INVESTIGATION OF THE EFFECTS OF SIRT1 AND SIRT2 MODULATORS IN NEUROINFLAMMATORY MODELS OF DEPRESSION

Yuqing Zhang

Doctor of Medicine, Master of Clinical Medicine

School of Pharmacy and Pharmacology

Griffith University

Supervisors: Prof. Andrew Davey

Assoc. Prof. Shailendra Anoopkumar-Dukie

Dr. Devinder Arora

Submitted in the fulfillment of the requirements of the degree of

Doctor of Philosophy

October 2020

Abstract

Depression is regarded as a manifestation of mood disorder and a complex phenomenon. The etiology can be primary and/or secondary to organic diseases. Neurodegenerative diseases such as Parkinson's disease, Alzheimer's disease and multiple sclerosis are often accompanied by the development of depression. A high prevalence of depression in populations with neurodegenerative diseases also indicates a close relationship between depression and neurodegeneration. There are several hypotheses of the pathogenesis of depression, including monoamine hypothesis, neurotrophic and the brain-derived neurotrophic factor (BDNF) hypothesis, HPA axis theory and circadian rhythm theory. There are apparently no infectious insults in the initiation of depression. However, depressed patients without apparent physical diseases showed an increased level of inflammatory markers. Evidence has indicated that neuroinflammation participates in the genesis and development of depression and interacts with other factors involved in depression. Excessive inflammatory cytokines can reduce the production of serotonin, fuel glutamate excitotoxicity, disturb neural plasticity, reduce the production of brain-derived neurotrophic factor and eventually prime the brain for neurodegeneration by facilitating inflammation and synaptic damage.

The target of current commercially available antidepressants is to increase levels of neurotransmitters including serotonin, noradrenaline and/or dopamine via different therapeutic mechanisms. However, the overall remission rate for the present medication options is under 30% according to the result of the National Institute of Mental Health (NIMH)-funded sequenced treatment alternatives to relieve depression (STAR*D) study. Additionally, they are frequently accompanied by undesirable side-effects and toxic effects in overdoses that limit their application. Therefore, there is an ongoing need to investigate the potential for novel medications that target neuroinflammation to address this underlying feature of depression.

Sirtuins are a unique class of nicotinamide adenine dinucleotide (NAD+)-dependent deacetylases that can affect multiple downstream targets by deacetylation activity. The sirtuin family consists of SIRT1-7 enzymes that differ in subcellular localization, enzymatic activities, physiological functions and pathological roles. Among these seven members, SIRT1 has been reported to exert neuroprotective effects in aging,

oxidative stress, neuronal survival, neurogenesis and neuroinflammation. SIRT2 also participates in numerous aging-related cellular activities including DNA repair, oxidative stress and autophagy. Based on these important roles, the pharmacological effects of SIRT1 and SIRT2 modulators have been investigated in numerous neurodegeneration studies where different models were conducted, and contradictory results were generated. Therefore, this thesis proposed a systematic investigation of the effects of SIRT1 and SIRT2 modulators in neuroinflammation and neurodegeneration models of depression including *in vitro* and *in vivo* studies. The pharmacological agents assessed in this study include: SIRT1 activator resveratrol; selective SIRT1 inhibitor EX527; dual SIRT1/SIRT2 inhibitor sirtinol; SIRT2 inhibitor AGK2; and positive controls for depression and inflammation, fluoxetine and ibuprofen, respectively.

Microglia are the resident macrophages that are regarded as the prime components of the intrinsic immune system in CNS parenchyma. Therefore, microglia play a dominant role in neuroinflammation. Injury or other pathological insults can result in the activation of microglia which are able to release inflammatory mediators and chemokines such as TNF-α, IL-1β, PGE_2 and reactive oxidative species. Thus the overall experimental design was to collect the supernatant from lipopolysaccharide (LPS)-stimulated microglia (HAPI cell line) and transfer it onto neuronal cells (SH-SY5Y cell line). Microglia were pre-treated with SIRT drugs to affect their biological performance under LPS stimulation and investigate the alteration of the subsequent outcome on neuronal cells.

To achieve this goal, methodology development was conducted to optimize the cell culture condition and differentiation method for SH-SY5Y cell line, which is key to achieve accurate results for this study. The glucose level in culture media needed to be correctly selected for the cell culture of SH-SY5Y cells in this supernatant transfer-based co-culture model. High glucose in culture media is considered a pre-diabetic condition for neurons. Data has shown that the cell viability of high-glucose cultured SH-SY5Y cells was reduced by treatment of HAPI cells-conditioned supernatant, which indicated the existence of low-glucose shock. Whereas, application of low-glucose media can effectively prevent SH-SY5Y cells from low-glucose shock after the treatment of the supernatant collected from HAPI cells. Moreover, the differentiation method for SH-SY5Y was also optimized. The combination induction treatment of retinoic acid and BDNF can successfully differentiate the SH-SY5Y cells

morphologically and genetically. The RNA expression of neuronal gene marker synaptophysin (SYP) and enolase 2 (ENO2) have shown to significantly increase after combination treatment of retinoic acid and BDNF.

In the *in vitro* pharmacological study, the effects of these SIRT1 and SIRT2 drugs on the production of inflammatory mediators including PGE_2, TNF-α, IL-1β and IL-10 on LPS (0.005 μg/L) -stimulated microglia were assessed. Resveratrol and sirtinol significantly reduced the TNF-α production in HAPI cells by up to 95% and 93% respectively. This result showed their potent inhibiting effects on TNF-α which can initiate cell death pathways by binding TNF receptors. Resveratrol, sirtinol, EX527 and AGK2 also significantly reduced PGE_2 production by up to 97%, 100%, 65% and 69% respectively in microglia under LPS stimulation. These results are significant given that prostaglandins contribute to prolonged acute inflammatory responses.

The supernatant from LPS-stimulated HAPI cells was transferred to SH-SY5Y cells. All SIRT drugs pre-treated of HAPI cells were shown to significantly increase the survival of undifferentiated SH-SY5Y cells, following the transfer of the supernatant. Their inhibiting effects on the production of inflammatory mediators including TNF-α and PGE_2 might contribute to this protection on SH-SY5Y cells. The SIRT1 activator resveratrol and dual SIRT1/SIRT2 inhibitor sirtinol demonstrated the most potent effect compared to others. Additionally, in undifferentiated cells, resveratrol was protective against apoptosis, as indicated by a reduction in Caspase 3/7 activity. However, in contrast, in differentiated SH-SY5Y cells, only sirtinol and AGK2 pre-treated supernatant were found to exert neuroprotective effects. Moreover, no increase in Caspase 3 activity was observed following treatment with supernatant indicating that protection against apoptosis is not the reason for increased cell survival.

In the animal study, the two most effective agents, SIRT1 activator resveratrol and dual SIRT1/2 inhibitor sirtinol, from the *in vitro* study were assessed in the acute phase of the LPS-induced depression mouse model and compared with fluoxetine. The behavioral parameters including locomotor activity and immobility time in the open field test, forced swim test and tail suspension test were significantly improved by resveratrol, sirtinol and fluoxetine in the acute sickness phase of the depression model.

In conclusion, this research has emphasized the necessity of increasing the understanding of the roles that neuroinflammation and neurodegeneration playing in

the pathophysiology of depression and the importance of investigating SIRT drugs as a novel class of drugs targeting neuroinflammation. This research has shown the effectiveness of SIRT modulators in inhibiting neuroinflammation and subsequent neurodegeneration through *in vitro* and *in vivo* studies. Further studies, including combining SIRT modulators and current antidepressant medications are warranted.

Statement of Original Authorship

I declare this work has not previously been submitted for a degree or diploma in any university. To the best of my knowledge and belief, the thesis contains no material previously published or written by another person except where due reference is made in the thesis itself. All sources of information have been fully acknowledged.

Yuqing Zhang

Table of Contents

List of Figures

List of Tables

List of Abbreviations

Aβ protein	Amyloid-β protein
ABC	Avidin-biotin-peroxidase complex
ACTH	Adrenocorticotropic hormone
AD	Alzheimer's disease
AMPAR	α-amino-3-hydroxy-5-methyl-4-isoxazolepropionic acid receptor
AMPK	5' AMP-activated protein kinase
ALS	Amyotrophic lateral sclerosis
ATP	Adenosine triphosphate
BBB	Blood-brain barrier
BDNF	Brain-derived neurotrophic factor
CNS	Central nervous system
COX-2	Cyclooxygenase-2
CR	Caloric restriction
CRF	Corticotropin-releasing factor
DA	Dopamine
DAMP	Danger-associated molecular pattern
DAT	Dopamine transporter
DCFH-DA	Dichloro-dihydro-fluorescein diacetate
DMEM	Dulbecco's modified eagle medium
DMSO	Dimethylsulphoxide
DSM-IV	Diagnostic and statistical manual of mental disorders-IV
ECM	Extracellular matrix
ECT	Electroconvulsive therapy
ENO2	Enolase 2
ER	Endoplasmic reticulum
FBS	Fetal bovine serum
FOXO	Forkhead box protein O
FST	Forced swim test
GWAS	Genome-wide association study
HAPI cell line	Highly aggressively proliferating immortalized cell line

HBSS	Hank’s balanced salt solution
HD	Huntington’s disease
HPA axis	Hypothalamic-pituitary-adrenal axis
HSF	Heat shock factor
HSP	Heat shock protein
ICD-10	International classification of diseases-10
IDO	Indoleamine 2, 3-dioxygenase
IFN-γ	Interferon-γ
IL	Interleukin
iNOS	Inducible nitric oxide synthase
LPS	Lipopolysaccharide
MAMP	Microbial-associated molecular pattern
MAO	Monoamine oxidase
MAOI	Monoamine oxidase inhibitor
MDD	Major depressive disorder
MMP	Mitochondrial membrane potential
MMP-9	Matrix metallopeptidase 9
MMSE	Mini-mental state examination
MPTP	1-methyl-4-phenyl-1, 2, 3, 6-tetrahydropyridine
MS	Multiple sclerosis
NA	Noradrenaline
NADPH	Dihydronicotinamide-adenine dinucleotide phosphate
NARI	Noradrenergic reuptake inhibitor
NASSA	Noradrenaline and serotonin-specific antidepressant
NDRI	Noradrenaline and dopamine reuptake inhibitor
NeuN	Neuronal nuclei
NSE	Neuron-specific enolase
NF-κB	Nuclear factor kappa-light-chain-enhancer of activated B cells
NMDAR	N-methyl-D-aspartate receptor
NSAIDs	Non-steroidal anti-inflammatory drugs
NTD	N-terminal domain
OFT	Open field test

PAMP	Pathogen-associated molecular pattern
PBS	Phosphate buffer saline
PD	Parkinson's disease
PGC-1α	Peroxisome proliferator-activated receptor gamma coactivator 1-α
PGE	Prostaglandin
PPAR	Peroxisome proliferator-activated receptor
PRR	Pattern recognition receptor
qPCR	Quantitative polymerase chain reaction
RA	Retinoic acid
RE	Response elements
ROCK1	Rho-associated, coiled-coil-containing protein kinase 1
ROS	Reactive oxidative stress
rtPCR	Real-time polymerase chain reaction
SARI	Dual 5HT-2 receptor antagonist/5-HT reuptake inhibitor
SIRT	Sirtuin
SOD	Superoxide dismutase
SSRI	Selective serotonin reuptake inhibitor
SNP	Single nucleotide polymorphism
SNRI	Dual serotonin and noradrenaline reuptake inhibitor
STAR*D study	Sequenced treatment alternatives to relieve depression study
SYN	Synaptophysin
TACE	TNF-α-converting enzyme
TADD	TNFR-associated death domain
TCA	Tricyclic antidepressant
TH	Tyrosine hydroxylase
TLR	Toll-like receptor
TNF	Tumor necrosis factor
TST	Tail suspension test
3-MA	3-methyladenine
5-HT	Serotonin/ 5-hydroxytryptamine

Publication during candidature

1. Zhang, Y. Anoopkumar-Dukie S. Arora, D. Davey, A.K. Review of the anti-inflammatory effect of SIRT1 and SIRT2 modulators on neurodegenerative diseases. European Journal of Pharmacology, Volume 867, 2020 (impact factor: 3.263)
2. Zhang, Y. Anoopkumar-Dukie S. Arora, D. Davey, A.K. SIRT1 and SIRT2 modulators: potential anti-inflammatory treatment for depression? Biomolecules, Special issue: Converging pathophysiologies of psychiatric and neurodegenerative disorders, Volume 353, Issue 11, 2021 (impact factor: 4.082)
3. Zhang, Y. Mallik, S.B. Davey, A.K. Arora, D. Anoopkumar-Dukie S. SIRT1 and SIRT2 modulators reduce LPS-induced inflammation in HAPI microglial cells and protect SH-SY5Y neuronal cells *in vitro*. Journal of Neural Transmission. Resubmission under review (impact factor: 3.505)
4. Zhang, Y. Davey, A.K. Anoopkumar-Dukie S. Arora, D. Effects of SIRT1 and SIRT2 modulators in lipopolysaccharide-induced sickness-like and depressive-like behavior in mice. In preparation.

Acknowledgments

This project was carried out in the School of Pharmacy and Pharmacology, Griffith University. This work was funded by a Griffith University International Postgraduate Scholarship and a Griffith University Postgraduate Research Scholarship. I would like to sincerely thank Griffith University for funding my Ph.D. research, and the School of Pharmacy and Pharmacology for providing me a lab and facilities to conduct my research project.

I would like to thank my supervisory team, Prof Andrew Davey, Assoc Prof Shailendra Dukie, and Dr Devinder Arora for giving me this opportunity to undertake this research project. I am grateful for their support, patience, help and guidance throughout my study and research. I also wish to express my sincere thanks to Dr Sanchari Basu Mallik for introducing me into the rt-PCR technique and her help and guidance for my Ph.D. study. I would also sincerely thank colleagues at Manipal University for their help in obtaining data as part of the *in vivo* study (Chapter 5).

I also would like to thank my husband and my parents. They have been unconditionally giving me constant help, support and faith and believing me through my whole Ph.D. journey. They had been giving me heart-warming support every time that I had a mental struggle and needed them the most. I could not successfully complete my Ph.D. without them. I like to dedicate my Ph.D. thesis to them. Thank you so much for your endless blessings!

Chapter 1 : Literature Review

1.1 Background

Depression is one of the leading causes of disability and had been predicted to be one of the largest health problems worldwide by 2020 (C. J. L. Murray et al., 1996). According to the data published by the World Health Organisation (WHO), over 264 million people of all ages suffer from depression. Approximately 800,000 people die from suicide every year (World Health Organization, 2020). In Australia, it is estimated that approximately 45% of the Australian population aged 16-85 years will experience a mental disorder at some age stage (Australian Institute of Health and Welfare, 2020).

The main theories of the underlying pathophysiology include deficiency of monoamine neurotransmitters such as 5-HT, noradrenaline and dopamine in the central nervous system (CNS), dysregulation of the hypothalamic-pituitary-adrenal (HPA) axis, and reduction of brain-derived neurotrophic factor (BDNF). However, the remission rate of depression patients who are having treatments with the currently available antidepressants is still low. Besides the low remission rate, current antidepressant medications, such as monoamine oxidase inhibitors (MAOIs), selective serotonin reuptake inhibitors (SSRIs) and tricyclic antidepressants (TCAs), have multiple types of toxicity, including serotonin syndrome, and withdrawal effects (J. M. Ferguson, 2001). However, there is strong evidence suggesting an intimate linkage between chronic neuroinflammation and the development of depression and associated manifestations, such as disturbed sleep and a loss of appetite (A. Roy and M. K. Campbell, 2013, O. Köhler et al., 2016, A. J. M. Loonen and S. A. Ivanova, 2016). This leads to the potential that neuroinflammation can be a novel treatment target for depression.

1.2 Depression

Depression is regarded as a manifestation of mood disorder and is a complex phenomenon. The symptoms include depressed emotion, a loss of interest and well-being, lack of motivation, suicidal thoughts and desperation, accompanied by somatic symptoms such as insomnia, decreased appetite and fatigue. However, depression is not a homogeneous condition. It has many categories and subtypes with multiple aetiologies in some cases (B. Brigitta, 2002). The uncertainty and complexity of the aetiology of depression results in different views and classifications of depressive disorders. Depression disorder can be categorized by the severity of clinical psychotic manifestations and features in the course of disease according to widely-used International Classification of Diseases (ICD-10) and Diagnostic and Statistical Manual of Mental Disorders (DSM-IV) (R. F. Garside et al., 1971, American Psychiatric Association, 2013, World Health Organization, 1992). Based on the classification DSM-IV, depression can

be classified into major depressive disorder, dysthymic disorder which is referred to as a persistent low mood, and unspecified depressive disorder (American Psychiatric Association, 2013). Additionally, mood disorder also can be separated into a primary group and a secondary group. It has been reported that medical disease load is possibly associated with a higher risk of hospital admission of depression, particularly among patients aged less than 65 (O. Köhler-Forsberg et al., 2020). There is a rough estimate on mood disorder that primary, secondary and undistinguishable mood disorder accounts for 55%, 35% and 12% respectively, which indicates that non-primary mood disorder accounts for almost half of all mood disorder cases (K. Jiang et al., 2010). Secondary depression can be a direct result of other psychotic diseases or other somatic diseases or substance abuse. Those types of depression caused by a medical condition can also be seen as an 'organic mood disorder' (N. R. C. Brian Walker, Stuart Ralston, Ian Penman, 2014). A variety of diseases are able to lead to depression such as stroke, Parkinson's disease (PD), Alzheimer's disease (AD), diabetes mellitus and epilepsy. Evidence has shown that depression and neurodegeneration are commonly co-morbid. For instance, depression symptoms commonly occur in neurodegenerative diseases such as AD (A. Burns and S. Iliffe, 2009), PD (S. Sveinbjornsdottir, 2016), amyotrophic lateral sclerosis (ALS) (E. Roos et al., 2016), Huntington's disease (HD) (Jane S. Paulsen et al., 2005) and multiple sclerosis (R. J. Siegert and D. A. Abernethy, 2005). Many patients in the early stages of neurologic diseases might be suffering from depression which could be the main symptom of these diseases. In some cases, the depressive manifestation can emerge late when the neurodegenerative disease is already well established (M. Baquero and N. Martín, 2015). For instance, according to descriptive population studies, approximately 80% of AD patients can develop depressive symptoms to some degree in the progression of AD (C. G. Lyketsos and H. B. Lee, 2004). Depressive symptoms as the main negative factor of PD often indicate rapid progression of motor disturbances and cognitive impairment. The prevalence of depressive symptoms in PD is approximately 20% to 50% (E. Tandberg et al., 1996, A. Schrag et al., 2007, R. C. Prado and E. R. Barbosa, 2005). In HD patients, the proportion of depression can reach up to 40% of cases (J. S. Paulsen et al., 2001, L. Di Maio et al., 1993). Thus, depression is not simply a mood disorder but also frequently a risk factor for the onset of neurodegenerative conditions from the epidemiological perspective, which indicates their close relationship (H. Rickards, 2006, M. Baquero and N. Martín, 2015).

1.2.1 Underlying pathogenesis of depression

Although many psychopharmacological agents are already available for the treatment of depression, the overall remission rate for the present medication options is under 30% according to the result of the National Institute of Mental Health (NIMH)-funded sequenced treatment alternatives to relieve depression (STAR*D) Study (NIMH, 2006, G. S. Malhi et al., 2015). The STAR*D study was conducted to determine the effectiveness of different treatments for people with major depression who have not responded to initial treatment with a current antidepressant (NIMH, 2006). This is the largest and longest study ever conducted to evaluate current depression medications so far (NIMH, 2006). The overall remission rates for the present medication options including citalopram, bupropion, venlafaxine, sertraline and mirtazapine were less than 30% (M. H. Trivedi et al., 2006a, B. N. Gaynes et al., 2009, A. J. Rush et al., 2006, M. H. Trivedi et al., 2006b, M. E. Thase et al., 2007, Maurizio Fava et al., 2006, Andrew A. Nierenberg et al., 2006, Patrick J. McGrath et al., 2006). In addition, that even after 4 sequential pharmacotherapies 19% of patients still have disease that is resistant to treatment (N. N. Huynh and R. S. McIntyre, 2008). The most important reason is that depression is a multifaceted disorder and that the understanding of the pathogenesis of depression is still poor (G. Racagni and M. Popoli, 2008). There are several hypotheses of the pathogenesis of depression, including monoamine hypothesis, neurotrophic and BDNF hypothesis, hypothalamic-pituitary-adrenal (HPA) axis theory and circadian rhythm theory. However, evidence has indicated that neuroinflammation participates in the genesis and development of depression and interacts with other factors involved in depression. There are apparently no infectious insults in the initiation of depression. Nevertheless, depressed patients without physical diseases showed an increased level of inflammatory markers (M. Uddin et al., 2011). Inflammatory markers such as TNF-α, IL-6 and C-reactive protein (CRP) in major depressive disorders are higher than normal (O. J. G. Schiepers et al., 2005); depression symptoms can also be induced by cytokine treatment such as IFN-γ therapy of hepatitis C and some types of cancers (R. Krishnadas and J. Cavanagh, 2012).

The monoamine hypothesis has long been recognized as a core concept in the pathogenesis of depression. According to this theory, depression can be caused by the deficiency of monoamine neurotransmitters including 5-HT, noradrenaline and dopamine. The alleviation of symptoms by application of selective serotonin reuptake inhibitors (SSRI) has provided further support for this hypothesis. The monoamine receptor sensitivity hypothesis supplemented this theory by suggesting that depression is induced by monoamine transporter up-regulation (S. W. Jeon

and Y.-K. Kim, 2016). Excessive inflammatory cytokines activate indoleamine 2, 3-dioxygenase (IDO) which is able to convert tryptophan, the precursor of 5-HT, into kynurenine, therefore reduce the production of 5-HT (C. Sahin et al., 2016, M. Maes et al., 2011). Kynurenine is further converted into quinolinic acid, an agonist of the N-methyl-D-aspartate receptor (NMDAR), which will fuel glutamate excitotoxicity in depression (D. C. Mathews et al., 2012). The interactions between pathways and other factors mentioned as followed are shown **Figure 1.1**.

The neurotrophic and BDNF hypothesis proposes that depression is on the basis of neurotrophin deficiency in the hippocampus (H. Yu and Z. Y. Chen, 2011, B. H. Lee and Y. K. Kim, 2010). The decreased BDNF with associated synaptic plasticity and increased apoptosis may be considered as a common pathway in various hypotheses of depression. BDNF is also known to improve neural plasticity, neurogenesis and increase survival of neurons (E. Castren and T. Rantamaki, 2010). Neural plasticity is defined as a neuronal adaptation, an individual response to the environment, which includes neurogenesis and apoptosis in the adult brain (R. S. Duman et al., 1999). The core function of neural plasticity is the signal-transduction-cascade which can be activated by learning, memory, stress or the environment (T. Tojima and E. Ito, 2004). The dysfunction or failure of signal-transduction-cascade and neural plasticity will eventually lead to the onset of depression. Many factors can affect BDNF synthesis, release, and function, such as changes in inflammatory cytokines and glutamate receptors, and hyperactivity of the HPA axis. Over-activation of neuro-immune responses and HPA axis synergistically disrupt the normal physiological microenvironment of neurons (S. Cai et al., 2015).

The HPA axis can also be excessively activated under severe stress, which will result in a sustained high blood concentration of glucocorticoids (J. Douglas Bremner et al., 2000). Glucocorticoid is secreted by the adrenal cortex under the regulation of corticotropin-releasing factor (CRF) and adrenocorticotropic hormone (ACTH) secretion from the hypothalamus and pituitary, which affects neurobehavioral functions in many brain domains (S. W. Jeon and Y.-K. Kim, 2016). Hypercortisolemia suppresses BDNF expression, attenuates synaptic plasticity, increases the excitotoxicity of neurons in the hippocampus and eventually causes atrophy or degeneration in neurons in extreme cases (C. Anacker et al., 2013, S. Cai et al., 2015). Excessive inflammation can disrupt glucocorticoid receptors and leads to glucocorticoid resistance as a result of which hypercortisolemia will reduce the BDNF production in the brain (X. Wang et al., 2004).

The abnormal glutamate receptor hypothesis is another vital theory of the pathophysiology of depression. There is also an intimate relationship between it and other theories mentioned above. Inflammatory cytokines can activate indoleamine 2, 3-dioxygenase (IDO) and kynurenine pathways which affect glutamate neurotransmission and contribute to glutamate dysfunction in the brain (J. C. Felger and F. E. Lotrich, 2013). Inotropic glutamate receptors, NMDARs and α-amino-3-hydroxy-5-methyl-4-isoxazolepropionic acid receptor (AMPARs), are also related to the onset of depression (S. Cai et al., 2015). Under the stimulation of excessive glutamate, activation of extra-synaptic glutamate receptors leads to detrimental episodes, including Ca^{2+} overload, oxidative stress injury, and apoptosis or degeneration which is reflected in the manifestation of depression (G. E. Hardingham et al., 2002, S. Cai et al., 2015). Besides, evidence has shown that the fast antidepressant effects of NMDAR antagonists are dependent on the rapid synthesis of BDNF, which indicates the close relationship between BDNF modulation and glutamate receptors (R. A. Crozier et al., 2008, S. Cai et al., 2015).

Disorganization of circadian rhythm has also been proposed to make individuals susceptible to depression (S. W. Jeon and Y.-K. Kim, 2016). The site of biological rhythm control in the hypothalamus receives inputs from varieties of signals, including a light signal from the retina, serotonin and melatonin, and transduces output signals to downstream targets, including the HPA axis, autonomic nervous system and the pineal gland (S. Cai et al., 2015). Therefore, biological rhythm control is able to regulate glucocorticoids or other hormones and sleep. The impairment of melatonin secretion directly disturbs normal sleep-wake rhythm (S. Cai et al., 2015). There is strong evidence that indicates that many depression patients manifest the disturbance of circadian rhythms and low melatonin syndrome (J. Beck-Friis et al., 1985). Sleep deprivation increases inflammatory biomarkers in patients and primes the brain for neurodegeneration by facilitating inflammation and synaptic damage (E. S. Musiek and D. M. Holtzman, 2016).

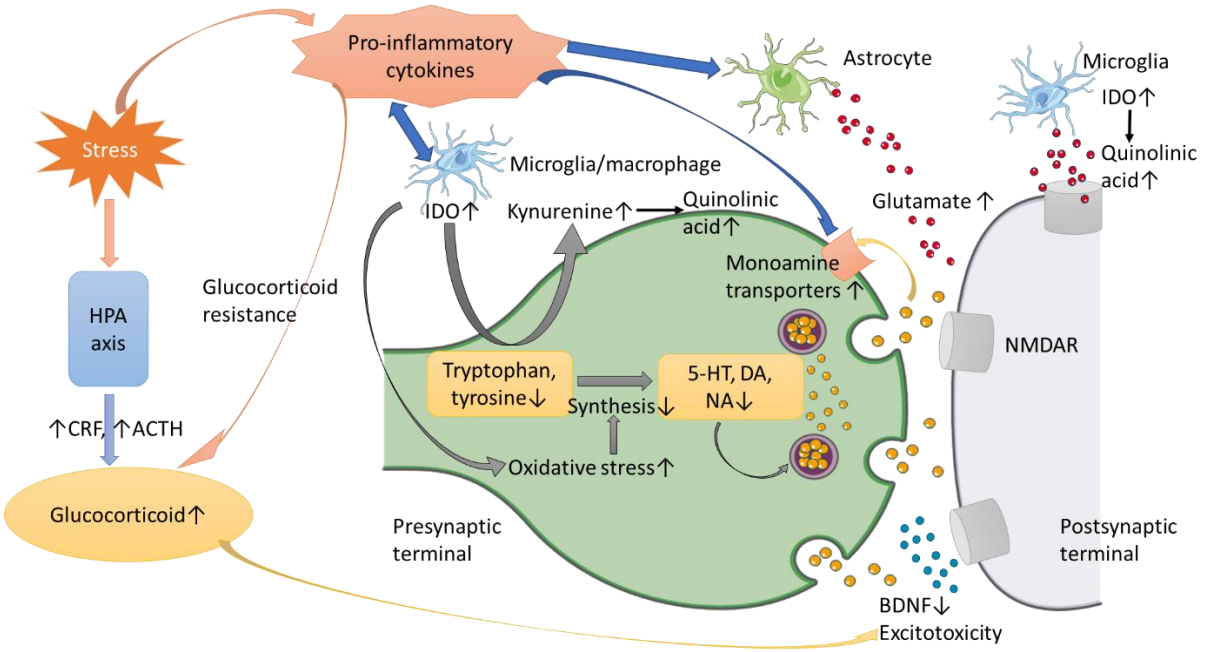

Figure 1.1 Inflammatory cytokines interfere with different factors in depression.

Inflammatory cytokines can be produced by macrophages or microglia under stress. Cytokines can manipulate the activities of monoamine neurotransmitters via different pathways. The activation of the IDO pathway along with the increased production of oxidative stress by cytokines in microglia leads to the reduction of the concentration of neurotransmitters, including 5HT, DA and NA, in the synaptic gaps. Cytokines also induce the up-regulation of the reuptake of neurotransmitters through monoamine transporters, which also contributes to the reduction of the concentration of these monoamines. Meanwhile, astrocytes can up-regulate the concentration of glutamate in the synaptic gaps. Glutamate receptors (NMDAR) can also be activated by kynurenine's by-product quinolinic acid. On the other hand, cytokines also can contribute to hypercortisolemia induced by excessively activated HPA axis under stress, which further induces the reduction of the production of BDNF. The combination of these effects can result in excitotoxicity that can eventually lead to cell damage and death. (IDO, indoleamine 2, 3-dioxygenase; 5-HT, serotonin; DA, dopamine; NA, noradrenaline; HPA axis, hypothalamic-pituitary-adrenal axis; CRF, corticotropin-releasing factor; ACTH, adrenocorticotropic hormone; BDNF, brain-derived neurotrophic factor; NMDAR, N-methyl-D-aspartate receptors)

1.2.2 Neuroinflammation and neurodegeneration

1.2.2.1 Neuroinflammation and sterile inflammation

Neuroinflammation is a generalized term to describe the immune response of the central nervous system (M. Lyman et al., 2014). Diverse triggers including peripheral infection, stroke, traumatic brain injury and autoimmune diseases can induce neuroinflammation (H. E. Gendelman, 2002). The blood-brain barrier (BBB), glia and neurons are all involved in this

immune response (N. J. Abbott et al., 2006, M. Lyman et al., 2014). The BBB is known as a highly selective semipermeable endothelial membrane that isolates the parenchyma of CNS from the circulatory system (I. Bechmann et al., 2006). IL-1β, IL-6, TNF-α, and other cytokines originating from the peripheral immune system are able to permeate across the BBB and intervene in the integrity of the BBB via adjusting the permeability of tight junctions (D. Wong et al., 2004). This also allows leucocytes such as monocytes and T immune cells from peripheral blood vessels (B. Becher et al., 2017) to cross the BBB and influx into the CNS and release inflammatory cytokines (H. E. de Vries et al., 1996, M. Russo and D. B. McGavern, 2015). This neuroinflammation eventually leads to synaptic dysfunction, restraint of neurogenesis and neuron death (M. Lyman et al., 2014).

Sterile inflammation of the CNS is an outcome of neurological and psychological diseases that do not involve microorganisms as the trigger (G. Y. Chen and G. Nuñez, 2010). Similar to microbially induced inflammation, the characteristic of sterile inflammation includes an assembly of neutrophils and macrophages and secretion of proinflammatory chemokines and cytokines, such as TNF-α and IL-1 (G. Y. Chen and G. Nuñez, 2010). As a result of sterile cell death, the inflammatory response and leukocyte infiltration, tissue injury is aggravated (K. L. Rock et al., 2010).

Nevertheless, neuroinflammation does not always meet the criteria discussed above, as the compromised BBB does not participate in some neuroinflammatory conditions (M. B. Graeber et al., 2011). The term ‘microglia activation’ is a better way to describe neuroinflammation with the absence of peripheral immune cells.

1.2.2.2 Cellular components and the cytokine network of neuroinflammation

Upon stimulation by a diverse range of agents, multiple types of cells including leukocytes, microglia, astrocytes, oligodendrocytes, monocyte-derived cells and even neurons are able to release chemokines and cytokines, and also have receptors to respond to chemokines and cytokines (E. N. Benveniste, 1992). Microglia are the resident macrophages that are regarded as the prime components of the intrinsic immune system in CNS parenchyma (W. J. Streit and C. A. Kincaid-Colton, 1995). Therefore, microglia play a dominant role in neuroinflammation (G. Ramesh et al., 2013). **Figure 1.2** shows the central role of microglia in neuroinflammation. In constant conditions, microglia stay in a resting status and protect the CNS through scavenging debris and pathogens such as damaged cells, apoptotic cells and DNA fragments (R. von Bernhardi et al., 2016). Injury or other pathological insults can result in the activation

of microglia which are able to release inflammatory mediators and chemokines such as TNF-α, IL-1β, PGE_2 and reactive oxidative species (ROS).

Cytokines normally maintain the homeostasis of the CNS, growth and survival factors, and brain development. However, classical neuroinflammatory diseases (i.e. multiple sclerosis) can be induced by cytokines such as IL-1, IL-6, and TNF which are secreted by invading leukocytes in pathological circumstances. In addition, the cytokines secreted by CNS-resident microglia in proteinopathies (i.e. Alzheimer's disease, Parkinson's disease) overlap to a large extent with that in classical neuroinflammatory diseases. Cytokines produced by invading leukocytes can initialize the inflammation cascade and microglia can increase the production of a diverse bulk of cytokines which enable more leukocytes to be recruited to inflame the cascades (B. Becher et al., 2017).

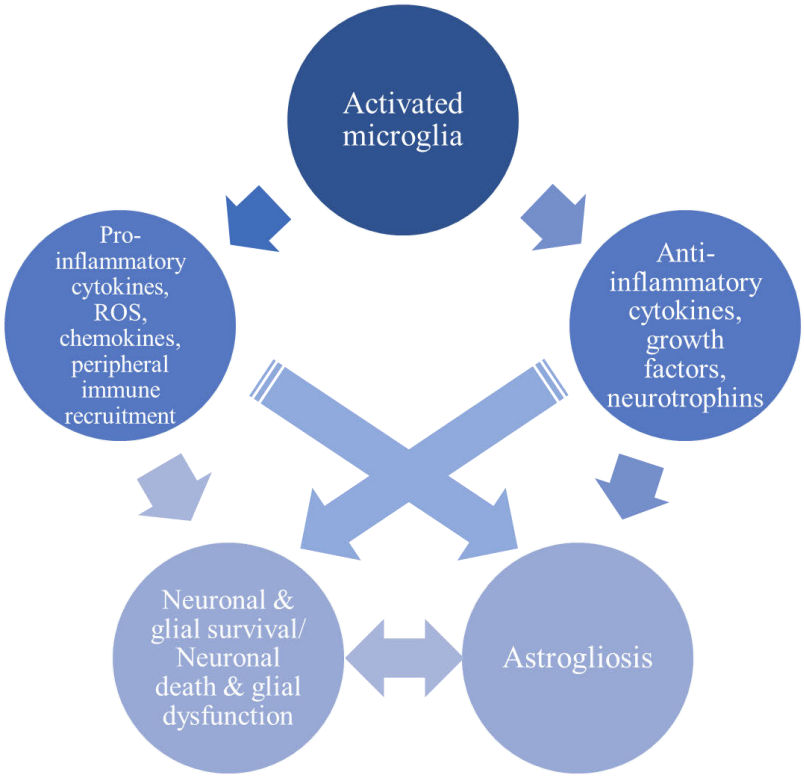

Figure 1.2 The central role of microglia in neuroinflammation.

Activated microglia after stimulation from infection, injury, and other triggers can release a variety of active mediators and factors. Proinflammatory cytokines partly can lead to direct neuronal death but also astrogliosis which can help with neuronal survival in return. Additionally, other cytotoxic factors such as ROS also contribute to the process of neuronal death. On the contrary, the anti-inflammatory cytokines can directly protect against neuronal death. Growth factors and neurotrophins also can benefit glial and neuronal survival.

1.2.2.3 Consequences of neuroinflammation

Excessive and protracted neuroinflammation can directly influence neuronal apoptosis and thus result in acute neurological damage or neuronal death and accelerate long-term neurodegeneration and neurological conditions such as Alzheimer's disease, Parkinson's disease, multiple sclerosis and cognitive impairment (M. Lyman et al., 2014). For instance, the tumor necrosis factor family of cytokines such as TNF-α display direct biological effects on neuronal survival and apoptosis (G. J. Harry et al., 2008).

Neuropathological and neuroradiological research show that the neuroinflammatory response is capable of fuelling a significant loss of neurons in neurodegenerative diseases (T. C. Frank-Cannon et al., 2009). For instance, a loss of dopaminergic neurons in the substantia nigra is a pathological feature of PD. Elevation of inflammatory mediators has been found in the cerebrospinal fluid of PD patients (M. P. Vawter et al., 1996, A. Gerhard et al., 2006). Inflammatory responses in the process of immune-mediated diseases such as MS lead to the pathophysiology characterized by the damage of myelinated cells and axonal injury. Regarding the neuroinflammation of AD, the relationship between the amyloid-β peptide (Aβ) accumulation, tauopathy and microglia activation is not yet fully understood. Oxidative stress led by the accumulation of misfolded protein can impair the mitochondrial function of microglia and neurons (K. A. Jellinger, 2010). Oxidative stress can also result in DNA damage and structural alteration of proteins and lipids. The imbalance between oxidative stress production and antioxidant defense is regarded as a vital hallmark of neurodegenerative diseases (E. Niedzielska et al., 2016). The excessive production of oxidative stress also further promotes redox imbalance and stimulates the transcription of the pro-inflammatory mediators such as IL-1β, IL-6, and TNF-α (M. Akbar et al., 2016).

Furthermore, neuroinflammation can disturb the synaptic function and destroy the connection between cells, which is an early feature of dementia (E. Masliah et al., 2001). The synaptic dysfunction turns out to affect neuroplasticity which plays a crucial role in depression and diseases with depressive symptoms (H. Eyre and B. T. Baune, 2012). The atrophy and loss of neuron and glial cells indicate a decreased synaptic plasticity. CNS imaging shows the loss of cellular population in the prefrontal cortex or amygdala is associated with a reduction of brain volume in depression (D. Cotter et al., 2001, I. M. Rosso et al., 2005, Y. I. Sheline et al., 1998). This depression-associated brain parenchyma volume decrease can also reflect the reduction of neurogenesis (C. Zhao et al., 2008).

1.2.3 The mechanism underlying the development of inflammation in depression

Recently numerous studies of neuropsychology have shifted their focus to inflammasomes which might be an important link between psychosocial stress, pathogens and inflammation. Inflammasomes are intracellular multiprotein complexes that function as sensors of danger-associated molecular patterns (DAMPs) and microbial or pathogen-associated molecular patterns (MAMPs or PAMPs) (M. Fleshner et al., 2016).

DAMPs are endogenous molecules such as extracellular heat-shock protein 72 (Hsp72) and adenosine triphosphate (ATP) which are derived from self or increased after cellular stress and tissue damage (M. Fleshner et al., 2016). MAMPs or PAMPs are referred to as small molecular motifs from infectious microbes such as lipopolysaccharides (LPS) (G. Santoni et al., 2015). The innate immune system can recognize and respond to DAMPs and PAMPs *via* pattern recognition receptors (PRRs) such as toll-like receptors (TLRs) (P. G. Vallés et al., 2014). The consequence of PRR-DAMP binding is sterile inflammation, and robust inflammatory response is the consequence of the PRR-PAMP binding (H. Kono and K. L. Rock, 2008). **Figure 1.3** shows the PAMPs, DAMPs, and inflammatory response.

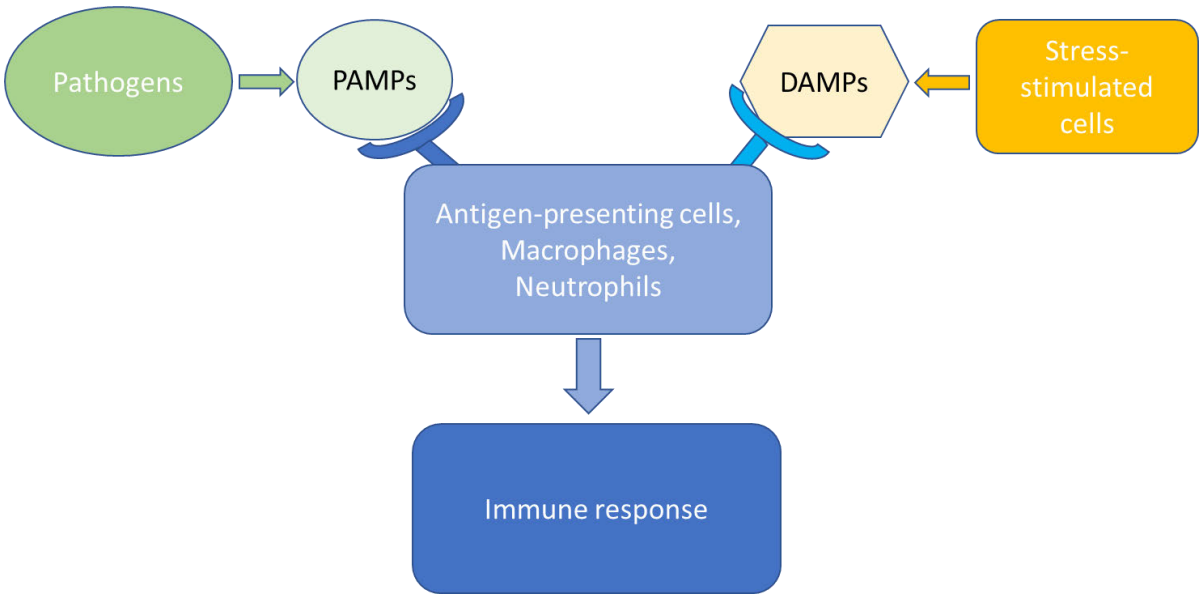

Figure 1.3 PAMPs, DAMPs, and inflammatory response.

Pathogen-associated molecular patterns (PAMPs) come from pathogens such as bacteria and viruses. Danger-associated molecular patterns (DAMPs) come from lysed dead cells including ATP and some intracellular proteins. They can bind to pattern recognition receptors (PRRs) or specialized receptors on immune cells, which will stimulate the immune response including the release of cytokines and chemokines and the recruitment of immune cells.

Activation of PRRs by cytoplasmic PAMPs and/or endogenous DAMPS provokes intracellular inflammatory signaling pathways such as nuclear factor-κB (NF-κB) which will lead to the generation of inflammasomes (NOD-, LRR- and NLRP3) (G. Santoni et al., 2015). Inflammasomes function as a molecular scaffold for the activation of caspase-1 which eventually leads to the maturation and the secretion of IL-1β and IL-18 by cleavage of pro-cytokines (S. P. Wilson and S. L. Cassel, 2010). Interestingly, an NLRP3 inflammasome can be activated by a range of stimuli which include both pathogenic microorganisms and endogenous mediators, such as reactive oxygen species, mitochondrial DAMPs and adenosine triphosphate (ATP), as well as by crystalline structures (e.g. uric acid crystals), other fibrillar proteins (e.g. β-amyloid fibrils) and environmental irritants (e.g. silica, alum) (B. K. Davis et al., 2011). A great variety of inflammatory proteins expressed in PAMP or DAMP pathways overlaps considerably such as IL-1β, TNF-α, IL-6, IL-10, and PGE_2 (M. Fleshner et al., 2016). Therefore, many researchers have chosen to apply lipopolysaccharide (LPS) to trigger inflammation, which can partly simulate sterile inflammation.

There are two ways of sterile inflammation which are inflammasome-independent and inflammasome-dependent (M. Fleshner et al., 2016). In the inflammasome-independent signaling pathway, the process begins with NF-κB activation after MAMPs or DAMPs binding to PRRs in monocytes. This binding initiates inflammatory protein gene transcription, translation, protein synthesis and release, which can stimulate the bone marrow to release more monocytes into the periphery (A. H. Miller and C. L. Raison, 2016). For the inflammasome-dependent pathway, once sufficient NLRP3 protein has been produced the activation/cleavage of procaspase 1 will be triggered (P. Duewell et al., 2010). Then mature, active caspase-1 acts to cleave pro-IL-1β into mature IL-1β (and IL-18) protein (M. Fleshner et al., 2016). **Figure 1.4** shows how the NLRP3 inflammasome matures IL-1β. Other pro-inflammatory cytokines including tumor necrosis factor and IL-6 from the activation of NF-κB can influx into the brain with IL-1β and IL-18 together through the humoral route where the blood-brain barrier lacks integrity and has small gaps on the structure congenitally (A. H. Miller and C. L. Raison, 2016). Microglia can also be activated into an M1 pro-inflammatory phenotype by psychosocial stress and secrete chemokines to attract peripheral monocytes to the brain through the cellular route (D. J. Stein et al., 2017, A. H. Miller and C. L. Raison, 2016)**.** The stimulation of NLRP3 inflammasome and the activation of caspase-1 can also mediate the cleavage of the glucocorticoid receptors (S. W. Paugh et al., 2015). It contributes to the resistance to the effects of glucocorticoids which are the most potent anti-inflammatory hormones (T. Rhen and J. A.

Cidlowski, 2005) and also participate in the pathophysiological process of depression (T. Steckler et al., 1999).

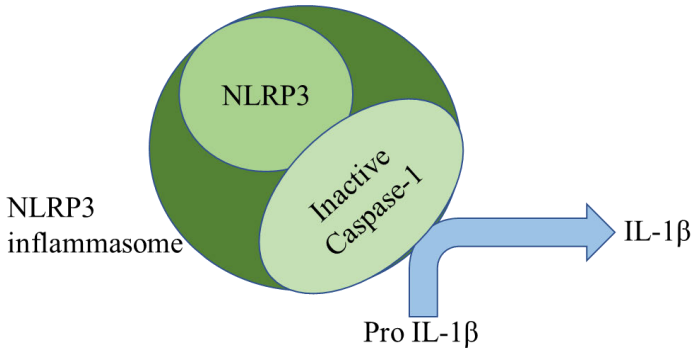

Figure 1.4 NLRP3 inflammasome matures IL-1β.

NLRP3 inflammasome assembly results in self-cleavage and activation of caspase-1 which further cleaves pro-IL-1β into mature IL-1β.

1.3 Current treatments of depression and their limitations

Current treatment practices of depression include antidepressant medication, cognitive therapy and other forms of psychotherapy, such as interpersonal therapy, electroconvulsive therapy (ECT) and electrical stimulation of the vagus nerve (UK ECT Review Group, 2003, M. F. de Mello et al., 2005, Z. Nahas et al., 2005, R. J. DeRubeis et al., 2008). Psychological treatments are equally important in the treatment of depression (G. S. Malhi et al., 2015). Many factors can impact the suitability for psychological therapy, including adherence to medications, the timing of treatment and formulation, and the extent of life stressors involved in the onset of the disease (G. S. Malhi et al., 2015). For instance, ECT applies to patients with a high risk of serious suicide attempts or experiencing evident psychosocial adversity or other specific indications (QueenslandHealth, 2017, G. S. Malhi et al., 2018). Also, psychological treatment may be better administered after initiating antidepressant treatment in some cases (G. S. Malhi et al., 2015). Therefore in this section, we mainly discuss the treatment outcomes of antidepressant medication.

Current commercially available antidepressants can increase levels of serotonin (5-HT), noradrenaline (NA), and/or dopamine (DA) via different therapeutic mechanisms (E. Penn and D. K. Tracy, 2012). First-generation antidepressants include tricyclic antidepressants (TCAs) and monoamine oxidase inhibitors (MAOIs), however, they are frequently accompanied by undesirable side-effects and toxic effects in overdose, limiting their application (E. Penn and

D. K. Tracy, 2012). Newer-generation antidepressants, including the well-known selective serotonin reuptake inhibitors (SSRIs), are more selective and offer improved safety and tolerability, but still have multiple side-effects which might result in poor compliance (E. Penn and D. K. Tracy, 2012, C. L. Bockting et al., 2008). **Table 1.1** shows a review of the therapeutic mechanism and side-effects of current antidepressants.

Toxicity might also occur with current antidepressant medication. Serotonin toxicity and withdrawal effects are the two main types of neurological toxicity. Serotonin toxicity is referred to as toxicity caused by a combination of >1 serotonergic agents or changing antidepressants with an inadequate washout period between drugs (AMH, 2018). The symptoms include hyperreflexia, mental state changes, shivering, and diarrhoea (AMH, 2018). Therefore, it is contraindicated to combine treatments of MAOIs, SSRIs, TCAs, NARIs, NaSSAs, SNRIs, and serotonin modulators. Missing 1 or 2 doses (especially with venlafaxine, paroxetine), high doses, long treatment course, stopping or rapid tapering antidepressants will cause withdrawal effects, including nausea, vomiting, anxiety and cholinergic rebound (AMH, 2018). Hepatotoxicity is also common in all categories of current antidepressants.

Besides the common types of toxicity, some data have suggested an increased risk of neonatal toxicity or symptoms (foetal heart defects, persistent pulmonary hypertension) after maternal use in late pregnancy with SSRIs, particularly with paroxetine (AMH, 2018). However, SSRIs have the least hepatic toxicity compared with the 2nd line and 3rd line antidepressants (C. S. Voican et al., 2014, G. S. Malhi et al., 2015, AMH, 2018). Besides neurological toxicity and high risk of hepatic impairment, TCAs also have cardiovascular toxicity (such as an increased risk of arrhythmia), overdose-related fatality (AMH, 2018). SNRIs increase bleeding risk and might cause cardiovascular events as well (AMH, 2018). MAOIs as 3rd line antidepressants also have multiple toxicities mentioned above (AMH, 2018). Other antidepressants such as mianserin and reboxetine also possess renal toxicity (AMH, 2018). In addition, bupropion might increase the risk of seizures (AMH, 2018).

Table 1.1 Review of antidepressants: mechanism and side-effects.

Typical recommendation	Antidepressant Class	Drug	Principal mechanism of action	Unwanted pharmacological action	Side effect
1st line	SSRI	Fluoxetine paroxetine sertraline fluvoxamine citalopram escitalopram	Selective inhibition of 5-HT reuptake transporter	Agonist of 5-HT_{2C} receptor	Gastrointestinal: reduced appetite, nausea, constipation, dry mouth Central Nervous: headache, insomnia, anxiety, fatigue, tremor Other: delayed orgasm, anorgasmia
	NARI	Reboxetine	Selective inhibition of NA reuptake	Muscarinic receptor blockade	Dry mouth, constipation, headaches
	NaSSA	Mianserin mirtazapine	5-HT_2 antagonism α_1-adrenoceptor antagonism	Histamine H_1 receptor blockade	Drowsiness, dry mouth, sedation, weight gain
	Melatonergic agonist	Agomelatine	Melatonin agonist (M1 and 2 receptors) 5-HT_{2C} antagonist		Nausea, dizziness, increase in serum hepatic transaminases (R. A. Sansone and L. A. Sansone, 2011)
	NDRI	Bupropion	Blockade of NA and DA reuptake transporters		Increased risk of seizures
2nd line	TCA	Clomipramine imipramine amitriptyline desipramine trimipramine nortriptyline protriptyline maprotiline amoxapine doxepin	Block reuptake transporters for serotonin and norepinephrine, and to a lesser extent dopamine	Muscarinic receptor blockade (anticholinergic) α_1-Adrenoceptor blockade Histamine H_1 receptor blockade	Dry mouth, tachycardia, blurred vision, glaucoma, constipation, urinary retention. Sexual dysfunction, cognitive impairment Drowsiness, postural hypotension, sexual dysfunction Drowsiness, weight gain

	SNRI	Venlafaxine duloxetine	Blockade of 5-HT and NA reuptake transporters		Nausea, dizziness, headache, dry mouth, insomnia, increases in blood pressure
	Serotonin modulator	Vortioxetine	5-HT_{1a} agonist, $5HT_{1b}$ partial agonist, 5-HT_{3a} and 5-HT_7 antagonist 5-HT transporter inhibitor		Nausea, diarrhea, dry mouth, constipation (A. D'Agostino et al., 2015)
3rd line	MAOI	Irreversible: phenelzine tranylcypromine isocarboxazid	Irreversible and nonselective inhibition of MAO	Irreversible blockade of MAO	Risk of hypertension from dietary amines-tyramine must be avoided, risk of intracerebral haemorrhage
		Reversible: moclobemide	Reversible and selective inhibition of MAO		
Adjunctive	SARI	Trazodone	Powerfully blocks serotonin-2 receptors with less potent inhibition of 5-HT reuptake	Histamine H_1 receptor blockade	Sedation, cognitive impairment
				α_1-Adrenoceptor blockade	Lowers blood pressure, postural hypotension Other: priapism (prolonged erections)
		Nefazodone		Histamine H_1 receptor blockade	Sedating, however less so than Trazodone

[TCA = tricyclic antidepressant, MAOI = monoamine oxidase inhibitor, MAO = monoamine oxidase, SSRI = selective serotonin reuptake inhibitor, NDRI = noradrenaline and dopamine reuptake inhibitor, SNRI = dual serotonin and noradrenaline reuptake inhibitor, SARI = dual 5HT-2 receptor antagonist/5-HT reuptake inhibitor, NASSA = noradrenaline and serotonin-specific antidepressant, NARI = noradrenergic reuptake inhibitor.]

(G. S. Malhi et al., 2015, E. Penn and D. K. Tracy, 2012, H. P. Gelder M., Cowen P. , 2006).

1.4 Sirtuins, neuroinflammation and neurodegeneration

Sirtuins are a unique class of nicotinamide adenine dinucleotide (NAD^+)-dependent deacetylases. The sirtuin family consists of SIRT1, SIRT2, SIRT3, SIRT4, SIRT5, SIRT6 and SIRT7 proteins that differ in subcellular localization, enzymatic activities, physiological functions and pathological roles. Each member of the sirtuin family also plays critical roles in chromatin silencing, genome stabilizing, longevity, aging and metabolic rate (L. Guarente, 2000). Sirtuins accomplish their primary enzymatic activities through NAD^+-nicotinamide exchange reaction in which lysines on histones are catalysed through deacetylation (J. Landry et al., 2000, Y. Jiang et al., 2017). A summary of SIRT1-7's pathological roles in neurodegeneration is shown in **Table 1.2**.

SIRT1 is involved in different physiological or pathological activities including cell differentiation, cell development, apoptosis, autophagy, circadian rhythm and cancer (M. M. Bellet et al., 2016, J. Gao et al., 2016, Y. L. Wang et al., 2016, I. Ben Salem et al., 2017, J. Heo et al., 2017, N. S. X. Ren et al., 2017, Q. Wang et al., 2017, Y. L. Cai et al., 2016). SIRT1 also exerts neuroprotective effects in aging, oxidative stress, neuronal survival, neurogenesis and neuroinflammation (A. F. Paraiso et al., 2013). Aging is the main risk factor for neurodegenerative diseases (Y. Hou et al., 2019). Additionally, animal studies have shown that aged mice show more severe sickness behaviour after LPS administration which indicates that aging is associated with increased activation of microglia or the innate immune system of the CNS (R. Dantzer et al., 2008). Numerous studies have shown that SIRT1 have anti-aging potential, such as inhibiting cell senescence, genomic instability and mitochondrial dysfunction which are hallmarks of aging (Y. Hou et al., 2019, W. Grabowska et al., 2017). The other factors are also important factors for the onset and the development of depression-related conditions as discussed above. In addition, SIRT2 is also considered to play a vital role in diverse pathophysiological processes of neurodegeneration. SIRT2 can directly deacetylases FOXO transcription factors which also participate in numerous aging-related cellular activities including DNA repair, oxidative stress and autophagy (G. Donmez and T. F. Outeiro, 2013). FOXO transcription factors are considered to promote life-span as sensors of insulin/insulin-like growth factor-1 (IGF-1) signalling pathway, which plays an important role in aging and longevity (R. Martins et al., 2016). This indicates the necessity and advantages of investigating the need for SIRT1 and SIRT2 intervention therapy for depression.

Table 1.2 Summary of SIRT1-7's pathological roles in neurodegeneration.

	Subcellular Localization	Tissue Distribution	Disease Involvement and Molecular Mechanisms
SIRT1	Nucleus Euchromatin (S. Michan and D. Sinclair, 2007)	Liver, pancreas, heart, muscle, adipose tissue, and brain (especially prefrontal cortex, hippocampus, basal ganglia, and metabolic centers) (R. Nogueiras et al., 2012)	SIRT1 presents protective effects in neurodegeneration through multiple mechanisms including lowering amyloid β (Aβ) accumulation by reducing its precursor protein and enhancing α-secretase activity. SIRT1 deficiency is also associated with the aggregation of acetylated tau. (S. W. Min et al., 2013) SIRT1 has also been indicated to deacetylate autophagy-related components to reduce α-synuclein aggregates (S. W. Min et al., 2013, B. L. Tang, 2017). However, the overall mechanism of SIRT1 in PD is not clear.
SIRT2	Cytoplasm Shift to the nucleus upon stress and mitosis (S. Michan and D. Sinclair, 2007)	Nervous tissue (particularly in the myelin sheaths, pre-myelinating cells, and oligodendrocytes), adipose tissue, muscle, heart, and lung (B. Shoba et al., 2009)	SIRT2 inhibition was found to attenuate the α-synuclein toxicity in *in vivo* or *in vitro* models of PD via stimulating the benign aggregation of α-synuclein toward acetylated microtubule (T. F. Outeiro et al., 2007). SIRT2 is also considered to influence neuronal cholesterol biosynthesis in *in vivo* HD models (G. Donmez and T. F. Outeiro, 2013).
SIRT3	Mitochondria (S. Michan and D. Sinclair, 2007)	Kidney, brain, heart, liver, testes, lung, ovary, spleen, and thymus (R. Nogueiras et al., 2012)	SIRT3, 4, 5 are associated with mitochondrial function, energy metabolism, and oxidative stress (L. Gan and L. Mucke, 2008). The mechanism of them in neurodegeneration needs further investigation.
SIRT4	Mitochondria (S. Michan and D. Sinclair, 2007)	Heart, brain, kidney, liver, and pancreas (B. Shoba et al., 2009)	
SIRT5	Mitochondria (S. Michan and D. Sinclair, 2007)	Expressed in a variety of tissue (Y. Du et al., 2018)	
SIRT6	Nucleus Heterochromatin (S. Michan and D. Sinclair, 2007)	Widely expressed in human tissues (E. Michishita et al., 2005)	SIRT6 may contribute to DNA repair in aging (H. Jesko et al., 2017).
SIRT7	Nucleolus (S. Michan and D. Sinclair, 2007)	Widely expressed in human tissues (E. Michishita et al., 2005)	Limited information

Taken from (Y. Zhang et al., 2020)

1.4.1 Polymorphisms of SIRT1 and SIRT2 gene in the population

Genetic polymorphism is referred to as the occurrence of at least two alleles at a particular locus in a population that occur with a frequency of more than 1% (Ann K. Daly, 2010). If the gene sequence differs by a single base, it is known as single nucleotide polymorphisms (SNPs) (G. Shaw, 2013). This genetic basis can affect individual response to drug treatment, which is known as pharmacogenetics and has been applied in cutting-edge drug discovery. The role of sirtuin polymorphisms has been investigated in many diseases, such as lung cancer, breast cancer and neurodegenerative diseases (Y. Lv et al., 2017, S. M. Rizk et al., 2016, M. Xia et al., 2014, S. Porcelli et al., 2013, L. Polito et al., 2013). There also have been several studies showing that SIRT1 and SIRT2 polymorphisms might be associated with the pathophysiology of depression.

It has been reported that SIRT1 expression reduction in peripheral blood was found in juvenile mice with isolation stress-induced depression, which indicates the involvement of SIRT1 in the development of depression (L. Lo Iacono et al., 2015). A genome-wide association study (GWAS) with more than 9000 cases conducted on Chinese women with major depressive disorder (MDD) identified that SNP rs12415800, a gene locus near SIRT1 on chromosome 10, might contribute to the risk of MDD (C. Na et al., 2015). Another GWAS study carried on the Chinese Han population has investigated the subsequent effect of the risk allele rs12415800 (W. Liu et al., 2019). It has been found that rs12415800 is associated with the reduction of cerebellar grey matter volume and lower brain SIRT1 mRNA expression (W. Liu et al., 2019). This SNP along with another SNP, rs4746720, were both found to have a significant association with suicide in Japanese women (778 suicide completers and 760 controls) (T. Hirata et al., 2019). In addition, a case-control study of SIRT1 SNPs and major depressive disorder patients (455 MDD patients and 766 controls) in the Japanese population has also suggested a significant association between SIRT1 rs10997875 polymorphism and depression (T. Kishi et al., 2010). However, further study is necessary for the investigation of this SNP's effect on the biological function of SIRT1. SIRT1 SNP rs12778366 has also been reported to be associated with age-related macular degeneration in the Chinese Han population (Z. Chen et al., 2015). It was also shown that homozygotes of the minor allele of SIRT1 had a higher risk of developing age-related macular degeneration (Z. Chen et al., 2015).

SIRT2 gene rs10410544 polymorphism has also been reported to associate with depressive symptoms in Alzheimer's disease in two independent European populations (S. Porcelli et al., 2013). It was also indicated that SIRT2 T/T genotype might exert protection against depression (S. Porcelli et al., 2013). However, two other studies found different results in rs10410544 and Alzheimer's disease. One study on the Caucasian population showed the rs10410544 T allele might have the potential to increase the risk of Alzheimer's disease (L. Polito et al., 2013). Another study on the Chinese Han population reported rs10415044 C/T genotype was related to late-onset Alzheimer's disease (M. Xia et al., 2014). Based on the limited evidence above, the variation of genotype in SIRT SNP might exert different subsequent SIRT functions and impacts on diseases.

1.4.2 Findings of effects of SIRT1 and SIRT2 modulators in neuroinflammation, neurodegeneration, and depression

Resveratrol

Resveratrol has long been regarded as a natural SIRT1 activator. Despite that, resveratrol is often considered to present pleiotropic effects (C. K. Cheng et al., 2019). However, the fact that evidence has shown the linkage between resveratrol and SIRT1 and the allosteric mechanism involved in the structure-activity relationship should not be neglected (D. Cao et al., 2015).

In the neuroinflammation area, it has been found that resveratrol can suppress the inflammation induced by LPS in microglial BV-2 cells and inhibit caspase-3-dependent apoptosis in neuronal PC12 cells via improving SIRT1 expression and the deacetylation of tumor suppressor p53 (J. Ye et al., 2013). In microglial N9 cells. matrix metalloproteinase-9 (MMP-9), IL-1β and IL-6 can also be attenuated by resveratrol (L. Li et al., 2015). Other studies also reported that resveratrol can inhibit MMP-2 and MMP-9 activities and the production of a range of cytokines (A. K. Pandey et al., 2015, R. L. Frozza et al., 2013). MMPs participate in disturbing the integrity of the BBB which allows inflammatory mediators and immune cells from the periphery to penetrate and influx into the brain parenchyma (G. A. Rosenberg, 2002, D. Wong et al., 2004). A clinical study in patients with Alzheimer's disease also found that 52-week resveratrol treatment MMP9 level in cerebrospinal fluid was decreased and the disease aggravation was attenuated (C. Moussa et al., 2017).

Moreover, in Alzheimer's disease field, resveratrol has been shown to promote cellular survival, suppress inflammation and toxicity induced by misfolded Aβ aggregation on multiple *in vitro* models including PC12, BV2 cell lines and primary cortical cultures (C. Scuderi et al., 2014, X. Feng et al., 2013, J. Chen et al., 2005). Accumulation of misfolded Aβ protein can cause oxidative stress, synaptic dysfunction and neuron loss in the brain of AD patients (W.-J. Huang et al., 2016). In an *in vivo* study of AD, resveratrol has been shown to improve the cognitive impairment of transgenic mice with the involvement of PGC-1α and tumor suppressor p53 that both participate in mitochondria biogenesis, oxidative response, and apoptosis (D. Kim et al., 2007, D. Porquet et al., 2013, J. R. Chang et al., 2012, G. Sweeney and J. Song, 2016).

In models of Parkinson's disease, resveratrol has been shown to reduce dopaminergic neuron loss and alleviate the decrease of tyrosine hydroxylase and dopamine levels in neurotoxin (MPTP)-induced PD mouse models via autophagy degradation of α-synuclein (Y. J. Guo et al., 2016). Mudo's research also reported resveratrol's protective effects against MPTP in the dopaminergic SN4741 cell line with an increase of PGC-1α and SIRT1 levels (G. Mudo et al., 2012). Resveratrol also attenuated the motor neuronal loss and promoted SIRT1 expression in the spinal cord and extended the lifespan of the SOD1G93A mouse model of amyotrophic lateral sclerosis (ALS) (L. Song et al., 2014). The neuroprotective effect of resveratrol was also reported in Machado-Joseph disease (MJD) mouse models and multiple sclerosis (MS) models (J. Cunha-Santos et al., 2016, K. S. Shindler et al., 2010).

The effect of resveratrol on mood disorder remains controversial. A study conducted on stressed mice indicated resveratrol could prevent anxiety and depression via SIRT1 activation and downstream extracellular signal-regulated kinases (ERK1/2) which has been reported participating in pro-depressive mechanism (N. Abe-Higuchi et al., 2016, G. Borges et al., 2015). Resveratrol also could alleviate depressive-like behaviours in LPS-induced models (L. Liu et al., 2016). Resveratrol also was indicated to induce the anti-anxiety effect and increase the mRNA level of SIRT1 in the striatum on prediabetic mice and stress-mice (B. R. Reddy et al., 2016). However, some studies found that resveratrol could induce depressive-like behaviour in stressed mouse models (H. D. Kim et al., 2016).

Table 1.3 shows the findings of SIRT1 activators in neuroinflammation and neurodegeneration.

EX527, sirtinol

Studies have found that the SIRT1 inhibitor EX527 can inhibit the toxicity of SOD1 in transgenic neuronal cells and increase the survival of transgenic SH-SY5Y cells as a model of ALS (C. Valle et al., 2014). In Huntington's disease model, EX527 was shown to improve voluntary movement and brain pathological impairment in transgenic R6/2 HD mice (M. R. Smith et al., 2014). However, there is also research showing EX527 can exacerbate tauopathy in primary neurons (S. W. Min et al., 2010) The effect of EX527 on depressive models is also uncertain. Kim's results show that EX527 protected stressed mice from depression and anxiety (H. D. Kim et al., 2016). But in Abe-Higuchi's research, EX527 led to mood disorders (N. Abe-Higuchi et al., 2016).

Sirtinol was originally found to manifest an inhibiting effect on SIRT2 in 2001 (C. M. Grozinger et al., 2001). After that, its analogues presenting both SIRT1 and SIRT2 inhibition were synthesized and evaluated (A. Mai et al., 2005). In neurodegeneration, it has been found that sirtinol can reverse the protective effect of resveratrol in 6-OHDA or α-synuclein-stimulated differentiated SK-N-BE cells where sirtinol was administered as a SIRT1 inhibitor (D. Albani et al., 2009). In the mood disorder area, sirtinol has been shown to prevent the disorder of memory function and mood of stress-mediated mouse models through SIRT1, ERK1/2 and downstream Bcl-2 pathway which is associated with apoptosis regulation (C. L. Ferland et al., 2013).

Table 1.4 shows the findings of SIRT1 inhibitors in neuroinflammation and neurodegeneration.

SIRT2 inhibitor

In neuroinflammation, AGK2 as a SIRT2 inhibitor has been found to suppress the activation of microglial BV2 cells under LPS stimulation and decrease the gene expression of inflammatory mediators such as TNF-α and IL-6 (B. Wang et al., 2016). Rat astrocyte activation and its release of pro-inflammatory factors can also be inhibited

by AGK2 (C. Scuderi et al., 2014). However, in the acute neuroinflammation model, AGK2 was reported to compound the injury (F. Yuan et al., 2016b). In neurodegeneration, SIRT2 has been discovered to exacerbate the toxicity of alpha-synuclein which is an important component of Lewy bodies, the characteristic marker of PD, in pathological conditions (R. M. de Oliveira et al., 2017). Additionally, in the primary culture of the midbrain, AGK2 and AK-1 have been found to protect dopaminergic cells from death induced by α-synuclein (T. F. Outeiro et al., 2007). It has also been reported that AK1 improved the acetylation level of tubulin, autophagy vesicular completion and the Aβ accumulation in a differentiated cybrid cell model of SH-SY5Y cells and platelets from sporadic AD subjects (D. F. Silva et al., 2016). AGK2 and AK1 protected the striatal neuron from death induced by mutant Huntingtin inclusion without altering the morphology (R. Luthi-Carter et al., 2010). According to findings described as following, it is interestingly implicated that SIRT1 and SIRT2 can exert the opposite effects on neurodegenerative diseases (S. A. Shah et al., 2017, Q. Wang et al., 2017, R. Luthi-Carter et al., 2010, B. Wang et al., 2016).

Regarding the findings in depression or mood disorder, 33i as a SIRT2 inhibitor has been indicated to have a protective effect on stress mouse models. Erburu's studies showed that 33i modulated excitatory neurotransmitters and prevented mood disorder (M. Erburu et al., 2017) and co-treatment with another deacetylase inhibitor MC158 increased synaptic plasticity and helped to build neuronal adaption in depression models (M. Erburu et al., 2015). The disturbance of synaptic function and the connection between cells is also an early feature of dementia (E. Masliah et al., 2001). The synaptic dysfunction turns out to affect neuroplasticity which plays a crucial role in depression (H. Eyre and B. T. Baune, 2012). The CNS imaging findings show the loss of cellular population in the prefrontal cortex or amygdala is associated with a certain reduction of brain volume in depression and neurogenesis (D. Cotter et al., 2001, I. M. Rosso et al., 2005, Y. I. Sheline et al., 1998). AK1 was also found to exert neuroprotection on frontotemporal dementia mouse models (T. L. Spires-Jones et al., 2012).

Table 1.5 shows evidence of several SIRT2 inhibitors found in research.

Table 1.3 Evidence that SIRT1 activators influence neuroinflammation and neurodegeneration.

Author	Title	Drug	Results	Study type
Moussa, C., et al.(C. Moussa et al., 2017)	Resveratrol regulates neuroinflammation and induces adaptive immunity in Alzheimer's disease	Resveratrol	Resveratrol alleviated MMP9 and Aβ42 level of cerebral spinal fluid and attenuated inflammation level in plasma of mild-moderate AD patients with 52-week oral treatment intake. MMSE scores declines were mitigated. But tau protein level was not altered.	Clinical Trial
Abe-Higuchi, N., et al.(N. Abe-Higuchi et al., 2016)	Hippocampal Sirtuin 1 Signaling Mediates Depression-like Behavior	Resveratrol SRT2104	Resveratrol could prevent BLAB mice from chronic ultra-mild stress-induced depressive-like and anxiety-like behavior. SRT2104 injection into bilateral dentate gyrus was also shown to improve the social interaction of BALB mice after exposure to repeated restraint stress.	*In vivo*
Kumar, R., et al.(R. Kumar et al., 2017)	Design, synthesis of allosteric peptide activator for human SIRT1 and its biological evaluation in cellular model of Alzheimer's disease.	CWR tripeptide	CWR tripeptide protected neurons from Aβ25-35 peptide-induced death in IMR32 human neuroblastoma AD models.	*In vitro*
Kim, H. D., et al.(H. D. Kim et al., 2016)	SIRT1 mediates depression-like behaviors in the nucleus accumbens	Resveratrol	Resveratrol improved depressive-like and anxiety-like behaviors in C57BL/6J mice exposed to chronic social defeat stress.	*In vivo*
Zou, X. D., et al.(X. D. Zou et al., 2016)	NAMPT protects against 6-hydroxydopamine-induced neurotoxicity in PC12 cells through modulating SIRT1 activity.	Resveratrol	Resveratrol increased the viability of PC12 cells as a Parkinson's disease model after 6-OHDA treatment.	*In vitro*
Liu, L., et al.(L. Liu et al., 2016)	Resveratrol counteracts lipopolysaccharide-induced depressive-like behaviors via enhanced hippocampal neurogenesis	Resveratrol	Resveratrol attenuated the depression-like behaviors in LPS-induced mouse models. LPS-triggered microglial activation in the subgranular zone of the dentate gyrus was inhibited by resveratrol treatment. Hippocampal neurogenesis suppression was also prevented by resveratrol. SIRT1 expression was found up-regulated after resveratrol treatment.	*In vivo*
Reddy, B. R., et al.(B. R. Reddy et al., 2016)	Sirtuin 1 and 7 mediate resveratrol-induced recovery from hyper-anxiety in high-fructose-fed prediabetic rats	Resveratrol	Resveratrol protected high-fructose diet-fed rat models from hyper-anxiety through the up-regulation of SIRT1 and SIRT7.	*In vivo*
Guo et al. (Y. J. Guo et al., 2016)	Resveratrol alleviates MPTP-induced motor impairments and pathological changes by autophagic degradation of alpha-synuclein via SIRT1-deacetylated LC3	Resveratrol	The loss of dopaminergic neurons, decrease of tyrosine hydroxylase and dopamine levels were attenuated by resveratrol treatment in 1-methyl-4-phenyl-1, 2, 3, 6-tetrahydropyridine (MPTP)-induced PD mouse models. SIRT1 was suggested to affect autophagy in the degradation of α-synuclein.	*In vivo*
Cunha-Santos, J., et al. (J. Cunha-Santos et al., 2016)	Caloric restriction blocks neuropathology and motor deficits in Machado-Joseph disease mouse models through SIRT1 pathway	Resveratrol	Resveratrol alleviated motor deficits and incoordination presentation of transgenic Machado-Joseph disease mouse models. The mRNA level of SIRT1 was also increased.	*In vivo*

Moorthi, P., et al. (P. Moorthi et al., 2015)	Pathological changes in hippocampal neuronal circuits underlie age-associated neurodegeneration and memory loss: positive clue toward SAD	Resveratrol	Resveratrol was found to decrease apoptosis and increase SIRT1 expression in aged rats. However, the presentation of learning and memory function remained unaltered.	*In vivo*
Li, L., et al. (L. Li et al., 2015)	Overexpression of SIRT1 Induced by Resveratrol and Inhibitor of miR-204 Suppresses Activation and Proliferation of Microglia	Resveratrol	Resveratrol treatment suppressed inflammatory mediators in mouse microglia N9 cells induced by LPS, including MMP-9, iNOS, IL-1β, and IL-6. It was found reversed by knockdown of SIRT1 expression.	*In vitro*
Diaz-Ruiz, C., et al.(C. Diaz-Ruiz et al., 2015)	Reciprocal regulation between sirtuin-1 and angiotensin-II in the substantia nigra: implications for aging and neurodegeneration	Resveratrol	Resveratrol reduced AT1receptors and NADPH activation in the substantia nigra of aged mouse models, which was verified by over-expression of SIRT1. Angiotensin-II receptor I level and NADPH-oxidative activity were reduced in MES 23.5 cells and microglial N9 cells.	*In vivo* *In vitro*
Ferretta, A., et al.(A. Ferretta et al., 2014)	Effect of resveratrol on mitochondrial function: implications in parkin-associated familiar Parkinson's disease	Resveratrol	Primary fibroblast carrying pathogenic mutation PARK2 from PD patients was cultured as an *in vitro* PD model. Resveratrol was found to improve mitochondrial oxidative capacity. SIRT1, 5'AMP-activated kinase (AMPK) and PPARG coactivator 1 alpha (PGC-1α) were indicated to participate in the mechanism.	*In vitro*
Song, L., et al. (L. Song et al., 2014)	Resveratrol ameliorates motor neuron degeneration and improves survival in SOD1(G93A) mouse model of amyotrophic lateral sclerosis	Resveratrol	Resveratrol attenuated motor neuronal loss and promoted SIRT1 expression in the spinal cord and extended lifespan of the $SOD1^{G93A}$ mouse model of ALS. The level of P53 acetylation and oxidative stress were also suppressed.	*In vivo*
Scuderi, C., et al.(C. Scuderi et al., 2014)	Sirtuin modulators control reactive gliosis in an *in vitro* model of Alzheimer's disease	Resveratrol	Resveratrol inhibited the activation and proliferation of primary astrocytes. Aβ-induced astrogliosis was alleviated by resveratrol. The expression of iNOS and COX-2 was also reduced.	*In vitro*
Mancuso R., et al.(R. Mancuso et al., 2014)	Resveratrol improves motoneuron function and extends survival in $SOD1^{G93A}$ ALS mice	Resveratrol	Resveratrol alleviated symptoms and promoted cell viability and lifespan of $SOD1^{G93A}$ ALS mouse models. The function of motoneuron in the spinal cord was improved. The regulation of autophagy and mitochondrial biogenesis were indicated to participate in the mechanism of resveratrol.	*In vivo*
Li, X. M., et al. (X. M. Li et al., 2014)	Resveratrol pretreatment attenuates the isoflurane-induced cognitive impairment through its anti-inflammation and -apoptosis actions in aged mice	Resveratrol	Cognitive impairment induced by isoflurane was alleviated by resveratrol. Inflammatory molecules including IL-1β and TNF-α were also down-regulated.	*In vivo*
Ye, J., et al.(J. Ye et al., 2013)	Protective effect of SIRT1 on the toxicity of microglial-derived factors induced by LPS to PC12 cells via the p53-caspase-3-dependent apoptotic pathway	Resveratrol	Resveratrol reversed the decrease of SIRT1 expression induced by LPS treatment. Resveratrol also protected PC12 cells from apoptosis via enhancing SIRT1 deacetylation of P53.	*In vitro*
Porquet, D., et al. (D. Porquet et al., 2013)	Dietary resveratrol prevents Alzheimer's markers and increases life span in SAMP8	Resveratrol	The lifespan of age-accelerated mouse models was extended. AMPK and SIRT1 were found elevated in the brain samples. Acetylation levels of P53, amyloid accumulation, and phosphorylated tau were reduced.	*In vivo*

Feng, X., et al. (X. Feng et al., 2013)	Resveratrol inhibits beta-amyloid-induced neuronal apoptosis through regulation of SIRT1-ROCK1 signaling pathway	Resveratrol	Resveratrol reduced the apoptosis of PC12 cells induced by $A\beta_{25-35}$ by the up-regulation of SIRT1.	*In vitro*
Mudo, G., et al. (G. Mudo et al., 2012)	Transgenic expression and activation of PGC-1alpha protect dopaminergic neurons in the MPTP mouse model of Parkinson's disease	Resveratrol	Reveratrol protected dopaminergic cells (SN4741) from cytotoxicity induced by MPTP treatment. PGC-1α and SIRT1 expression were also found elevated by resveratrol treatment.	*In vivo* *In vitro*
Khan, R. S., et al. (R. S. Khan et al., 2012)	SIRT1 activating compounds reduce oxidative stress and prevent cell death in neuronal cells	Resveratrol SRTAW04	The combined treatment of resveratrol and SRTAW04 extended cell viability, alleviated reactive oxygen species (ROS) and repressed damage of mitochondrial membrane in the retinal ganglion cell model. This effect is demonstrated SIRT1-dependent.	*In vitro*
Han, S., et al. (S. Han et al., 2012)	Resveratrol upregulated heat shock proteins and extended the survival of G93A-SOD1 mice	Resveratrol	Resveratrol protected transgenic mutant- SOD1 mice from neurodegeneration. However, the gliosis was not altered. The deacetylation of heat shock factor 1(HSF1) and the level of Hsp were enhanced.	*In vivo*
Wang, J., et al. (J. Wang et al., 2011)	Protective effects of resveratrol through the up-regulation of SIRT1 expression in the mutant hSOD1-G93A-bearing motor neuron-like cell culture model of amyotrophic lateral sclerosis.	Resveratrol	The apoptosis induced by mutant SOD1 in ALS cellular models was inhibited via the improvement of mitochondrial function by resveratrol. The protective effect could be suppressed by SIRT1 inhibition.	*In vitro*
Shindler, K. S., et al. (K. S. Shindler et al., 2010)	Oral resveratrol reduces neuronal damage in a model of multiple sclerosis	Resveratrol SRT1720	Resveratrol and SRT170 were able to protect optic neurons from death without decreasing neuroinflammation. The effect was reversed by the SIRT1 inhibitor.	*In vivo*
Markert, C. D., et al. (C. D. Markert et al., 2010)	A single-dose resveratrol treatment in a mouse model of amyotrophic lateral sclerosis	Resveratrol	Resveratrol could not expand the viability of ALS mouse models or exert a protective effect via regulating P53 acetylation.	*In vivo*
Albani, D., et al.(D. Albani et al., 2009)	The SIRT1 activator resveratrol protects SK-N-BE cells from oxidative stress and against toxicity caused by alpha-synuclein or amyloid-beta (1-42) peptide	Resveratrol	The anti-oxidative protection effect of resveratrol on SK-N-BE cells was blocked by SIRT1 inhibitor sirtinol. Resveratrol also prevented the toxicity of α-synuclein and amyloid-β in a SIRT1-independent way.	*In vitro*
Kim, D., et al. (D. Kim et al., 2007)	SIRT1 deacetylase protects against neurodegeneration in models for Alzheimer's disease and amyotrophic lateral sclerosis	Resveratrol	Resveratrol protected primary mouse neurons from the toxicity of p25 and mutant SOD1. The deacetylation of PGC-1α was decreased. The deacetylation activity of SIRT1 was verified *in vitro*. Resveratrol also protected P25 transgenic mice from neurodegeneration and cognitive impairment.	*In vitro* *In vivo*
Chen, J., et al. (J. Chen et al., 2005)	SIRT1 protects against microglia-dependent amyloid-beta toxicity through inhibiting NF-κB signalling	Resveratrol	Resveratrol suppressed NF-κB activation induced by amyloid-β and toxicity via SIRT1 activation in microglia.	*In vitro*
Valle, C., et al.(C. Valle et al., 2014)	Tissue-specific deregulation of selected HDACs characterizes ALS progression in mouse models: pharmacological characterization of SIRT1 and SIRT2 pathways	SRT1720	SRT1720 could not protect the transgenic neuronal cells from mutant SOD1 injury and death.	*In vitro*

Xiang, Z. and D. Krainc (Z. Xiang and D. Krainc, 2013)	Pharmacological upregulation of PGC1alpha in oligodendrocytes: implications for Huntington's Disease	SRT1720	SRT1720 promoted the differentiation of oligodendrocytes and the expression of PGC-1α.	*In vitro*

Table 1.4 Evidence that SIRT1 inhibitors influence neuroinflammation and neurodegeneration.

Author	Title	Drug	Results	Study Type
Sussmuth, S. D., et al.(S. D. Sussmuth et al., 2015)	An exploratory double-blind, randomized clinical trial with selisistat, a SIRT1 inhibitor, in patients with Huntington's disease	Selisistat (EX527)	Selisistat treatment was shown safe and tolerant in patients in early Huntington's Disease without adverse effects on cognitive, motor and functional status.	Clinical trial
Smith, M. R., et al.(M. R. Smith et al., 2014)	A potent and selective Sirtuin 1 inhibitor alleviates pathology in multiple animal and cell models of Huntington's disease.	Selisistat (EX527)	Selisistat inhibited the deacetylation activities of Sir2 in a Drosophila HD model and human SIRT1 in HEK293 cells. It also protected PC12 cells and primary rat striatal neurons from death resulted from mutant Huntingtin infection. The voluntary movement of transgenic R6/2 mouse models was improved by selisistat treatment.	*In vivo* *In vitro* (Drosophila, mammalian cells, mice)
Shah, S. A., et al.(S. A. Shah et al., 2017)	Melatonin Stimulates the SIRT1/Nrf2 Signaling Pathway Counteracting Lipopolysaccharide (LPS)-Induced Oxidative Stress to Rescue Postnatal Rat Brain	EX527	EX527 inhibited the neuroprotective effect of melatonin on neuroinflammation, neurodegeneration and oxidative stress in postnatal Sprague-Dawley rat models after LPS treatment.	*In vivo*
Guo et al. (Y. J. Guo et al., 2016)	Resveratrol alleviates MPTP-induced motor impairments and pathological changes by autophagic degradation of alpha-synuclein via SIRT1-deacetylated LC3	EX527	The protective effects of resveratrol on dopaminergic neuron loss, the decrease of tyrosine hydroxylase and dopamine level was reversed by EX527 in MPTP-induced PD mice.	*In vivo*
Diaz-Ruiz, C., et al.(C. Diaz-Ruiz et al., 2015)	Reciprocal regulation between sirtuin-1 and angiotensin-II in the substantia nigra: implications for aging and neurodegeneration	EX527	EX527 blocked the effect that resveratrol inhibited angiotensin-II receptor I and NADPH-oxidative activity in primary mesencephalic culture, N9 microglia, and MES 23.5 dopaminergic cells.	*In vitro*
Kim, H. D., et al.(H. D. Kim et al., 2016)	SIRT1 Mediates Depression-Like Behaviors in the Nucleus Accumbens	EX527	EX527 attenuated depression-like and anxiety-like behaviors in mice after chronic social defeat stress. EX527 also protected stress-naïve mice from acute stress.	*In vivo*
Valle, C., et al.(C. Valle et al., 2014)	Tissue-specific deregulation of selected HDACs characterizes ALS progression in mouse models: pharmacological characterization of SIRT1 and SIRT2 pathways	EX527 Sirtinol	EX527 protected the transgenic neuronal SH-SY5Y cells from mutant SOD1 toxicity and increased the viability of neurons in a SIRT1-independent way. Sirtinol showed no protective effect on differentiated SH-SY5Y cells.	*In vitro*
Min, S. W., et al. (S. W. Min et al., 2010)	Acetylation of tau inhibits its degradation and contributes to tauopathy.	EX527	EX527 increased the acetylation of tau, which directly resulted in tau accumulation and inhibition of polyubiquitination of tau in primary neurons and transgenic HEK293T cells.	*In vitro*

Liu, S. Y., et al. (S. Y. Liu et al., 2017)	Hydrogen sulfide inhibits chronic unpredictable mild stress-induced depressive-like behavior by upregulation of Sirt-1: involvement in suppression of hippocampal endoplasmic reticulum stress	Sirtinol	Sirtinol reversed the antidepressant-like effect of H_2S on chronic unpredictable mild stress-induced mouse models through SIRT1 pathway.	*In vivo*
Abe-Higuchi, N., et al.(N. Abe-Higuchi et al., 2016)	Hippocampal Sirtuin 1 Signaling Mediates Depression-like Behavior	EX527 Sirtinol	Sirtinol and EX527 bilateral injection treatment in dentate gyrus could induce depression-like behaviors in BALB mice.	*In vivo*
Ferland, C. L., et al. (C. L. Ferland et al., 2013)	Sirtuin activity in dentate gyrus contributes to chronic stress-induced behavior and extracellular signal-regulated protein kinases 1 and 2 cascade changes in the hippocampus.	Sirtinol	Sirtinol infusion reversed the chronic variable stress-induced dysfunction of memory and anhedonia of stressed rat models. The extracellular signal-regulated protein kinases1 and 2 activities and Bcl-2 expression were increased by SIRT1 inhibition in the hippocampus.	*In vivo*
Ferland, C. L. and L. A. Schrader (C. L. Ferland and L. A. Schrader, 2011)	Regulation of histone acetylation in the hippocampus of chronically stressed rats: a potential role of sirtuins	Sirtinol	Sirtinol increased histone acetylation activity in chronic variable stress-induced rats.	*In vivo*
Albani, D., et al.(D. Albani et al., 2009)	The SIRT1 activator resveratrol protects SK-N-BE cells from oxidative stress and against toxicity caused by alpha-synuclein or amyloid-beta (1-42) peptide	Sirtinol	The anti-oxidative protection effect of resveratrol on SK-N-BE cells was blocked by sirtinol.	*In vitro*
Ye, J., et al.(J. Ye et al., 2013)	Protective effect of SIRT1 on the toxicity of microglial-derived factors induced by LPS to PC12 cells via the p53-caspase-3-dependent apoptotic pathway	Sirtinol Nicotinamide	Sirtinol enhanced the inhibition of SIRT1 expression induced by LPS treatment in PC12 cells. Nicotinamide treatment increased the apoptosis of PC12 cells.	*In vitro*
Green, K. N., et al.(K. N. Green et al., 2008)	Nicotinamide restores cognition in Alzheimer's disease transgenic mice via a mechanism involving sirtuin inhibition and selective reduction of Thr231-phosphotau	Nicotinamide	Nicotinamide protected transgenic 3xTg-AD mice from cognitive impairment. Phosphorylated Tau protein Th231 was decreased.	*In vivo*

Table 1.5 Evidence that SIRT2 inhibitors influence neuroinflammation and neurodegeneration.

Author	Title	Drug	Results	Study Type
Guan, Q., et al.(Q. Guan et al., 2016)	Aging-related 1-methyl-4-phenyl-1,2,3,6-tetrahydropyridine-induced neurochemical and behavioral deficits and redox dysfunction: improvement by AK-7	AK-7	The acetylation of α-tubulin was increased by AK-7 application in MPTP-induced aging mouse models. AK-7 also attenuated behavioral abnormality and dopamine depletion.	*In vivo*
Chen, X., et al.(X. Chen et al., 2015)	The sirtuin-2 inhibitor AK7 is neuroprotective in models of Parkinson's disease but not amyotrophic lateral sclerosis and cerebral ischemia	AK-7	AK-7 diminished α-synuclein cytotoxicity in human fetal dopaminergic neuron-like LUHMES cells in a dose-dependent way. It also prevented dopamine depletion and dopaminergic cell death in mice after MPTP injection. However, it did not affect amyotrophic lateral sclerosis and cerebral ischemia mouse models.	*In vitro* *In vivo*
Wang, X., et al. (X. Wang et al., 2015)	Aging-related rotenone-induced neurochemical and behavioral deficits: role of SIRT2 and redox imbalance, and neuroprotection by AK-7	AK-7	AK-7 attenuated the redox reaction and behavior abnormality and dopamine decreasing in rotenone-induced PD mouse models. The superoxide flux was reduced in primary neuron/glial cell models treated with AK-7.	*In vivo* *In vitro*
Chopra, V., et al.(V. Chopra et al., 2012)	The sirtuin 2 inhibitor AK-7 is neuroprotective in Huntington's disease mouse models.	AK-7	AK-7 promoted behavioral performance and motor function of HD (R6/2) mice and ameliorated striatal and neuronal atrophy. The level of polyglutamine aggregation was decreased the brain of R6/2 mice.	*In vivo*
Erburu, M., et al.(M. Erburu et al., 2017)	SIRT2 inhibition modulate glutamate and serotonin systems in the prefrontal cortex and induces antidepressant-like action	33i	Chronic 33i was applied in chronic mild stress mouse models (C57B16). GluN2A, GluN2B, and serotonin were improved in the prefrontal cortex. The anhedonia and decreasing social interaction were reversed.	*In vivo*
Erburu, M., et al.(M. Erburu et al., 2015)	Chronic stress and antidepressant induced changes in Hdac5 and Sirt2 affect synaptic plasticity	33i	Co-treatment with Class II histone deacetylase inhibitor MC1568 and 33i was a benefit to synaptic plasticity in the prefrontal cortex. Upregulation of them helped to build neuronal adaption under chronic stress and depression.	*In vivo*
Wang, B., et al.(B. Wang et al., 2016)	SIRT2 Plays Significant Roles in Lipopolysaccharides-Induced Neuroinflammation and Brain Injury in Mice.	AGK2	AGK2 inhibited the microglial activation induced by LPS and reduced the mRNA levels of TNF-α and IL-6. It also prevented nuclear translocation of NF-κB and the rising activation of Caspase 3 and Bax protein.	*In vivo*
Scuderi, C., et al.(C. Scuderi et al., 2014)	Sirtuin modulators control reactive gliosis in an *in vitro* model of Alzheimer's disease	AGK2	Astrocytes were treated with Aβ 1-42. AGK2 improved the cell viability but generated cytotoxicity at a concentration of 35μM on normal astrocytes and suppressed proliferation of astrocytes. Aβ-induced astrogliosis was alleviated by AGK2. The expression of iNOS and COX-2 were reduced.	*In vitro*

Outeiro, T. F., et al.(T. F. Outeiro et al., 2007)	Sirtuin 2 inhibitors rescue α-synuclein-mediated toxicity in models of Parkinson's disease	AGK2	AGK2 protected HeLa cells applied from the toxicity of α-synuclein. AGK2 protected dopaminergic cells from α-Syn-induced death in primary midbrain cultures. In a Drosophila PD model, AGK2 showed a significant protective effect on dorsomedial neurons without changing α-synuclein levels.	*In vitro* *In vivo*
Luthi-Carter, R., et al.(R. Luthi-Carter et al., 2010)	SIRT2 inhibition achieves neuroprotection by decreasing sterol biosynthesis	AGK2 AK1	AGK2 and AK1 generated neuroprotection in HD fly models. AGK2 and AK1 protected the striatal neurons from mutant Huntingtin inclusion, but the morphology was not altered. They decreased cholesterol and cholesteryl esters synthesis via inhibition of SIRT2.	*In vivo* *Drosophila* *In vitro*
Silva, D. F., et al.(D. F. Silva et al., 2016)	Mitochondrial Metabolism Power SIRT2-Dependent Deficient Traffic Causing Alzheimer's-Disease Related Pathology.	AK1	AK1 improved the acetylation level of tubulin, the autophagy vesicles and the Aβ aggregation in sporadic AD cybrid cells, which might improve microtubule stabilization.	*In vitro*
Spires-Jones, T. L., et al.(T. L. Spires-Jones et al., 2012)	Inhibition of Sirtuin 2 with Sulfobenzoic Acid Derivative AK1 is Non-Toxic and Potentially Neuroprotective in a Mouse Model of Frontotemporal Dementia	AK1	AK1 was injected into the hippocampus of rTg4510 mouse models expressing mutant tau protein. It was non-toxic in the mouse brain and showed a neuroprotective effect, but it did not affect neurofibrillary.	*In vivo*
Valle, C., et al.(C. Valle et al., 2014)	Tissue-specific deregulation of selected HDACs characterizes ALS progression in mouse models: pharmacological characterization of SIRT1 and SIRT2 pathways	AGK2	AGK2 failed to protect the transgenic neuronal cells from mutant SOD1 toxicity and death.	*In vitro*
Di Fruscia, P., et al.(P. Di Fruscia et al., 2015)	The discovery of a highly selective 5,6,7,8-tetrahydrobenzo[4,5]thieno[2,3-d]pyrimidin-4(3H)-one SIRT2 inhibitor that is neuroprotective in an *in vitro* Parkinson's disease model	ICL-SIRT078	ICL-SIRTO78 showed a protective effect of cellular survival and cytotoxicity on lactacystin-induced PD models in N27 cells.	*In vitro*

1.4.3 Targets of SIRT1 and SIRT2

1.4.3.1 Autophagy

Autophagy is a general term for the degradation of cytoplasmic components within lysosomes (N. Mizushima, 2007). Autophagy participates in the degradation of damaged organelles such as mitochondria, endoplasmic reticulum, and peroxisomes, as well as eliminating intracellular pathogens and recycling of cellular metabolites (D. Glick et al., 2010). This process can be initiated in response to a pathogenic insult to enclose the infection and promote the clearance of the pathogen (C. S. Shi et al., 2012).

The correlation between SIRT1 and autophagy has been implied by numerous findings which can be generally classified into three types (F. Ng and B. L. Tang, 2013). The first type of evidence is that SIRT1 and autophagy activities are simultaneously activated in some experiments. For instance, inhibition of autophagy by 3-methyladenine (3-MA) suppresses SIRT1 expression in some *in vitro* studies (Q. Cui et al., 2006); resveratrol induces autophagy which acts in a SIRT1-dependent manner (E. Morselli et al., 2011, R. Zeng et al., 2011, R. Zeng et al., 2012). Another connection is that SIRT1 expression and autophagy can be induced by implementing caloric restriction (CR) and interact with each other (S. Kume et al., 2010). The more direct evidence is that overexpression and silencing of SIRT1 levels could exert or inhibit the effect of autophagy (J.-K. Jeong et al., 2013, R. R. Alcendor et al., 2007). It is considered that SIRT1 can influence autophagy via its deacetylation of FOXO family members (F. Ng and B. L. Tang, 2013). SIRT2 is also implicated to play a role in modulation of autophagy through the FOXO1 pathway (F. Ng and B. L. Tang, 2013).

Autophagy has been identified as a major regulator of inflammasomes. In some inflammatory conditions where autophagy is restricted or diminished, there is over-activation of inflammation and inflammasomes (B. Levine et al., 2011, V. Deretic et al., 2013). Similarly, inflammasome activation is able to induce autophagy which protects tissues and cells from excessive inflammation and subsequent injury (K. Cadwell, 2016). Autophagic removal of intracellular DAMPs, inflammasome components or cytokines can negatively regulate inflammasome activation and inhibit the following maturation and release of cytokines (S. Qian et al., 2017). Manipulation of autophagy pathways leads to caspase-1 activation and cytokine production deficiency in the macrophage (T. Saitoh et al., 2008).

1.4.3.2 NF-κB

SIRT1 inhibits NF-κB signal pathway directly through the deacetylation of the p65 subunit of the NF-κB complex. SIRT1 stimulates oxidative energy production via the activation of AMPK, PPARα and PGC-1α, which will inhibit NF-κB signaling and suppress inflammation simultaneously. NF-κB, in turn, can down-regulate SIRT1 activities through the regulation of the expression of miR-34a, IFN-γ, and the production of reactive oxygen species. The inhibition of SIRT1 can disrupt oxidative energy metabolism and stimulates the NF-κB-induced inflammatory responses present in many chronic metabolic and age-related diseases (A. Kauppinen et al., 2013).

NF-κB is also a target of nucleus SIRT2 but not cytoplasm SIRT2. AGK2, an inhibitor of SIRT2, suppresses the microglial activation induced by LPS and reduces the mRNA levels of TNF-α and IL-6. SIRT2 inhibitors block the nuclear translocation of NF-κB and the following activation of Caspase 3 (B. Wang et al., 2016). On the other hand, SIRT2 deacetylates the NF-κB p65 unit and inhibits NF-κB-dependent transcription in microglia (T. F. Pais et al., 2013). Collectively, SIRT2 might be required for NF-κB-mediated neuroinflammation, which indicates an opposite effect on the NF-κB pathway.

NF-κB is known as a protein complex family that modulates the transcription of diverse genes, cytokine production and cell survival. There are five members in the NF-κB family: p65 (RelA), RelB, c-Rel, p50/p105 (NF-κB1), and p52/p100 (NF-κB2) (L. F. Chen and W. C. Greene, 2004). NF-κB plays a crucial role in regulating the immune response to inflammation in the nervous system. Numerous chemokines, cytokines, enzymes, other molecules or factors in the inflammatory process are regulated by NF-κB. The classic NF-κB pathways can be activated by pro-inflammatory molecules such as IL-1, LPS and TNF. The activated NF-κB (p65) translocates from the cytoplasm into the nucleus where it binds to specific sequences of DNA called response elements (RE) and activates target gene transcription. At the molecular level, neuroinflammation is modulated by diverse molecules and factors, including chemokines, cytokines, pro-inflammatory enzymes and transcription factor NF- κB. Among these mediators, NF-κB is the central regulator of neuroinflammation (B. B. Aggarwal, 2004, W. J. Lukiw and N. G. Bazan, 1998, K. S. Ahn and B. B. Aggarwal, 2005).

1.6 Knowledge gaps and significance

There is no systematic research investigating and comparing the effects of selective SIRT1 modulators, selective SIRT2 modulators or dual SIRT1/2 modulators on depression models. The studies of depressive-like behaviours in literature applied different triggers and different methods of drug administration.

SIRT1 and SIRT2 modulators both appear to be able to influence the development of neurodegeneration. Whether both SIRT1 and SIRT2 are required for suppressing neuroinflammation activities in depression has not been investigated yet. Similarly, the mechanism of pathways of how SIRT1, 2 modulators affect neuroinflammation is unknown.

Augmentation treatment is required to enhance the therapeutic effect of a current antidepressant. Augmentation with NSAIDs has been studied in clinical trials. However, firm conclusions cannot be drawn on the anti-depressant effects of NSAIDs in depression. Augmentation strategies of SIRT1, 2 modulators need to be designed and investigated.

Despite the advances of current medications and psychotherapy, over 65,000 Australians still make a suicide attempt every year, and 3 million Australians are currently experiencing anxiety or depression. Depression is one of the leading causes of disability and remains difficult-to-treat. Thus exploration of new potential treatment is urgent.

1.6.1 Effect of SIRT1, 2 modulators on depression is unclear

Plenty of studies show that SIRT1 and SIRT2 are involved in the pathophysiology of neuroinflammation, neurodegeneration and depression. However, the results of these studies contradict each other. It has been found that both neuroprotective effects and negative effects of SIRT1 activators, SIRT1 inhibitors, SIRT2 activators and dual SIRT1/2 inhibitors. The anti-degeneration or anti-inflammation effects discovered in each study were investigated via different disease models, including *in vitro* or *in vivo* AD, PD, HD and ALS models. The studies of depressive-like behaviours in animals applied different triggers of depression (stress or LPS) and different methods of drug administration (intracerebral ventricular injection or intraperitoneal injection). In addition, there is no clinical trial related to this field. Therefore, it is difficult to conclude whether SIRT1 and SIRT2 modulators will benefit depression or not. There is no

systematic research investigating and comparing the effects of selective SIRT1 modulators, selective SIRT2 modulators or dual SIRT1/2 modulators on depression models.

1.6.2 Mechanism of the anti-inflammatory action of SIRT1, 2 modulators in depression models is unclear

SIRT1 and SIRT2 modulators both appear to be able to influence the development of neurodegeneration. However, the evidence of the effects of SIRT1, 2 modulators on neuroinflammation is not robust. Resveratrol as a SIRT1 activator has been shown to exert an inhibiting effect on neuroinflammation in *in vitro* models by a research group while the other animal study failed to achieve the same observation result. SIRT2 also was considered to take part in neuroinflammation. But only an *in vivo* study reported that AGK2 as a SIRT2 inhibitor inhibited microglial activation. Therefore, whether both SIRT1 and SIRT2 are required for inhibiting neuroinflammation activities in depression has not been investigated yet. Besides, the mechanism of pathways of how SIRT1, 2 modulators affect neuroinflammation was not further demonstrated. Therefore, the investigation of the mechanism requires designed experiments to be conducted.

1.6.3 Augmentative anti-inflammatory effect of SIRT modulators with current antidepressants is unknown

For those patients who fail to respond to the initial antidepressant therapy, alternative treatment includes switching medication, augmentation or combination treatment. A novel solution for augmentation treatment is required to enhance the therapeutic effect of a current antidepressant. Augmentation with traditional anti-inflammatory agents (NSAIDs) has been studied in some clinical trials. However, firm conclusions cannot be drawn on the anti-depressant effects of NSAIDs in depression. NSAIDs also increase the risk of cardiovascular adverse events and infections. Thus whether SIRT1 and SIRT 2 modulators can be potential medication candidates urgently needs to be investigated.

1.7 Research aims and objectives

To study the effect of SIRT1 and SIRT 2 modulators on *in vitro* model of neuroinflammation and *in vivo* LPS-induced rodent models,

Objective 1: To establish an *in vitro* differentiated model of LPS-induced neuroinflammation and subsequent neurodegeneration

Objective 2: To determine if SIRT1 and SIRT 2 modulators decrease neuroinflammation and subsequent neurodegeneration and mechanism in the *in vitro* model

Objective 3: To determine the effects of SIRT1 and SIRT 2 modulators on LPS-induced anxiety-like and sickness behaviours.

Chapter 2 : Methods development

2.1 Introduction

Establishing a suitable model is crucial for *in vitro* drug evaluation. Methods development optimizes the appropriate conditions of experiments and prevents the final evaluation results of the drugs from being misinterpreted, exaggerated or neglected due to the use of the wrong model. Well-developed methods provide advantages including validity, reliability and reproducibility to the study. Therefore, in this introduction, different experiment conditions and concerns are discussed as follows.

2.1.1 Overview

The overall experimental design of the *in vitro* study is to collect the supernatant from lipopolysaccharide (LPS)-stimulated microglia and transfer it onto neuronal cells. Essentially, this design is a 2D microglia-neuron co-culture model to investigate the effects of inflammatory mediators produced by microglia on neuronal cells. Pre-treatment of microglia with SIRT modulators prior to LPS stimulation will be used to investigate their effects on the subsequent outcome on neuronal cells. To conduct this experiment design, the rat highly aggressively proliferating immortalized (HAPI) cell line was selected as the microglia model. HAPI cell line is derived from microglia-enriched neonatal primary cultures. It expresses microglial markers and is able to well respond to LPS stimulation and phagocytize (R. Timmerman et al., 2018). The SH-SY5Y cell line was selected as the neuronal model, which is attributed to its human derivation and capability of differentiation to mature and neuron-like phenotype (J. Kovalevich and D. Langford, 2013). In this chapter, several optimization processes were conducted to establish a suitable *in vitro* neuroinflammation-neurodegeneration model in order to achieve an accurate evaluation of the pharmacological and biological effects of SIRT drugs.

2.1.2 LPS-induced inflammatory response in microglia

A suitable concentration for LPS treatment on HAPI cells should be optimized to better mimic the neuroinflammation underlying the pathology of the depressive condition in the central nervous system. Microglia are macrophages that reside in the central nervous system as the prime component of its immune system. Thus, they are widely used as an *in vitro* model of neuroinflammation. Microglia can be activated by many stimuli such as cytokines, interferon and toxins. LPS is derived from the outer membrane of Gram-negative bacteria and targets on toll-like receptors 4 (TLR4) (B. Boonen et al., 2018). LPS has been recognized as an important molecule in modeling neuroinflammation-

related disorders, including Alzheimer's disease, Parkinson's disease, Huntington's disease and depression (C. R. A. Batista et al., 2019, J. C. O'Connor et al., 2009). HAPI cell line originates from rat neonatal primary brain cultures and can generate multiple kinds of cytokine and ROS under LPS stimulation (W. Zheng et al., 2012, R. J. Horvath et al., 2008, P. Cheepsunthorn et al., 2001). After LPS combines to and activates toll-like receptor 4, the mitogen-activated protein kinase (MAPK) pathways are initiated and followed by activation of downstream transcription factor NF-κB, which subsequently results in the production of inflammatory mediators, including TNF-α, the IL-1 family, IL-6, the IL-10 family and cyclooxygenase-2 (COX-2) (B. Kaminska et al., 2016, B. L. Fiebich et al., 2018, T. Kawai and S. Akira, 2011, M. Rossol et al., 2011). COX-2 and its secondary product PGE_2 can also be induced by LPS in macrophages (S. H. Lee et al., 1992). There is literature showing that the PGE_2 level is elevated in depression patients (J. Lieb et al., 1983) and COX-2 signaling is involved in depression models (Q. Chen et al., 2017).

As cytokines are the main biomarkers to assess the inflammatory status of microglia in experimental systems, the dynamic time course of LPS-induced response in gene expression and protein level is crucial guidance for successful measurement of these cytokines. According to literature, the production cytokines in primary microglia including TNF-α, IL-1β, IL-10 and PGE_2 have shown an ascending tendency after LPS stimulation and the increasing slope tends to slow down from 20 h post-treatment and stops elevating afterward (S. Lund et al., 2006).

2.1.3 Cell culture condition for SH-SY5Y cell line

The SH-SY5Y cell line has been used as neuroblastoma for cancer-related research and as neuron substitutes for neurology studies. However, the culture conditions for these two applications should not be the same. Even though numerous studies have used culture media containing high glucose (24 mM) to culture SH-SY5Y cells (J. I. Forster et al., 2016, A. J. McFarland et al., 2018), some studies had also reported that a high concentration of glucose can affect the performance of SH-SY5Y cell line, which affects researchers' ability to correctly interpret the published results and apply the knowledge to other research (H. Smerker, 2014). Additionally, the neuroinflammation-neurodegeneration model employed in this study is based on the supernatant transfer between microglia and neurons, where the components in the supernatant produced by cell lines can affect one another. Thus, the fluctuation of the concentration of glucose

during the supernatant transfer can be avoided by culturing both the microglia and neurons with the same level of glucose. Therefore, optimization of the culture condition especially glucose concentration for SH-SY5Y cell culture must be conducted.

2.1.4 Differentiation methods for SH-SY5Y cell line

Another issue to be considered in the experimental design is whether differentiation of SH-SY5Y cells should be conducted. The SH-SY5Y cell line has been used as a model of dopaminergic neurons in neurological studies as it expresses a few dopaminergic makers including dopamine transporter (DAT) and tyrosine hydroxylase (TH) (R. Constantinescu et al., 2007, S. P. Presgraves et al., 2004). SH-SY5Y cell line is human-derived neuroblastoma cells which are subclones of SK-N-SH cells and contain two distinct phenotypes, neuroblastic type (N) or neuronal-like type and substrate-adherent type (S) or epithelial-like type (M. Encinas et al., 2000). The undifferentiated SH-SY5Y cell line still conserves proliferative characteristics of stem cells and cancer cell and tends to grow in clusters where there are clumps of cells in the center and the surrounding cells radiate gradually from the center (J. Kovalevich and D. Langford, 2013). They proliferate aggressively in a certain period of culture and express immature gene markers (J. Kovalevich and D. Langford, 2013). By contrast, differentiated neuroblastoma cells present distinct features in morphology and gene expression. They distribute more evenly without overlapping each other and more in polarized or neuronal-like shape with longer projections (J. Kovalevich and D. Langford, 2013). Fully differentiated SH-SY5Y cells have been reported to express a range of mature neuronal gene markers, including synaptophysin (SYN), ENO2 (enolase 2) or neuron-specific enolase (NSE), and neuronal nuclei (NeuN) (M. M. Shipley et al., 2016). Thus, a differentiation procedure to cease mitosis is necessary to obtain the accuracy of results of experimental assessments.

Within the literature, there is a range of applicable differentiation methodologies for the SH-SY5Y cell line. These methodologies vary in aspects of duration, chemical treatment, media preference and assessment means. Some studies reported that retinoic acid (RA) alone can successfully differentiate the SH-SY5Y cell line (Y. T. Cheung et al., 2009). Retinoic acid is a derivative of vitamin A that exerts morphogenic and teratogenic effects and influences gene expression *in vivo* (J. Rohwedel et al., 1999). *In vitro*, RA can inhibit DNA synthesis and suppress the growth of tumor cells by inducing differentiation and/or apoptosis of S-type cells (G. Melino et al., 1997). However, some

clinical research has shown that RA treatment alone can not fully differentiate neuroblastoma *in vivo* (H. Teppola et al., 2016). However, other agents such as brain-derived neurotrophic factor (BDNF) has also been used to maintain the differentiated status of SH-SY5Y cells (M. M. Shipley et al., 2016). BDNF has been shown to enhance RA-induced differentiation and support the survival of differentiated neurons (H. Teppola et al., 2016).

2.1.5 Application of extracellular matrix gel in cell culture

Two-dimensional neuroinflammation models have been widely used for pharmacological research of the central nervous system, which is either conducted by culturing commercially available neuronal and microglial cell lines or primary cells extracted from mammals. In the majority of *in vitro* studies, each cell line is cultured separately in an isolated 2D environment. The transfer of supernatants containing varieties of molecules secreted by cells can mimic neuron-to-glia interaction to some extent. However, the results of supernatant transfer can only be measured in one direction. In other words, the status of the co-existence of neurons and glia cannot be determined or observed simultaneously. In addition, isolated culture itself can lead to a shift in the morphology, function and gene expression compared to those in the CNS environment (Z. Szepesi et al., 2018). Many physiological or pathological activities rely on the interplay between neurons, astrocytes, and microglia, such as the formation of synaptic circuits and immune modulation (J. A. Stogsdill and C. Eroglu, 2017, Z. Szepesi et al., 2018) Thus, a 3D neuroinflammation model where neurons and glia grow together can mimic neuron-glia interaction more realistically.

Extracellular matrix (ECM) is a mixture with a protein concentration of 8-12 mg/mL, containing laminin as a major component, collagen type IV, heparin sulfate proteoglycan, entactin and other minor components (Sigma-Aldrich, 2018b). Using ECM as a fundamental environment for cell culture can establish a structural framework providing mechanical support for cell attachment. Drug treatments are also able to affect the microglia and neurons in the same condition. The inflammatory mediators secreted by microglia can act on neurons directly, which improves the reliability of the drug assessment results.

The components of ECM and its receptors have been studied for neural proliferation and differentiation for decades (K. R. Long and W. B. Huttner, 2019). The key

components of ECM that have been demonstrated to modulate proliferation are proteoglycans, laminins, and integrins. Proteoglycans along with laminins have been shown to provide structural support and modulate the proliferation of neural progenitors (K. R. Long and W. B. Huttner, 2019). It has also been discovered that laminin contributes to neuron differentiation in chick retina samples and neural tube progenitor from the chick embryo (J. M. Frade et al., 1996). Similar effects were found in mouse and human neural stem cells (J. Drago et al., 1991, W. Ma et al., 2008). Additionally, ECM has long been considered to promote neurite outgrowth (P. C. Letourneau et al., 1992). The integrins are the essential members of ECM receptors and an important marker of early developing human neocortex (R. O. Hynes, 2002, K. R. Long and W. B. Huttner, 2019). It has been shown that integrins help with the formation of neurospheres, cortical progenitor proliferation, cooperating with laminins in promoting the initiation of differentiation network (K. R. Long and W. B. Huttner, 2019).

SH-SY5Y has been long discovered the potential of differentiating to mature neurons under chemical induction. However, the induction of multiple reagents in the differentiation process would also disturb the accuracy of the results obtained from any experiment taken in this type of culture system. Therefore, a cleaner and more realistic model to mimic the microenvironment of the central nervous system is necessary. A study reported the combination of ECM proteins and growth factor modified SH-SY5Y cells morphologically and biochemically (S. Dwane et al., 2013). However, this study obtained this conclusion based on a 2D experimental system, which only reflects the role of ECM proteins in influencing the differentiation of neuroblastoma from an indirect perspective. Another study reported having built up a 3D model for SH-SY5Y cells using bacterial nanocellulose scaffolds as the supportive material with the addition of retinoic acid treatment for 17 days (M. Innala et al., 2014). A collagen-based 3D hydrogel culture study of SH-SY5Y found a significantly less amount of release in intracellular Ca^{2+} in the response to high K^{+} depolarization in 3D culture compared to 2D culture, which indicates the result generated 2D culture system might be exaggerated and misleading (A. Desai et al., 2006). Therefore, in this study, a preliminary study was also conducted to explore several potential conditions for ECM to differentiate SH-SY5Y cells and elucidate the limitations to it in our microglia-neuron co-culture system.

2.2 Aims and Objectives

To optimize the LPS-induced neuroinflammation-neurodegeneration model composed of HAPI and SH-SY5Y cell line,

Objective 1: To measure LPS dose-response on HAPI cells and select a comparable concentration to mimic neuroinflammation in depression.

Objective 2: To determine whether the result of supernatant treatment can be affected by high-glucose cell culture for SH-SY5Y cells.

Objective 3: To determine the morphological and gene expression alterations in SH-SY5Y cells after different differentiation treatments.

Objective 4: To preliminarily observe the 3D morphology of SH-SY5Y cells and the co-culture with HAPI cells in the ECM environment.

2.3 Methods and materials

2.3.1 Cell culture

All operations and experiments which were required to be sterile were performed in Biology Safety Cabinets. Highly Aggressively Proliferating Immortalised (HAPI) cell line (Merck, USA) was used as a model of microglia to observe the inflammatory response. SH-SY5Y cell line (Sigma-Aldrich, USA) was used as a model of neuronal cells.

HAPI cells were grown in ATCC-formulated DMEM (Gibco by Life Technologies, 11885084) which contains low glucose (1 g/L D-Glucose), L-glutamine (584 mg/L), sodium pyruvate (110 mg/L) and phenol red (15 mg/L). For SH-SY5Y cells, two types of ATCC-formulated DMEM were used. One is DMEM (Gibco by Life Technologies, 11885084). The other one is DMEM (Gibco by Life Technologies, 11965092) that contains D-Glucose (4.5 g/L), L-glutamine (584 mg/L), and phenol red (15 mg/L). The media was additionally supplemented with 1% penicillin/streptomycin and 10% fetal bovine serum (FBS). Cells were grown in sterile T-75 cm^2 flasks and cultured in an incubator at 37°C with 5% CO_2 and high humidity. Cells were passaged with various ratios after they reached 80-90% confluence based on cell number needed.

2.3.2 Weaning and adaption of SH-SY5Y cell line to low-glucose media

To adapt the SH-SY5Y cells that are cultured in high-glucose media into low-glucose media, weaning and adapting procedures need to be conducted prior to low-glucose cell

culture based on literature (H. Smerker, 2014). SH-SY5Y cells in 100% DMEM high-glucose media were cultured to reach 80-90% confluence and regarded as passage one. The following ratios of media were used as shown in **Figure 2.1**. SH-SY5Y cells were eventually adapted into low-glucose media after 8 passages.

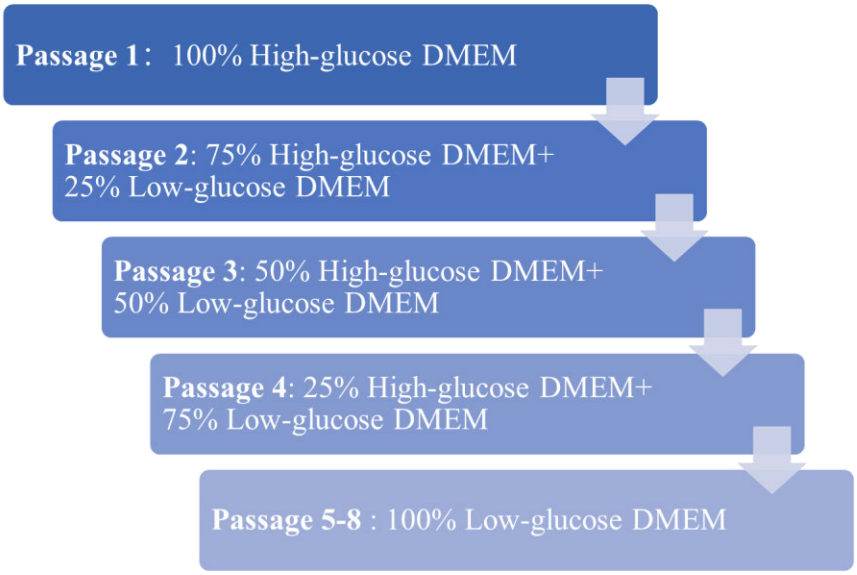

Figure 2.1 Ratios of media in weaning and adaption of the SH-SY5Y cell line.

2.3.3 Extracellular matrix gel

Extracellular matrix (ECM) gel from Engelbreth-Holm-Swarm murine sarcoma (Sigma Aldrich, Australia) was applied in cell culture for the SH-SY5Y cell line. The protein concentration in ECM gel is 8-12 mg/mL, which contains laminin (major), collagen type IV (increases polymerization), heparin sulfate proteoglycan, entactin, other minor components, and 50 mg/L gentamicin sulfate. ECM gel can be stored at -20°C in a solid form for the long term and stored at 2-8°C in a liquid form for up to 72 h. It can gel within 5 min at room temperature and cannot liquefy after polarization. Thus the operation of ECM gel should be done on top of the ice to prevent polarization in the short term. ECM gel was placed at 2-8˚C to thaw out overnight before use. Seeding plates and pipettes were pre-cooled at 2-8˚C in the fridge.

For a 2D cell culture, ECM gel was diluted with serum-free media (2-8˚C) to twofold (1:2) and 500 µL of the diluted gel was added into wells in a 6-well plate. After the gel solidified in an incubator, SH-SY5Y cells were seeded at 1.4 $\times 10^4$ cells/well on the surface of the gel with the addition of serum-containing media on top and cultured for 5 days.

To build a 3D cell culture model, ECM gel was mixed with SH-SY5Y cell suspension (1.4×10^4 cells/well) to 1:4 dilution. Then 50 µL of the mixture was added into wells in a 96-well plate and cultured for 6 days.

Cells were visualized and photographed using an Olympus IX53 microscope.

2.3.4 Treatment preparation

LPS was dissolved in PBS solution at the stock concentration of 1 mg/mL and aliquoted and stored in a -20°C freezer. Before treatments were conducted, the LPS stock solution was diluted from 1:10 to a working solution. BDNF was reconstituted in distilled water to a concentration of 10 µg/mL as stock and stored in a -20°C freezer. RA was dissolved in DMSO at a concentration of 25 mM and stored in a -20°C freezer and protected from light when operation.

2.3.5 Resazurin assay

A resazurin assay was used to determine cell viability. Viable cells are able to reduce resazurin to resorufin, leading to a visible colour change and a difference in fluorescence. Cell lines were plated and seeded on 24-wells or 96-wells plates. The resazurin stock (440 µM) solution was diluted 1:10 with culture media. Then, the supernatant was collected and discarded before conducting resazurin assays. Three wells without cells were set up as a blank. Five hundred µL of the resazurin solution (44 µM) was added to each well and incubated for 4 h at 37°C with 5% CO_2. After this, fluorescence (excitation: 530 nm and emission: 590 nm) was measured and recorded using a Tecan Infinite 200 Pro microplate reader (Tecan, Australia).

HAPI cells were seeded at 10^5 cells/well on 24-well plates and incubated in an incubator for 24 h. Then, for cytotoxicity measurement, cells were treated with LPS (0.0001 µg/mL-10 µg/mL) for 20 h and the supernatant was collected for transfer onto SH-SY5Y cells or ELISA measurement. Then the cell viabilities of HAPI cells were measured by conducting resazurin assay. Each treatment on HAPI cells had 3 replicates. SH-SY5Y cells were seeded on 96-well plates with a cell density of 10^5 cells/mL (100 µL) and incubated for 24 h. Then, the supernatant of SH-SY5Y cells was replaced by the supernatant collected from HAPI cells and incubated for 24 h. Each treatment on SH-SY5Y cells had 6 replicates. Then, resazurin assay was conducted to test the cell viability of them.

2.3.6 Trypan blue dye exclusion assay

Cell concentration was measured by the trypan blue dye exclusion method. Cell numbers were counted through the automatic cell counter or the hemocytometer under an inverted light microscope.

2.3.7 Dichloro-dihydro-fluorescein diacetate (DCFH-DA) assay

DCFH-DA assay was used to determine the oxidative reaction of cells. Reactive oxygen species (ROS) can oxidize DCFH-DA into the highly fluorescent compound dichlorofluorescein (DCF). The DCFH-DA stock solution (50 mM) was diluted into a working solution (25 µM) with culture media. HAPI cells were seeded at 10^5 cells/well on 24-well plates and incubated for 24 h. Then HAPI cells were treated with a series of concentrations of LPS (10-0.0001 µg/mL) for 20 h. Each treatment had 3 replicates. The supernatant above cells was removed and discarded. The media containing DCFH-DA was added to respective wells and incubated for 1 h in an incubator. After that, the solution above cells was replaced with 200 µL of the PBS and washed out. Following this, PBS (100 µL) was added into each well. Fluorescence (excitation: 485 nm and emission: 535 nm) was measured and recorded using a Tecan Infinite 200 Pro microplate reader (Tecan, Australia).

To calculate the final DCF fluorescence value, an adjusted cell number was needed. The following formula was used to calculate the final DCF fluorescence value:

Final DCF fluorescence value = original DCF fluorescence value × 100%/cell viability (%)

2.3.8 Enzyme-linked immunosorbent assays (ELISA)

HAPI cells were seeded at 2.5×10^5 cells/well on 24-well plates and incubated for 24 h. Then, cells were stimulated with LPS (0.1-0.001 µg/mL) treatment for 20 h in an incubator. The supernatant was collected fresh and stored at room temperature before running ELISA using PGE_2 (Cayman), TNF-α and IL-1β using ELISA kits (Biosensis). ELISA kits were taken out from a freezer to equilibrate them to room temperature except for standards. All reservoirs and cylinders were labeled.

2.3.8.1 Reagent preparation

Buffer preparation

ELISA buffer concentration or wash buffer concentration was dissolved and diluted in distilled water. The reconstituted buffer solution was stored at 4°C for up to two months when not conducting assays.

Standards preparation

Firstly the whole vial of the standard was reconstituted with ELISA buffer and sat at ambient temperature for 10 min. This reconstituted standard was stored at 4°C for up to four weeks when not using. After that, the reconstituted standard was serially diluted into several standards with different concentrations in descending order.

Microplate preparation

96-well plates pre-coated by capture antibodies were provided in the ELISA kits and ready to use. A layout was designed for sample dispensing locations. Samples were tested in replicates according to the layout design.

Sample preparation

Cell supernatant was prepared at a minimum of two 1:10 dilutions with ELISA buffer during the temperature equilibrium time.

Standards preparation

The standards were reconstituted with ELISA buffer. Several descending concentrations of standard solutions were prepared and kept at a temperature required by ELISA manuals.

Tracer and antibody solution preparation

Antibodies were diluted with ELISA buffer and mixed thoroughly in 2 h prior to running assays. Tracers were diluted with ELISA buffer and mixed thoroughly in 1 h prior to running assays.

2.3.8.2 Performing assays

Competitive ELISA

ELISA buffer, standards, diluted samples, tracer, and monoclonal antibodies were added into each well according to the designed plate format. After that, the plate was covered with a plastic film provided by ELISA kits and incubated 60 min at room temperature on an orbital shaker.

Ellman's reagent was reconstituted immediately before use. After incubation, the solution in each well was removed and washed with wash buffer for 5 times. Then, Ellman's reagent was added to each well according to the plate format. The plate was covered with plastic film and incubated in dark on an orbital shaker for 90 min.

Sandwich ELISA

Standards, diluted samples, and buffer were added into wells according to the designed plate format. Then, the plate was sealed with parafilm and incubated at 4°C overnight.

After that, the plate was emptied and washed with wash buffer five times. Following that, the biotinylated antibody was added to each well and incubated at room temperature on an orbital shaker for 2-3 h.

After 3 times of rinsing with wash buffer, diluted Avidin-Biotin-Peroxidase complex solution was added to each well. The plate was covered and incubated at room temperature on an orbital shaker for 1 h. Then, five wash cycles were conducted.

TMB color developing reagent was warmed up and to 37°C and added into each well. Then, the plate was incubated at room temperature for 5-20 min in the dark. The TMB stop solution was added to each well to stop the reaction.

2.3.8.3 Reading plates

A Tecan infinite 200 Pro (Tecan, Australia) microplate reader was used to read the absorbance of the plate. A wavelength was set up according to the requirement of different manuals.

2.3.9 Neurite outgrowth staining

Neurite outgrowth staining kit (life technologies, Australia) was used to visualize and quantify cell viability and relative neurite outgrowth of differentiated neurons in the same sample.

2.3.9.1 Material preparation

Hank's balanced salt solution (HBSS) was prepared by dissolving Hank's balanced salts (Sigma Aldrich, Australia) in less than 1 L of distilled water. Then, the pH of the solution was adjusted to 0.1-0.3 pH units by adding the appropriate amount of sodium dihydrogen phosphate. After that, the final volume was supplemented to 1 L.

The 1X working stain solution was prepared by combining 10 µL of cell viability indicator and 10 µL of the cell membrane stain in 10 mL of Hank's balanced salt solution.

2.3.9.2 Live-cell staining

The medium above the cells was removed and the cells were washed with PBS twice. To each well of a 6-well plate was added 1.5 mL of 1X working stain solution, which was then incubated for 10-20 min in the incubator at 37°C. Meanwhile, 1X working solution of background suppression dye was prepared by diluting it with HBSS to 1:100. After the incubation, the staining solution on top of cells was removed and cells were washed with PBS twice. Then 1X background solution (1.5 mL) was added to each well.

2.3.9.3 Fluorescence imaging and analysis

Standard FITC filter was used to visualize the green cell viability indicator and standard Cy3 filter for the red cell membrane stain using an Olympus IX53 microscope. For fluorescence measurement, the cell viability indicator was measured at 495 nm for excitation and 515 nm for emission and recorded using a Tecan Infinite 200 Pro microplate reader (Tecan, Australia). The cell membrane stain was measured at 555 nm for excitation and 565 nm for emission.

Adjusted cell membrane fluorescence value = sample viability fluorescence value ÷ control viability fluorescence value × corresponding cell membrane fluorescence value.

2.3.10 Crystal violet staining

The crystal violet solution (5%) was prepared by dissolving 0.125 g of crystal violet powder in 20 mL of distilled water. Then, 5 mL of methanol was added.

Cells were first washed with cold PBS twice. Then, cells were fixed with cold methanol in an ice-cold condition (freezer) for 10 min. After that, methanol was aspirated and replaced with 50 µL of crystal violet solution. The cells were stained for 20 min and washed with water 3 times. Cells were visualized and photographed using an Olympus IX53 microscope.

2.3.11 Neurite length analysis

Five photos of random different fields were taken from both control and retinoic acid wells using an Olympus IX53 microscope and Cellsens software. Cell counts and neurite length analysis of differentiated SH-SY5Y cells were conducted ImageJ software Fiji version with plugin NeuronJ (M. D. M. Abràmoff, P. J. Ram, S. J, 2004, E. Meijering et al., 2004). Neuron processes were categorized as followed according to literature (J. F. da Rocha et al., 2015).

Pre-neurites: $\geq$ 20 µm, $<$ 35 µm; neurites: $\geq$ 35 µm.

Process/cell (each field) = Total number of processes ÷ total cell number.

Total neurite length average = 15 longest neurite lengths of five fields ÷ 75

2.3.12 Quantitative real-time PCR

The total RNA was extracted using TRIzol^{TM} reagent (Invitrogen). The concentration of RNA was measured using a Nanodrop spectrophotometer (Thermo Fisher Scientific, Australia). cDNA was synthesized using Verso cDNA synthesis kit (Thermo Scientific) and ProFlex PCR System (Life technology). Primer sequences (Sigman Aldrich) for rt-PCR are shown in **Table 2.1**. Rt-PCR was performed using PowerUp^{TM}SYBR^{TM} Green Master Mix kit and QuantStudioTM Real-Time PCR systems (Thermo Fisher Scientific Australia) according to manufactures' guidelines. The thermal cycling conditions were 50°C for 2 min, 95°C for 2 min followed by 40 cycles of 95°C for 1 s and 60°C for 20 s. The dissociation curve conditions were 95°C for 15 s and 60°C for 1 min followed by 95°C for 15 min. The comparative threshold cycles (CT) or $2^{-\Delta\Delta CT}$ method was used to analyze the CT values of samples of interest and control samples. All CT values were normalized against GAPDH gene.

Table 2.1 List of oligonucleotides for gene markers used in rtPCR of neuronal differentiation.

Primer	Sequence
SYP (Human)	Forward: 5'-TCCTCGTCAGCCGAATTCTTT-3'
	Reverse: 5'-CTCGCTACTTGTTCTGCAGGAA-3'
ENO2 (Human)	Forward: 5'-CGGGAACTGCCCCTGTATC-3'
	Reverse: 5'-CATGAGAGCCACCATTGATCA-3'
NeuN (Human)	Forward: 5'-CTACAGCGACAGTTACGGCA-3'

	Reverse: 5’- ATGGTCCGAGAAGGAAACGG-3’
GAPDH (Human)	Forward: 5’-TGCACCACCAACTGCTTAGC-3’
	Reverse: 5’-GGCATGGACTGTGGTCATGAG-3’

2.3.13 Statistical analysis

All data were analyzed by GraphPad Prism 5 and presented as mean ± SD. One-way ANOVA and post hoc tests and t tests were used to determine the significant difference. $P < 0.05$ was considered a significant difference.

2.4 Processes and results for method optimization

2.4.1 Lipopolysaccharide (LPS) induced the cytotoxicity and inflammation in HAPI cells in a dose-dependent way

To select a suitable concentration of LPS to simulate a mild inflammatory environment of depression, the cytotoxic and inflammatory effects of LPS were measured on HAPI cells using different assays. LPS treatment with 10 μg/mL, 1 μg/mL, and 0.1 μg/mL produced significant cytotoxicity on HAPI cells (**Figure 2.2 A**). Concentrations induced obvious cell death were not suitable as microglial models.

Oxidative stress is an also important hallmark of cell injury. DCF fluorescence assay was used to measure the oxidative stress level of HAPI cells induced by LPS (0.0001 μg/mL-10 μg/mL) treatment for 20 h. LPS with concentrations of 10 μg/mL and 1 μg/mL produced significantly greater ROS production than the control group (**Figure 2.2 B**).

Then, one concentration to induce mild inflammation in HAPI cells was estimated. Cells were plated and incubated as mentioned above and treated with a series of concentrations of LPS (0.1 μg/mL-0.001 μg/mL). The supernatant was collected after 20 h and the concentrations of inflammatory mediators were measured by running ELISA. The production of PGE_2 and TNF-α of HAPI cells has been shown a dose-response after LPS stimulation with a series of concentrations (**Figure 2.2 C, D**). According to the result, LPS with a concentration of 0.005 μg/mL induced mild but sufficient level of inflammation.

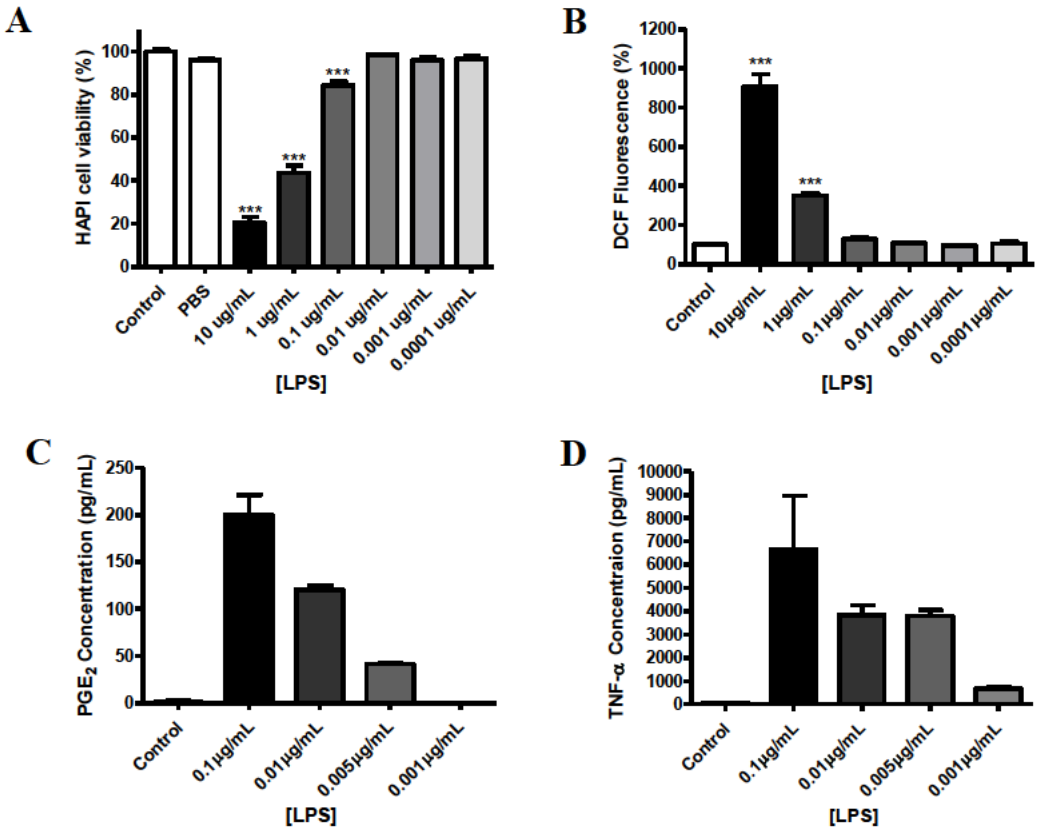

Figure 2.2 LPS induces the cytotoxicity and inflammation in HAPI cells in a dose-dependent way.

A, B, HAPI cells were treated with LPS (0.0001-10 µg/mL) for 20 h, then assessed for cell viability using resazurin assay (A) and assessed for ROS production using DCF-DA assay (B). **C, D,** HAPI cells were treated with LPS (0.001-0.1 µg/mL) for 20 h. The concentration of PGE_2 (C) and TNF-α (D) in the supernatant was measured by running ELISA. One-way ANOVA followed by Turkey's multiple comparison test was applied. Significance levels were shown as $P< 0.001$ (***). Data indicate mean ± SD of three independent experiments.

2.4.2 High-glucose cell culture for SH-SY5Y cells interferes with the microglia-neuron 2D co-culture model of neuroinflammation and neurodegeneration

First, in this microglia-neuron co-culture model, LPS-conditioned supernatant was transferred onto high glucose-cultured SH-SY5Y cells and the cell viability was tested. As shown in **Figure 2.4 A**, SH-SY5Y cultured in high-glucose media showed decreases in cell viabilities after exposure to HAPI supernatant exposed to all concentrations of LPS (10 - 0.0001 µg/mL). Besides, supernatant exposed to high concentrations of LPS, such as 10, 1, 0.1 µg/mL, did not exert strong inhibiting effects on SH-SY5Y cells. Additionally, LPS does not have toxicity on SH-SH5Y cells according to literature (Y. Liu et al., 2020). Thus, we suspected that some factor in HAPI supernatant apart from LPS stimulation had also affected the cell viability after transfer. Then the cell viability of SH-SY5Y cells after exposure to high-glucose media and pure HAPI-conditioned supernatant were compared. It was found that pure HAPI-conditioned supernatant itself decreased the viability of SH-SY5Y cells as shown in **Figure 2.4 B**. This indicates the glucose level in HAPI supernatant after 2 days of culturing had been consumed more, which could shock the high-glucose cultured SH-SY5Y cells when exposed to supernatant transfer. Then, SH-SY5Y cells were weaned and adapted from high-glucose media to low-glucose media, which did not alter the morphology of them as shown in **Figure 2.3**. After this, the same experiment was conducted on SH-SY5Y cells cultured in low-glucose media. It was found that the supernatant collected from HAPI cells exposed to low concentrations of LPS (0.001, 0.0001 µg/mL) did not affect the viability of SH-SY5Y cells cultured in low-glucose media as shown in **Figure 2.4 C**. Then the cell viability of SH-SY5Y cells after exposure to low-glucose media and pure HAPI-conditioned supernatant were also compared. It was found that the low-glucose shock after transfer was no longer exhibited, as shown in **Figure 2.4 D**.

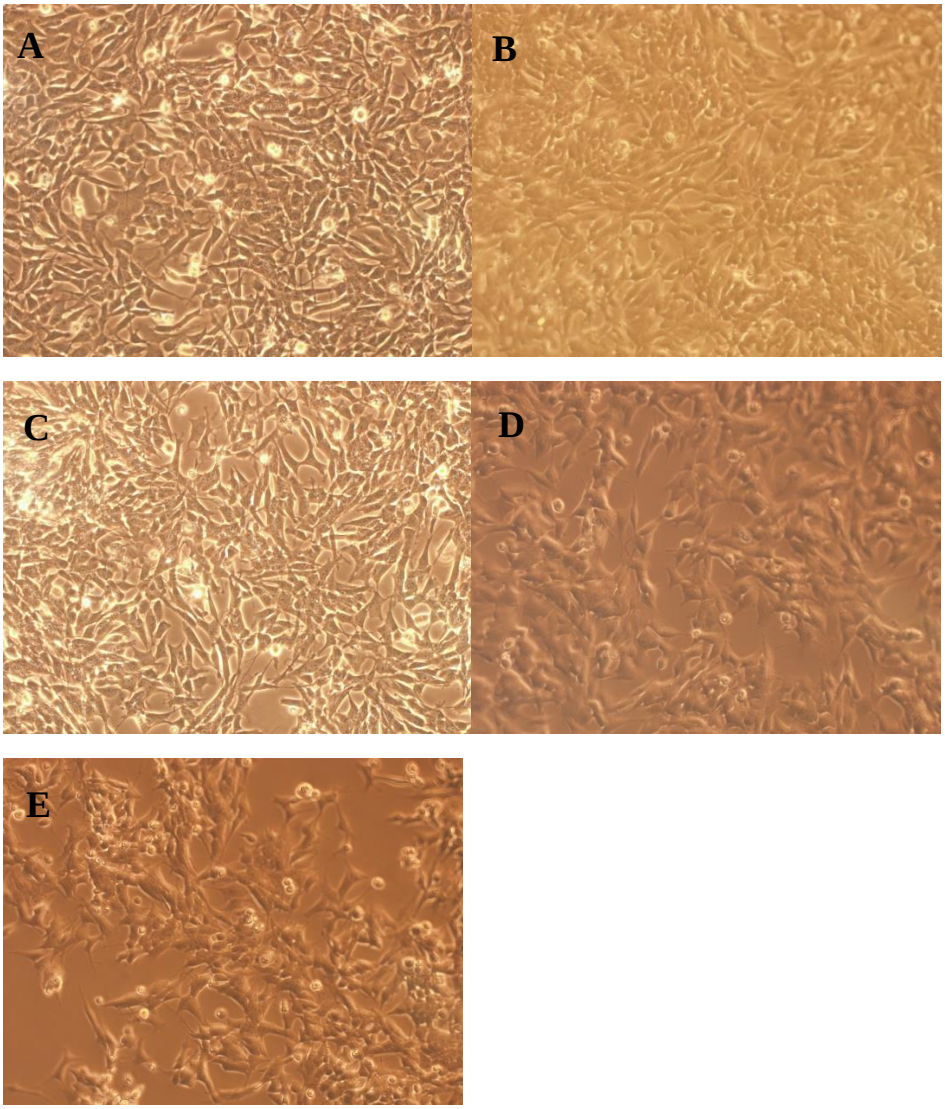

Figure 2.3 Morphology of SH-SY5Y cells in weaning and adapting the process to low-glucose DMEM.

SH-SY5Y cells were cultured in T75 flasks and passaged with a series of ratios of media. A. Passage 1 in 100% high-glucose DMEM + 0% low-glucose DMEM B. Passage 2 in 75% high-glucose DMEM + 25% low-glucose DMEM C. Passage 3 in 50% high-glucose DMEM + 50% low-glucose DMEM D. Passage 4 in 25% high-glucose DMEM + 75% low-glucose DMEM E. Passage 5 in 0% high-glucose DMEM + 100% low-glucose DMEM. The morphology of SH-SY5Ycells during 5 passages shows no alteration. SH-SY5Y cells present neuroblast-like or migratory feature that forms cells in clusters, non-polarised cell bodies and short processes.

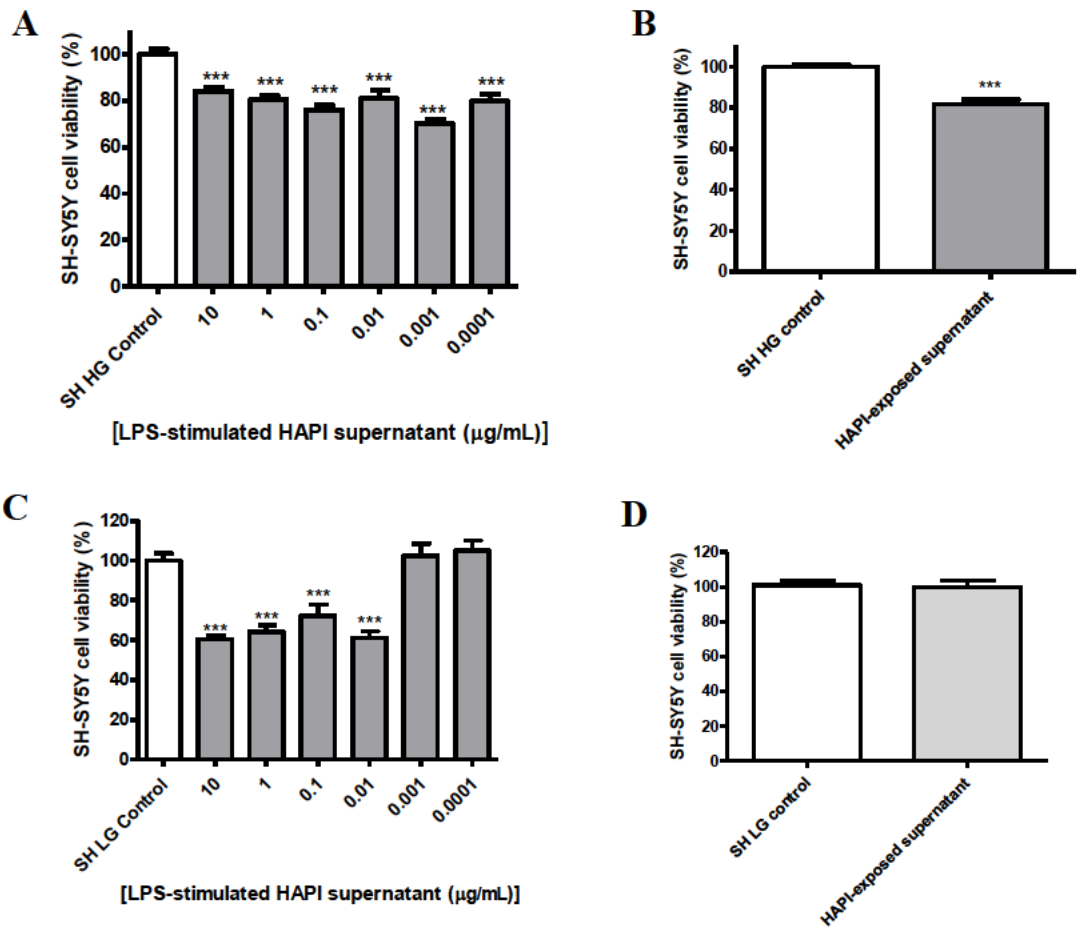

Figure 2.4 High-glucose cell culture primes SH-SY5Y for low-glucose shock during supernatant transfer treatment

Undifferentiated SH-SY5Y cells were treated with supernatant produced by HAPI cells after different treatments. Resazurin assays were conducted to measure the cell viability of SH-SY5Y cells. (A) SH-SY5Y cells cultured with high-glucose media were treated with LPS (10-0.0001 µg/mL)-conditioned HAPI supernatant for 24 h. (B) SH-SY5Y cells cultured with high-glucose media were treated with 2-day cultured HAPI supernatant for 24 h. (C) SH-SY5Y cells cultured with low-glucose media were treated with LPS (10-0.0001 µg/mL)-conditioned HAPI supernatant for 24 h. (D) SH-SY5Y cells cultured with low-glucose media were treated with 2-day cultured HAPI supernatant for 24 h. One-way ANOVA followed by Turkey's multiple comparison test and t tests were applied. Significance levels were shown as and $P < 0.001$ (***). Data indicate mean ± SD of three independent experiments. (SH HG control, SH-SY5Y cells cultured with high-glucose media; SH LG control, SH-SY5Y cells cultured with low-glucose media; HAPI-exposed supernatant, 2-day cultured HAPI supernatant)

2.4.3 Differentiation by retinoic acid with serum starvation suppresses the expression of mature neuronal markers in SH-SY5Y

To optimize the suitable conditions for SH-SY5Y cells to differentiate, several conditions were tested including retinoic acid (RA), serum starvation and addition of BDNF based on varieties of differentiation methodology from literature.

To assess whether RA treatment alone can initiate the differentiation of SH-SY5Y cells as reported in some studies, cells were first seeded on 6-well plates on Day 0 at 1.4×10^4 cells/well (2 mL) to prevent overgrowth throughout the five days. Then on Day 1, Day 3, and Day 5, the supernatant was replaced with new media containing 10 µM of RA with 10% serum (FBS). As we can observe from the morphology, SH-SY5Y cells have overgrown after 5-day culture with RA (10 µM) in 10% FBS media (**Figure 2.5**).

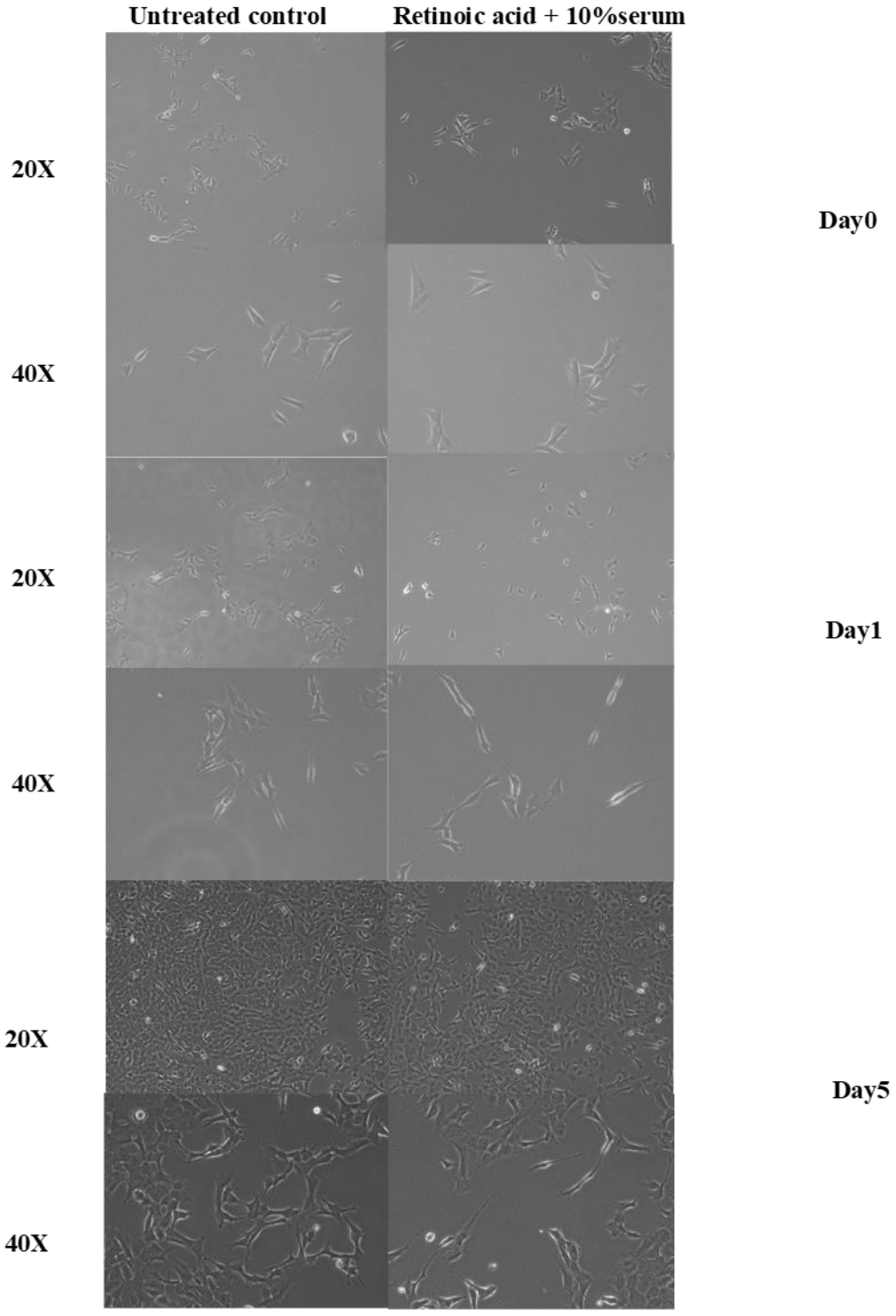

Figure 2.5: RA (10 µM) treatment only in 10%-serum media for 5 days does not cease the proliferation of the SH-SY5Y cell line.

SH-SY5Y cells have aggressively proliferated and migrated along with each other forming clusters after 5 days without showing differences between control and treatment containing RA and 10% serum.

Then, we tested whether 10% serum would inhibit the differentiation process of SH-SY5Y, cells were first seeded on 6-well plates on Day 0 at 1.4×10^4 cells/well (2 mL) to prevent overgrowth throughout five days. Then on Day 1, Day 3, and Day 5, the supernatant was replaced with new media containing 10 μM of RA without serum (FBS). As we can observe from the morphology, the majority of SH-SY5Y cells become swollen and break down on Day 1 (**Figure 2.6**). Therefore, complete serum deprivation is not healthy for SH-SY5Y in differentiation.

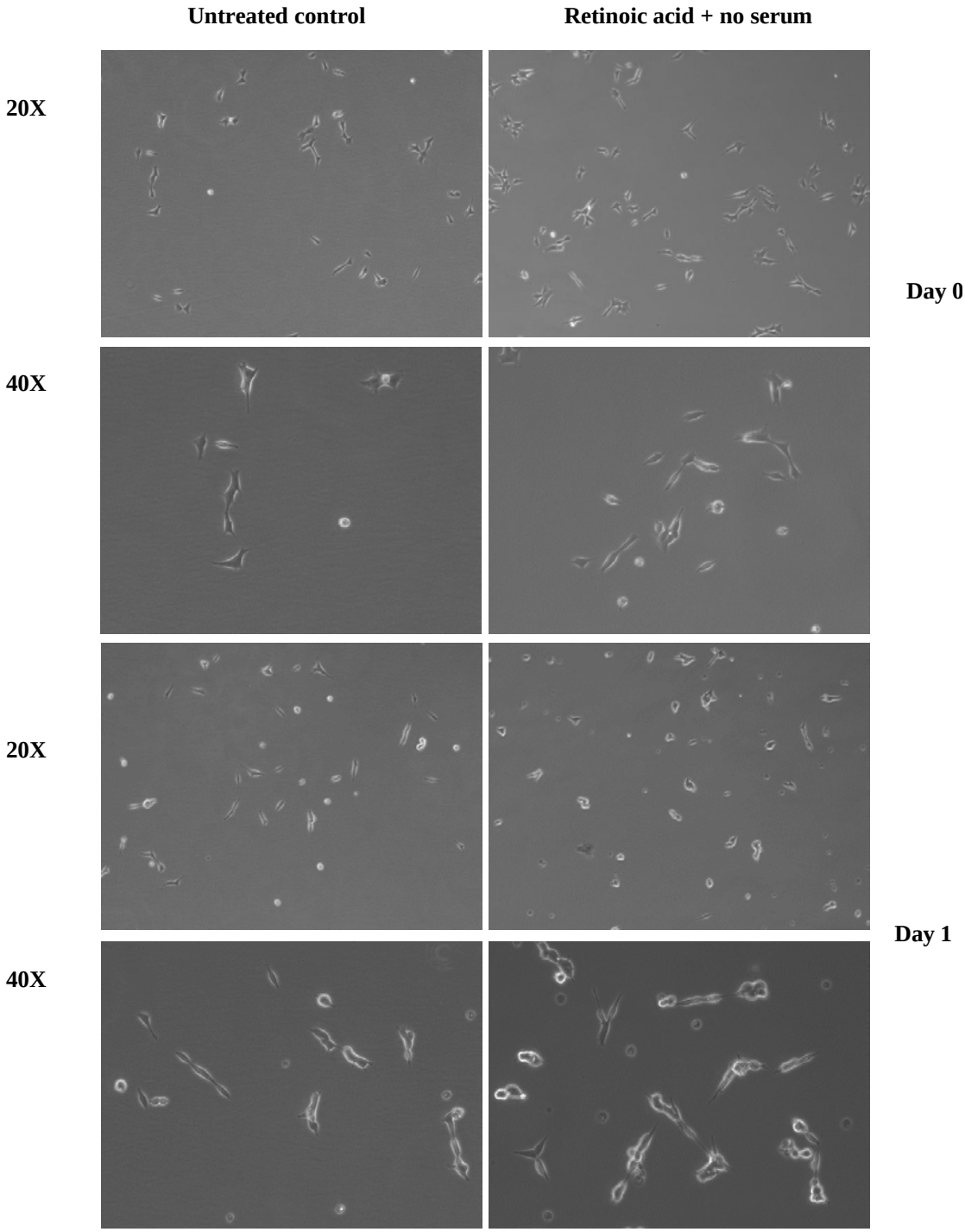

Figure 2.6 RA (10 μM) treatment with complete serum deprivation is toxic for SH-SY5Y cells.

SH-SY5Y cells in untreated control manifest in non-polarized shape, short neurites and intact cell membranes after 1-day cell culture. By contrast, after 1-day treatment with serum-free media containing RA, SH-SY5Y cells present cell membrane blebbing and cytoplasm shrinkage.

Then, we considered whether appropriate serum starvation would be a suitable condition for SH-SY5Y differentiation, cells were first seeded on 6-well plates on Day 0 at 1.4×10^4 cells/well (2 mL) to prevent overgrowth throughout five days. Then on Day 1, Day 3, and Day 5, the supernatant was replaced with new media containing 10μM of RA with 2.5% serum (FBS). As it can be observed from the morphology, SH-SY5Y cells have stopped proliferating and grown out longer processes in polarized shapes compared to control after 5-day culture with RA (10 μM) in 2.5% FBS media (**Figure 2.7**).

To obtain clearer observation and analyse neurite lengths, crystal violet staining was applied to stain the cells (**Figure 2.7**). The result of neurite length analysis shows that 5-day treatment of RA (10 μM) in 2.5% FBS significantly stimulates the process elongation of SH-SY5Y cells in the aspects of process/cell ratio and total neurite length average (**Figure 2.8 A, B**). To further assess neurite outgrowth, cell membrane outgrowth fluorescence was obtained using the neurite outgrowth kit. The result shows increased cell membrane fluorescence, which can indirectly indicate neurite outgrowth (**Figure 2.9 A, B**).

Then, in order to assess whether the 5-day treatment of RA (10 μM) in 2.5% FBS would modify the gene expression, the mRNA was extracted from SH-SY5Y cells after the differentiation treatment and measure the gene expression of gene marker SYP, NeuN, and NeuN using rt-PCR. However, the result showed the gene expression of these gene markers were undetermined. Then, a cDNA dilution study was further conducted to test whether the concentration of cDNA would affect the accuracy of rt-PCR. The concentrations of cDNA at 2 μg, 1 μg and 0.5 μg were used to retest the expression of these gene markers, but the result remained undetermined. Therefore, RA (2.5%) treatment with 2.5% serum starvation for 5 days can not stimulate the expression of these mature neuronal gene markers in SH-SY5Y.

Then, 3-day treatment of BDNF (50 nM) was added to supplement the differentiation of RA treatment in 2.5% serum. The gene expression of SYP and ENO2 from this method was compared with RA treatment in 10% serum plus BDNF treatment. The result shows that serum starvation suppresses the expression of mature genes to some extent (**Figure 2.10**).

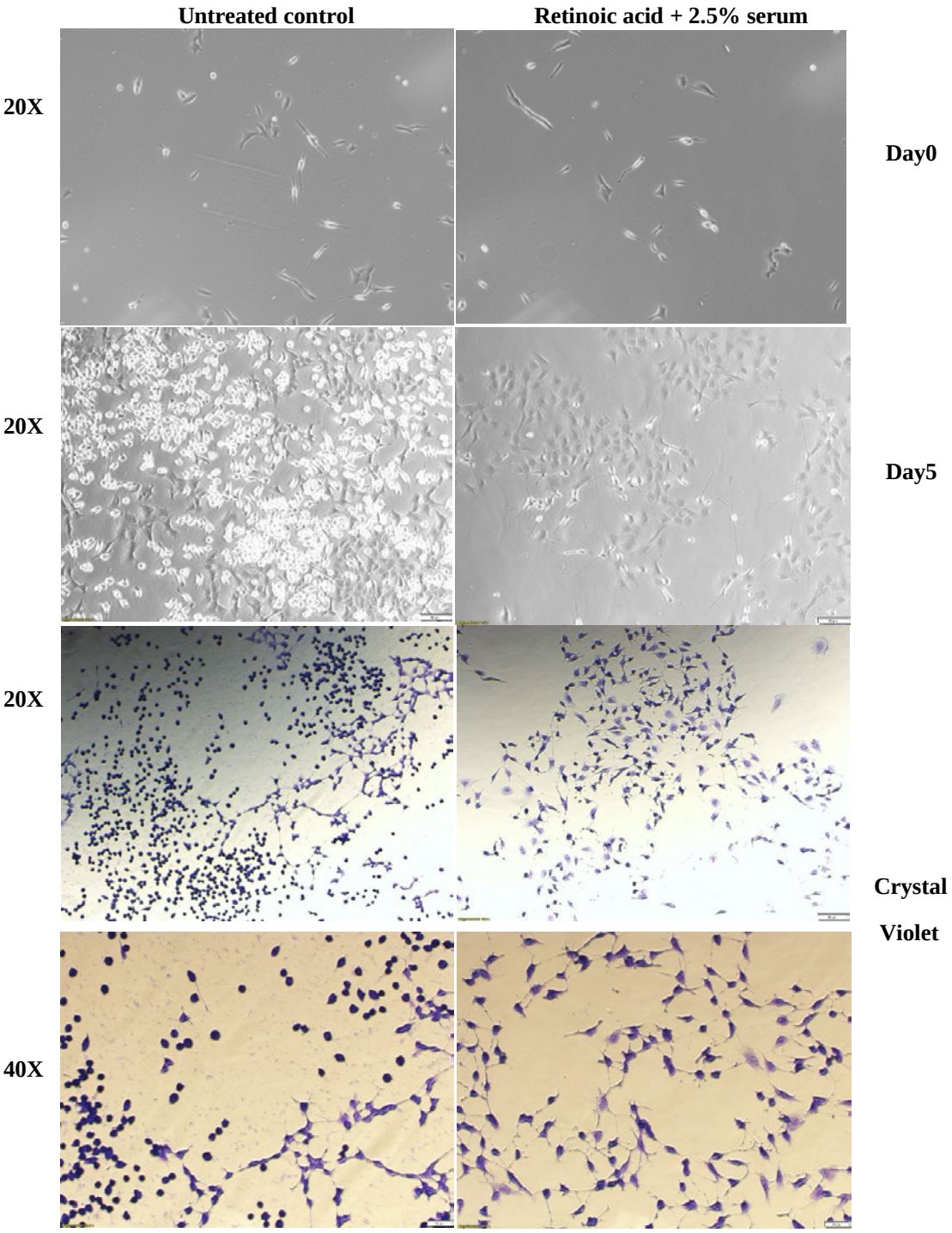

Figure 2.7 RA (10 µM) treatment with 2.5% FBS differentiates SH-SY5Y morphologically after 5 days.

SH-SY5Y cells in untreated control manifest in a mixture of cells with heterogeneous morphologies due to overgrowth after 5 days, including non-polarized shape with/without short processes and longer neurites showing in some cells. By contrast, after 5-day treatment with media containing 2.5% serum and RA, SH-SY5Y cells

manifest a homogeneous and polarized shape with longer neurites connecting each other and spread out evenly. Scale bars represent 50 µm at 20X and 25 µm at 40X.

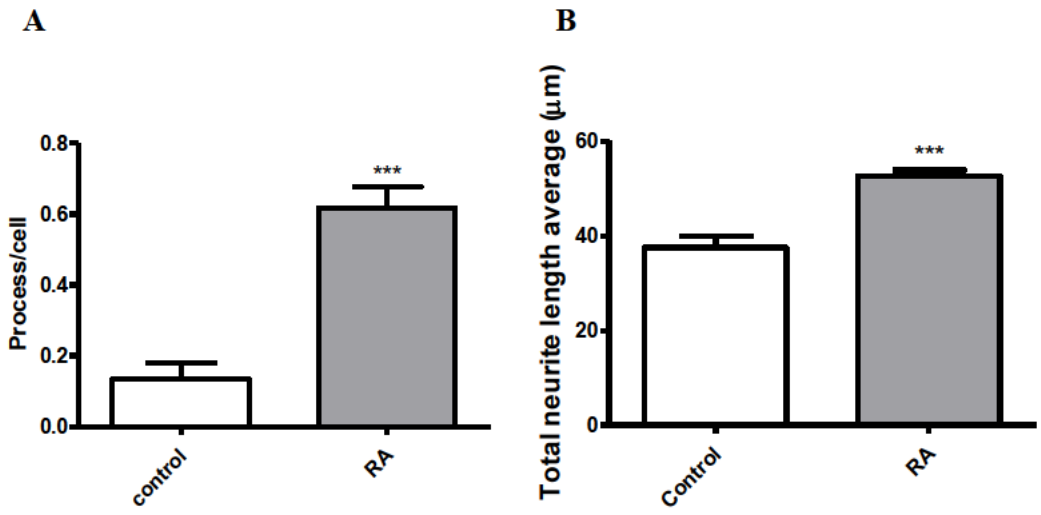

Figure 2.8 5-day treatment of RA (10 µM) in 2.5% serum stimulates the process elongation of SH-SY5Y cells.

Undifferentiated SH-SY5Y cells were treated with RA (10 µM) in 2.5% serum for 5 days and stained with crystal violet. NeuronJ plugin of ImageJ software was used to measure neurite lengths. Process/cell ratio (A) and total neurite length average (B) were analysed to assess the lengths of neurites. T tests were applied. Significance levels were shown as and $P < 0.001$ (***). Data indicate mean ± SD of three independent experiments.

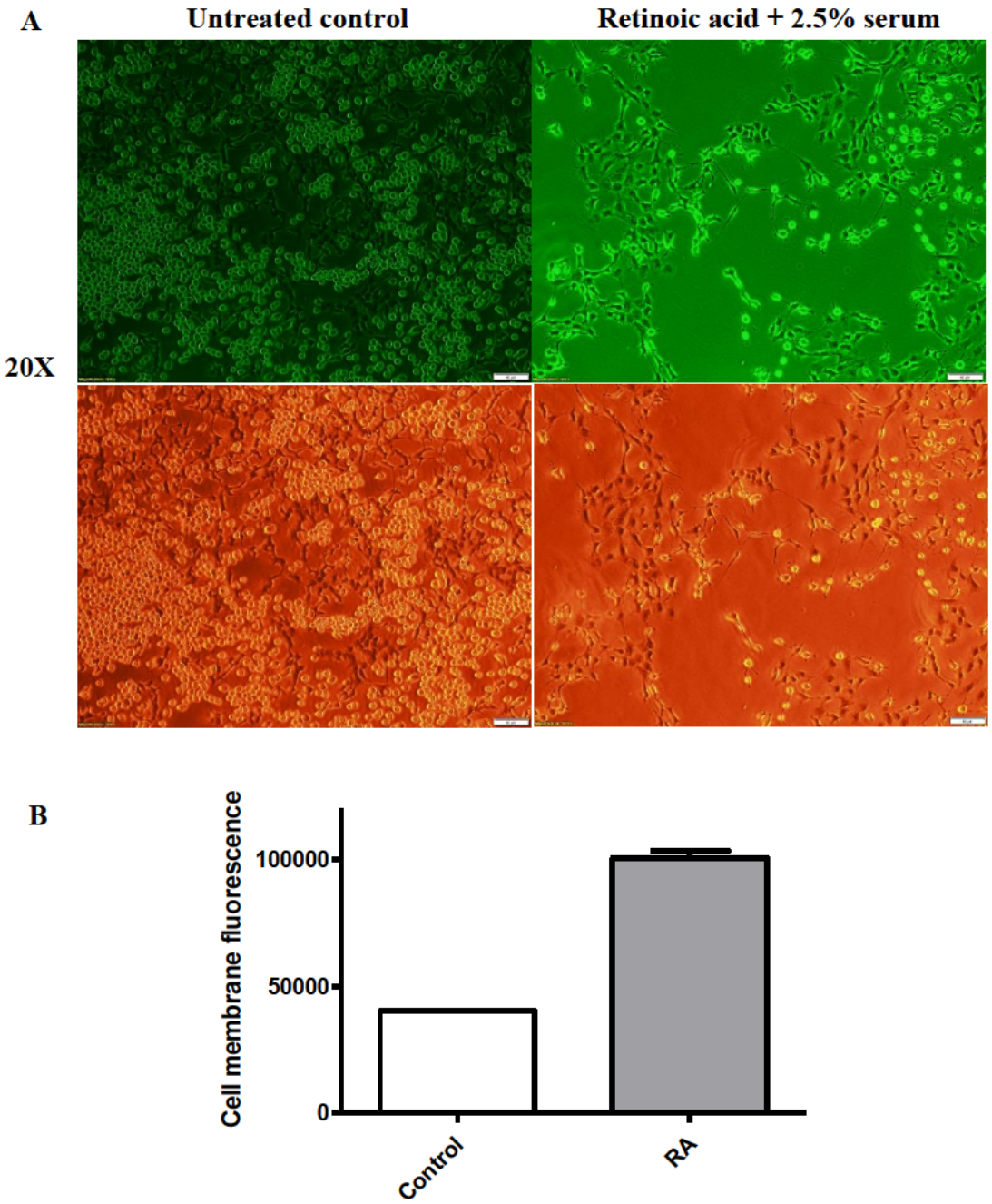

Figure 2.9 5-day treatment of RA (10 µM) in 2.5% serum stimulates the cellular outgrowth of SH-SY5Y cells

Undifferentiated SH-SY5Y cells were treated with RA (10 µM) in 2.5% serum for 5 days and stained using the neurite outgrowth kit. Cell viability staining is shown in green and cell membrane staining in red (A). Adjusted cell membrane fluorescence is adjusted to cell viability (B). Scale bar represents 50 µm at 20X.

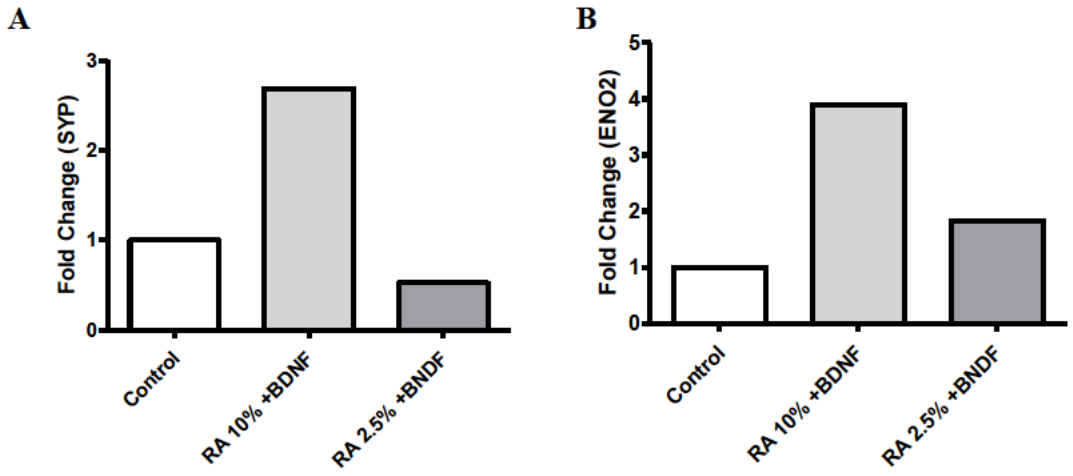

Figure 2.10 Serum starvation might suppress the gene expression of mature neuronal gene expression in SH-SY5Y cells

SH-SY5Y cells were treated with two differentiation methods: 5-day treatment of RA (10 μM) in 2.5% serum followed by 3-day treatment of BDNF (50 nM) treatment; 5-day treatment of RA (10 μM) in 10% serum followed by 3-day treatment of BDNF (50 nM) treatment. mRNA was extracted from these samples and tested for the expression level of SYP (A) and ENO2 (B) using rt-PCR.

2.4.4 Retinoic acid and BDNF combination treatment without serum starvation stimulates the expression of mature neuronal markers in SH-SY5Y

To observe the morphology of differentiated SH-SY5Y cells, SH-SY5Y cells were seeded on 96-well plates at 10^5 cells/mL (100 µL) and incubated for 24 h. Retinoic acid (10 µM) in 10%-serum media was added onto the cells every other day for a 5-day period and followed by BDNF (50 µg/mL) treatment in serum-free media for three executive days. Crystal violet staining was applied to stain differentiated SH-SY5Y cells.

As it is shown in **Figure 2.11**, undifferentiated SH-SY5Y cells as the control (**Figure 2.11 A**) tend to grow in forms of clusters or clumps surrounded by cells with short processes. On the contrary, differentiated cells (**Figure 2.11 B, C**) spread out and have longer neurites and pyramidal-shaped cell bodies.

A

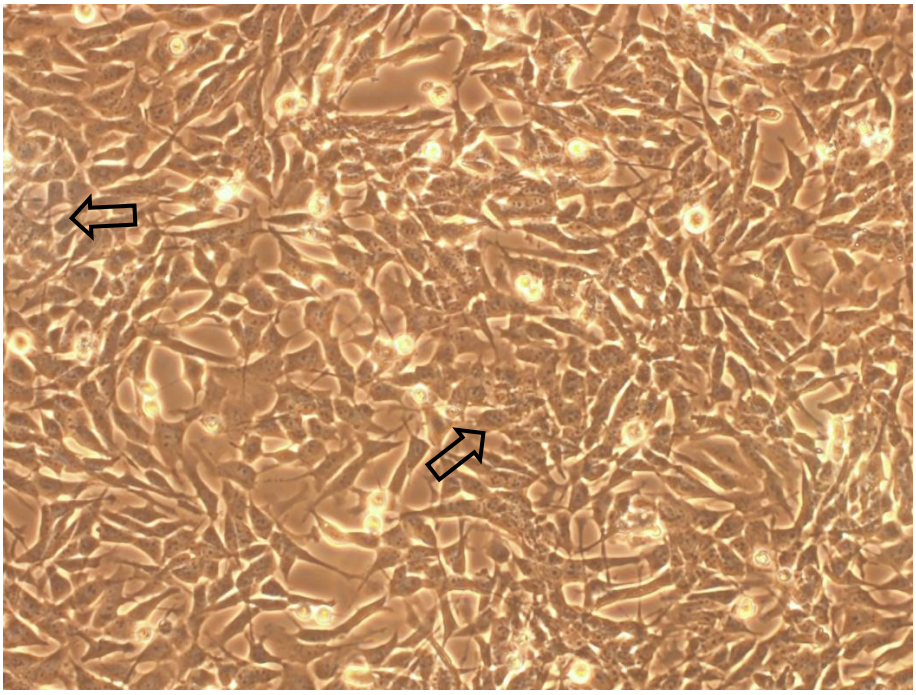

B

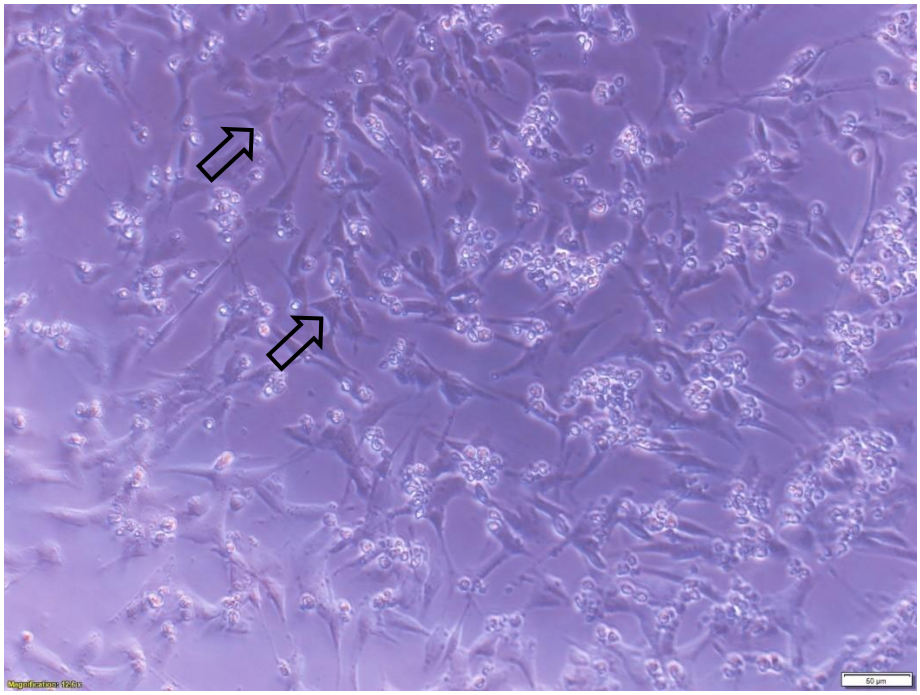

C

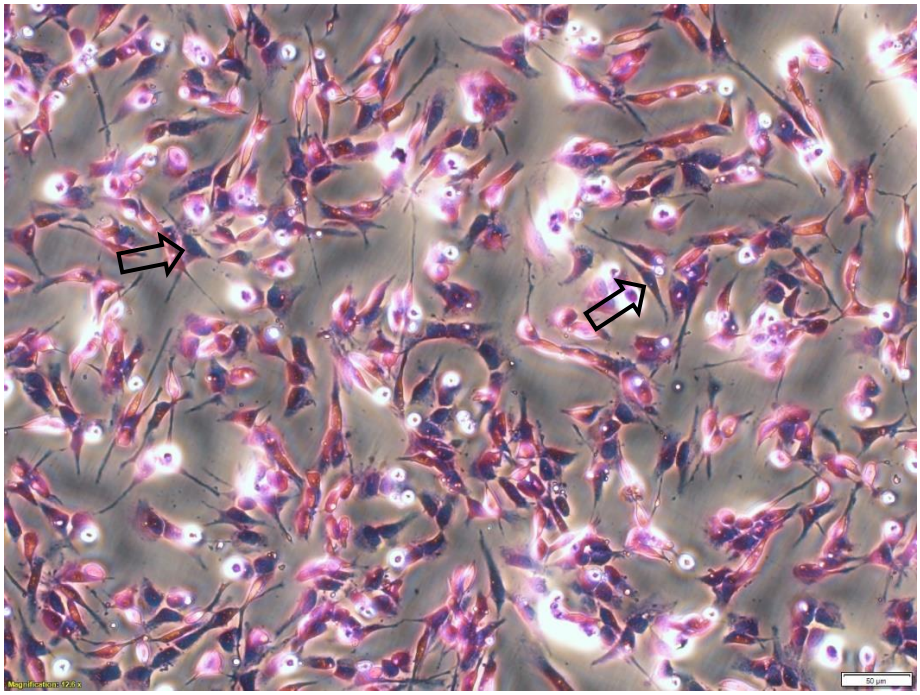

Figure 2.11 Morphology of undifferentiated and differentiated SH-SY5Y cells

Undifferentiated SH-SY5Y cells (A) showed clusters of cells (arrowed). Differentiated SH-SY5Y cells (C) and after crystal violet staining (D) showed more pyramidal-shaped cell bodies (arrowed) and grow more dispersedly. Scale bar represent 25 µm at 40X.

To verify whether the differentiation treatment of retinoic acid and BDNF combination can alter the gene expression of SH-SY5Y cells, synaptophysin (SYP), neuronal nuclei (NeuN), and enolase 2 (ENO2) or neuron-specific enolase (NSE) were used as the markers of mature neurons to indicate differentiation. To collect sufficient cells to extract mRNA, SH-SY5Y cells were seeded on 6-well plates at 5×10^5 cells/well and treated with retinoic acid (10 µg/mL) every other day for a 5-day period and BDNF (50 ng/mL) for 3 days. Real-time PCR was conducted to measure the gene expression level of the two gene markers.

Gene marker SYP and ENO2 in differentiated SH-SY5Y cells showed significant increases in gene expression compared to undifferentiated ones (**Figure 2.12 A, B**). However, NeuN showed expression in neither of them.

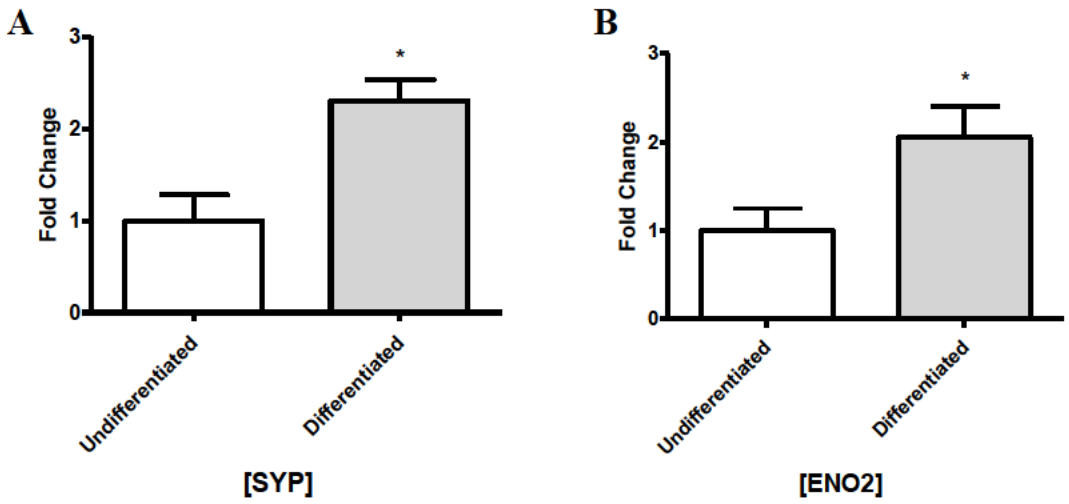

Figure 2.12 Gene expression of SYP and ENO2 as neuronal markers in SH-SY5Y cells were elevated after differentiation

SH-SY5Y cells were treated with RA for 5 days and followed by BDNF treatment for 3 days. One-way ANOVA followed by Turkey's multiple comparison test was applied. Significance levels were shown as $P< 0.05$ (*). Data indicate mean ± SD of three independent experiments.

2.4.5 ECM alone is not sufficient for SH-SY5Y differentiation or 3D co-culture with HAPI cells

To assess whether ECM culture alone can initiate the differentiation of SH-SY5Y cells as reported in numerous studies, ECM as a culture base cannot cease the proliferation of SH-SY5Y cells in 2D cell culture after 5 days as shown in **Figure 2.13**.

Then SH-SY5Y cells were suspended and cultured in the ECM gel for 6 days. several spheroids with a radiating structure and short neurites can be observed as shown in **Figure 2.14 A**. However, this morphology still lacks characteristics of mature neurons such as long neurites and connections between neurons.

HAPI cells and SH-SY5Y cells were also cultured in ECM together for 6 days. From **Figure 2.14 B, C**, it is found that HAPI cells have overgrown as clusters and SH-SY5Y can be found under the whole microscopic vision.

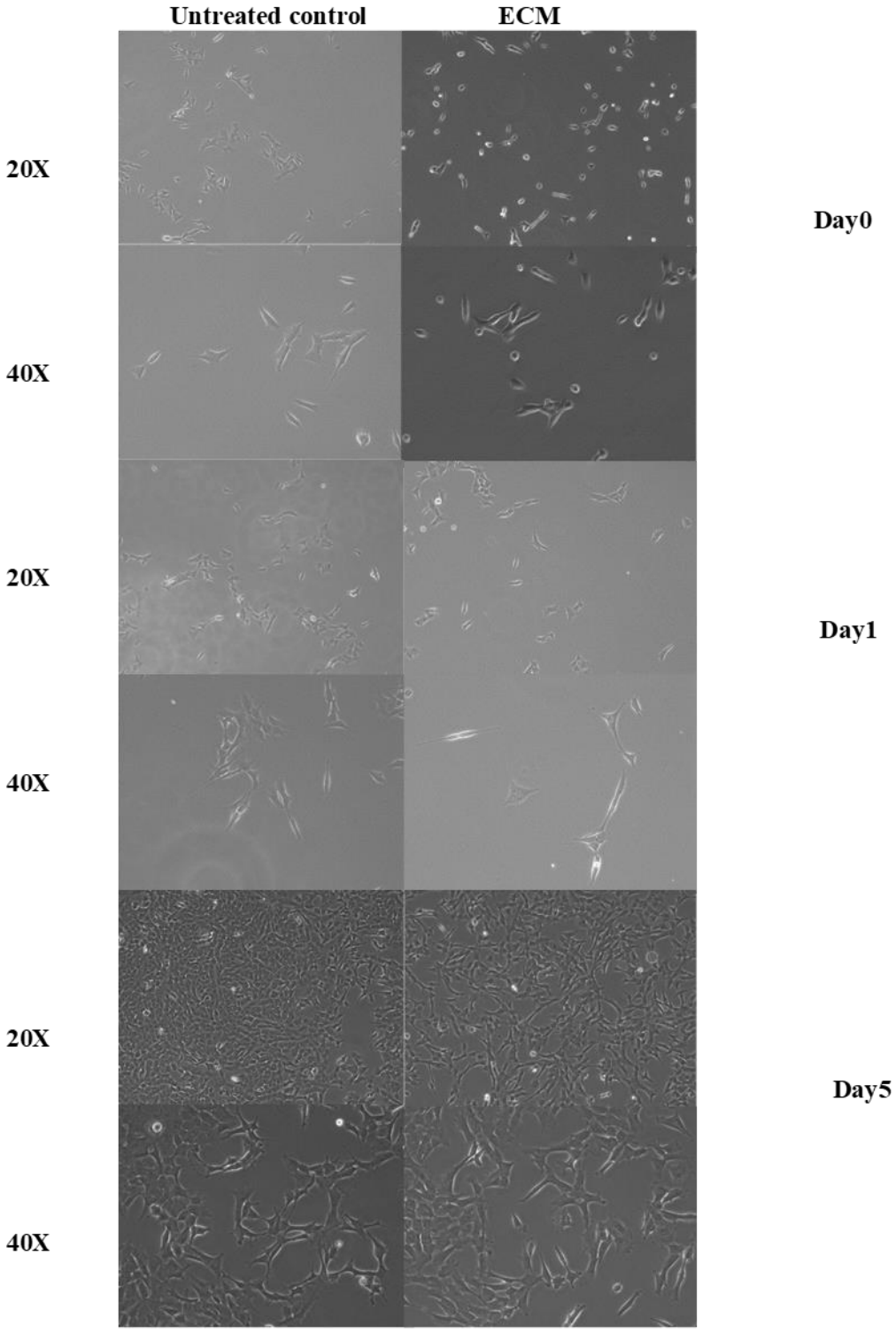

Figure 2.13 ECM only does not cease the proliferation of SH-SY5Y cells in 2D culture.

SH-SY5Y cells have aggressively proliferated and grown in clusters after 5 days without showing differences between control and treatment with ECM gel as a base for cells to adhere.

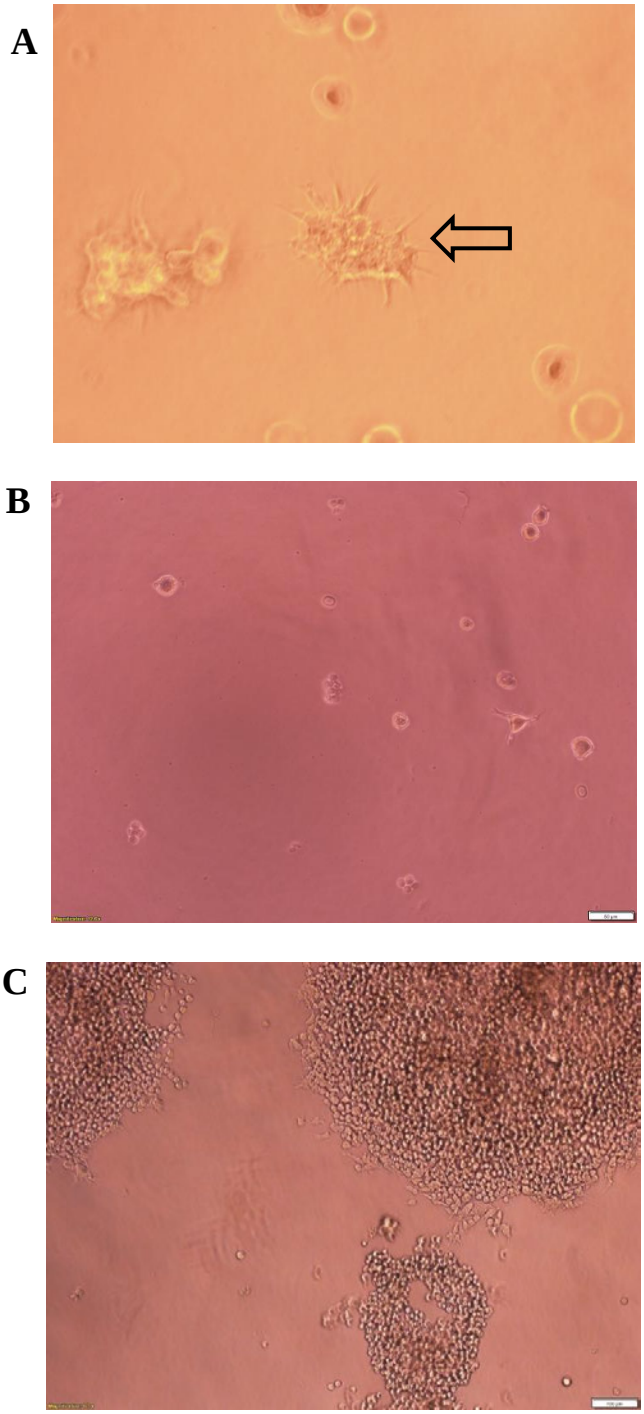

Figure 2.14 Morphology of SH-SY5Y and HAPI cells growing in ECM gel.

A. SH-SY5Y cells suspend in the ECM gel in a 96-well plate. Several spheroids displayed a radiating structure with short neurites on Day 6 of cell culture. **B.** Day 1 of 3D co-culture of HAPI cells and SH-SH5Y cells. **C.** Day 6 of 3D co-culture. HAPI cells overgrow in clusters with the absence of SH-SY5Y cells.

2.5 Discussion and conclusions

In this chapter of methods development, optimization for several methods for 2D microglia-neuron co-culture model for our pharmacological study was completed, including LPS dose-response, cell culture conditions for SH-SY5Y cells, differentiation method for SH-SY5Y differentiation and a preliminary study of ECM-based 3D co-culture.

Lipopolysaccharide has been widely used as a stimulus to induce inflammation in macrophages, which can be used to mimic different inflammatory conditions such as septic infection and sterile inflammation. Thus, it is important to narrow down an appropriate range of inflammation levels to mimic the inflammatory response of depression conditions. Based on our results and literature, HAPI cells can produce varieties of inflammatory mediators under LPS stimulation, such as TNF-α, IL-1β, PGE_2 and ROS, which indicates that HAPI cells can be used as a microglia model in our study (A. J. McFarland et al., 2018). According to the dose-response of LPS in the results, the productions of inflammatory mediators in HAPI cells increase in a dose-dependent fashion. Five ng/mL of LPS induced a lesser degree of inflammation than 10 ng/mL and above. Additionally, an *in vitro* study of HIV on rodent microglia has also regarded the inflammatory response induced by 10 ng/mL of LPS as comparable to the inflammatory environment in a co-infection of bacteria and viruses (S. Dallas et al., 2013). Clearly, microorganism infection is not a cause of depression. Selecting the correct dosage of LPS as a stimulus should be close to or in accord with the true microenvironment in the pathological condition that a model is built for. The inflammatory environment of depression in the CNS is not comparable to the situation in bacterial and viral co-infection. Therefore, concentrations of LPS under 10 ng/mL should be regarded as a safer choice to induce a mild level of neuroinflammation to better align with the inflammation level in depression patients.

Then the culture media condition has also been optimized. Culturing SH-SY5Y cells in culture media containing low-glucose not only eliminates the low-glucose shock when transferring the supernatant between cell lines but also has avoided the potential biological impacts induced by high-glucose cell culture. D-glucose concentrations reaching 10 mM are considered to be pre-diabetic to diabetic levels (Sigma-Aldrich, 2018a). The concentration glucose in high-glucose DMEM is approximately 25 mM which is far higher than the pre-diabetic glucose level. There is also evidence showing

that high concentrations of glucose can induce amplified mitochondrial respiration and increased ROS production in the SH-SY5Y cell line, which further activates the NF-κB pathway and induces subsequent inflammation (P. Van Dyken and B. Lacoste, 2018, V. C. Russo et al., 2012). Therefore, 5.5 mM of glucose that was chosen in the culture media is better suitable for SH-SY5Y cells, which is more comparable to that in the true glucose level in the CNS. It has been demonstrated that the extracellular glucose concentration varies during hyperglycemia and hypoglycemia. In hyperglycemia, the plasma glucose concentration ranges from 15.2 mM to 2.8 mM. In hypoglycemia, the plasma level fluctuates between 4.5 mM to 0.16 mM (A. M. Kleman et al., 2008).

Regarding the optimization process conducted for the differentiation method of SH-SY5Y, it has been found that retinoic acid treatment alone on SH-SY5Y can only alter the morphology of neuroblastoma to a neuronal-like shape with longer processes but not the gene expression. The result is in line with the findings in a study of Nishida's group. SH-SY5Y cell line has two subtypes which are SH-SY5Y-A and SH-SY5Y-E from different two different bioresource centers (Y. Nishida et al., 2008). They reported that SH-SY5Y-A cells from the American Type Culture Collection (ATCC) can fully differentiate in the presence of retinoic acid, whereas SH-SY5Y-E from European Collection of Authenticated Cell Cultures (ECACC) requires additional BDNF for full differentiation (Y. Nishida et al., 2008). The SH-SY5Y cell line in this study was procured from Sigma Aldrich which obtains this cell line from ECACC. Hence, this might potentially be the reason that our differentiation methodology needs both retinoic acid and BDNF treatment. Besides, the expression of NeuN could be not detected in both undifferentiated and differentiated SH-SY5Y cells. The origin of the cell line might also be a factor that affects the expression of gene marker NeuN.

Last but not least, a preliminary study for the ECM-based models has also been conducted. The aggressive proliferation of SH-SY5Y cells could not be ceased by cell culture with ECM as a 2D base. A study reported that SH-SY5Y cell line is a high-grade, namely, the most tumorigenic neuroblastoma, expressing the least integrin which correlates with the adhesion and differentiation of neuroblastoma (A. Meyer et al., 2004). However, SH-SY5Y cells can manifest with radiating neurites in a suspending form growing in ECM gel. This can be regarded as a new culture model for SH-SY5Y cells compared to monolayer 2D cell culture. The expression of varieties of markers might also be different from those in 2D cell culture as other studies have shown that

cell lines manifest different morphology and gene expression in 2D and 3D models (D. L. Kiss et al., 2013). From the result of the co-culture of HAPI cells and SH-SY5Y cells, it is found that the overgrowth of HAPI cells severely inhibits the survival of SH-SY5Y cells. Therefore, other microglial cell lines and other culture conditions apart from ECM gel as a base need to be explored in future work.

Therefore, to summarize based on the optimization, in the following two chapters, the inflammatory response in HAPI microglial cells will be induced by LPS with a concentration of 0.005 μg/mL to mimic the inflammation level in depression patients. SH-SY5Y cells will be cultured in the same low-glucose media as HAPI cells to avoid the low-glucose shock produced during supernatant transfer treatment. In regards to the differentiation method for SH-SY5Y cells, the combination treatment with RA and BDNF will be employed to ensure cells differentiate to mature neuronal cells morphologically and genetically.

Chapter 3 : SIRT1 and SIRT2 modulators inhibit LPS-induced neuroinflammation in microglia

3.1 Introduction

3.1.1 Neuroinflammation in depression

Monoamine metabolism is the main theory of depression. It is considered that the deficiency of neurotransmitters such as serotonin, dopamine and noradrenaline result in the onset of depression. Microglia are the prime component of the intrinsic immune system of the central nervous system (R. von Bernhardi et al., 2016). They can be activated by diverse pathogens, cytokines, neurotoxins and injuries (M. B. Graeber et al., 2011). Activated microglia can convert the precursor of serotonin into kynurenine, which leads to a decrease in serotonin production (A. H. Miller and C. L. Raison, 2016). The cytokines also increase the reuptake of neurotransmitters, which further reduce the secretion of neurotransmitters into the synaptic cleft (A. H. Miller and C. L. Raison, 2016). Kynurenine is further converted into quinolinic acid to activate glutamate receptors, which subsequently produces excessive excitatory neurotransmitter glutamate and leads to excitotoxicity (A. H. Miller and C. L. Raison, 2016).

Excessive neuroinflammation also can directly influence neuronal dysfunction, damage and death in the pathology of depression (B. E. Leonard, 2018). Resting microglia convert into activated microglia and release inflammatory mediators including tumor necrosis factor (TNF)-α, interleukin (IL)-1β, IL-10, reactive oxygen species (ROS) and prostaglandin E_2 (PGE_2), the imbalance of which eventually lead to dysfunction, damage and death of neurons (B. E. Leonard, 2018). Cytokines also activate the astrocyte which can increase the production of glutamate. These all eventually result in the excitotoxicity of glutamate and a decrease of brain-derived neurotrophic factors which will affect the neuronal integrity and lead to neurodegeneration.

3.1.2 Elevated immune profile in depression population

While the direct relationship of the inflammatory mediators and the pathology of depression and related neurodegenerative diseases is not fully elucidated, the evidence of the elevation of cytokines provided by clinical studies is considerable (H. Himmerich et al., 2019). Even though high variation in the serum level of the inflammatory mediators in depression patients was found, studies are showing significant differences in serum levels of TNF-α, IL-1β and IL-10 compared to healthy controls (W. Zou et al., 2018). In mild, moderate, severe MDD patients and healthy control, the mean serum levels of TNF-α are3.35, 3.79, 6.19 and 2.96 pg/mL respectively. The mean IL-1β serum levels are 0.65, 0.87, 1.07 and 0.38 pg/mL for the same classification

aforementioned. The mean IL-10 serum levels are 0.51, 0.55, 0.49 and 0.26 pg/mL for mild, moderate, severe MDD patients and healthy subjects (W. Zou et al., 2018). From these groups of data, it has been found that the serum levels of TNF-α and IL-1β in any severity stage are significantly higher than those in healthy controls. Whereas anti-inflammatory cytokine IL-10 level is significantly higher than the normal level, which has also been reported in other studies (W. Zou et al., 2018). It is considered that the elevation of serum IL-10 might be associated with late-onset of depression instead of an indicator for lesser severity of depression (W. Zou et al., 2018). Moreover, another study of depression in patients with Alzheimer's disease showed a correlation between elevated cytokine levels and associated depression presentation (V. K. Khemka et al., 2014). In this study, the serum levels of TNF-α, IL-6 and IL-1β levels are 10 pg/mL, 8.8 pg/mL, and 6.8 pg/mL respectively in AD patients with depression, which are significantly higher than the serum levels in healthy controls (V. K. Khemka et al., 2014). This study also reported a strong correlation between unsatisfactory mini-mental state exam (MMSE) scores and high serum levels of TNF-α and IL-6 in AD patients with depression (V. K. Khemka et al., 2014). There is also a study showing that the level of TNF-α can exceed 50 pg/mL and IL-10 level can be approximately 5 pg/mL in depressed subjects (F. M. Schmidt et al., 2014). Based on these studies, deviations can be found on serum levels of inflammatory mediators between different studies, but the serum levels of these cytokines have not exceeded 100 pg/mL yet. Even though PGE_2 has been researched in numerous animal studies for depression and neurodegenerative diseases, there is still no abundant data for serum PGE_2 levels in clinical research. However, one study on major depressive disorder reported a salivary level of PGE_2 of around 498 pg/mL, which can be an indicator of the serum level (K. Ohishi et al., 1988). Therefore, the level of cytokines induced in *in vitro* neuroinflammation model should mimic the serum levels from the clinical data of depression as much as possible, which can be beneficial for obtaining accurate data.

3.1.3 Potential treatment for neuroinflammation

Based on accumulating evidence showing the association between depression and neuroinflammation, different medication options have been proposed as potential treatments for neuroinflammation. Non-Steroidal Anti-inflammatory Drugs (NSAIDs) have been proposed to treat against inflammation as part of an anti-depression regimen (O. Köhler et al., 2014). However, results from the currently available studies have

found inconsistent data showing different efficacies (H. A. Eyre et al., 2015). Also, some studies reported NSAIDs could reduce the effectiveness of antidepressant treatment (R. C. Shelton, 2012). However, there is no sufficient and consistent clinical data to prove the experimental theory. Another perspective is that numerous studies have demonstrated the anti-inflammatory effect of fluoxetine, including data from animal models (I. Kostadinov et al., 2015, F. Zhang et al., 2012). One study of adolescent depression found fluoxetine treatment slightly reduced the serum levels of TNF-α, IL-6, and IL-1β at week 4 of treatment, which slightly bounced back but was still less than the pre-treatment level at week 8 (G. Pérez-Sánchez et al., 2018). In contrast, another study of depressed patients with 6-week treatment of fluoxetine reported that fluoxetine slightly increased the serum level of TNF-α but reduced the serum levels of IL-1β and IL-10 (C. Song et al., 2009). As the efficacy of the current medication treatment for neuroinflammation is not as potent as might be anticipated, investigation and development of a novel class of medication treatment for neuroinflammation are necessary. Additionally, NSAIDs and fluoxetine can be administered as positive controls to compare the anti-inflammatory effects within this study.

Based on the background in the literature review, SIRT1 and SIRT2 drugs have been proposed as a potential treatment for neuroinflammation by targeting SIRT1 and/or SIRT2 activity. Resveratrol has been used as a natural SIRT1 activator and also found to have pleiotropic effects. Some studies have proposed that resveratrol's SIRT1 activating effect is conducted via 5' AMP-activated protein kinase (AMPK) and peroxisome proliferator-activated receptor δ (PPARδ) pathways (C. K. Cheng et al., 2019). It was also discovered that resveratrol has a direct structure-activity relationship with the SIRT1 enzyme. Several studies reported that resveratrol can stabilize the loose-binding between the SIRT1 enzyme and its substrates, with three resveratrol molecules needed to alter the conformation of the N-terminal domain (NTD) of SIRT1 (X. Hou et al., 2016, Z. Ovesna and K. Horvathova-Kozics, 2005, D. Cao et al., 2015). Sirtinol was originally discovered to exert the SIRT2 inhibition effect in 2001 by Grozinger's team (C. M. Grozinger et al., 2001). After that, Mai's team further synthesized and evaluated sirtinol and its analogues which exert both SIRT1 and SIRT2 inhibition (A. Mai et al., 2005). EX527 is currently used as a selective SIRT1 inhibitor. It is reported that EX527 exerts the SIRT1 inhibition effect through depriving SIRT1's NAD+-

dependent deacetylation catalysis (M. Gertz et al., 2013). AGK2 has been claimed as the most potent inhibitor of SIRT2 activity in a study of Parkinson's disease (T. F. Outeiro et al., 2007). **Figure 3.1** shows the chemical structure of resveratrol (A), sirtinol (B), EX527 (C), and AGK2 (D).

Based on the dose-response of LPS presented in the method development chapter, the levels of inflammatory mediators induced by 0.005 µg/mL of LPS are lower than those induced by higher concentrations of LPS. As the *in vitro* neuroinflammation induced by LPS should be aligned with the true serum level of inflammation, this Chapter will use a concentration of LPS of 0.005µg/mL to investigate the anti-inflammatory effects of representative SIRT1 and SIRT2 drugs on the inflammatory response in microglial HAPI cells.

3.2 Materials and methods

3.2.1 Cells and reagents

HAPI cells were purchased from Sigma-Aldrich (Merck). They were grown in ATCC-formulated DMEM (Gibco by Life Technologies, 11885084) which contains low glucose (1 g/L D-Glucose), L-glutamine (584 mg/L), sodium pyruvate (110 mg/L) and phenol red (15 mg/L). The media was additionally supplemented with 1% penicillin-streptomycin (10000 U/mL) (Gibco by Life Technologies) and 10% fetal bovine serum (FBS) (Scientifix life). HAPI cells were grown in sterile T-75 cm^2 flasks and cultured in an incubator at 37°C with 5% CO_2 and high humidity.

3.2.2 Treatment preparation

Resveratrol (RSV), sirtinol (SIR), EX527 and AGK2 (Selleck Chemicals, Australia) were chosen as SIRT1 activator, dual SIRT1/SIRT2 inhibitor, selective SIRT1 inhibitor and SIRT2 inhibitor respectively. Fluoxetine (FLU) and ibuprofen (IBU) were chosen as positive controls. **Figure 3.2** shows the structure of the agents. The resveratrol, sirtinol, EX527, AGK2, fluoxetine and ibuprofen were dissolved in DMSO at the stock concentration of 10 mM and aliquoted and stored at -20°C. Before treatments were conducted, all stocks (10 mM) were diluted to a working solution (1:10). The final proportion of DMSO in each well of plates was below 0.01%. LPS was dissolved in PBS solution at the stock concentration of 1 mg/mL and aliquoted and stored in a -20°C freezer. Before treatments were conducted, the LPS stock solution was diluted from 1:10 to a working solution.

A

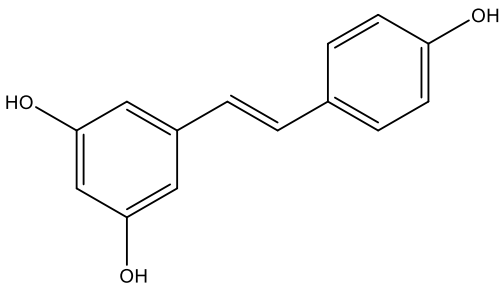

resveratrol

B

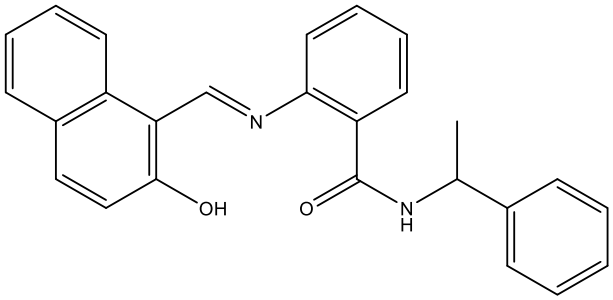

sirtinol

C

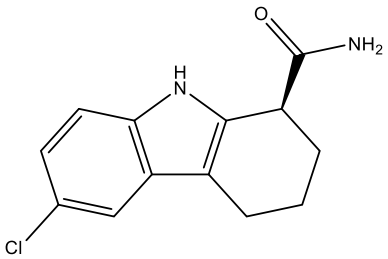

EX527

D

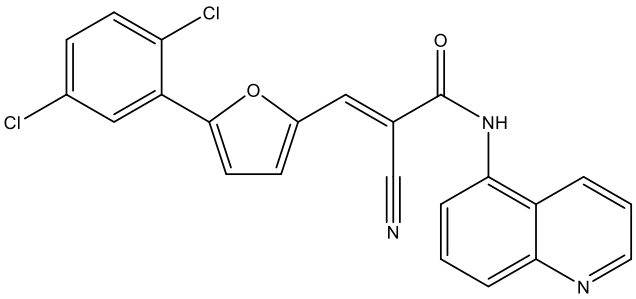

AGK2

Figure 3.1 Chemical structure of SIRT modulators.

3.2.3 Establishment of *in vitro* model of neuroinflammation

To induce neuroinflammation of HAPI cells, LPS (E. coli O111: B4) was used as a stimulus. HAPI cells were seeded at 2.5 $\times 10^5$ cells/mL with 400 µL per well in 24-well plates and placed in an incubator for 24 h. LPS solution (50 µL) with a concentration of 0.005 µg/mL was added to HAPI cells. Then, HAPI cells treated with LPS were incubated for 20 h. Treatments (50 µL) were added into corresponding wells 4 h prior to LPS treatment. Solvent (PBS) controls and media controls were set up as well. After that, the supernatant was collected as samples for running ELISAs. Resazurin assays were run to determine the cell viability.

3.2.4 Resazurin assay

To assess the cytotoxicity of resveratrol, sirtinol, EX527, AGK2, fluoxetine and ibuprofen on microglia, HAPI cells were seeded at 2×10^4 cells/well on 96-well plates for 24 h and then treated with a series of concentrations (0.001-100 µM) of the agents for 24 h. Each treatment had 6 replicates. Then, resazurin assay was applied for cell viabilities.

The resazurin reagent was purchased from Sigma-Aldrich. Resazurin assays were run to detect cell viabilities of HAPI cells. After treatment, the supernatant above cells was removed and replaced with diluted resazurin solution (44 µM) and incubated for 3 h. After that, fluorescence (excitation: 530 nm and emission: 590 nm) value was read and recorded using a Tecan Infinite 200 Pro microplate reader (Tecan, Australia).

3.2.5 Enzyme-linked immunosorbent assay (ELISA)

To investigate the effect of resveratrol, sirtinol, EX527 and AGK2 on the production of inflammatory mediators, HAPI cells were seeded at 2.5 × 10^5 cells/well on 24-well plates and incubated for 24 h. Pre-treatment was conducted after 20 h post-seeding. After 4 h, cells were challenged with LPS (0.005 µg/mL) for 20 h in an incubator. The supernatant was collected fresh for running ELISA of PGE_2, TNF-α, IL-1β, and IL-10 using ELISA kits.

3.2.5.1 PGE_2 production measurement

For measurement of PGE_2 production in HAPI cells after treatment and LPS challenge, prostaglandin E_2 express ELISA kit (Cayman chemical, 500141, Australia) was used to conduct the assay. The protocol in the instruction was followed. Samples were tested in replicates according to the layout design. The absorbance was measured at a

wavelength of 410 nm using a Tecan infinite 200 microplate reader for several times until the value of B_0 reached above 0.3 A.U. with blank value subtracted. The raw data was calculated according to the instruction of the protocol and input into Graphpad Prism 5 and interpreted into concentration by performing a 4-parameter logistic (4-PL) regression analysis.

3.2.5.2 TNF-α, IL-1β and IL-10 production measurement

For measurement of cytokine production of HAPI cells after pre-treatment and LPS stimulation, rat TNF-α ELISA kit (Biosensis BEK-2101, Australia), rat IL-1β ELISA kit (Biosensis BEK-2309, Australia) and rat IL-10 ELISA kit (Biosensis BEK-2047, Australia) were used to conduct the measurement of the concentration of TNF-α in the supernatant.

All supernatant samples were produced and collected fresh before running the assay. Diluted samples (100 µL) and buffer control were added into corresponding wells of the pre-coated plates and incubated overnight in a 4°C fridge. All steps are followed according to the instructions. Samples were tested in replicates according to the layout design. TMB colour developing reagent was added into each well and incubated for 20 to 35 min at room temperature. The TMB stop solution was added when the colour of the highest four concentrations of the standard became obvious blue shades and other standards remained clear.

The absorbance of the yellow shade was measured at 450 nm by using a Tecan Infinite 200 Pro microplate reader (Tecan, Australia). The raw data were input into Graphpad Prism 5 and interpreted into concentration by performing a 4-PL regression analysis.

3.2.6 Measurement of intracellular oxidative reaction

HAPI cells were seeded at 2×10^4 cells/well on 96-well plates and incubated for 24 h in an incubator. Then, pre-treatment was applied to HAPI cells 20 h post-seeding. After 4 h, the LPS solution was added to each well to challenge HAPI cells for 20 h in an incubator. Each treatment had 5 replicates. After that, ROS production was measured by conducting DCF assay.

DCFH-DA assay was used to determine the oxidative reaction of HAPI cells. After the treatment of LPS solution and control solution, the supernatant above HAPI cells was removed and discarded. The diluted DCFH-DA solution (10 µM) was added to respective wells and incubated for 1 h in an incubator. Then the solution above the cells

was replaced with 200 µL of PBS and washed out. Following this, PBS (100 µL) was added into each well. Fluorescence (excitation: 485 nm and emission: 535 nm) was measured and recorded using a Tecan Infinite 200 Pro microplate reader (Tecan, Australia).

3.2.7 Trypan blue dye exclusion assay

Cell concentration was measured by the trypan blue dye exclusion method. Cell numbers were counted through the automatic cell counter or the hemocytometer under an inverted light microscope.

3.2.8 Quantitative real-time PCR

HAPI cells were plated at 5×10^5/well on 6-well plates and incubated for 24 h. Then cells were treated with the investigational agents for 4 h and total RNA was extracted using TRIzol™ reagent (Invitrogen). The concentration of RNA was measured using a Nanodrop spectrophotometer (Thermo Fisher Scientific, Australia). cDNA was synthesized using Verso cDNA synthesis kit (Thermo Scientific) and ProFlex PCR System (Life technology). Primer sequences (Sigman Aldrich) for rt-PCR are shown in **Table 3.1**. Rt-PCR was performed using PowerUp™SYBR™ Green Master Mix kit and QuantStudio™ Real-Time PCR systems (Thermo Fisher Scientific Australia) according to manufactures' guidelines. The thermal cycling conditions were 50°C for 2 min, 95°C for 2 min followed by 40 cycles of 95°C for 1 s and 60°C for 20 s. The dissociation curve conditions were 95°C for 15 s and 60°C for 1 min followed by 95°C for 15 min. The comparative threshold cycles (C_T) or $2^{-\Delta\Delta C_T}$ method was used to analyze the C_T values of samples of interest and control samples. All C_T values were normalized against GAPDH gene.

Table 3.1 List of oligonucleotides for SIRT gene expression in rt-PCR

Primer	Sequence
SIRT1 (Rat)	Forward: 5'-CGCCTTATCCTCTAGTTCCTGTG-3'
	Reverse: 5'-CGGTCTGTCAGCATCATCTTCC-3'
SIRT2 (Rat)	Forward: 5'-CTCCCACCAAACAGATGACC-3'
	Reverse: 5'-ATTCAGACTCGGACACTGAGG-3'
GAPDH (Rat)	Forward: 5'-TCCCTCAAGATTGTCAGCAA-3'
	Reverse: 5'-AGATCCACAACGGATACATT-3'

3.2.9 Statistical analysis

All data were analyzed by GraphPad Prism 5 and presented as mean ± SD. One-way ANOVA and t tests were used to determine the significant difference. $P < 0.05$ was considered a significant difference.

3.4 Results

3.4.1 SIRT1 and SIRT2 modulators induced cytotoxicity in HAPI cells in a dose-dependent way

The cytotoxicities of SIRT1 and SIRT2 modulators on HAPI cells including SIRT1 activator resveratrol, dual SIRT1/2 inhibitor sirtinol, selective SIRT1 inhibitor EX527 and SIRT2 inhibitor AGK2 were tested through resazurin assays. The cytotoxicity of control drugs, fluoxetine as a selective serotonin reuptake inhibitor (SSRI) and ibuprofen as a non-steroidal anti-inflammatory drug, was also tested simultaneously. Resveratrol and sirtinol showed high cytotoxicity at the concentrations of 100 µM and 50 µM and mild cytotoxicity at 25 µM (**Figure 3.2 A, B**). EX527 and fluoxetine exerted high cytotoxicity at concentrations of 100 µM, 50 µM, and 25 µM and mild cytotoxicity at 10 µM (**Figure 3.2 C, E**). AGK2 produced high cytotoxicity at 100 µM, 50 µM, 25 µM, and 10 µM (**Figure 3.2 D**). Data showed increasing concentrations reduced cell viability. Ibuprofen only produced mild cytotoxicity at 100 µM (**Figure 3.2 F**). Ibuprofen apparently is the safest drug as it exerts almost no dramatic cytotoxicity on rat microglia even at 100 µM in this study. Comparing to fluoxetine on rat microglia, resveratrol, sirtinol and EX527 treatment are non-toxic under 25 µM, whereas AGK2 is safe to use on microglia under concentrations of 1 µM.

Next, the cytotoxicity of DMSO with a range of proportions on HAPI cells was examined. The result showed DMSO as the solvent of the treatments did not induce cytotoxicity at proportions from 1% to 0.00001% on HAPI cells (**Figure 3.2 G**).

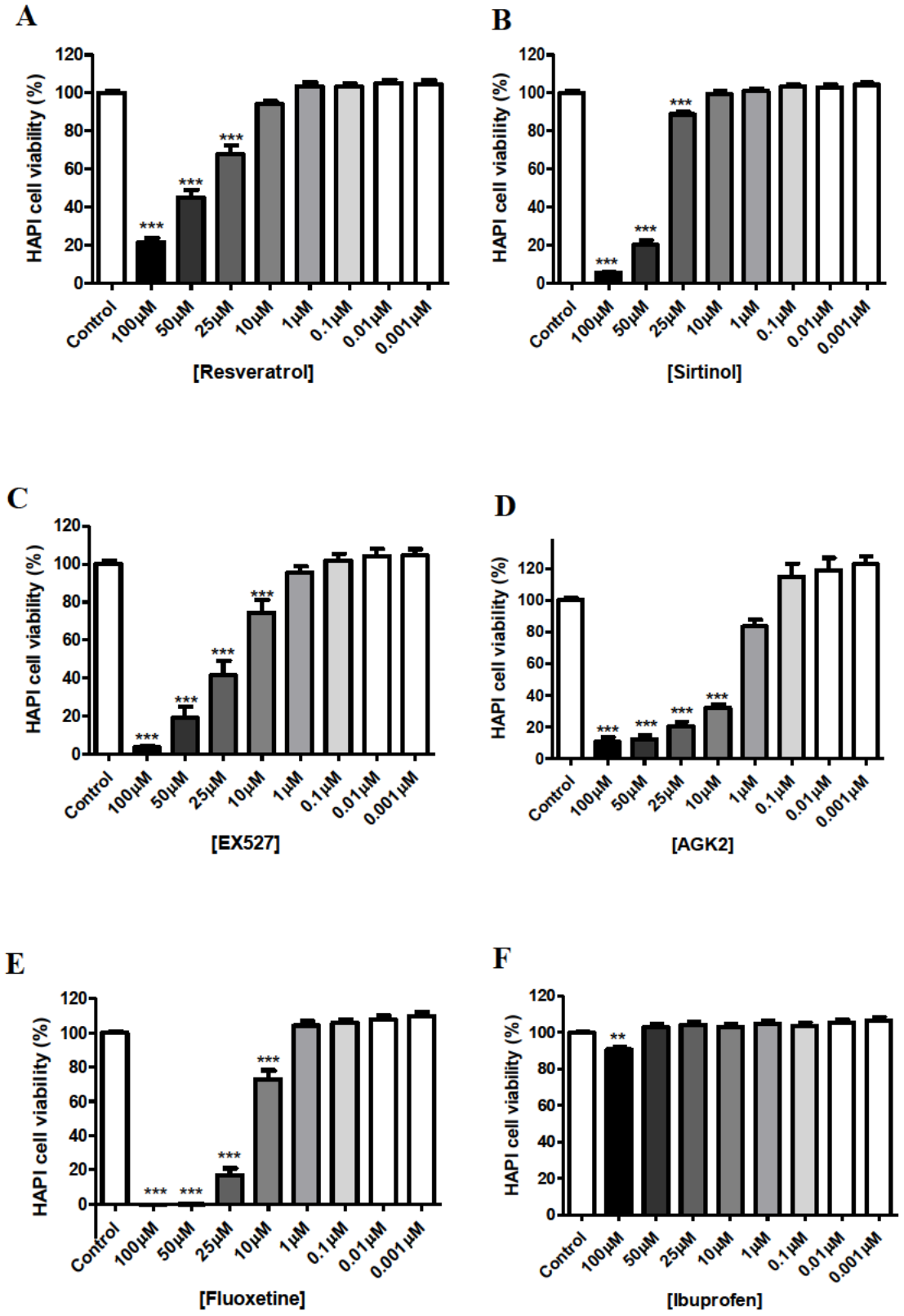
A
HAPI cell viability (%)
120
100
80
60
40
20
0
***
***
***
Control
100μM
50μM
25μM
10μM
1μM
0.1μM
0.01μM
0.001μM
[Resveratrol]
B
HAPI cell viability (%)
***
***
***
[Sirtinol]
C
HAPI cell viability (%)
***
***
***
***
[EX527]
D
HAPI cell viability (%)
***
***
***
***
[AGK2]
E
HAPI cell viability (%)
***
***
***
***
[Fluoxetine]
F
HAPI cell viability (%)
**
[Ibuprofen]

G

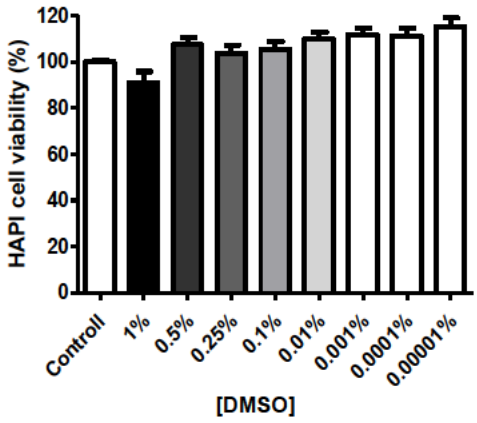

Figure 3.2 SIRT1 and SIRT2 modulators induce cytotoxicity in HAPI cells in a dose-dependent way.

HAPI cells were treated with resveratrol (A) (0.001-100 μM), sirtinol (B) (0.001-100 μM), EX527 (C) (0.001-100 μM), AGK2 (D) (0.001-100 μM), fluoxetine (E) (0.001-100 μM), ibuprofen (F) (0.001-100 μM), and DMSO (G) (0.00001-1%) for 24 h and assessed for cell viability using resazurin assay. One-way ANOVA followed by Turkey's multiple comparison test was applied. Significance levels were shown as $P< 0.05$ (*), $P<0.01$ (**) and $P< 0.001$ (***). Data indicate mean ± SD of three independent experiments.

3.4.2 SIRT1 and SIRT2 modulators inhibit the production of LPS-induced neuroinflammation in HAPI cells

PGE_2 production by HAPI cells after LPS (0.005 μg/mL) challenge for 20 h was significantly reduced by 24-h treatments of SIRT1 and SIRT2 modulators with a series of concentrations. Resveratrol significantly reduced PGE_2 production at 20 μM by approximately 97% but showed no significant differences in the reduction compared to fluoxetine (1 μM) and ibuprofen (1 μM) (**Figure 3.3 A**). Sirtinol concentrations of 20 μM, 10 μM and 1 μM significantly decreased PGE_2 production by approximately 79%, 83%, and 100% respectively but showed no significant differences in the reduction compared to fluoxetine (1 μM) and ibuprofen (1 μM) (**Figure 3.3 B**). EX527 (0.1 μM) significantly repressed PGE_2 production of HAPI cells by approximately 65% but showed no significant differences in the reduction compared to fluoxetine (1 μM) and ibuprofen (1 μM) (**Figure 3.3 C**). AGK2 also significantly repressed PGE2 production of HAPI cells at 0.1 μM by approximately 69% but has been shown no significant

differences in the reduction compared to fluoxetine (1 µM) and ibuprofen (1 µM) (**Figure 3.3 D**).

Fluoxetine had a significant effect on the reduction of PGE_2 production of HAPI cells, which is approximately 91% at 1 µM and 72% at 0.1 µM (**Figure 3.3 E**). Ibuprofen also generated a significant effect on the reduction of PGE_2 production of HAPI cells, which is approximately 90% at 1 µM and 76% at 0.1 µM (**Figure 3.3 F**).

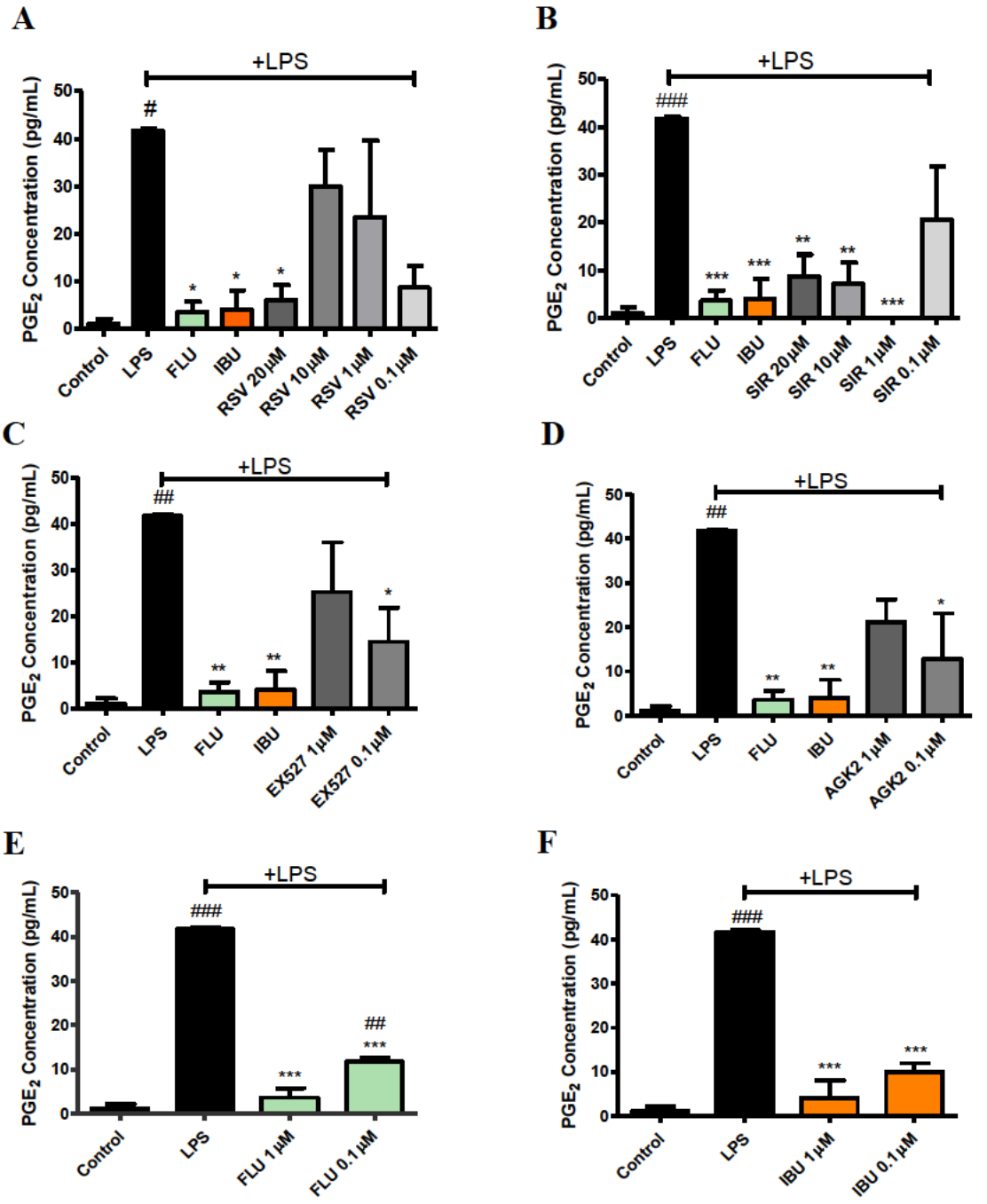

Figure 3.3 SIRT1 and SIRT2 modulators repress LPS-induced PGE_2 production in HAPI cells.

HAPI cells were treated with resveratrol (A) (0.1-20 µM), sirtinol (B) (0.1-20 µM), EX527 (C) (0.1, 1 µM), AGK2 (D) (0.1, 1 µM), fluoxetine (E) (0.1, 1 µM) and ibuprofen (F) (0.1, 1 µM) 4 h prior to LPS (0.005 µg/mL) challenge for 20 h and assessed for PGE_2 production using ELISA. Fluoxetine (1 µM) and ibuprofen (1 µM) were used as reference drugs. One-way ANOVA followed by Turkey's multiple comparison test was applied. Significance levels were shown as $P< 0.05$ (*, #), $P<0.01$ (**, ##) and $P< 0.001$ (***, ###). Data indicate mean ± SD of three independent experiments. # *vs* untreated media control only, * *vs* LPS only

TNF-α production by HAPI cells after LPS (0.005 μg/mL) challenge for 20 h was significantly repressed by 24-h treatments of SIRT1 and SIRT2 modulators with a series of concentrations. Resveratrol significantly decreased TNF-α production by approximately 95% at 20 μM, 90% at 10 μM, 70% at 1 μM, and 61% at 0.1 μM (**Figure 3.4 A**). Resveratrol also has been shown significant differences in the affecting TNF-α production of HAPI cells at 20-0.1 μM compared to both fluoxetine (1 μM) and ibuprofen (1 μM).

Sirtinol also significantly suppressed TNF-α production by approximately 93% at 20 μM and 85% at 10 μM respectively (**Figure 3.4 B**). Moreover, compared to fluoxetine, sirtinol at 20-0.1 μM has been shown significant differences in effect. Furthermore, 20 μM and 10 μM of sirtinol has been shown significant differences to ibuprofen treatment.

EX527 (**Figure 3.4 C**), AGK2 (**Figure 3.4 D**), fluoxetine (**Figure 3.4 E**), and ibuprofen (**Figure 3.4 F**) have been shown no significant difference in TNF-α production of HAPI cells after LPS treatment.

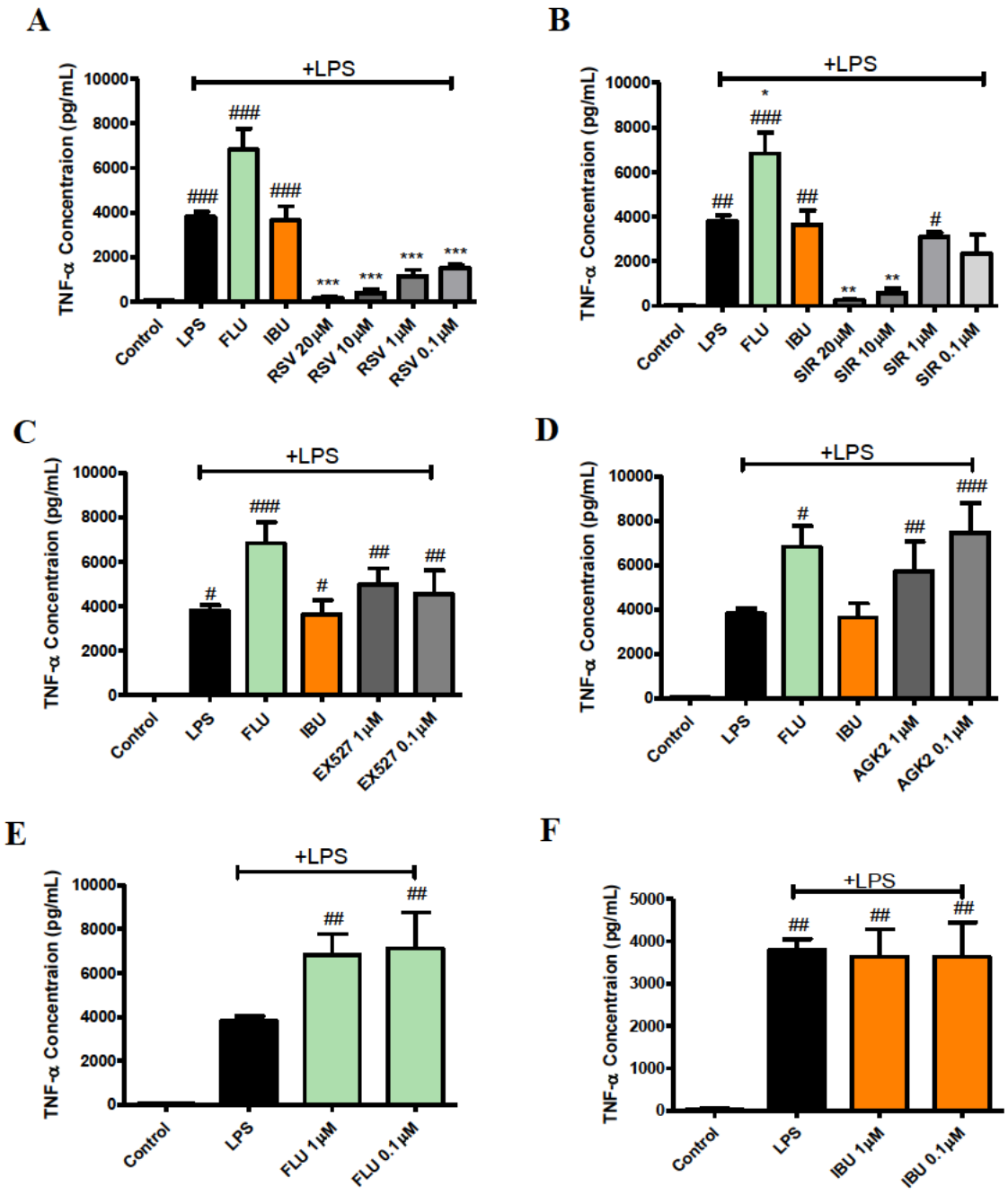

Figure 3.4 SIRT1 and SIRT2 modulators repress LPS-induced TNF-α production in HAPI cells

HAPI cells were treated with resveratrol (A), sirtinol (B), EX527 (C), AGK2 (D), fluoxetine (E) and ibuprofen (F) at a series of concentrations 4 h prior to LPS (0.005 μg/mL) challenge for 20 h and assessed for TNF-α production using ELISA. One-way ANOVA followed by Turkey's multiple comparison test was applied. Significance levels were shown as P< 0.05 (*, #), P<0.01 (**, ##) and P< 0.001 (***, ###). Data indicate mean ± SD of three independent experiments. # *vs* untreated media control only, * *vs* LPS only.

SIRT1 and SIRT2 modulators including resveratrol (20 µM, 10 µM, 1 µM, 0.1 µM), sirtinol (20 µM, 10 µM, 1 µM, 0.1 µM), EX527 (1 µM, 0.1 µM) and AGK2 (1 µM, 0.1 µM) did not stimulate the production of IL-1β and IL-10 in LPS (0.005 µg/mL)-induced HAPI cells. Fluoxetine and ibuprofen (1 µM, 0.1 µM) did not exert any effect on the production of IL-1β and IL-10 in LPS (0.005 µg/mL)-induced HAPI cells.

3.4.3 SIRT1 and SIRT2 modulators affect the production of LPS-induced reactive oxidative species in HAPI cells

We aimed to test whether SIRT1 and SIRT2 modulators affect the production of reactive oxidative species (ROS) in LPS-challenged (0.005 µg/mL) HAPI cells.

Resveratrol significantly reduced ROS production of LPS-challenged HAPI cells by approximately 37% at 20 µM, 27% at 10 µM, 23% at 1 µM, and 13% at 0.1 µM (**Figure 3.5 A**). Resveratrol at 20 µM has been shown a significant difference from fluoxetine (1 µM) and ibuprofen (1 µM) in the reduction of ROS level. In contrast, sirtinol significantly stimulated the increase of the ROS level of LPS-challenged HAPI cells at 20 µM and 10 µM (**Figure 3.5 B**).

EX527 (1 µM) significantly decreased ROS production of LPS-challenged HAPI cells by approximately 10% but had similar effects to fluoxetine (1 µM) and ibuprofen (1 µM) (**Figure 3.5 C**). AGK2 did not affect the ROS production of LPS-challenged HAPI cells (**Figure 3.5 D**).

Fluoxetine significantly reduced the ROS production of LPS-challenged HAPI cells by approximately 21% at 1 µM and 0.1 µM (**Figure 3.5 E**). Ibuprofen significantly reduced the ROS production of LPS-challenged HAPI cells by approximately 21% at 1 µM and 26% at 0.1 µM (**Figure 3.5 F**).

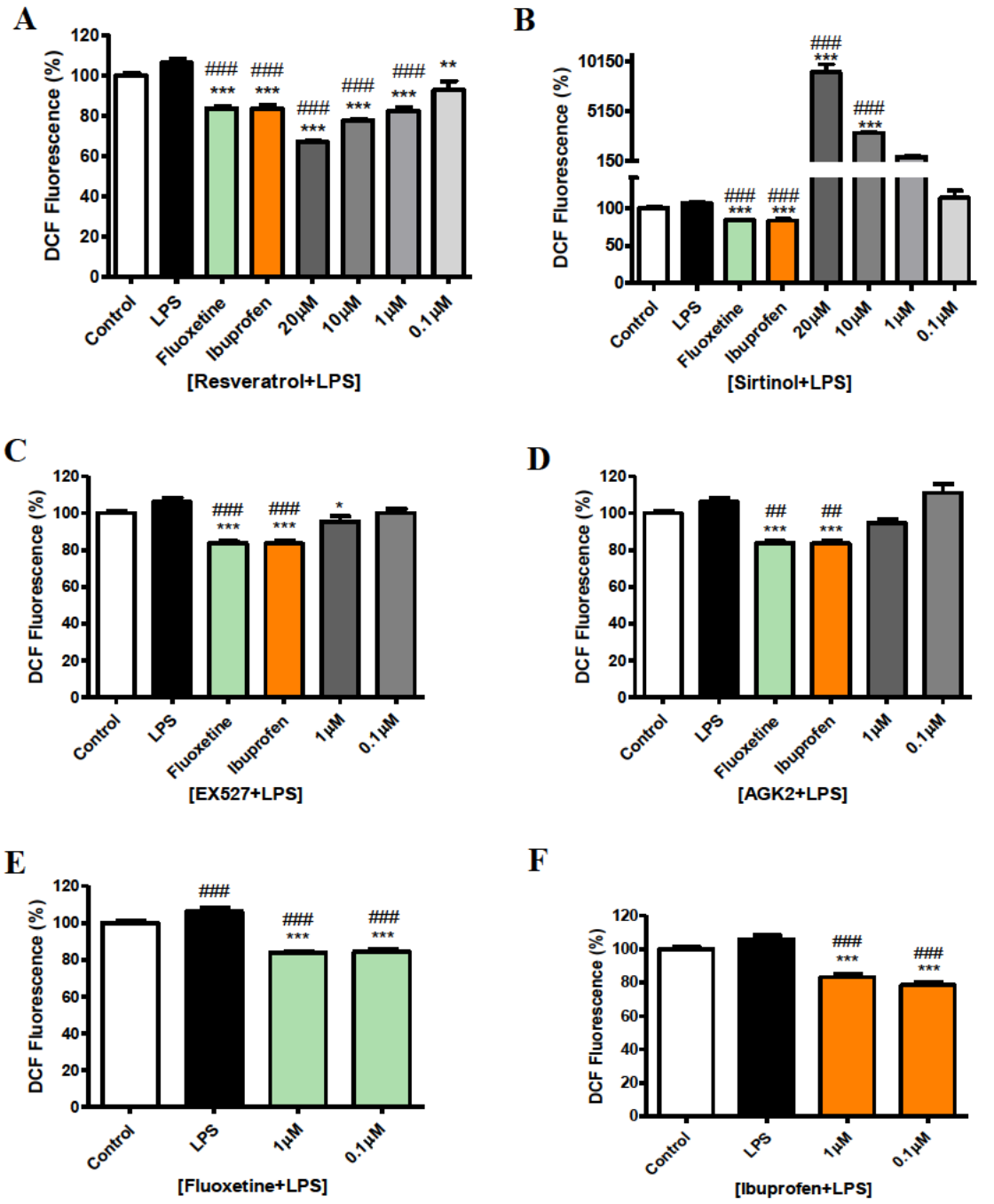

Figure 3.5 SIRT1 and SIRT2 drugs affect LPS-induced oxidative stress production in HAPI cells.

HAPI cells were treated with resveratrol (A) (0.1-20 µM), sirtinol (B) (0.1-20 µM), EX527 (C) (0.1, 1 µM), AGK2 (D) (0.1, 1 µM), fluoxetine (E) (0.1, 1 µM) and ibuprofen (F) (0.1, 1 µM) 4 h prior to LPS (0.005 µg/mL) challenge for 20 h and assessed for oxidative stress production using DCF assay. Fluoxetine (1 µM) and ibuprofen (1 µM) were used as reference drugs. One-way ANOVA followed by Turkey's multiple comparison test was applied. Significance levels were shown as P< 0.05 (*), P<0.01 (**, ##) and P< 0.001 (***, ###). Data indicate mean ± SD of three independent experiments. # *vs* untreated media control only, * *vs* LPS only.

3.4.4 SIRT1 and SIRT2 expression in HAPI cells after 4h treatment of SIRT1 and SIRT2 modulators

To investigate whether resveratrol, EX527 can affect the gene expression of SIRT1 and whether sirtinol and AGK2 can affect SIRT2 expression, rt-PCR was conducted to measure SIRT1 and SIRT2 expression after 4 h drug treatment. As shown in **Figure 3.6 A**, resveratrol (20 μM) is not shown to significantly affect SIRT1 expression in HAPI microglial cells. The expression of SIRT1 under EX527 (1 μM) was undetermined. SIRT2 expression was also not shown significantly affected by sirtinol (20 μM) and AGK2 (1 μM) (**Figure 3.6 B**).

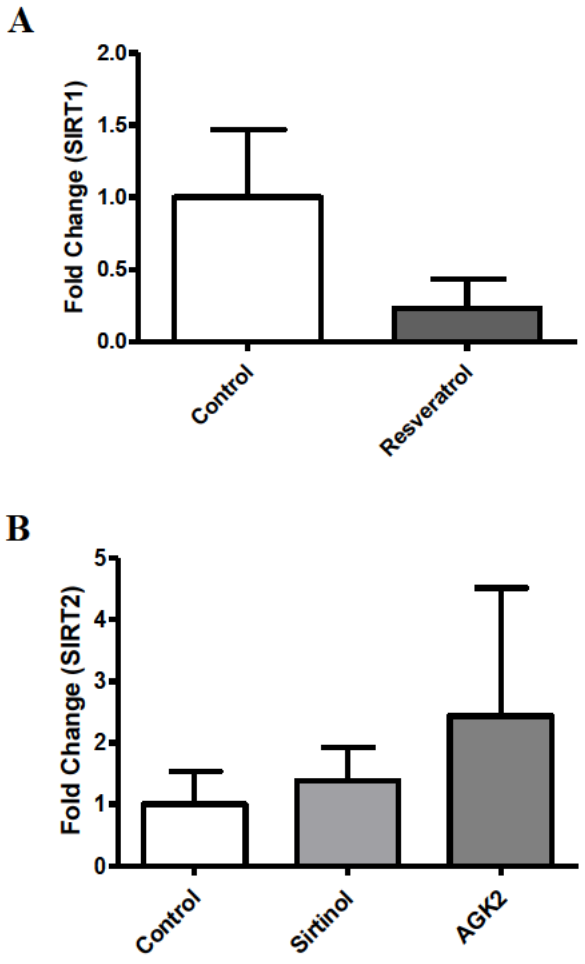

Figure 3.6 SIRT1 and SIRT2 mRNA expression after 4 h drug pre-treatment.

HAPI cells were treated with resveratrol (20 μM), sirtinol (20 μM), EX527 (1 μM), AGK2 (1 μM) for 4 h prior to mRNA extraction. Rt-PCT was applied to measure the expression of SIRT1 (A) and SIRT2 (B).

3.5 Discussion

The effects of these SIRT1 and SIRT2 drugs on the production of inflammatory mediators on LPS-stimulated microglia have been assessed in this chapter. All SIRT drugs, fluoxetine and ibuprofen were shown to significantly reduce PGE_2 production. Prostaglandins are synthesized by COX 1 and 2 which can be induced by LPS and/or by pro-inflammatory cytokines in the brain (B. E. Leonard, 2018). It has been demonstrated that prostaglandins play an important role in the development of chronic inflammation (S. Narumiya, 2009, T. Honda et al., 2006). Prostaglandins contribute to prolonged acute inflammatory responses by activating chronic gene expression by inhibiting the differentiation of Th2 cells which produce anti-inflammatory cytokine IL-10 (B. E. Leonard, 2018). In terms of PGE_2 and associated contribution to chronic inflammation, resveratrol, EX527, sirtinol and AGK2 have shown a potential benefit in the enhancement of anti-inflammatory mediators. However, the production of prostaglandins can also be affected by nitric oxide (NO). It has been reported that NO can activate COX in a macrophage cell line after LPS stimulation (D. Salvemini et al., 1993). Moreover, fluoxetine has been found to suppress NO production, which might contribute to the inhibiting effect on PGE_2 (I. Yaron et al., 1999). However, the crosstalk between NO and COX can alter between activation and inhibition (S. F. Kim, 2011). In some conditions, NO can inactivate COX2 expression and related PGE_2 production in LPS-stimulated macrophages (R. Clancy et al., 2000, L. Minghetti et al., 1996).

Only resveratrol and sirtinol were shown to significantly reduce the production of TNF-α, whereas EX527, AGK2, fluoxetine and ibuprofen did not show inhibitory effects on TNF-α production of HAPI cells in the presence of LPS. TNF-α is first produced as a precursor in a transmembrane form. Then it can be transformed into a soluble form by TNF-α-converting enzyme (TACE) and released outside the cell membrane (T. Horiuchi et al., 2010). Both transmembrane and soluble forms of TNF-α can bind to TNF receptors and exert physiological functions (T. Horiuchi et al., 2010). However, the mechanism of release of LPS-induced IL-1β is unclear as it does not follow the conventional endoplasmic reticulum (ER)-Golgi route (G. Lopez-Castejon and D. Brough, 2011). Under the stimulation of LPS, IL-1β is first generated as an inactive precursor pro-IL-1β which is subsequently cleaved by IL-1 converting enzyme (ICE), a member of caspase-1. Caspase-1 also needs to be activated by the formation of

inflammasome which contains pro-caspase-1 (G. Lopez-Castejon and D. Brough, 2011). Also, the assembly of inflammasomes is dependent upon the activation of P2X7 receptors on the cell membrane by extracellular adenosine triphosphate (ATP) (M. Stoffels et al., 2015a). Therefore, this might be a reason that IL-1β was not detected through ELISA measurement in this LPS-induced (0.005 μg/mL) neuroinflammation model. In this model, LPS did not result in acute cell death of HAPI cells, which means there was not a large amount of ATP release following cell membrane damage to activate the P2X7 receptors on the remaining HAPI cells and lead to the maturation and release of IL-1β (J. M. Sanz and F. Di Virgilio, 2000). Thus, to stimulate the maturation and secretion of IL-1β, 1 mM of ATP should be dissolved 2 min before adding into the wells and incubated for 15 min before the collection of supernatant before running ELSIA (M. Stoffels et al., 2015b).

The IL-10 family is another important cytokine produced by microglia upon TLR stimulation, which can be regulated by adenosine and further inhibit the production of other pro-inflammatory cytokines *in vitro* (D. Lobo-Silva et al., 2016). However, IL-10 was not detected in HAPI cells after LPS stimulation and drug treatment in this study. This result indicates that IL-10 production might not participate in the anti-inflammatory effects of SIRT1 and SIRT2 drugs in mild neuroinflammation circumstances.

Resveratrol as a SIRT1 activator and sirtinol as a dual SIRT1/2 inhibitor had a better anti-inflammatory effect than the selective SIRT1 inhibitor EX527 and the SIRT2 inhibitor AGK2 in our *in vitro* neuroinflammation study. EX527 has been often administered to verify the effects of SIRT1 activator resveratrol in other neurodegeneration studies (Y. J. Guo et al., 2016, C. Diaz-Ruiz et al., 2015). However, based on our results, whether EX527 should be recommended to be used as a pharmacological suppressor to inhibit the SIRT1 pathway in the application of inflammation research still needs further discussion. AGK2 as a SIRT2 inhibitor also did not show a very promising inhibitory effect on inhibiting LPS-induced neuroinflammation. However, as discussed in the literature, SIRT2 inhibitors could potentially be beneficial in antagonizing neuroinflammation and neurodegeneration (B. Wang et al., 2016, C. Scuderi et al., 2014). There can be several factors that may cause the result to be inconsistent, such as different cell lines, experimental systems, types of stimuli and animal experiments.

In regards to the anti-inflammatory effects of fluoxetine, it has been reported that fluoxetine can inhibit the production of TNF-α, PGE_2 and IL-6 in the LPS-stimulated BV-2 microglial cells by influencing multiple pathways such as NF-κB and mitogen-activated protein kinase (MAPK) (D. Liu et al., 2011), which is not completely in line with our results in HAPI cells. Additionally, as mentioned above, fluoxetine has been reported to suppress the production of PGE_2 and nitric oxide simultaneously, the mechanism might be the interaction between NO and COX activities (I. Yaron et al., 1999, S. F. Kim, 2011). The controversy of fluoxetine was also discussed in the introduction, as the data provided by the limited clinical studies are highly variable and contradictory between studies. Therefore, it cannot yet be concluded that the antidepressant therapeutic effect of fluoxetine is partially attributed to its anti-inflammatory effect.

Regarding the oxidative stress, resveratrol, EX527, fluoxetine and ibuprofen have shown significant inhibitory effects on HAPI cells in the presence of LPS. Whereas, sirtinol was shown to trigger the production of reactive oxygen species (ROS). ROS is a metabolic by-product of normal metabolism and causes damage to crucial cellular components including DNA, protein and lipids (D. G. Deavall et al., 2012). This result indicates that sirtinol may potentially be causing some unknown drug-related side effects to tissues and organ systems. Other agents including resveratrol, EX527, AGK2, fluoxetine and ibuprofen might exert lesser damage to the target tissue in terms of oxidative stress. Regarding whether the gene expression of SIRT1 and SIRT2 can be affected by these SIRT modulators, only one pre-treatment condition with limited concentrations was assessed on HAPI microglial cells, which cannot represent all other conditions including adding LPS trigger or other disease models. Further development is needed to investigate the impact the SIRT drugs on gene expression.

In conclusion, this chapter has assessed drug cytotoxicity, anti-inflammatory effects and induced ROS production of resveratrol, sirtinol, EX527 and AGK2 in microglial HAPI cells and compared them with fluoxetine and ibuprofen. Although, SIRT1 activator and inhibitor or SIRT2 inhibitor did not exert exact similar or opposites effects in regards of PGE_2, cytokines and ROS production in this study. SIRT2 is often reported to exert the opposing effect to SIRT1 in neurodegeneration studies (G. Donmez and T. F. Outeiro, 2013). However, based on available *in vitro* studies of inflammation, different reports using various *in vitro* models and stimuli have reported contradictory

findings, suggesting that the effect of SIRT2 modulators needs to be interpreted based on the biochemical conditions of different models. For example, an *in vitro* study of brain injury showed that the SIRT2 inhibitor AK-7 can increase the expression of pro-inflammatory cytokines in primary microglia after stretch-induced injury (F. Yuan et al., 2016a), and a similar pro-inflammatory effect of AK7 was reported in a cell culture system that investigated spinal cord injury (D. Romeo-Guitart et al., 2018). However, in a study of allergic asthmatic inflammation, SIRT2 inhibitor AGK2 diminished inflammatory manifestations, including the activation of lung macrophages and expression of chemokine CCL17 (Y. G. Lee et al., 2019). Sirtinol, as a dual inhibitor of SIRT1 and SIRT2, was also shown to reduce inflammation in primary dermal microvascular endothelial cells (A. Orecchia et al., 2011). The data in this study has shown the potential of employing these agents to treat the activation of microglia as the primary component of the innate immune system of the CNS and the release of inflammatory mediators from them. However, a more comprehensive understanding and further discovery of more effective SIRT1 and SIRT2 modulators or a specific modulator type need to be established on larger scale of drug scanning and pharmacological evaluation on different cell lines. In the next chapter, SH-SY5Y cells as neuronal models will be used to investigate the effects of SIRT1 and SIRT2 drugs on subsequent neurodegeneration after exposure to neuroinflammation. To achieve this aim, the conditioned supernatant of HAPI cells collected by the methods mentioned in this chapter will be transferred onto SH-SY5Y cells and assays conducted on them. Detailed methods and results are shown in the next chapter.

Chapter 4 : SIRT1 and SIRT2 modulators inhibit neuroinflammation-induced subsequent neurodegeneration in *in vitro* neuronal models

4.1 Introduction

4.1.1 Neuroinflammation and subsequent neurodegeneration

Physiologically, the existence of inflammation including cytokine networks and COX-2 activity plays a protective role in regulating learning and memory, development of synaptic remodeling and upregulating synaptic activities (R. A. Khairova et al., 2009, N. G. Bazan, 2001). However, prolonged and accumulating inflammatory mediators can have pathological effects such as synaptic impairment, disturbance of neurogenesis and neuronal death (M. Lyman et al., 2014). The IL-1 family is a pivotal member of the inflammatory mediators that respond and take controls of pro-inflammatory reactions to diverse stimuli, injury and stress (A. Weber et al., 2010a). IL-1α is mainly binding on cell membranes and secreted through autocrine and juxtracrine pathways (A. Weber et al., 2010a). It is present in varieties of cells in healthy conditions. Under stress stimulation without cell death, the binding of membrane IL-1α and IL-1R can initiate more cytokine production from neighbouring cells and recruit other myeloid cells to the site (N. C. Di Paolo and D. M. Shayakhmetov, 2016). Unlike IL-1α functioning as an alarm signal or DAMP itself, IL-1β is produced under stimulation by DAMPs and PAMPs and secreted through paracrine or endocrine in a systemic manner (A. Weber et al., 2010a). IL-1β regulates inflammation by binding to receptor IL-1R and sequentially activating mitogen-activated protein kinase (MAPK) signalling and the NF-κB pathway to mediate the expression of a secondary inflammation (A. Weber et al., 2010a, A. Weber et al., 2010b). It has been reported that IL-1β contributes to the loss of synaptic connections with the participation of PGE_2 and activation of NMDA receptors which lead to excitotoxicity (A. Mishra et al., 2012). TNF-α can bind to tumor necrosis factor receptor 1 (TNFR1), one pathway of which subsequently recruits TNFR-associated death domain (TADD) that further activates caspase 8, sequentially caspase-3 activation and induces apoptosis (B. B. Aggarwal, 2003). Whereas, the other pathway of TADD binding with TNFR2 leads to the activation of NF-κB which in turn promotes neuron survival (B. B. Aggarwal, 2003). Also, the level of TNF-α production and the balance between the two TNF pathways determines the initiation of apoptosis or survival and the degree of neuronal apoptosis (M. Lyman et al., 2014, B. B. Aggarwal, 2003).

4.1.2 SIRT1 and SIRT2 modulators in neuroprotection

SIRT1 and SIRT2 drugs have been shown to exert neuroprotective effects in numerous neurodegenerative disease studies. However, there has still not been a systematic analysis of the effects of this class of drugs on neurodegeneration.

Resveratrol is a natural SIRT1 activator that has been investigated in cellular and animal models of Alzheimer's disease, Parkinson's disease, amyotrophic lateral sclerosis and aging. In an AD study on p25 transgenic mice, resveratrol was found to prevent neurodegeneration and cognitive decrease via acetylation of peroxisome proliferator-activated receptor-gamma coactivator (PGC)-1α, a master regulator of mitochondrial biogenesis, and up-regulation of SIRT1 (D. Kim et al., 2007). Similarly, in a PD study on dopaminergic SN4741 cell line reported increases of PGC-1α and SIRT1 levels induced by resveratrol treatment (G. Mudo et al., 2012). The up-regulation of SIRT1 by resveratrol has also been reported to benefit mitochondria function in motor neuron-like cell line VSC 4.1 (J. Wang et al., 2011). Besides, AMPK activation and tumor suppressor p53 acetylation has also been reported to participate in the mechanism in SOD^{G93A} transgenic mice (R. Mancuso et al., 2014). In aged mouse models, resveratrol also has been shown to increase SIRT1 expression and decrease apoptosis (P. Moorthi et al., 2015).

EX527 is a selective SIRT1 inhibitor the effect of which remains controversial due to lack of research. It has been found that EX527 prevented transgenic neuronal cells from death after treatment of mutant SOD1 toxicity and improved the survival of transgenic SH-SY5Y cells as ALS models (C. Valle et al., 2014). However, it was also reported that EX527 could exacerbate protein aggregation in primary neurons, which indicates more consideration and investigation should be done before administration (S. W. Min et al., 2010). Besides, sirtinol is a dual inhibitor of SIRT1 and SIRT2 as introduced in Chapter 3 that also was shown to exacerbate neurodegeneration of differentiated SK-N-BE cells (D. Albani et al., 2009). AGK2 is a selective SIRT2 inhibitor. Some studies show that AKG2 can protect dopaminergic cells from toxicity induced by α-synuclein and protect primary rat striatal neurons from toxicity induced by mutant Huntingtin (T. F. Outeiro et al., 2007, R. Luthi-Carter et al., 2010).

Based on these findings above, it is found that all these drugs were employed in different disease models or used under different forms of stimuli. Therefore, a uniform

neurodegeneration model needs to be applied to assess SIRT1 and SIRT2 drugs and compare their effects in the same condition. In this chapter, to achieve this aim, undifferentiated and differentiated SH-SY5Y cells were treated with the conditioned supernatant collected from HAPI cells after drug pre-treatment and exposure to LPS. Then the alteration of apoptosis during this supernatant transfer was further assessed.

4.2 Materials and methods

4.2.1 Cells and reagents

SH-SY5Y cells were purchased from Sigma-Aldrich. They were grown in ATCC-formulated DMEM (Gibco by Life Technologies, 11885084) which contains low glucose (1 g/L D-Glucose), L-glutamine (584 mg/L), sodium pyruvate (110 mg/L) and phenol red (15 mg/L). The media was additionally supplemented with 1% penicillin-streptomycin (Gibco by Life Technologies) and 10% fetal bovine serum (FBS) (Scientifix Life). SH-SY5Y cells were grown in sterile T-75 cm^2 flasks and cultured in an incubator at 37°C with 5% CO_2 and high humidity.

4.2.2 Treatment preparation

Prior to treatment, all stocks (10 mM: resveratrol (RSV), sirtinol (SIR), EX527, AGK2, fluoxetine (FLU) and ibuprofen (IBU)) were diluted to a working solution (1:10). The final proportion of DMSO in each well of plates was below 0.01%. BDNF was reconstituted in distilled water to a concentration of 10 µg/mL as stock and stored in a -20°C freezer for future use. RA was dissolved in DMSO at a concentration of 25 mM and stored in a -20°C freezer for future use and protected from light when applying. The LPS stock solution (1 mg/mL) was diluted from 1:10 to a working solution before treatments were conducted.

4.2.3 Establishment of neuroinflammation-induced neurodegeneration *in vitro* neuronal model

4.2.3.1 Undifferentiated neuronal model

SH-SY5Y cells were seeded at 10^5 cells/mL on 96-well plates and placed in an incubator for 24 h. To induce neuroinflammation-induced neurodegeneration, the supernatant above SH-SY5Y cells was removed and treated with conditioned-supernatant of HAPI cells for 24 h. The conditioned supernatant was collected from HAPI cells in 24-well plates after 20 h LPS treatment with/without 4 h pre-treatment

of resveratrol, sirtinol, EX527, AGK2, fluoxetine and ibuprofen in a series of concentrations.

4.2.3.2 Differentiated neuronal model

SH-SY5Y cells were seeded at 10^5 cells/mL (100 µL) on 96-well plates and placed in an incubator for 24 h. Then, cells were treated with 10 µM of retinoic acid (RA) every other day for a 5-day period in complete medium containing 10% FBS, followed with a treatment of 50 ng/mL of BDNF for 3 executive days in serum-free medium. After that, the supernatant above SH-SY5Y cells was removed and treated with conditioned-supernatant of HAPI cells for 24 h. The conditioned supernatant was collected from HAPI cells in 24-well plates after 20 h LPS treatment with/without 4 h pre-treatment of resveratrol, sirtinol, EX527, AGK2, fluoxetine, and ibuprofen in a series of concentrations.

4.2.4 Resazurin assay

To test the cytotoxicity induced by SIRT1 and SIRT2 drugs on undifferentiated SH-SY5Y cells, cells were seeded on 96-well plates with a cell density of 10^5 cells/mL (100 µL) and incubated for 24 h. After that, cells were treated with resveratrol, sirtinol, EX527, AGK2, fluoxetine, ibuprofen, and DMSO with a series of concentrations and LPS (0.005 µg/mL) for 24 h. For differentiated cells, after the last treatment of BDNF, the same drug treatments were conducted. Each treatment had 6 replicates. Then, the resazurin assay was conducted for cell viabilities.

To test whether SIRT1 and SIRT2 modulators can alleviate neuroinflammation-induced subsequent neurodegeneration on undifferentiated cells, cells were seeded on 96-well plates with a cell density of 10^5 cells/mL (100 µL) and incubated for 24 h. Then, the supernatant was replaced by the supernatant collected from HAPI cells after LPS (0.005 µg/mL) challenge and the combination pre-treatment with resveratrol, sirtinol, EX527, AGK2, fluoxetine and ibuprofen. For differentiated cells, after the last treatment of BDNF, the same supernatant treatments were added onto them and incubated for 24 h. Then, resazurin assay was conducted for measurement of cell viabilities.

Resazurin assays were run to detect cell viabilities of undifferentiated and differentiated SH-SY5Y cells. After treatment, the supernatant above cells was removed and replaced with diluted resazurin solution (44 µM) and incubated for 3 h. After that, fluorescence

(excitation: 530 nm and emission: 590 nm) value was read and recorded using a Tecan Infinite 200 Pro microplate reader (Tecan, Australia).

4.2.5 Caspase 3/7 assay

SH-SY5Y cells were seeded at 10^5 cells/mL (100 µL) on 96-well plates and incubated for 24 h. For the undifferentiated cells, the supernatant of HAPI cells after LPS challenge and drug treatment was transferred onto the cells in the 96-well plates and incubated for 24 h. For the differentiated model, SH-SY5Y cells were induced to differentiated after seeding for an 8-day period, then the same supernatant was transferred onto the differentiated cells and incubated for 24 h. After that, caspase 3/7 assays (Cayman Chemical, Australia) were conducted to measure the apoptosis level of cells. The cells were centrifuged to the bottom of the plates and rinsed with assay buffer and lysed afterward. The supernatant containing caspase 3/7 was collected and transferred to corresponding wells on a black plate. Caspase 3/7 substrate was added into each well and incubated for 30-90 min at 37°C. After that, the fluorescence (excitation: 485 nm and emission: 535 nm) intensity value was read and recorded using a Tecan Infinite 200 Pro microplate reader (Tecan, Australia).

4.2.6 Trypan blue dye exclusion assay

Trypan blue dye was used to differentiate dead cells and viable cells. Cell concentrations were measured using an automatic cell counter or hemocytometer under Olympus IX53 microscope.

4.2.7 Statistical analysis

All data were analyzed by GraphPad Prism 5 and presented as mean ± SD. One-way ANOVA and t tests were used to determine the significant difference. $P<0.05$ was considered a significant difference.

4.3 Results

4.3.1 SIRT1 and SIRT2 modulators induced cytotoxicity in SH-SY5Y cells in a dose-dependent way

Resveratrol exerted significant cytotoxicity on undifferentiated SH-SY5Y cells at 100, 50, 25, 10, 1 and 0.1 µM (**Figure 4.1 A**). The graph shows increasing concentrations reduced cell viability. Data showed no significant difference between 1 and 0.1 µM.

Sirtinol produced significant cytotoxicity on undifferentiated SH-SY5Y cells at 100 µM and 50 µM (**Figure 4.1 B**). The graph shows increasing concentrations reduced cell viability. Data showed no significant difference between 10, 1 and 0.1 µM.

EX527 exerted significant cytotoxicity on undifferentiated SH-SY5Y cells at 100 µM (**Figure 4.1 C**). The graph shows increasing concentrations reduced cell viability. Data showed no significant difference between 10, 1 and 0.1 µM.

AGK2 produced significant cytotoxicity on undifferentiated SH-SY5Y cells at 100 µM (**Figure 4.1 D**). The graph shows increasing concentrations reduced cell viability. Data showed no significant difference between 10, 1 and 0.1 µM.

As control drugs, the results showed that fluoxetine showed significant cytotoxicity on undifferentiated SH-SY5Y cells at 10 and 1 µM (**Figure 4.1 E**). Ibuprofen showed no cytotoxicity from 10 to 0.1 µM (**Figure 4.1 F**).

DMSO exerted no significant cytotoxicity under 0.5% (**Figure 4.1 G**). LPS with a concentration of 0.005 µg/mL showed no cytotoxicity on undifferentiated SH-SY5Y cells (**Figure 4.1 H**).

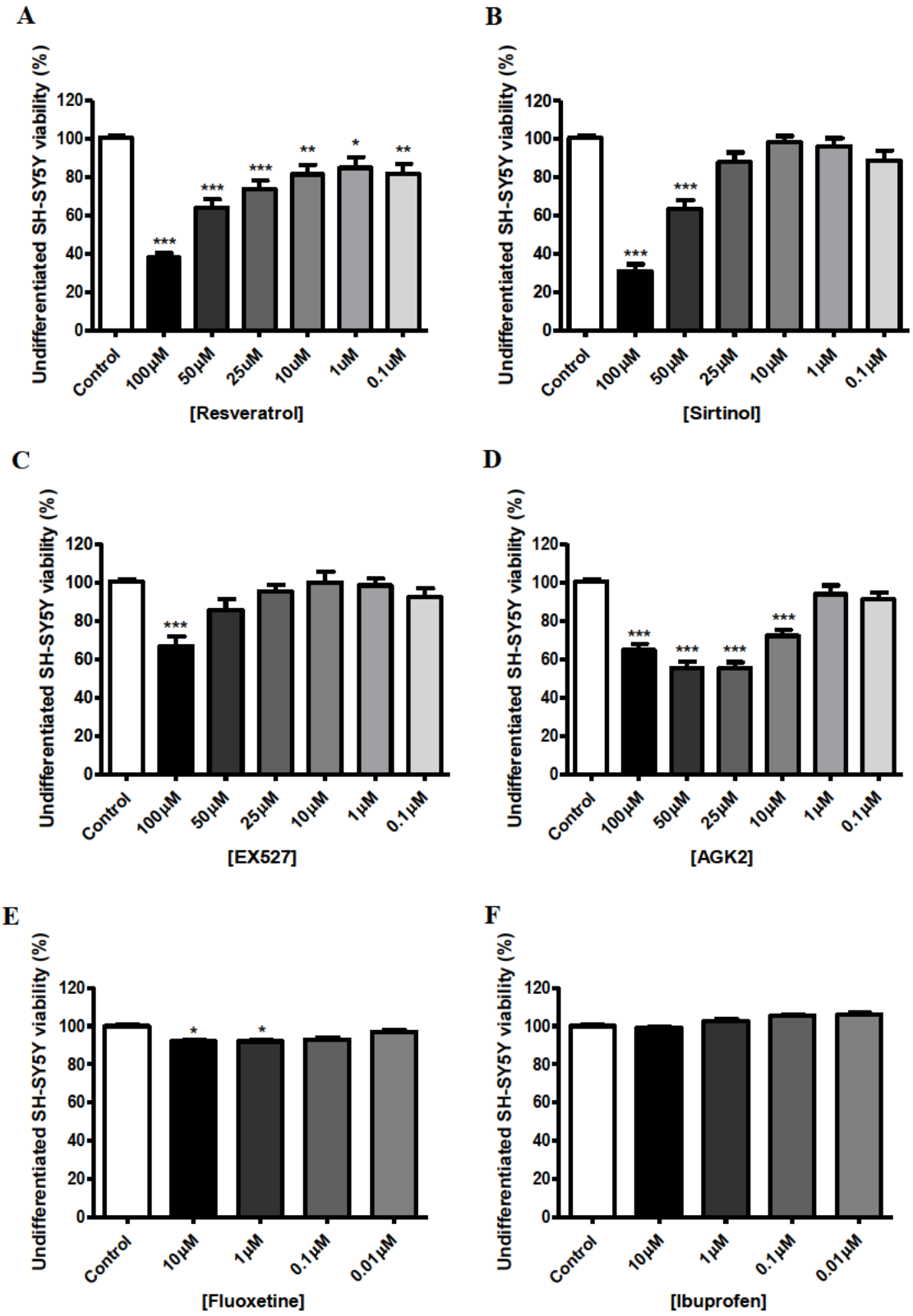
A
Undifferentiated SH-SY5Y viability (%)
120
100
80
60
40
20
0
***
***
***
**
*
**
Control
100µM
50µM
25µM
10µM
1µM
0.1µM
[Resveratrol]
B
Undifferentiated SH-SY5Y viability (%)
***
***
Control
100µM
50µM
25µM
10µM
1µM
0.1µM
[Sirtinol]
C
Undifferentiated SH-SY5Y viability (%)
***
Control
100µM
50µM
25µM
10µM
1µM
0.1µM
[EX527]
D
Undifferentiated SH-SY5Y viability (%)
***
***
***
***
Control
100µM
50µM
25µM
10µM
1µM
0.1µM
[AGK2]
E
Undifferentiated SH-SY5Y viability (%)
*
*
Control
10µM
1µM
0.1µM
0.01µM
[Fluoxetine]
F
Undifferentiated SH-SY5Y viability (%)
Control
10µM
1µM
0.1µM
0.01µM
[Ibuprofen]

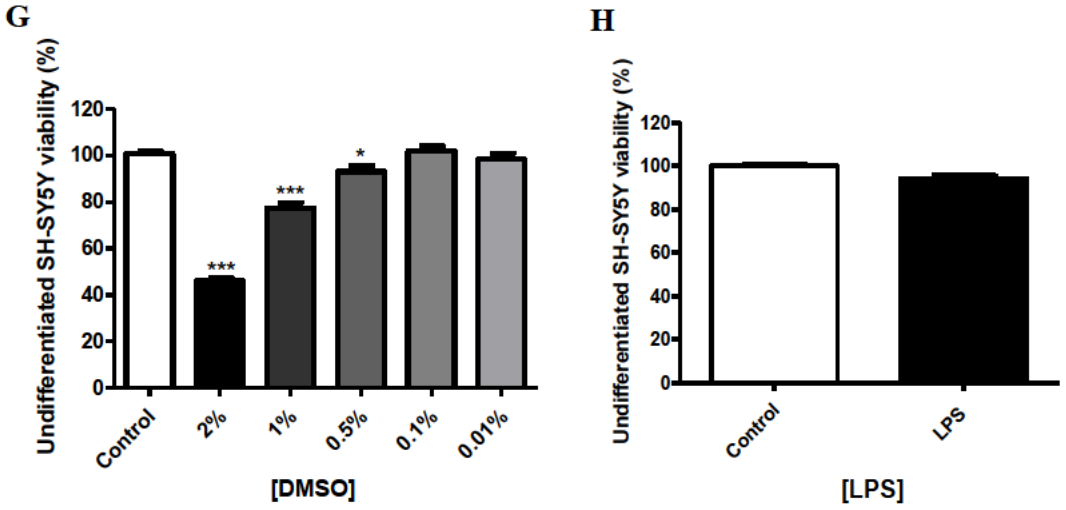

Figure 4.1 SIRT1 and SIRT2 modulators induced cytotoxicity in undifferentiated SH-SY5Y cells in a dose-dependent way

Undifferentiated SH-SY5Y cells were treated with resveratrol (A) (0.1-100 µM), sirtinol (B) (0.1-100 µM), EX527 (C) (0.1-100 µM), AGK2 (D) (0.1-100 µM), fluoxetine (E) (0.01-10 µM), ibuprofen (F) (0.01-10 µM), DMSO (G) (0.01-2%), and LPS (0.005 µg/mL) (H) for 24 h and assessed for cell viability using resazurin assay. One-way ANOVA followed by Turkey's multiple comparison test and t tests were applied. Significance levels were shown as $P< 0.05$ (*), $P<0.01$ (**) and $P< 0.001$ (***). Data indicate mean ± SD of three independent experiments.

4.3.2 SIRT1 and SIRT2 modulators protected undifferentiated SH-SY5Y cells from death induced by HAPI-conditioned supernatant

To test whether SIRT1 and SIRT2 modulators can attenuate neuroinflammation-induced subsequent neurodegeneration, undifferentiated SH-SY5Y cells were seeded on 96-well plates with a cell density of 10^5 cells/mL (100 µL) and incubated for 24 h in an incubator. After that, supernatant of HAPI cells after LPS (0.005 µg/mL) challenge and the combination treatment with resveratrol, sirtinol, EX527, AGK2, fluoxetine and ibuprofen for 24 h was transferred onto the undifferentiated SH-SY5Y cells and incubated for 24 h. Then, resazurin assay was conducted for measurement of cell viability.

The survival rate of undifferentiated SH-SY5Y cells significantly improved after the challenge of HAPI cells' LPS and resveratrol-conditioned supernatant by approximately 11% at 20 µM, 24% at 10 µM, 21% at 1 µM, and 11% at 0.1 µM (**Figure 4.2 A**). Resveratrol demonstrated significant differences in greater survival improvement than fluoxetine (1 µM) at 10 µM and 1 µM. Resveratrol (10 µM) also demonstrated a significant difference from ibuprofen (1 µM).

Sirtinol also significantly promoted the survival rate of SH-SY5Y cells after the conditioned-supernatant challenge by approximately 35% at 20 µM, 40% at 10 µM, 24% at 1 µM, and 15% at 0.1 µM (**Figure 4.2 B**). It demonstrated significant differences in greater survival improvement from fluoxetine (1 µM) and ibuprofen (1 µM) at 20 µM, 10 µM, and 1 µM.

EX527 significantly increased the survival rate of SH-SY5Y cells after the conditioned-supernatant challenge by approximately 8% at 1 µM and 9% at 0.1 µM (**Figure 4.2 C**). There were no significant differences in the survival improvement from fluoxetine (1 µM) and ibuprofen (1 µM).

AGK2 (0.1 µM) significantly improved the survival rate of SH-SY5Y cells after the conditioned-supernatant challenge by approximately 10% (**Figure 4.2 D**). No significant differences were shown in the survival improvement from fluoxetine (1 µM) and ibuprofen (1 µM).

As control drugs, fluoxetine (0.1 µM) significantly improved the survival rate of SH-SY5Y cells after the conditioned-supernatant challenge by approximately 6% (**Figure**

4.2 E). Ibuprofen significantly increased the survival rate of SH-SY5Y cells after the LPS challenge by approximately 11% at 1 µM and 14% at 0.1 µM (**Figure 4.2 F**).

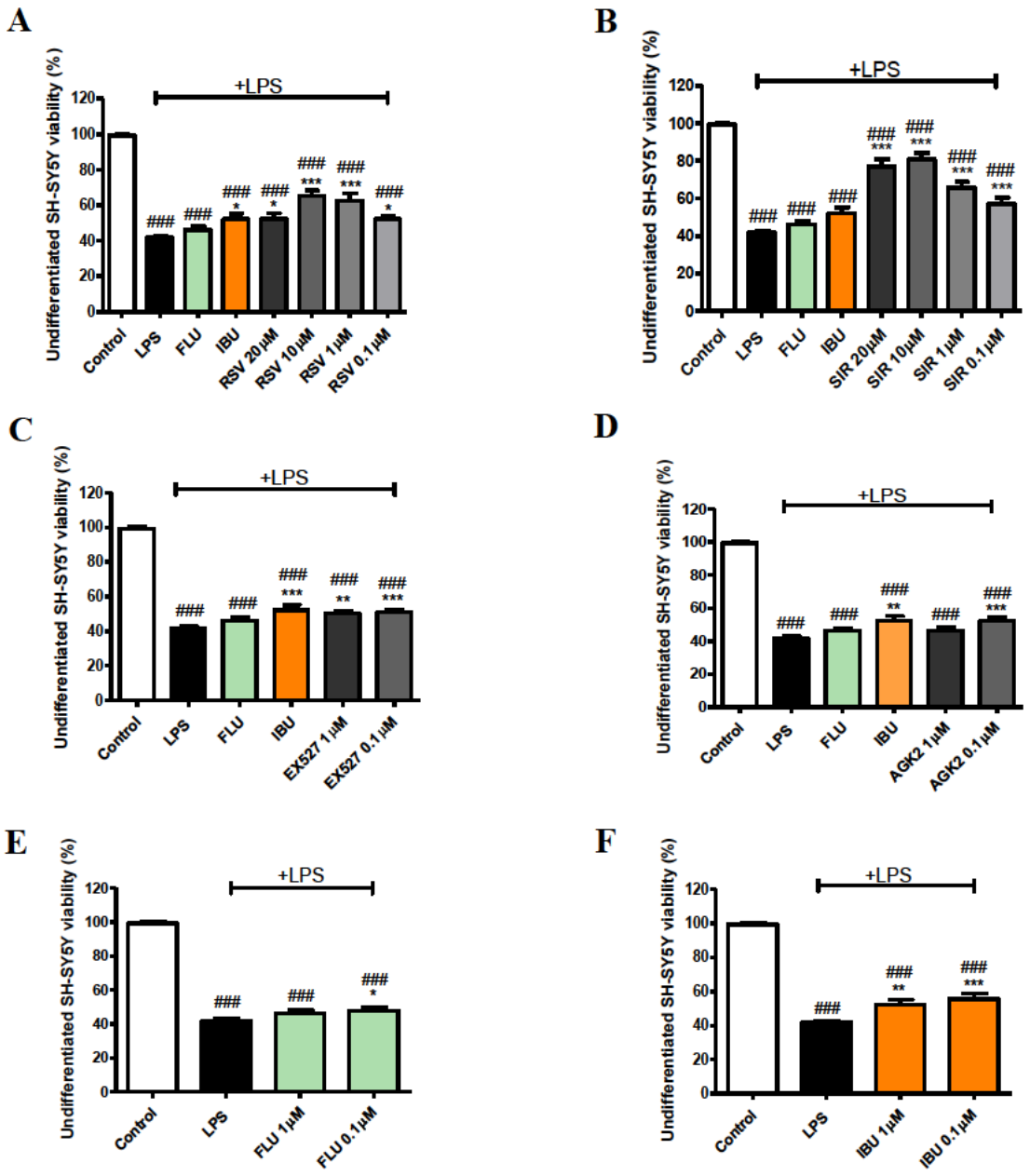

Figure 4.2 SIRT1 and SIRT2 modulators protected undifferentiated SH-SY5Y cells from death induced by supernatant of LPS-challenged HAPI cells

Undifferentiated SH-SY5Y cells were treated with supernatant produced by HAPI cells after treatment of resveratrol (A) (0.1-20 µM), sirtinol (B) (0.1-20 µM), EX527 (C) (0.1, 1 µM), AGK2 (D) (0.1, 1 µM), fluoxetine (E) (0.1, 1 µM) and ibuprofen (F) (0.1, 1 µM) 4 h prior to LPS (0.005 µg/mL) challenge for 20 h. Fluoxetine (1 µM) and ibuprofen (1 µM) were used as reference drugs. One-way ANOVA followed by Turkey's multiple comparison test was applied. Significance levels were shown as P< 0.05 (*, #), P<0.01 (**) and P< 0.001 (***, ###). Data indicate mean ± SD of three independent experiments. # *vs* untreated media control only, * *vs* LPS only

4.3.3 SIRT1 and SIRT2 modulators induced lesser cytotoxicity in differentiated SH-SY5Y cells.

Resveratrol produced no significant cytotoxicity on differentiated SH-SY5Y cells at 25 µM, 10 µM, 1 µM and 0.1 µM (**Figure 4.3 A**). Sirtinol exerted no significant cytotoxicity on differentiated SH-SY5Y cells below 25 µM (**Figure 4.3 B**). None of EX527, AGK2, fluoxetine, and ibuprofen had significant cytotoxicity on differentiated SH-SY5Y cells at 10 µM, 1 µM and 0.1 µM (**Figure 4.3 C, D, E, F**). However, there were small but statistically significant improvements in cell viability seen with resveratrol, sirtinol, EX527, AGK2 and fluoxetine at some concentrations as shown in **Figure 4.3 A, B, C, D, E**.

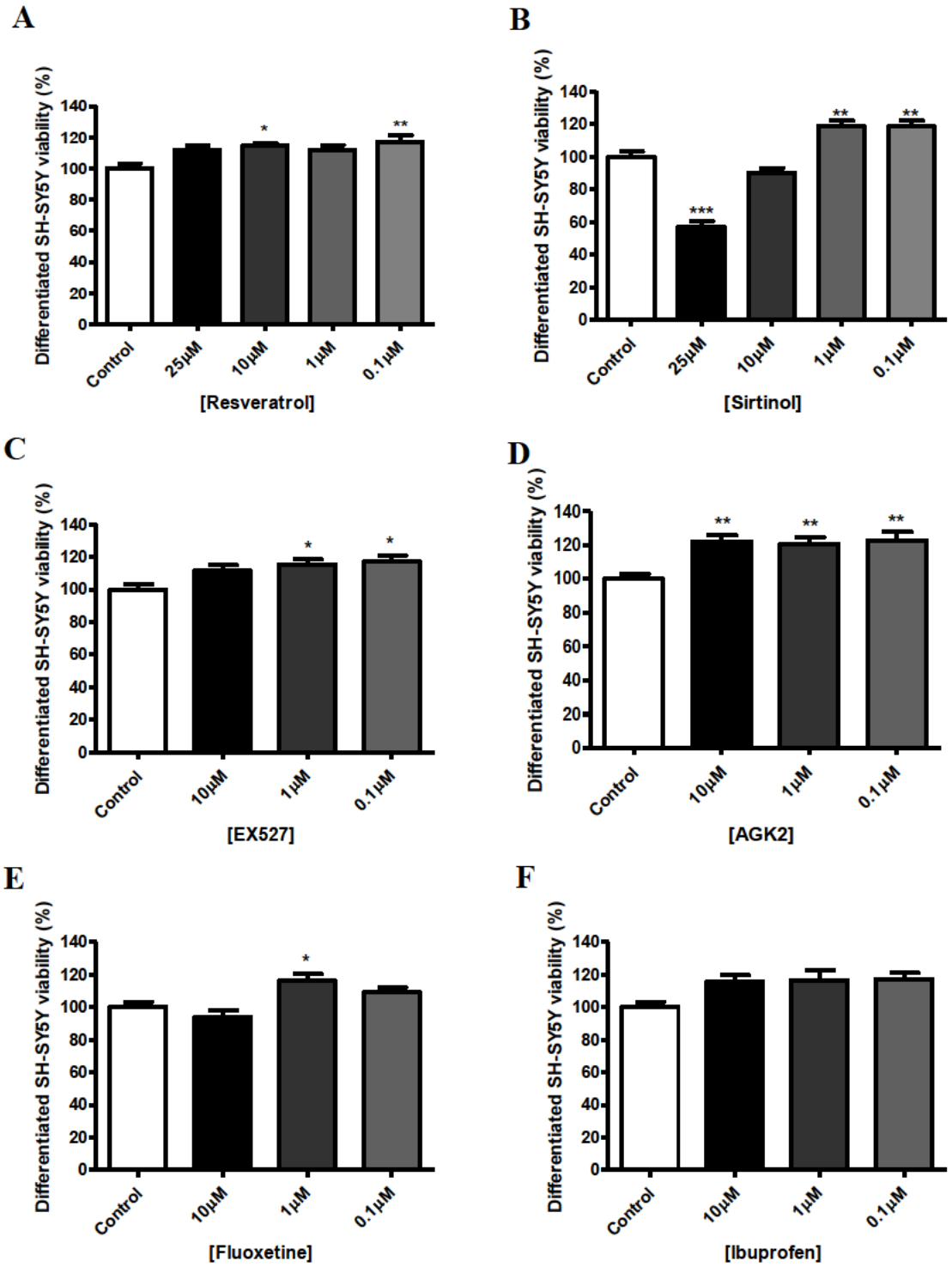

Figure 4.3 SIRT1 and SIRT2 modulators induced lesser cytotoxicity in differentiated SH-SY5Y cells.

Differentiated SH-SY5Y cells were treated with resveratrol (A) (0.1-20 μM), sirtinol (B) (0.1-20 μM), EX527 (C) (0.1-10 μM), AGK2 (D) (0.1-10 μM), fluoxetine (E) (0.1-10 μM) and ibuprofen (F) (0.1-10 μM) for 24 h and assessed for cell viability using resazurin assay. One-way ANOVA followed by Turkey's multiple comparison test was

applied. Significance levels were shown as P<0.05 (*), P<0.01 (**) and P< 0.001 (***). Data indicate mean ± SD of three independent experiments.

4.3.4 Sirtinol and AGK2 protected differentiated SH-SY5Y cells from death induced by HAPI-conditioned supernatant

The survival rate of differentiated SH-SY5Y cells did not improve after the challenge of HAPI cells' LPS and resveratrol-conditioned supernatant at 20 µM, 10 µM, 1 µM and 0.1 µM (**Figure 4.4 A**). Significant differences were found between all concentrations of resveratrol and ibuprofen (10 µM).

Sirtinol significantly promoted the survival rate of differentiated SH-SY5Y cells after the conditioned-supernatant challenge by approximately 30% at 20 µM and 19% at 10 µM (**Figure 4.4 B**). It demonstrated significant differences in greater survival improvement from 20 µM of sirtinol and fluoxetine (1 µM). There is no significant difference between ibuprofen (1 µM) and all concentrations of sirtinol.

EX527 exerted no significant effect on the survival rate of SH-SY5Y cells after the conditioned-supernatant challenge (**Figure 4.4 C**). Significant differences were found between all concentrations of EX527 and ibuprofen (10 µM).

AGK2 (0.1 µM) significantly improved the survival rate of SH-SY5Y cells after the conditioned-supernatant challenge by approximately 20% (**Figure 4.4 D**). No significant differences were found in the survival improvement from fluoxetine (1 µM) and ibuprofen (1 µM).

As control drugs, fluoxetine (1, 0.1 µM) did not significantly improve the survival rate of SH-SY5Y cells after the conditioned-supernatant challenge (**Figure 4.4 E**). Ibuprofen significantly increased the survival rate of SH-SY5Y cells after the conditioned-supernatant challenge by approximately 22% at 1 µM and 21% at 0.1 µM (**Figure 4.4 F**).

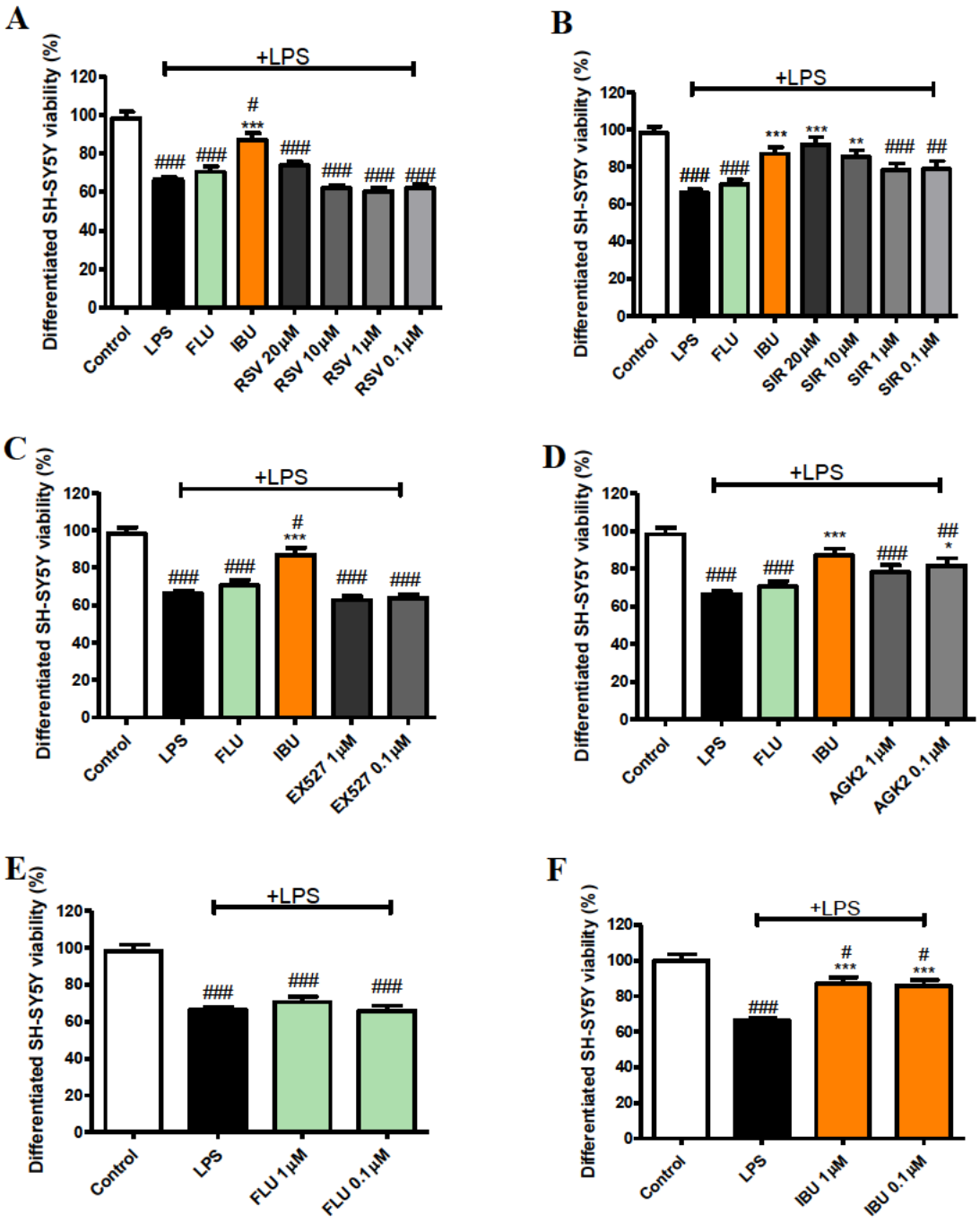

Figure 4.4 Effects of SIRT1 and SIRT2 modulators on neuroinflammation-induced neurodegeneration in differentiated SH-SY5Y cells.

Differentiated SH-SY5Y cells were treated with supernatant produced by HAPI cells after treatment of resveratrol (A) (0.1-20 µM), sirtinol (B) (0.1-20 µM), EX527 (C) (0.1, 1 µM), AGK2 (D) (0.1, 1 µM), fluoxetine (E) (0.1, 1 µM) and ibuprofen (F) (0.1, 1 µM) 4 h prior to LPS (0.005 µg/mL) challenge for 20 h and assessed for cell viability using resazurin assay. Fluoxetine (1 µM) and ibuprofen (1 µM) were used as reference drugs. One-way ANOVA followed by Turkey's multiple comparison test was applied.

Significance levels were shown as P< 0.05 (*, #), P<0.01 (**, ##) and P< 0.001 (***, ###). Data indicate mean ± SD of three independent experiments.

4.3.5 Caspase 3/7 activation does not participate in SIRT drugs' protective effects in mild neuroinflammation-induced neurodegeneration

To measure caspase 3/7 activation in mild neuroinflammation-induced subsequent neurodegeneration, undifferentiated SH-SY5Y cells were seeded on 96-well plates at 10^5 cells/mL (100 µL) and after 24 h cells were treated with supernatant collected from HAPI cells after 24-h exposure to LPS (0.005 µg/mL) combining with the treatment of resveratrol, sirtinol, EX527, AGK2, fluoxetine and ibuprofen for 24 h. Differentiated SH-SY5Y cells were treated with the same supernatant collected from HAPI cells for 24 h. Caspase 3/7 fluorescence assay was applied to measure caspase 3/7 activities.

In undifferentiated SH-SY5Y cells (**Figure 4.5**), resveratrol (20, 10 µM) significantly decreased the elevation of caspase 3/7 activity induced by LPS treatment by approximately 20% and 16% (**Figure 4.5 A**). It also shows significant differences than fluoxetine (1 µM) and ibuprofen (1 µM).

Sirtinol did not have a significantly different affect on caspase 3/7 activities compared to LPS alone (**Figure 4.5 B**). However, sirtinol (1, 0.1 µM) did exert an increasing effect on caspase 3/7 compared to control and also shown significant differences to ibuprofen (1 µM).

EX527 had no significant effects on caspase 3/7 activation (**Figure 4.5 C**). However, there is a significant difference between EX527 and fluoxetine.

AGK2 had no significant effects on caspase 3/7 activities compared to LPS stimulation (**Figure 4.5 D**). However, AGK2 (0.1 µM) had an increasing effect on caspase 3/7 compared to control, but without significant differences to fluoxetine (1 µM) or ibuprofen (1 µM).

Fluoxetine increased caspase 3/7 activities, but this was not significantly different compared to LPS alone (**Figure 4.5 E**). Ibuprofen (1 µM) significantly decreased the elevation of caspase 3/7 activity induced by LPS treatment by approximately 6% (**Figure 4.5 F**).

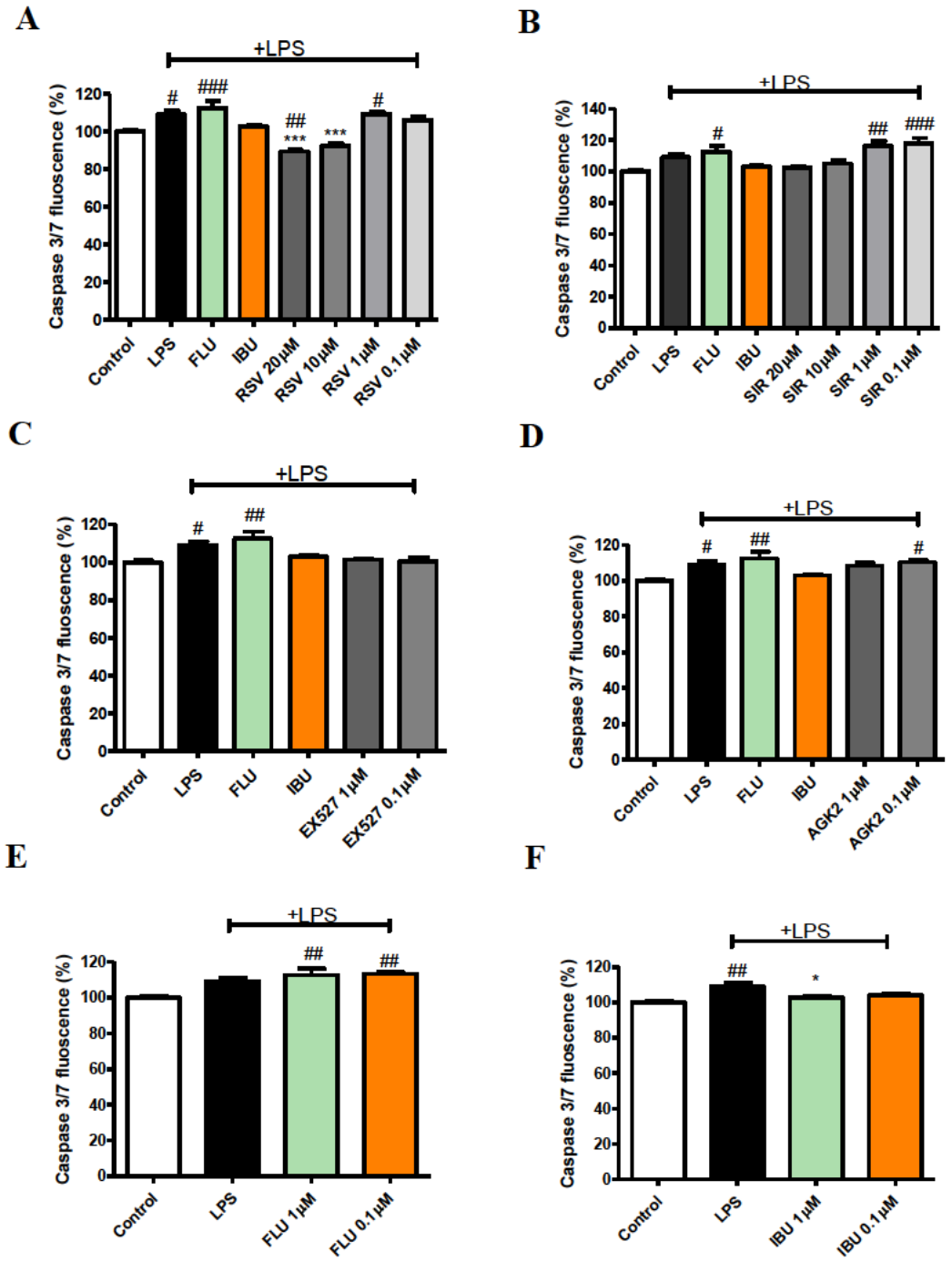

Figure 4.5 Effects of SIRT1 and SIRT2 modulators on caspase 3/7 activation in neuroinflammation-induced neurodegeneration in undifferentiated SH-SY5Y cells.

Undifferentiated SH-SY5Y cells were treated with supernatant produced by HAPI cells after treatment of resveratrol (A) (0.1-20 µM), sirtinol (B) (0.1-20 µM), EX527 (C) (0.1, 1 µM), AGK2 (D) (0.1, 1 µM), fluoxetine (E) (0.1, 1 µM) and ibuprofen (F) (0.1, 1 µM) 4 h prior to LPS (0.005 µg/mL) challenge for 20 h and assessed for caspase 3/7 activation. One-way ANOVA followed by Turkey's multiple comparison test was

applied. Significance levels were shown as P<0.05 (*, #), P<0.01 (**, ##) and P< 0.001 (***, ###). Data indicate mean ± SD of three independent experiments.

In differentiated SH-SY5Y cells (**Figure 4.6**), all concentrations of resveratrol do not significantly affect caspase 3/7 activity (**Figure 4.6 A**). No significant differences were shown compared with fluoxetine (1 µM) and ibuprofen (1 µM).

Sirtinol at 20 µM has exerted a significant effect on increasing caspase 3/7 activities compared to LPS stimulation, fluoxetine (1 µM), and ibuprofen (1 µM) (**Figure 4.6 B**).

EX527 at 1 µM and 0.1 µM also have been shown to exert significant effects on increasing caspase 3/7 activation compared to LPS stimulation, fluoxetine (1 µM), and ibuprofen (1 µM) (**Figure 4.6 C**).

Similarly, AGK2 at 1 µM and 0.1 µM have been shown no significant effects on reducing caspase 3/7 activities compared to LPS stimulation and fluoxetine (1 µM) (**Figure 4.6 D).** AGK2 at 0.1 µM has produced an increasing effect on caspase 3/7 compared to control but without significant differences than fluoxetine (1 µM) and ibuprofen (1 µM).

Fluoxetine (1 µM) exerted a significant effect on reducing caspase 3/7 activities compared to control but LPS stimulation (**Figure 4.6 E**). Whereas, ibuprofen has been shown no effects on caspase 3/7 activity compared to control or LPS stimulation (Figure **4.6 F**).

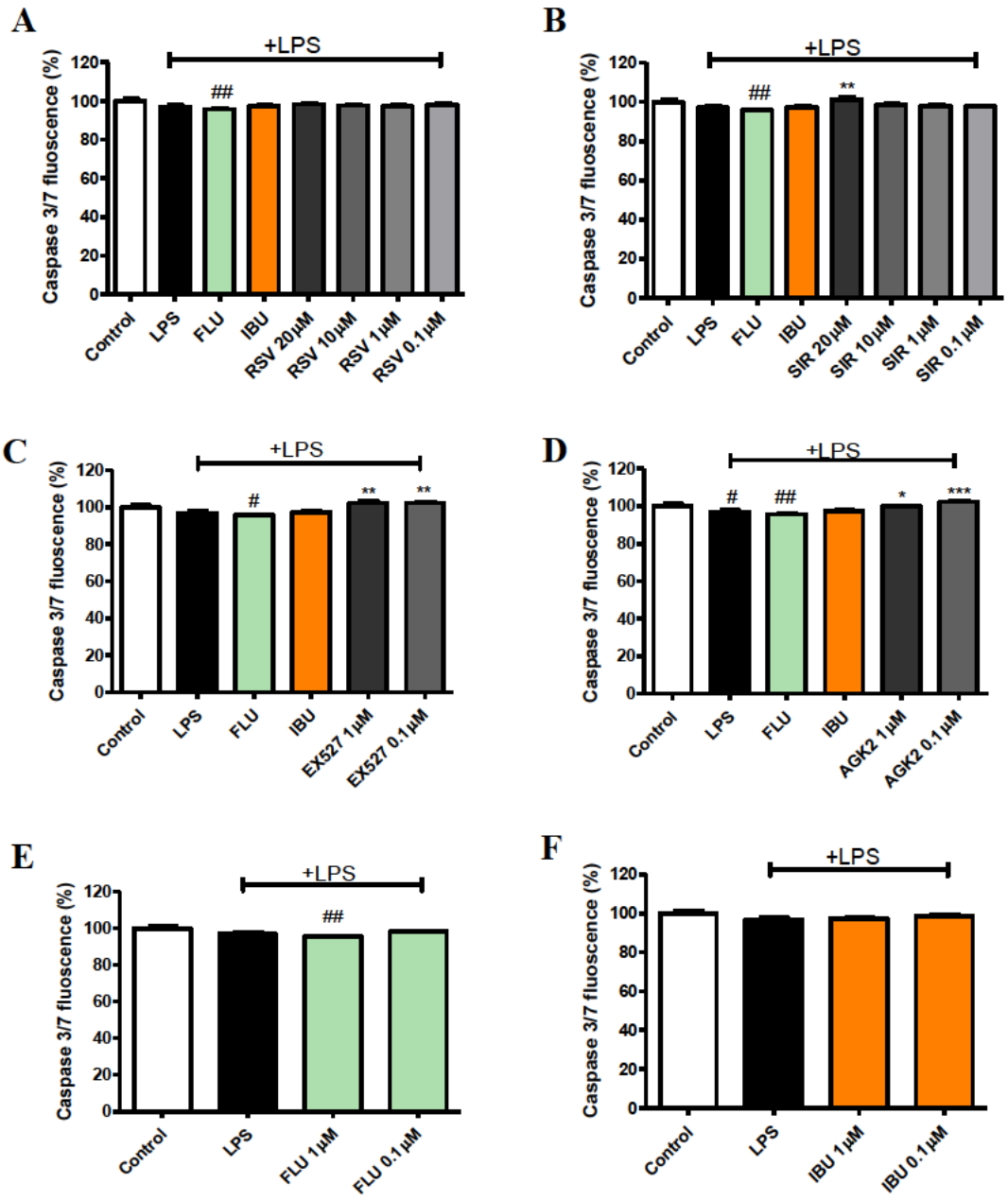

Figure 4.6 Effects of SIRT1 and SIRT2 drugs on caspase 3/7 activation in neuroinflammation-induced neurodegeneration in differentiated SH-SY5Y cells.

Differentiated SH-SY5Y cells were treated with supernatant produced by HAPI cells after treatment of resveratrol (A) (0.1-20 µM), sirtinol (B) (0.1-20 µM), EX527 (C) (0.1, 1 µM), AGK2 (D) (0.1, 1 µM), fluoxetine (E) (0.1, 1 µM) and ibuprofen (F) (0.1, 1 µM) 4 h prior to LPS (0.005 µg/mL) challenge for 20 h and assessed for caspase 3/7 activation. One-way ANOVA followed by Turkey's multiple comparison test was applied. Significance levels were shown as $P<0.01$ (**) and $P< 0.001$ (***). Data indicate mean ± SD of three independent experiments.

4.4 Discussion

The effects of SIRT1 and SIRT2 modulators on neuroinflammation-induced neurodegeneration on both undifferentiated and differentiated SH-SY5Y cells have been assessed. Compared to the effects of SIRT drugs on the HAPI cell line in chapter 3, human neuroblastoma cells and differentiated neuroblastoma cells have shown to be more tolerant of higher concentrations of SIRT1 and SIRT2 modulators than observed in the rat microglia. This indicates that microglia and neurons have different tolerances to cytotoxicity including from resveratrol, sirtinol, EX527, AGK2 and fluoxetine. Based on the cell culture of HAPI and SH-SY5Y cell lines, it has been observed that the HAPI cell line proliferates or divides markedly faster than the SH-SY5Y cell line. HAPI cells in a T75 flask can reach 80-90% confluence in 48-72 h. In contrast, with the same amount of SH-SY5Y cells, it takes them at least 72 h to reach 80-90% confluence. Thus, this might render HAPI cells to be more sensitive to these SIRT drugs. Besides, SIRT drugs and fluoxetine also slightly increased the cell viability of differentiated SH-SY5Y cells. The reason could be that SIRT1 and SIRT2 modulators and fluoxetine have been found to have a positive effect on cell survival and longevity (S. Lavu et al., 2008, G. Fu et al., 2021, F. Zavvari and A. Nahavandi, 2020).

Then the supernatant collected from pre-treated HAPI cells after LPS stimulation was transferred onto both undifferentiated and differentiated SH-SY5Y cells respectively. It has been found that the degeneration of undifferentiated SH-SY5Y can be alleviated by resveratrol, sirtinol, EX527 and AGK2 –pre-treated supernatant from LPS-challenged microglia. Additionally, SIRT1 activator resveratrol and dual SIRT1/SIRT2 inhibitor sirtinol both show significantly better performance than fluoxetine and ibuprofen in undifferentiated SH-SY5Y cells. However, in differentiated SH-SY5Y cells, this effect of sirtinol is relatively diminished but still greater than fluoxetine, and SIRT2 inhibitor AGK2's effect is relatively increased but not greater than fluoxetine or ibuprofen. But resveratrol and selective inhibitor EX527 fail to significantly reduce the neurodegeneration in differentiated SH-SY5Y cells. In this comparison between the two different systems, it has been found that dual SIRT1/SIRT2 inhibitor sirtinol and SIRT2 inhibitor AGK2 exert potent protective effects on neurodegeneration.

This neuroprotective effect might be most likely due to that the production of inflammatory mediators in the supernatant from LPS-induced HAPI cells is suppressed by drug pre-treatment. In this microglia-neuron 2D co-culture model, the supernatant

containing a mixture of LPS, the drug and cytokines from the HAPI cells were transferred onto SH-SY5Y cells without further additional treatment of any SIRT modulators. However, it is well known that only free drug concentrations act biologically in both pharmacokinetics and pharmacodynamics way (K. Jaroch et al., 2018). Whether the remaining mixture of LPS and drugs in the supernatant can pharmacologically affect SH-SY5Y cells after transfer depends on the unbound fraction of the agents and LPS that exhibit biological activities. Based on our data and literature, LPS does not affect the survival of SH-SY5Y cells, which means LPS most likely does not participate in the biological effects of the supernatant transfer (Y. Liu et al., 2020). Moreover, the targets of these SIRT modulators are intracellular SIRT1 and SIRT2 enzymes. Whereas, for intracellular acting drugs, free drug concentrations in the supernatant do not necessarily correspond with intracellular free drug concentrations (K. Jaroch et al., 2018). Therefore, whether any free drug molecules can be transported into SH-SY5Y cells and exert biological action and the intracellular drug concentrations of them are unknown. From the results, it has also been found that resveratrol and sirtinol are the two most effective agents in protecting neurodegeneration. These two SIRT modulators exerted strong inhibiting effects on the production of TNF-α in HAPI cells, which is in line with the result that the survival of SH-SY5Y cells is most protected by resveratrol and sirtinol pre-treated supernatant. TNF-α can induce cell death by binding with TNF receptors (H. Wajant et al., 2003). Thus, the decrease of TNF-α after treatment of resveratrol and sirtinol can effectively attenuate the cell death of SH-SY5Y cells.

Based on this discussion, the reduction of cytokine release by LPS-stimulated HAPI cells might most likely be the reason for neuroprotection results that were acquired on SH-SY5Y cells. The drugs in the supernatant have been either degraded or transported into HAPI cells and metabolized or some have precipitated on the bottom of cell culture plates. To further investigate this, the whole method development of high-performance liquid chromatography needs to be employed to assess the drug concentrations in extracellular supernatant and intracellular cytoplasm respectively.

However, in differentiated SH-SY5Y cells, the results were found to be different from those in undifferentiated results. LPS-stimulated supernatant with resveratrol and EX527 pre-treatment failed to reverse the reduction of survival of SH-SY5Ycells. Supernatant with sirtinol and AGK2 pre-treatment still exert neuroprotection on SH-

SY5Y cells. It can be found that both SIRT1 activation and inhibition both could not significantly affect the survival of SH-SY5Y cells. Whereas, SIRT2 inhibition by sirtinol and AGK2 both again present positive effects.

Multiple factors may have led to this finding. The proliferation of differentiated SH-SY5Y cells is reduced compared with the undifferentiated, and once SH-SY5Y cells stop dividing they become less sensitive to stress such as inflammation. Secondly, the differentiation method by combination treatment of retinoic acid and BDNF is not ideal and still has some limitations. For example, during this process of differentiation, the condition change for SH-SY5Y in different periods can have an impact on pharmacological evaluation. Factors include the toxicity of retinoic acid, serum starvation in BDNF treatment, and serum refill when applying subsequent treatment or experiments. Therefore, potentially, further optimisation of the differentiation model might have yielded different results. A similar situation has also been reported where an undifferentiated model was considered more appropriate than a differentiated model (Y. T. Cheung et al., 2009). Cheung's team recommended expanding their study on the primary cell culture of neurons to further compare with the experimental findings (D. W. Luchtman and C. Song, 2010). However, a more physiologically relevant option might be to utilise a spheroid model of differentiated SH-SY5Y cells. Literature shows that the results from 2D and 3D can be different so there are potential benefits in developing an applicable 3D model (K. Jaroch et al., 2018). In the method development chapter, a preliminary study of SH-SY5Y 3D culture showed the morphology of the formation of SH-SY5Y spheroids. Further method development for spheroid differentiation of SH-SY5Y cells needs to be conducted in the future.

Then the alteration of apoptosis level was assessed by conducting the caspase3/7 fluorescence assay. LPS (0.005 μg/mL) conditioned supernatant collected from HAPI cells only significantly increased the level of caspase 3/7 in undifferentiated SH-SY5Ycells but not the differentiated. The result also showed only resveratrol and ibuprofen could significantly decrease the apoptosis level in undifferentiated SH-SY5Y cells after exposure to LPS-conditioned supernatant collected from HAPI cells. In differentiated SH-SY5Y cells, the apoptosis level was not reduced by pre-treatment of any SIRT1 and SIRT2 drugs including resveratrol, sirtinol, EX527 and AGK2. Since our *in vitro* neuroinflammation-neurodegeneration model of depression was established on the activation of microglia induced by mild LPS treatment with a relatively low

concentration of 0.005 µg/mL, apoptosis induced by LPS might not participate in our model of neurodegeneration. However, other pathways leading to cell death could also exist in this *in vitro* model. As the concentration of stimuli and the variety of them increases, certain cell death pathways will be triggered consequently. Cell death mechanisms have been continued to expand over the past decades. Based on the guideline of the Nomenclature Committee on Cell Death (NCCD), cell death according to the morphological manifestation can be classified into three major categories which are apoptosis, autophagy, and necrosis (L. Galluzzi et al., 2018). Apoptosis manifests with shrinkage of cytoplasm, chromatin condensation, nuclear fragmentation, formation of cell membrane blebbing and apoptotic bodies or vesicles which eventually are phagocytized by surrounding cells and degraded in lysosomes (J.-U. Schweichel and H.-J. Merker, 1973, L. Galluzzi et al., 2007). Apoptosis can be categorized as intrinsic apoptosis and/or extrinsic apoptosis. Intrinsic apoptosis is caused by different intracellular and extracellular stimuli including genetic damage, ROS injury, alteration of supportive microenvironment and features with mitochondrial outer membrane permeabilization (MOMP) (L. Galluzzi et al., 2018). Extrinsic apoptosis can be initiated by death receptors, which several TNF receptor superfamily members belong to, and dependence receptors (L. Galluzzi et al., 2018). Autophagy exhibits extensive cytoplasmic vacuolization leading to phagocytosis and lysosomal degradation. Necrosis does not display any manifestations of apoptosis and autophagy, including phagocytic activities and lysosomal degradation, but only terminates with the disposal of cell corpses (L. Galluzzi et al., 2007, J.-U. Schweichel and H.-J. Merker, 1973, L. Galluzzi et al., 2018). Therefore, in our *in vitro* neurodegeneration model based on cell culture of SH-SY5Y cells, the phagocytic activity and lysosomal degradation in the end-stage of apoptosis and autophagy cannot be observed due to the absence of macrophages in the microenvironment. Other than this, other subroutes of cell death also have been supplemented to the whole underlying mechanism, such as necroptosis, ferroptosis, pyroptosis and parthanatos (L. Galluzzi et al., 2018). More investigation regarding the neurodegeneration mechanism and SIRT drugs' effects on it needs to be conducted in the future.

Chapter 5 : SIRT1 and SIRT2 modulators attenuate LPS-induced anxiety and sickness behaviors in *in vivo* model

5.1 Introduction

Animal models of depression are widely used in the pharmacological assessment of antidepressants, even though there are still some deviations between animal models and human depression in terms of the three key criteria of etiologic validity, face validity and predictive validity, that an ideal animal model of depression should meet (W. T. McKinney, Jr. and W. E. Bunney, Jr., 1969). Etiologic validity is the most difficult criterion to implement because the ideal method to fully mimic the mechanisms of human diseases is genetic modification (N. Dedic et al., 2011). However, the aetiology and mechanism of the development of depression are complex and controversial, which creates substantial difficulty in establishing a reliable disease model on the basis of a single genetic alteration. Nonetheless, face validity still can be procured by mimicking the pathology of diseases biochemically or in behavioural ways (N. Dedic et al., 2011). Predictive validity refers to models such that the animals correctly respond to pharmacological treatment the results of which can accord with those from clinical trials (N. Dedic et al., 2011).

Lipopolysaccharide (LPS)-induced sickness behaviour and depressive-like behaviour are two commonly employed models to quantify the neuroinflammation-induced changes in rodents. Systemic administration of LPS upregulates the mRNA expression of pro-inflammatory cytokines including IL-1β, IL-6 and TNF-α in the periphery. These pro-inflammatory cytokines are transmitted to the brain via neural, humoral communication pathways, cytokine transporters at the BBB and receptors on brain venules (R. Dantzer et al., 2008). Then they can stimulate the cytokine expression in the hypothalamus accompanied by activation of microglia and astrocytes in the dentate gyrus (S. Layé et al., 1994). Local production of prostaglandins can also be activated by these circulating cytokines combining with corresponding receptors (R. Dantzer et al., 2008, S. Biesmans et al., 2013). These meditators also act on the brain to elicit behavioural symptoms of sickness to enable ill individuals to re-organize perceptions and actions which develop acutely after 2-4 h after LPS injection and last for 4-6 h (R. Dantzer et al., 2008). Sickness behavior is defined as a complex of subjective behavioral and physiological modifications. It is an adaptive response of the host to an infection, which is in the same manner that fear is an adaptive response to potential dangers (R. Dantzer, 2004). Moreover, some sickness manifestations that mirror the clinical symptoms of depression show up after systemic LPS treatment, including

weight gain or loss, eating or drinking less, and lack of local mobility, which is also accompanied by the elevation of inflammatory mediator levels (J. L. Remus and R. Dantzer, 2016).

Stress is one of the major predisposing factors in major depressive disorder (J. F. Cryan and A. Holmes, 2005). Thus, some behavioural tests are designed based on the mechanisms of stress, coping and learning helplessness (J. F. Cryan and A. Holmes, 2005). For example, in the forced swim test (FST) and tail suspension test (TST) animals are put in an environment where they constantly have to face the stressor but fail to escape and ultimately have learned helplessness. Anxiety is referred to as a persistent fear or cognitive preparedness in response to a potential threat or danger (N. Dedic et al., 2011, J. F. Cryan and A. Holmes, 2005). The comorbidity of the two is quite common in clinical depression cases. In animal models, anxiety is also regarded as the main endophenotype of depression, which is assessed by exploratory-based approach-avoidance conflict (AAC) tests (N. Dedic et al., 2011, J. F. Cryan and A. Holmes, 2005). They are designed based on the nature of rodents that they tend to explore novel environments but also have an innate aversion to exposed and well-lit spaces (J. F. Cryan and A. Holmes, 2005). For example, in the open field test (OFT) and dark-light chamber (DLC) test, the averseness is procured by the central area of a brightly lit open field and brightly illuminated compartment respectively (J. F. Cryan and A. Holmes, 2005). Literature has shown that the behavioural parameters acquired from these tests are well-established in assessing behavioural despair of inflammation-induced model of depression (S. Basu Mallik et al., 2016, J. Mudgal et al., 2020).

The symptoms of cytokine-induced sickness behaviour and depression have striking similarities. For instance, they both manifest with a withdrawal from the physical and social environment, reduced reactivity to reward. Some symptoms of sickness behaviour can also be improved by antidepressant treatment, including a decreased preference for sweet solutions and reduced social exploration (R. Dantzer et al., 2008). In the background of our study, we not only highlighted the importance of inflammation in the pathology of primary depression but also emphasized the prevalence of depression in physically ill patients who are suffered from neurodegenerative diseases and co-morbid organic depression associated with them. Therefore, the employment of these sickness behaviour models in the following method section can be beneficial for us to investigate and understand the pharmacological effects of SIRT modulators on

inflammation-induced depression. In this chapter, the effects of SIRT1 activator resveratrol and dual SIRT1/SIRT2 inhibitor sirtinol on the acute behavioural parameters of OFT, FST and TST in LPS-induced mouse model of depression have been assessed.

5.2 Materials and methods

5.2.1 Animals and sample size

Male Swiss albino mice (8−10 weeks, 20−30 g) procured from the inbred strains of central animal research facility (CARF), Manipal Academy of Higher Education (MAHE) were used in this study. The animals were housed in groups of 6, under controlled laboratory conditions, maintained on 12 h day and night cycle with free access to food and tap water.

5.2.2 Ethical approval

Ethical approval was obtained from the Institutional Animal Ethics Committee (IAEC) of Manipal University, which is in compliance with the Guide for the Care and Use of Laboratory Animals by National Research Council (US) Committee (National Research Council, 2011). The approval number is IAEC/KMC/25/2020.

5.2.2 Drugs and treatments

All the chemicals used in this study were of analytical grade. Lipopolysaccharide (LPS; *Escherichia coli* 0111:B4), resveratrol, sirtinol and fluoxetine were all procured from Sigma-Aldrich Co. LLC (St Louis, MO, USA).

Animals were randomly assigned into 5 groups (n = 6), including; group I: saline (SAL); group II: LPS; group III: resveratrol (RSV) + LPS; group IV: sirtinol (SIR) + LPS and group V: fluoxetine (FLU) + LPS. Saline and LPS groups were administered with vehicle (normal saline) at a dose of 10mL/kg. RSV + LPS; SIR + LPS and FLU + LPS groups were treated with resveratrol (50 mg/kg); sirtinol (2 mg/kg); and fluoxetine (10 mg/kg) respectively. All the treatments were administered by intraperitoneal (i.p.) route. Sickness behaviour was induced in all the animals except the saline-treated group using LPS (2 mg/kg). The selection of treatment doses was based on our preliminary studies and supporting literature. Fluoxetine served as a positive control as a standard selective serotonin reuptake inhibitor (SSRI) that acts by inhibiting the reuptake of serotonin. Behavioural assays were performed within 1-2 h of LPS administration, and were video recorded. The recorded data were analysed by a well-trained observer as well as the

blinded observer to reduce bias. For all behavioural endpoints, the animals were brought to the observation room for acclimatization 2 h before the experimental procedures.

5.2.3 Behavioural studies

Open field test

The open-field test (OFT) was used to assess the effect of LPS and the other treatment groups on the exploratory behaviour of the animals. Locomotor Activity (LMA) was assessed in mice individually placed into a clean, novel plexiglass arena (30 x 30 x 60 cm) which was divided into nine virtual quadrants (10 x 10 cm each). LMA was measured by counting the number of square crossings over a 5 min period. The apparatus was cleaned with 50% ethanol between the experiments (Mudgal et al., 2020).

Tail suspension test

The tail suspension test (TST) was performed to quantify the effect of various treatment groups on LPS-induced sickness behaviour (J. C. O'Connor et al., 2009). A small piece of medical adhesive tape was placed approximately 1 – 1.5 cm from the tip of the tail and mice were hung individually for a period of 5 min at 15 cm away from the nearest surface. The tail climbing was prevented by placing a plastic tubing around the tail prior to applying the adhesive tape. The duration of immobility was then measured during the final 4 min of the total 5 min of the test (Mudgal et al., 2020).

Forced swim test

The forced swim test (FST) was employed to study the effect of treatment groups on LPS-induced behavioural despair. The mice were forced to swim individually in a transparent plexiglass cylindrical tank (30 x 20 cm) containing water maintained at 22 ± 2°C. The water level was adjusted to a height of 15 cm. After an initial period of vigorous activity, the animals assume a type of immobile posture. The immobility stage was quantified when the animal ceases to struggle and make minimal movements of limbs to keep the head above water. Animals were allowed to swim for a total of 6 min and the immobility was recorded over the last 5 min (Basu Mallik et al., 2016; Sahu et al., 2019; Mudgal et al., 2020).

5.2.4 Statistical Analysis

All the results were statistically analysed using GraphPad Prism 5 (GraphPad Software Inc., San Diego, CA, USA). Results are expressed as means ± SEM. Treatment and

control groups were compared by one-way analysis of variance (ANOVA) followed by Dunnett's multiple comparison test. Statistical significance was determined at the p value < 0.05 ($p < 0.05$*, $p < 0.01$** and $p < 0.001$***).

5.3 Results

5.3.1 Resveratrol and sirtinol increased the locomotor activity in the open field test

The number of crossings in the open field test indicates the locomotor activity of the mice. After LPS (2 mg/kg) intraperitoneal injection, the number of crossings of the mice significantly reduced compared to the saline group (12.7 ± 3.9 vs 97.0 ± 12.5, F = 7.5, p < 0.05), which indicates the mice were in a status of sickness and lack of movement (**Figure 5.1**). Resveratrol (50 mg/kg), sirtinol (2 mg/kg) and fluoxetine (10 mg/kg) significantly increased the number of crossings compared to the LPS group (70.5 ± 12.3, 59.3 ± 15.9, 57.83 ± 6.8 vs 12.7± 3.9 respectively; F = 7.5; p < 0.05) as shown in **Figure 5.1**. However, there is no significant difference between these drug treatments on the open field test.

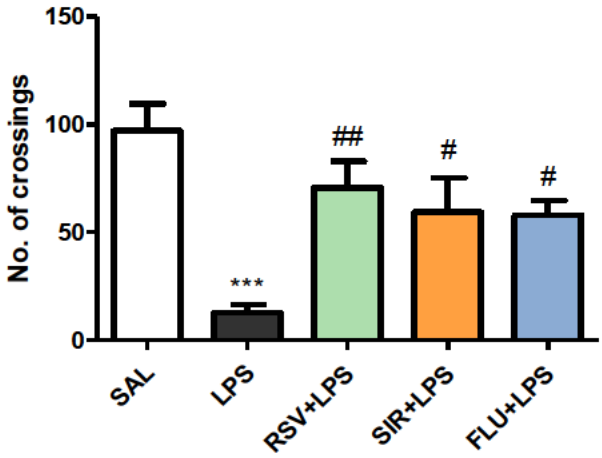

Figure 5.1 Effects of resveratrol (RSV), sirtinol (SIR) and fluoxetine (FLU) on LPS-induced changes in the locomotor activity in the open field test.

LPS (2 mg/kg, i.p.) was administered to drug pre-treated mice, including resveratrol (50 mg/kg.), sirtinol (2 mg/kg) and fluoxetine (10 mg/kg). OFT was conducted 1-2 h post LPS administration. One-way ANOVA followed by Dunnett's multiple comparison test was applied. $^{***}p < 0.001$ as compared with saline group (SAL); $^{\#}p < 0.05$, $^{\#\#}p < 0.01$ as compared with LPS group.

5.3.2 Resveratrol and sirtinol alleviated the learned helplessness in the forced swim test

The immobility time in the forced swim test indicates the learned helplessness of the mice in a situation where there is no escape. After LPS (2 mg/kg) intraperitoneal injection, the immobility time of the mice significantly increased compared to the saline group (214.3 ± 15.4 vs 128.0 ± 9.0, $F = 9.7$, $p < 0.05$) as shown in **Figure 5.2**, which indicates the mice developed failure of the persistence of escape-directed behaviour, namely, behavioural despair or passive behaviour (J. F. Cryan, 2010). Resveratrol (50 mg/kg), sirtinol (2 mg/kg) and fluoxetine (10 mg/kg) significantly reduced the immobility time compared to the LPS group (114.3 ± 15.4, 97.7 ± 16.9, 122 ± 15.1 vs 214.3 ± 9.0 respectively; $F = 9.7$; $p < 0.05$) as shown in **Figure 5.2**. However, there is no significant difference between these drug treatments on the forced swim test.

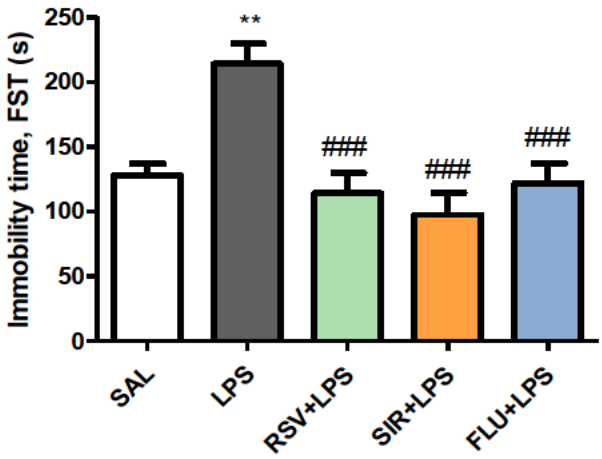

Figure 5.2 Effects of resveratrol (RSV), sirtinol (SIR), and fluoxetine (FLU) on LPS-induced immobility time (s) as observed by FST.

LPS (2 mg/kg, i.p.) was administered to drug pre-treated mice, including resveratrol (50 mg/kg.), sirtinol (2 mg/kg) and fluoxetine (10 mg/kg). FST was conducted 1-2 h post LPS administration. One-way ANOVA followed by Dunnett's multiple comparison test was applied. $^{**}p < 0.01$ as compared with saline group (SAL); $^{###}p < 0.001$ as compared with LPS group.

5.3.3 Resveratrol and sirtinol attenuated the learned helplessness in the tail suspension test

The immobility time in the tail suspension test can double test the effects of the drugs on the learned helplessness of the mice in a situation where there is no escape, as in some cases drugs' potency and sensitivity can be reduced in the tail suspension test (L. Steru et al., 1987, R. Chermat et al., 1986). After LPS (2 mg/kg) intraperitoneal injection, the immobility time of the mice significantly increased compared to the saline group (185.7 ± 17.7 vs 106.8 ± 14.9, $F = 7.0$, $p < 0.05$) as shown in **Figure 5.3**, which indicates the behavioural despair or passive behaviour (J. F. Cryan, 2010). Resveratrol (50 mg/kg), sirtinol (2 mg/kg) and fluoxetine (10 mg/kg) significantly reduced the immobility time compared to the LPS group (109.7 ± 14.1, 94.8 ± 10.1, 117.5 ± 9.5 vs 185.7 ± 17.7 respectively; $F = 7.0$; $p < 0.05$) as shown in **Figure 5.3**. However, there is no significant difference between these drug treatments on the tail suspension test.

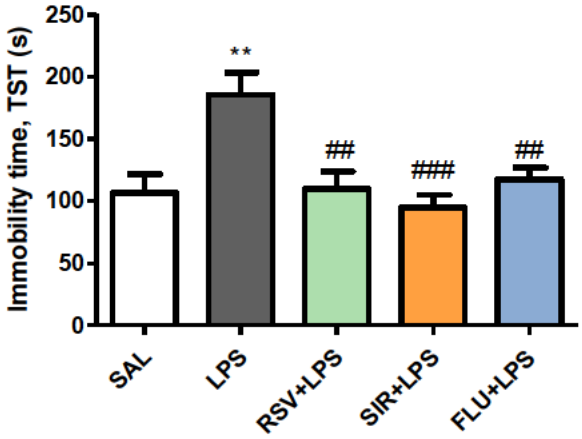

Figure 5.3 Effects of resveratrol (RSV), sirtinol (SIR), and fluoxetine (FLU) on LPS-induced immobility time (s), as observed by TST.

LPS (2 mg/kg, i.p.) was administered to drug pre-treated mice, including resveratrol (50 mg/kg.), sirtinol (2 mg/kg) and fluoxetine (10 mg/kg). TST was conducted 1-2 h post LPS administration. One-way ANOVA followed by Dunnett's multiple comparison test was applied. $^{**}p < 0.01$ as compared with saline group (SAL); $^{###}p < 0.001$ as compared with LPS group.

5.4 Discussion

In this chapter, the effects of resveratrol, sirtinol and fluoxetine on behavior changes in the LPS-induced model of depression have been assessed. Systemic LPS administration can elicit two phases of states, sickness for acute phase and depression for chronic phase. In the acute phase which lasts 2-6 h, mice manifest with lack of movement and less intake of food and water (J. L. Remus and R. Dantzer, 2016). The underlying mechanism is that the inflammatory mediators from the periphery arouse the inflammatory response of the innate immune system in the brain which acts on the brain to elicit sickness behaviours aforementioned.

In our study, the behavioural despair was assessed in the acute phase of LPS-induced model by measuring locomotor activity in OFT, immobility time in FST and TST. SIRT1 activator resveratrol, dual SIRT1/SIRT2 inhibitor sirtinol and fluoxetine were all shown to significantly reverse the decrease of locomotor activity and the increase of immobility time, which is in alignment with the results in *in vitro* study where these drugs have shown anti-inflammatory effects on LPS-stimulated microglia. Resveratrol and sirtinol have shown potent inhibiting effects on the production of TNF-α and secondary inflammatory product PGE_2 which can contribute to the reduction of serotonin precursor tryptophan and mediation various behavioural actions respectively (R. Dantzer et al., 2008). Moreover, resveratrol and sirtinol have shown similar results on sickness behaviours as the antidepressant fluoxetine as a positive control. In a previous *in vitro* study, resveratrol and sirtinol have shown significant stronger inhibiting effects on TNF-α than fluoxetine, which indicates the possibility that resveratrol and sirtinol might be able to elicit antidepressant effects in animal models via an anti-inflammatory mechanism. To test their subsequent anti-depressant effects, further depressive-like behaviour study needs to be conducted, which leads to the importance of the chronic phase of LPS-induced mouse models.

In the chronic phase of this model, the sickness behaviours generally disappear within 24 h of LPS administration (J. L. Remus and R. Dantzer, 2016). While the motor activity and appetite of animals are back to normal, the animals will develop depressive-like behaviours (J. L. Remus and R. Dantzer, 2016). Meanwhile, the depressive-like behaviour in the LPS-induced model is elicited via the activation of indoleamine-2,3-deoxygenase (IDO) induced by cytokines (R. Yoshida and O. Hayaishi, 1987). The precursor to the neurotransmitter serotonin is tryptophan which exists both in the peripheral and the brain. IDO activity can convert tryptophan to kynurenine (R.

Yoshida and O. Hayaishi, 1987). However, the depressive-like behaviour in the LPS-induced model has been demonstrated not to be caused by the depletion of serotonin turnover through this IDO pathway (J. L. Remus and R. Dantzer, 2016). It has been found that the elevation of the downstream metabolite of kynurenine, quinolinic acid, contributes to the depressive-like behaviours by activating NMDA receptors, which results in excitotoxicity and oxidative damage to the CNS (J. L. Remus and R. Dantzer, 2016). The evidence of this mechanism has also been verified in many clinical cases (J. L. Remus and R. Dantzer, 2016). Therefore, behaviour tests in the chronic phase are suitable for assessing the effects of SIRT1 and SIRT2 drugs on IDO-associated pathways which further indicate their effects on serotonin metabolism on the foundation of inflammation. The use of a chronic model of depression as a future direction maybe as a way of exploring the time course of neurological changes and the influence of SIRT during this process.

Chapter 6 : Discussion

6.1 Final discussion

The overall aim of this project is to investigate the effects of SIRT1 and SIRT2 modulators including SIRT1 activator resveratrol, SIRT1/SIRT2 dual inhibitor sirtinol, selective SIRT1 inhibitor EX527, and SIRT2 inhibitor AGK2 on neuroinflammation in depression. We also aimed to compare the anti-inflammatory effects between this class of drugs with antidepressant fluoxetine and nonsteroidal anti-inflammatory drug (NSAID) ibuprofen. Additionally, this project was also aimed at investigating the mechanism underlying the protective effects against neuroinflammation-induced neurodegeneration.

This research first highlighted the crucial role of neuroinflammation playing in the pathogenesis of depression. Prolonged and excessive neuroinflammation can directly result in disruption of synaptic circuits, neuronal apoptosis, and subsequent neuron death or long-term neurodegeneration (M. Lyman et al., 2014). It also exacerbates or interacts with other pathological factors that contribute to the development of depression including deficiency of monoamine neurotransmitter, neurotrophin deficiency, dysfunction of the hippocampus-pituitary-adrenal axis, excessive production of glutamate and dysfunction of the circadian rhythm. Therefore, neuroinflammation as an overall underlying factor can influence every element of depression and neurodegeneration. Moreover, we also emphasized the importance of raising awareness of treating the population suffered from 'organic depression' that is secondary to neurodegenerative diseases. Not only is depression highly prevalent in the population of neurodegenerative diseases but both depression and neurodegenerative diseases share the same mechanism foundation of neuroinflammation. Importantly, in the current medication strategy or guidelines for depression, a suitable treatment against neuroinflammation is not considered for incorporation in treatment regimens. Therefore, there would be a potential benefit, including increasing the remission rate or decreasing relapse rates of depression, to incorporating a treatment to target neuroinflammation and augment the therapeutic effect of current antidepressants.

Existing pharmacological studies for supporting SIRT1 and SIRT2 drugs as an anti-inflammatory agent in neuroinflammation and neurodegeneration have been reviewed. SIRT1 and SIRT2 are two members of the sirtuin family that function as deacetylases and influencing downstream pathways by deacetylation such as NF-κB, PGC-1α, and AMPK (Y. Zhang et al., 2020). It has been found that SIRT1 activation and SIRT2

inhibition are the most reported investigations in these studies. SIRT741 activation has shown a promising effect on inhibiting inflammation and oxidative stress induced by amyloid deposition (D. Porquet et al., 2013, J. Chen et al., 2005, D. Kim et al., 2007). In regards to SIRT1 inhibition's effect on neuroinflammation and neurodegeneration, the existing studies have shown some contradictory results because of a lack of sufficient supporting data, which needs further investigation. The studies of SIRT2 also proposed a hypothesis that its inhibition may exert neuroprotective effects by affecting autophagy activities and sterol biosynthesis (R. Luthi-Carter et al., 2010, D. F. Silva et al., 2016). Additionally, the few available genetic studies have discovered the association between the onset of depression and the genetic polymorphism of SIRT1 and SIRT2, which indicates the potential value to design and investigate new SIRT agents based on the knowledge of pharmacogenetic to better target the depression population (T. Hirata et al., 2019, S. Porcelli et al., 2013, T. Kishi et al., 2010). Therefore, based on the findings from the neurodegeneration field and the pharmacogenetics angle, we are the first to propose to explore the class of SIRT1 and SIRT2 drugs to be a potential treatment for neuroinflammation in depression.

Regarding the methodology development, we emphasized the importance of glucose selection in the cell culture of SH-SY5Y cells. High-glucose cell culture is considered a pre-diabetic condition and not supposed to be applied in *in vitro* neurological studies except for diabetes-associated studies. Clearly, this 2D co-culture model of microglia and neuronal cells was not intended to mimic any pre-diabetic condition. Instead, in order to prevent SH-SY5Y from the low-glucose shock during the supernatant transfer, low-glucose media can have made SH-SY5Y cells adapted to the supernatant change before transfer. This finding can facilitate future studies using this model to achieve more accurate and interpretable results.

Moreover, to better investigate the subsequent neurodegeneration following LPS-conditioned supernatant treatment, the differentiation methodology for the SH-SY5Y cell line was also optimized in this study. Based on our data, it has been found that retinoic acid treatment alone can stimulate SH-SY5Y to generate neurite outgrowth and transform into neuronal-like shape. However, retinoic acid could not modify the genetic expression of SH-SY5Y cells, which thus affects the phenotype change of this neuroblastoma cell line. Instead, the combination induction treatment of retinoic acid and BDNF can successfully differentiate the SH-SY5Y cell line morphologically and

genetically to some extent. This finding indicates that even though morphology analysis can show positive results as literature also has reported (J. F. da Rocha et al., 2015), a differentiation method for SH-SY5Y cells should be assessed from both morphologic aspects and genetic aspects.

The *in vitro* study within this thesis tested the drug cytotoxicity on the microglia cell line, neuroblastoma cell line, and its differentiated cell line after treatments of resveratrol, sirtinol, EX527, AGK2, fluoxetine and ibuprofen. These results provide a general range for safe dose selection for these drugs in *in vitro* neurological studies, especially where HAPI cell line and SH-SY5Y cell line are employed. This research also measured and compared the effects of these SIRT1 and SIRT2 drugs on the production of pro- and anti-inflammatory cytokines, inflammatory mediators, and oxidative stress in the *in vitro* neuroinflammation model of depression induced by LPS. Then the effects of SIRT1 and SIRT2 drugs on neuroinflammation-induced neurodegeneration by treating undifferentiated and differentiated neuroblastoma cells with supernatant from the microglial cells after LPS challenge or with drug pre-treatment have been investigated. The different manifestations that these drugs result in on undifferentiated and differentiated neuroblastoma indicate the importance of applying differentiation to SH-SY5Y cells in order to obtain relatively more accurate data in research where SH-SY5Y cells are regarded as neuronal cells.

Resveratrol has long been regarded as a potent pleiotropic agent that exerts multiple effects in neuroinflammation and neurodegeneration. The anti-inflammatory effect in microglia is in line with the available literature that resveratrol has been reported to suppress the inflammation expression induced by LPS in mouse microglial cell line N9 (L. Li et al., 2015). Regarding neurodegeneration, resveratrol has been reported in numerous studies to present the protective effects against many neurodegenerative conditions as mentioned in inductions including Alzheimer's disease, Parkinson's disease, amyotrophic lateral sclerosis and Hungtington's disease. However, there is no research investigating resveratrol on direct neuroinflammation-induced neurodegeneration. Resveratrol failed to significantly increase the survival of differentiated SH-SY5Y cells under LPS stimulation. However, resveratrol was still shown to exert potent anti-inflammatory traits in LPS-stimulated microglia and neuroprotection against the degeneration of undifferentiated SH-SY5Y cells. The data also suggests that effects on apoptosis activity might participate in this neuroprotection.

EX527 as a selective SIRT1 inhibitor exerts inhibiting effects on PGE_2 but not as potent as the SIRT1 activator resveratrol. In contrast, the production of TNF-α was not reduced by EX527 treatment. Also, EX527 could exert a slight neuroprotective effect against inflammation-induced neurodegeneration on undifferentiated SH-SY5Y cells. The overall result indicates that EX527 did not exacerbate the neurodegeneration of SH-SY5Y cells under inflammation. In the literature, the combination treatment of resveratrol and EX527 was often administered to pharmacologically block the SIRT1 activation induced by resveratrol in previous studies where EX527 could reduce but not completely suppress resveratrol's protective effects (C. Diaz-Ruiz et al., 2015, Y. J. Guo et al., 2016). Another study by Valle's team also reported that EX527 showed protective effects on the survival of neuronal cells, which is in line with our aforementioned result. However, Valle's study found EX527's effect is SIRT1-independent (C. Valle et al., 2014). Therefore, whether EX527 should be recommended as an ideal SIRT1 antagonist to use to pharmacologically suppress the activity of SIRT1 as opposed to the activation by resveratrol in neuroinflammation research is yet to be confirmed through further investigation.

Based on the result, it has also been found sirtinol as a dual SIRT1 and SIRT2 inhibitor has shown very promising protective effects in both undifferentiated and differentiated SH-SY5Y cells, which is also in line with its anti-inflammatory effects in microglia. Sirtinol has been used as a SIRT1 inhibitor to reverse the protective effects of SIRT1 activator resveratrol in some studies, which means sirtinol hypothetically should present effects as opposed to resveratrol. For instance, sirtinol has been shown to reverse the anti-oxidative effect of resveratrol in α-synuclein-stimulated SK-N-BE cells, which are also a neuroblastoma cell line (D. Albani et al., 2009). Sirtinol has also been reported to aggravate the activation of microglia cell line BV-2 induced by LPS (1 μg/mL) (J. Ye et al., 2013). Sirtinol was shown to not exert antagonism effects solely against SIRT1 activation in this study. There are some perspectives regarding SIRT inhibition by sirtinol that should be emphasized. In a number of studies, sirtinol is administered as a SIRT1 inhibitor (C. Valle et al., 2014, S. Y. Liu et al., 2017). However, there is literature showing that sirtinol exerts a potent inhibiting effect on SIRT2 which is stronger than SIRT1 (C. M. Grozinger et al., 2001, M. Zhang et al., 2017, Selleckchem, 2020). Therefore, sirtinol is not recommended as a pharmacological

suppressor for selective SIRT1 activation in research with inflammation-related mechanisms.

The other SIRT2 inhibitor AGK2 also showed similar protective effects to sirtinol. AGK2 had significant protective effects in differentiated SH-SY5Y cells after exposure to LPS-conditioned supernatant from HAPI cells, even though AGK2 only reduced the production of PGE_2 but not TNF-α in LPS-stimulated HAPI cells. It indicates that SIRT2 inhibition and reduced inflammation are beneficial in neuroinflammation-induced neurodegeneration. This result is in line with previous literature and can be used as a pharmacological suppressor for SIRT2 activity in SIRT2-related studies (G. Donmez and T. F. Outeiro, 2013, C. Scuderi et al., 2014). However, caspase 3/7 activity is not shown to be decreased in the neuroprotection of AGK2 in the neuroinflammation-neurodegeneration model induced by 0.005 µg/mL of LPS.

In the animal study, the two most effective drugs SIRT1 activator resveratrol and dual SIRT1/2 inhibitor sirtinol tested in the *in vitro* study were assessed in the acute phase of LPS-induced depression mouse model and compared with fluoxetine. The behavioural parameters including locomotor activity and immobility time in the open field test, forced swim test and tail suspension test were significantly improved by resveratrol, sirtinol and antidepressant fluoxetine in the acute sickness phase of the depression model, which verified the anti-inflammatory effects of the two drugs from the *in vitro* study. However, in several previous studies, sirtinol has been shown to elicit contradictory effects on stressed-induced depression models including mice and rats (N. Abe-Higuchi et al., 2016, C. L. Ferland et al., 2013). Additionally, in these two studies, sirtinol was administered through direct drug infusion in the hippocampus. Based on the ROS production test in the *in vitro* study, sirtinol induced a dramatic amount of ROS in microglial HAPI cells, which indicates its potential toxicity to the CNS. However, in our animal study, sirtinol was administered orally and metabolized systematically instead of locally in the brain. A study based on silico drug-likeness parameters reported that sirtinol presents high lipophilicity and BBB penetration ability which is an advantage of sirtinol to treat neurological conditions (M. Schnekenburger et al., 2018). But overall. there is limited information about the pharmacokinetics of sirtinol. Sirtinol's effects on depressive-like behaviour need to be further assessed in the chronic phase of the LPS-induced depression model and also compared with

fluoxetine. It would also be informative to obtain systemic and localised cytokine profiles in this model.

In conclusion, this research has emphasized the necessity of increasing the understanding of the roles that neuroinflammation and neurodegeneration playing in the pathophysiology of depression and the urge of investigating SIRT drugs as a novel class of drugs targeting neuroinflammation. This study has shown the effectiveness of SIRT drugs in inhibiting neuroinflammation and subsequent neurodegeneration through *in vitro* and *in vivo* studies. It has provided the potential prospect for validating the logic of further investigating the therapeutic effect of combining treatment of SIRT drug and current antidepressant medication in the population of depression.

However, in *in vitro* study, the 2D microglia-neuron co-culture model is achieved through supernatant transfer. The development and application of the 3D microglia-neuron model can facilitate researchers detecting the mechanism of neuroinflammation and neurodegeneration and conducting the pharmacological assessment. Additionally, several SIRT modulators were assessed as representatives of this class of drugs. Other SIRT modulators should also be assessed in the same experimental system. It also should be emphasized that more novel and advanced SIRT1 and SIRT2 drugs need to be developed on the foundation of understanding the drug-protein catalytic relationship to facilitate 3D structure-based drug design **(Y. Jiang et al., 2017)**, so that pharmacological agonism or antagonism of sirtuins can be more effective, targeted and precise.

6.2 Future work

Regarding future directions, there are still several aspects of this study where further investigation to obtain more rigorous conclusions would be beneficial. This includes further studies to investigate and elucidate the mechanisms of action.

In our *in vitro* model, supernatant collected from HAPI cells after LPS and drug exposure was transferred onto undifferentiated and differentiated SH-SY5Y cells to measure the degeneration. It has been observed that drug-conditioned supernatant can reduce neurodegeneration, which is in line with our theory that SIRT drugs reduce the cytokines and mediators which lead to neuronal death. However, the situation cannot be excluded that the residue drug remaining in the supernatant can contribute to the protection against neurodegeneration of SH-SY5Y cells. The relevant evidence of the

neuroprotection of SIRT drugs against neurodegeneration has been reviewed in the introduction chapter. Therefore, to estimate this potential factor, high-performance liquid chromatography (HPLC) can be used to analyse the concentration of drugs and their derivatives in the supernatant.

Based on the result of this thesis, it is evident that SIRT1 and SIRT2 modulators can exert anti-inflammatory effects and protect against neurodegeneration. In order to confirm the core role of SIRT1 and SIRT2 in the process, it is necessary to measure the activation of enzyme SIRT1 and enzyme SIRT2 and the extent of this. Also, siRNAs can be used to interfere with the expression of SIRT1 and SIRT2 to test if the anti-inflammatory effects are suppressed. SIRT1-specific siRNA or SIRT2-specific siRNA allows the researcher to specifically inhibit SIRT1 or SIRT2 expression via RNA interference, a method whereby gene expression can be selectively silenced through the delivery of double-stranded RNA molecules into the cells. The SIRT1/2-specific siRNA and control siRNA can be predesigned by and purchased from Life Technologies. The dynamic regulation of NAD metabolism in mitochondria is important for mitochondrial function and the regulation of NAD-consuming enzymes like sirtuins (L. R. Stein and S.-i. Imai, 2012). Therefore, ultra-high performance liquid chromatography (UPLC) can be used to determine the quantity and ratio of NAD and NADH. Mitochondrial membrane potential (MMP) is also a key parameter for evaluating the mitochondrial function. JC-1 assay can be used to determine the MMP of microglial mitochondria.

To test whether the downstream targets of SIRT1 and SIRT2 such as NF-κB and autophagy pathway are involved in the neuroprotection as mentioned in the introduction chapter, the corresponding methodology can be conducted to measure the activity of them. Electrophoretic mobility shift assay (EMSA) is a common technique to determine the interaction between protein and DNA or protein and RNA. This assay can be used to qualitatively and half quantitatively determine the amount of NF-κB binding to DNA. Nuclear isolation kits can be applied to extract cell nuclei. The cell nuclei can be collected after 1 h of LPS treatment to ensure that the activated NF-κB translocates to the nucleus and binds to κB DNA site. DNA probe can be synthesized and labeled by biotin. The biotin-labeled DNA probe can be incubated with isolated protein. Then, the mixture can be separated on a non-denaturing polyacrylamide gel. The shifted bands that correspond to the protein/DNA complexes can be visualized

eventually (B. Poljsak and I. Milisav, 2016). Regarding the measurement for autophagy, according to the guideline of interpretation of the methodology in monitoring autophagy, the assessment of autophagy is complex and needs to be considered integrally and multiple methods are recommended to determine simultaneously (D. J. Klionsky et al., 2016). Monodansylcadaverine (MDC) is an autofluorescent compound which can be used to label autophagic vacuoles (AV) *in vitro*. The accumulation of MDC-labelled vesicles is indicative of autophagy induction. Western blot also can be used to determine the expression level of LC3 protein which is an essential component on the membrane of autophagic vacuoles.

For determining whether there are augmentation synergistic effects among the combination treatments of SIRT drugs and antidepressants such as fluoxetine, combination index (CI) values with their indication can be used to assess the effects. The combination index is calculated from drug cytotoxicity or growth inhibition curves. The computer software Calcusyn can be used to calculate a CI, taking the entire shape of the growth inhibition curve into account for calculating whether a combination is synergistic, additive or antagonistic (I. V. Bijnsdorp et al., 2011). Median-drug effect analysis through Calcusyn is the most widely used method. CI value below 0.8 can simply be considered synergism. CI values between 0.8 and 1.2 can be additive. CI value above 1.2 can be seen as antagonism. A more detailed classification of CI value can indicate the grade of the strength in synergism and antagonism effects.

Regarding the animal study, behavioural parameters in the chronic phase of the LPS-induced depression model need to be assessed in the future, including OFT, TST and FST. Additionally, the biochemical evaluation needs to be conducted to verify whether the plasma level of inflammatory mediators can be reduced by SIRT drugs and compared with fluoxetine. The evaluation should include the determination of plasma level of IL-1β, TNF-α and PGE_2 and oxidative stress markers such as the amount of malondialdehyde (MDA) for peroxidation of lipids, glutathione assay (GSH) and catalase assay (CAT) for antioxidants.

Appendices

S1 Materials

Table S 1 Chemicals and reagents

Reagents	Supplier
Dulbecco's Modified Eagle Medium (DMEM) Low-glucose	Gibco by Life Technologies
Dulbecco's Modified Eagle Medium (DMEM) high-glucose	Gibco by Life Technologies
Fetal bovine serum (FBS)	Scientifix Life
Phosphate buffered saline (PBS)	Sigma-Aldrich, Merck
2.5% Trypsin-EDTA (10×)	Gibco by Life Technologies
Penicillin-streptomycin (10000 U/mL)	Gibco by Life Technologies
Trypan blue solution (0.4%)	Sigma-Aldrich, Merck
Resazurin (7-hydroxy-3H-phenoxazin-3-one-10-oxide sodium salt)	Sigma-Aldrich, Merck
Lipopolysaccharide (LPS from E. coli O111: B4 serotype)	Sigma-Aldrich, Merck
Resveratrol	Selleck Chemicals
EX527	Cayman Chemical
Sirtinol	Cayman Chemical
AGK2	Selleck Chemicals
Fluoxetine	Sigma-Aldrich, Merck
Ibuprofen	Sigma-Aldrich, Merck
Retinoic acid (RA)	Abcam
Recombinant Human/Murine/Rat brain-derived neurotrophic factor (BDNF) protein	Abcam/Sigma-Aldrich, Merck
Dimethylsulfoxide (DMSO)	Sigma-Aldrich, Merck
Dichloro-dihydro-fluorescein diacetate (DCFH-DA)	Sigma-Aldrich, Merck
Tubes and Ultra clear Caps for qPCR (strips of 8)	Thermo Fisher
TRIzol™ reagent	Thermo Fisher
UltraPure™ DNase/RNase-Free Distilled Water	Thermo Fisher
RNaseZap™ RNase Decontamination Solution	Thermo Fisher
Hank's balanced salt	Sigma-Aldrich, Merck
Sodium dihydrogen phosphate	Sigma-Aldrich, Merck
ECM Gel from Engelbreth-Holm-Swarm murine sarcoma	Sigma-Aldrich, Merck
Crystal violet	Sigma-Aldrich, Merck

Table S 2 Commercial kits

Kits	Supplier
Neurite outgrowth staining kit	Life technologies
Verso cDNA synthesis Kit	Thermo Fisher
PowerUp™ SYBR™ Green Master Mix	Thermo Fisher
Prostaglandin E_2 Express ELISA kit (500141)	Cayman Chemical
Rat IL-10 ELISA kit (BEK--2047)	Biosensis
Rat IL-1β ELISA kit (BEK-2309)	Biosensis
Rat TNF-α ELISA kit (BEK-2101)	Biosensis
Caspase 3/7 fluorescence assay kit	Cayman Chemical

Table S 3 List of Oligonucleotides

Oligonucleotide	Sequence	Application
SIRT1 (Rat) Forward	5'-CGCCTTATCCTCTAGTTCCTGTG-3'	rt-PCR
SIRT1 (Rat) Reverse	5'-CGGTCTGTCAGCATCATCTTCC-3'	rt-PCR
SIRT2 (Rat) Forward	5'-CTCCCACCAAACAGATGACC-3'	rt-PCR
SIRT2 (Rat) Reverse	5'-ATTCAGACTCGGACACTGAGG-3'	rt-PCR
GAPDH (Rat) Forward	5'-TCCCTCAAGATTGTCAGCAA-3'	rt-PCR
GAPDH (Rat) Reverse	5'-AGATCCACAACGGATACATT-3'	rt-PCR
SYP (Human) Forward	5'-TCCTCGTCAGCCGAATTCTTT-3'	rt-PCR
SYP (Human) Reverse	5'-CTCGCTACTTGTTCTGCAGGAA-3'	rt-PCR
ENO2 (Human) Forward	5'-CGGGAACTGCCCCTGTATC-3'	rt-PCR
ENO2 (Human) Reverse	5'-CATGAGAGCCACCATTGATCA-3'	rt-PCR
GAPDH (Human) Forward	5'-TGCACCACCAACTGCTTAGC-3'	rt-PCR
GAPDH (Human) Reverse	5'-GGCATGGACTGTGGTCATGAG-3'	rt-PCR

S2 Cell culture

All operations and experiments which were required to be sterile were performed in Biology Safety Cabinets.

S2.1 Monolayer cellular models

HAPI cells and SH-SY5Y cells were grown separately in ATCC-formulated DMEM (Gibco by Life Technologies, 11885084) which contains low glucose (1 g/L D-Glucose), L-glutamine (584 mg/L), sodium pyruvate (110 mg/L) and phenol red (15 mg/L). The media was additionally supplemented with 0.2% gentamicin and 10% fetal bovine serum (FBS). Cells were grown in sterile T-75 cm^2 flasks and cultured in an incubator at 37°C with 5% CO_2 and certain humidity. Cells were passaged with various ratios after they reached 80-90% confluence.

S2.2 Basic cell culture

To split and subculture cells to maintain cell viability

All items were sprayed with 80% ethanol before being put into the Biological Safety Cabinet. First, all culture media from the flask where cells were grown was removed. 10 mL of phosphate buffer solution (PBS) was added into the flask to wash out the media residue and the mixture was discarded using a pipette. Then, warmed 0.05% trypsin-EDTA solution (3 mL) was added into the flask to detach the cells which were placed in an incubator for 3 min. After that, warmed media (7 mL) was added into the mixture of cell suspension and the trypsin solution to obtain 10 mL cell suspension in total which was transferred into a 15 mL centrifuge tube. HAPI cells were centrifuged for 3 min at 1200 rpm/2790 × g in a centrifuge (Eppendorf centrifuge 5810 R). SH-SY5Y cells were centrifuged for 5 min at 900 rpm/1569 × g. The supernatant in the centrifuge tube was then carefully aspirated without disturbing the cell pellet. The cell pellet was resuspended thoroughly in various volumes of media using a pipette. Based on different splitting ratios (1:3, 1:5, 1:8), various volumes of this cell suspension was added into a new sterile flask supplemented with 15 mL of culture media. At last, this new passage of cells was taken into an incubator.

S2.3 Cell counting/ trypan blue exclusion assay

Counting with an automatic cell counter

Cells were split as the protocol mentioned above to obtain the cell suspension. Then, the well-mixed cell suspension (250 µL) was transferred into a 1.5 µL microcentrifuge

tube. The well-mixed cell suspension (100 µL) and trypan blue dye solution (0.4%, 100 µL) were transferred into a clean well of a 96-well plate. After evenly mixing, this mixed cell suspension (10 µL) was loaded into each chamber of a Countess slide. Then, the slide was inserted into an automatic cell counter. Cell density and cell viability were calculated and given by an automatically.

Counting with a hemocytometer

Cells were split as the protocol mentioned above to obtain the cell suspension. Then, well-mixed cell suspension (100 µL) and trypan blue dye solution (0.4%, 100 µL) were transferred into a clean 1.5 µL microcentrifuge tube and evenly mixed. A clean glass coverslip was placed on the top of the hemocytometer counting chamber. Dead cells were dyed blue color and viable cells were translucent. Both dead and viable cells in four corner squares and one center square of the grid were counted.

The following formula was used to calculate the viability and concentration of cells:

Cell viability = number of viable cells/total of cells × 100

Average number of viable cells per square = total of viable cells/5

Dilution factor = final volume/volume of cells = 200 µL/100 µL = 2

Concentration of cell suspension (cells/mL) = average number of cells per square × dilution factor × 10^4

S2.4 Thawing cells from -80℃ stocks

A cryogenic vial of cells was taken out from -80℃ freezer and swirled in a water bath immediately until the color turned pink and the cell suspension was defrosted thoroughly. Then, cells were transferred to a Biological Safety Hood. Twenty mL of warmed media was prepared in a sterile flask. The cell suspension was gently dropped into the media using a pipette and mixed by inverting gently. After that, this flask of cells was labeled and incubated for 24 h. The media was changed the next day.

S2.5 Freezing down cells for long-term storage

Cells were split as the protocol mentioned above and a cell pellet was obtained. Media containing 10% DMSO was used to resuspend the cells. Each 2 mL aliquot of the cell suspension was transferred to a cryogenic vial. The vial was placed in a Mr. Frosty

Freezing container in a freezer overnight and transferred to -80℃ freezer for long-term storage.

S3 Enzyme-linked immunosorbent assays (ELISA)

S3.1 Prostaglandins E_2 (PGE_2) production measurement

For measurement of PGE_2 production in HAPI cells after drug treatment and LPS challenge, prostaglandin E_2 express ELISA kit (Cayman chemical, 500141, Australia) was used to conduct the assay. ELISA buffer was prepared by diluting ELISA buffer concentrate (10X) with 90 mL of ultrapure distilled water. Wash buffer was prepared by diluting 5 mL of wash buffer concentrate into 1 L of ultrapure distilled water with a supplement of 500 µL polysorbate 20. PGE_2 standard was reconstituted with 1 mL of ELISA buffer and diluted into a series of concentrations with serum-free DMEM. PGE_2 express AChE tracer and monoclonal antibody were reconstituted with ELISA buffer respectively and supplemented with different dyes (1:100). According to the instruction of the protocol, blank (Blk) well, total activity (TA) wells, non-specific binding (NSB) wells, and maximum binding (B_0) wells were set up for data analysis and troubleshooting.

All standard solutions of a series of concentrations, samples, and the controls mentioned above were added into corresponding wells and incubated at room temperature on an orbital shaker for 60 min. Meanwhile, Ellman's reagent was reconstituted with 20 mL of ultrapure distilled water and protected from light. After incubation, all the contents were discarded by flicking the liquid vigorously out of the wells followed by gentle tapping onto blotting paper towels. Then the plates were washed 5 times using wash buffer. After that, Ellman's reagent (200 µL) was added into each well. Tracer (5 µL) was added into the TA wells and then the plate was sealed with a plastic film and incubated at room temperature on an orbital shaker for 60-90 min and protected from light. The absorbance was measured at 410 nm using a Tecan infinite 200 Pro microplate reader until the value of B_0 reached above 0.3 A.U. with blank value subtracted.

The raw data was calculated according to the instruction of the protocol and input into Graphpad Prism 5 and interpreted into concentration by performing a 4-parameter logistic (4-PL) regression analysis.

S3.2 TNF-α, IL-1β and IL-10 production measurement

For measurement of the production of TNF-α, IL-1β and IL-10 in HAPI cells after drug pre-treatment and LPS stimulation, rat TNF-α ELISA kit (Biosensis BEK-2101, Australia), rat IL-1β ELISA kit (Biosensis BEK-2309, Australia) and rat IL-10 ELISA kit (Biosensis BEK-2047, Australia) were used to conduct the measurement of the concentration of TNF-α in the supernatant. In order to avoid exceeding the range of measurement, preliminary dilution studies were conducted to estimate the level ranges of these cytokines produced by LPS-induced HAPI cells. For TNF-α measurement, the final samples were diluted in 1:10. For IL-1β and IL-10 measurement, dilution was not needed.

Wash buffer was prepared by dissolving the packet of PBS buffer concentrate with 900 mL of distilled water and adjusting pH to 7.2-7.6 with potassium phosphate monobasic or sodium phosphate dibasic to make 1000 mL as the final volume.

All supernatant samples were produced and collected fresh before running the assay. Diluted samples (100 µL) and buffer control were added into corresponding wells of the pre-coated plates and incubated overnight in a 4°C fridge. Then, the plate was emptied by a flicking movement and gently blotted on paper towels. After that, the plate was washed with wash buffer 5 times. Each wash took 1-2 min. Meanwhile, biotinylated antibody working solution was prepared by 1:100 dilution with antibody diluent buffer. Then, biotinylated antibody solution (100 µL) was added to corresponding wells and the plate was incubated at room temperature on an orbital shaker for 2-3 h. After that, the plate was washed 3 times with wash buffer. Meanwhile, avidin-biotin-peroxidase complex (ABC) working solution was prepared by 1:100 dilution with ABC diluent buffer. Then, ABC working solution (100 µL) was added into corresponding wells and incubated for 1 h on an obrbital shaker. After that, the plate was washed 3 times with wash buffer and 90 µL of warm TMB color developing reagent was added into each well and incubated for 20 to 35 min at room temperature. The TMB stop solution (100µL) was added when the color of the highest four concentrations of standard became obvious blue shades and other standands remained clear.

The absorbance of the yellow shade was measured at 450 nm by using a Tecan Infinite 200 Pro microplate reader (Tecan, Australia). The raw data were input into Graphpad Prism 5 and interpreted into concentration by performing a 4-PL regression analysis.

S4 Caspase-3/7 assay

S4.1 Seeding cells

SH-SY5Y cells were seeded in a 96-well plate at a density of 10^5 cells/mL. Then they were treated with conditioned supernatant collected from HAPI cells for 24 h.

S4.2 Reagent preparation

Assay buffer was prepared by dissolving a cell-based buffer tablet in 100 mL of distilled water. Caspase-3/7 substrate solution was prepared by dissolving 100 µL of caspase-3/7 substrate, 400 µL of DTT assay reagent in 9.5 mL of assay buffer. Active caspase-3 positive control and caspase-3/7 inhibitor solution were prepared by dilution with assay buffer.

S4.3 Performing assay

The plates were centrifuged (Eppendorf, 5810 R) at 800 × g (rcf) for 5 min. Then the supernatant was discarded by aspiration. Assay buffer (200 µL) was added into each well to rinse out medium residue. After that, the plates were centrifuged at 800 × g (rcf) for 5 min and the supernatant was aspirated. Then, cell-based assay lysis buffer (100 µL) was added into each well and incubated on an orbital shaker for 30 min at room temperature. After that, the plates were centrifuged for at 800 × g (rcf) for 10 min. The supernatant (90 µL) in each well was transferred to corresponding well in another black 96-well plate with the addition of 10 µL of assay buffer. For an indication of assay specificity, caspase-3/7 (10 µL) inhibitor was added to in the 90 µL of supernatant in separate wells. Then, the caspase-3/7 substrate solution (100 µL) was added into each well and incubated for 30-90 min at 37°C. Fluorescence (excitation: 485 nm and emission: 535 nm) was measured and recorded using a Tecan Infinite 200 Pro microplate reader (Tecan, Australia).

S5 Quantitative real-time PCR

S5.1 Isolation of total RNA

Lyse samples and separate phases

After the treatment, the supernatant above cells was aspirated. TRIzol™ reagent (Invitrogen) (0.5 mL) was added per 1×10^5-10^7 cells directly into wells to lyse the cells in a fume hood. The surface of the flask was gently washed across with TRIzol™ reagent to harvest all cells. All cell lysis was collected into PCR-grade microcentrifuge tubes. Chloroform (0.2 mL per 1 mL TRIzol™ used for lysis) was added into the cell lysis and shaken for 10 min. After that, the mixture was centrifuged for 15 min at 12000 × g at 4°C in a cooling centrifuge. The aqueous phase containing RNA was transferred to a new tube without pipetting any of the interphase or organic phase at the bottom of the tube.

Precipitate the RNA

An equivalent volume of isopropanol was added into the aqueous phase and incubated for 10 min. After then, the samples were centrifuged for 10 min at 12000 × g at 4°C. RNA gel pellet was obtained by removing the supernatant without disturbing the white feather-like pellet on the wall of the tube.

Wash the RNA

Ethanol (75%, 1 mL per 1 mL of TRIzol™ reagent used for lysis) was added to resuspend the RNA pellet. The samples were vortexed briefly and centrifuged for 5 min at 7500 × g at 4°C. The supernatant was discarded with a PCR-grade aerosol barrier tip and micropipette. The RNA pellet was air-dried for 5-10 min.

Solubilize the RNA

The RNA pellet was resuspended in 20 μL of RNase-free water by pipetting up and down. All samples were stored at -80°C until required.

Determine the concentration of RNA

The concentration and purity of RNA were measured using a Nanodrop Spectrophotometer (Thermo Fisher Scientific Australia). The RNA solution was spun down to the bottom of microcentrifuge tubes to obtain the whole droplets before measurement.

S5.2 cDNA synthesis

cDNA was synthesized using Verso cDNA synthesis kit (Thermo Scientific) and RNase-free PCR tubes. All cDNA samples were stored at -80°C until required. Each reaction mix was set up on ice as followed below:

Table S 4 System of cDNA synthesis.

Component	Volume
RNA template	0.5 µg/RNA concentration
Verso enzyme mix	1 µL
RT Enhancer	1 µL
A blend of random hemaxers and oligoDT (3:1)	1 µL
dNTP Mix	2 µL
cDNA sythesis buffer	4 µL
RNase-free water	11 µL – volume of RNA
Total volume	20 µL

The cDNA synthesis was performed using ProFlex PCR System (Life techonology). The reverse transcription cycling program was set up as followed below:

Table S 5 Condition setup for cDNA synthesis.

Step	Temperature	Time	Number of cycles
cDNA synthesis	42°C	30 min	1 cycle
Inactivation	95°C	2 min	1 cycle
Final	4°C		

S5.3 Real-time PCR

The real-time PCR (rt-PCR) reaction was preformed using PowerUp™ SYBR™ Green Master Mix (Thermo Fisher Scientific Australia) and qPCR tubes with ultra clear caps. Each reaction system was set up on ice as followed below:

Table S 6 System of rt-PCR.

Component	Volume	Final concentration

Forward primer (10 μM)	1 μL	500 nM
Reverse primer (10 μM)	1 μL	500 nM
cDNA	2 μL	
SYBR Green Mix	10 μL	
RNase-free water	6 μL	
Total volume	20 μL	

The rt-PCR was performed using QuantStudio™ 3 Real-Time PCR Systems (Thermo Fisher Scientific Australia). The thermal cycling conditions were set up as followed below:

Table S 7 Fast cycling condition setup for running rt-PCR.

Step	Temperature	Duration	Cycles
UDG activation	50°C	2 min	Hold
Dual-Lock™ DNA polymerase	95°C	2 min	Hold
Denature	95°C	1 s	40
Anneal/extend	60°C	30 s	

Table S 8 Dissociation curve conditions setup for rt-PCR.

Step	Ramp rate	Temperature	Time
1	1.6°C/s	95°C	15 s
2	1.6°C/s	60°C	1 min
3 (Dissociation)	0.15°C/s	95°C	15 min

The comparative threshold cycles (C_T) or $2^{-\Delta\Delta C_T}$ method was used to compare the C_T values of samples of interest with control samples. All C_T values were normalized against GAPDH gene. The equation is showed as followed below:

Normalisation: $\Delta C_T = C_T$ (gene of interest) $- C_T$ (GAPDH)

$\Delta\Delta C_T = \Delta C_T$ (sample) $- \Delta C_T$ (control)

Fold change = $2^{-\Delta\Delta C_T}$

Reference

American Psychiatric Association, 2013. Diagnostic and statistical manual of mental disorders V, Washington, DC: American Psychiatric Association.

AMH, 2018. Australian medicines handbook (online). Adelaide: Australian medicines handbook Pty Ltd; Retrieved from: https://amhonline.amh.net.au/.

Australian Institute of Health and Welfare, 2020. Mental health services in Australia. Retrieved from https://www.aihw.gov.au/reports/mental-health-services/mental-health-services-in-australia.

National Research Council, 2011. Guide for the care and use of laboratory animals. 8th ed. Washington (DC): National Academies Press (US).

Selleckchem, 2020. Sirtinol catalog No.S2804. Retrieved from https://www.selleckchem.com/products/sirtinol.html [Online]. [Accessed 5 July 2020].

Sigma-Aldrich, 2018a. Glucose in cell culture. Retrieved from Sigma-Aldrich learning center media expert: www.sigmaaldrich.com/life-science/cell-culture/learning-center/media-expert/glucose.html.

Sigma-Aldrich, 2018b. Sigma aldrich ECM Gel from Engelbreth-Holm-Swarm murine sarcoma. Retrieved from https://www.sigmaaldrich.com/content/dam/sigma-aldrich/docs/Sigma/Datasheet/3/e1270dat.pdf.

UK ECT Review Group, 2003. Efficacy and safety of electroconvulsive therapy in depressive disorders: a systematic review and meta-analysis. *Lancet,* 361**,** 799-808.

World Health Organization, 1992. The ICD-10 classification of mental and behavioral disorders. Clinical descriptions and diagnostic guidelines. Geneva, Switzerland: World Health Organization.

World Health Organization, 2020. Depression key facts. Retrieved from https://www.who.int/news-room/fact-sheets/detail/depression.

Abbott, N. J., Ronnback, L. & Hansson, E. 2006. Astrocyte-endothelial interactions at the blood-brain barrier. *Nat Re Neurosci,* 7**,** 41-53.

Abe-Higuchi, N., Uchida, S., Yamagata, H., Higuchi, F., Hobara, T., Hara, K., Kobayashi, A. & Watanabe, Y. 2016. Hippocampal sirtuin 1 signaling mediates depression-like behavior. *Biol Psychiatry,* 80**,** 815-826.

Abràmoff, M. D. Magalhães, P. J. Ram, S. J 2004. Image processing with ImageJ. *Biophotonics Int,* 11**,** 36-42.

Aggarwal, B. B. 2003. Signalling pathways of the TNF superfamily: A double-edged sword. *Nat Rev Immunol,* 3**,** 745-756.

Aggarwal, B. B. 2004. Nuclear factor-kappaB: the enemy within. *Cancer Cell,* 6**,** 203-8.

Ahn, K. S. & Aggarwal, B. B. 2005. Transcription factor NF-kappaB: a sensor for smoke and stress signals. *Ann N Y Acad Sci,* 1056**,** 218-33.

Akbar, Mohammed, Essa, Musthafa Mohamed, Daradkeh, Ghazi, Abdelmegeed, Mohamed A., Choi, Youngshim, Mahmood, Lubna & Song, Byoung-Joon 2016. Mitochondrial dysfunction and cell death in neurodegenerative diseases through nitroxidative stress. *Brain Res,* 1637**,** 34-55.

Albani, D., Polito, L., Batelli, S., De Mauro, S., Fracasso, C., Martelli, G., Colombo, L., Manzoni, C., Salmona, M., Caccia, S., Negro, A. & Forloni, G. 2009. The SIRT1 activator resveratrol protects SK-N-BE cells from oxidative stress and against toxicity caused by alpha-synuclein or amyloid-beta (1-42) peptide. *J Neurochem,* 110**,** 1445-56.

Alcendor, Ralph R., Gao, Shumin, Zhai, Peiyong, Zablocki, Daniela, Holle, Eric, Yu, Xianzhong, Tian, Bin, Wagner, Thomas, Vatner, Stephen F. & Sadoshima, Junichi 2007. Sirt1 regulates aging and resistance to oxidative stress in the heart. *Circ Res,* 100**,** 1512-1521.

Anacker, C., Cattaneo, A., Luoni, A., Musaelyan, K., Zunszain, P. A., Milanesi, E., Rybka, J., Berry, A., Cirulli, F., Thuret, S., Price, J., Riva, M. A., Gennarelli, M. & Pariante, C.

M. 2013. Glucocorticoid-related molecular signaling pathways regulating hippocampal neurogenesis. *Neuropsychopharmacology,* 38**,** 872-83.

Andrew A. Nierenberg, Maurizio Fava, Madhukar H. Trivedi, Stephen R. Wisniewski, Michael E. Thase, Patrick J. Mcgrath, Jonathan E. Alpert, Diane Warden, James F. Luther, George Niederehe, Barry Lebowitz, Kathy Shores-Wilson & A. John Rush 2006. A comparison of Lithium and T 3 augmentation following two failed medication treatments for depression: a STAR*D report. *Am J Psychiatry,* 163**,** 1519-1530.

Baquero, Miquel & Martín, Nuria 2015. Depressive symptoms in neurodegenerative diseases. *World J Clin Cases,* 3**,** 682-693.

Basu Mallik, Sanchari, Mudgal, Jayesh, Nampoothiri, Madhavan, Hall, Susan, Dukie, Shailendra Anoopkumar, Grant, Gary, Rao, C. Mallikarjuna & Arora, Devinder 2016. Caffeic acid attenuates lipopolysaccharide-induced sickness behaviour and neuroinflammation in mice. *Neurosci Lett,* 632**,** 218-223.

Batista, Carla Ribeiro Alvares, Gomes, Giovanni Freitas, Candelario-Jalil, Eduardo, Fiebich, Bernd L. & De Oliveira, Antonio Carlos Pinheiro 2019. Lipopolysaccharide-induced neuroinflammation as a bridge to understand neurodegeneration. *Int J Mol Sci,* 20**,** 2293.

Bazan, Nicolas G. 2001. COX-2 as a multifunctional neuronal modulator. *Nat Med,* 7**,** 414-415.

Becher, B., Spath, S. & Goverman, J. 2017. Cytokine networks in neuroinflammation. *Nat Rev Immunol,* 17**,** 49-59.

Bechmann, Ingo, Galea, Ian & Perry, V. Hugh 2006. What is the blood-brain barrier (not)? *Trends Immunol,* 28**,** 5-11.

Beck-Friis, J., Kjellman, B. F., Aperia, B., Unden, F., Von Rosen, D., Ljunggren, J. G. & Wetterberg, L. 1985. Serum melatonin in relation to clinical variables in patients with major depressive disorder and a hypothesis of a low melatonin syndrome. *Acta Psychiatr Scand,* 71**,** 319-30.

Bellet, M. M., Masri, S., Astarita, G., Sassone-Corsi, P., Della Fazia, M. A. & Servillo, G. 2016. Histone deacetylase SIRT1 controls proliferation, circadian rhythm, and lipid metabolism during liver regeneration in mice. *J Biol Chem,* 291**,** 23318-23329.

Ben Salem, I., Boussabbeh, M., Da Silva, J. P., Guilbert, A., Bacha, H., Abid-Essefi, S. & Lemaire, C. 2017. SIRT1 protects cardiac cells against apoptosis induced by zearalenone or its metabolites alpha- and beta-zearalenol through an autophagy-dependent pathway. *Toxicol Appl Pharmacol,* 314**,** 82-90.

Benveniste, E. N. 1992. Inflammatory cytokines within the central nervous system: sources, function, and mechanism of action. *Am J Physiol Cell Physiol,* 263**,** C1-C16.

Biesmans, Steven, Meert, Theo F., Bouwknecht, Jan A., Acton, Paul D., Davoodi, Nima, De Haes, Patrick, Kuijlaars, Jacobine, Langlois, Xavier, Matthews, Liam J. R., Ver Donck, Luc, Hellings, Niels & Nuydens, Rony 2013. Systemic immune activation leads to neuroinflammation and sickness behavior in mice. *Mediators Inflamm.,* 2013**,** 271359.

Bijnsdorp, Irene V., Giovannetti, Elisa & Peters, Godefridus J. 2011. Analysis of drug interactions. *In:* CREE, I. A. (ed.) Cancer Cell Culture: Methods and Protocols. Totowa, NJ: Humana Press.

Bockting, C. L., Ten Doesschate, M. C., Spijker, J., Spinhoven, P., Koeter, M. W. & Schene, A. H. 2008. Continuation and maintenance use of antidepressants in recurrent depression. *Psychother Psychosom,* 77**,** 17-26.

Boonen, B., Alpizar, Y. A., Sanchez, A., Lopez-Requena, A., Voets, T. & Talavera, K. 2018. Differential effects of lipopolysaccharide on mouse sensory TRP channels. *Cell Calcium,* 73**,** 72-81.

Borges, G., Berrocoso, E., Mico, J. A. & Neto, F. 2015. ERK1/2: Function, signaling and implication in pain and pain-related anxio-depressive disorders. *Prog Neuropsychopharmacol Biol Psychiatry,* 60**,** 77-92.

Brian Walker, Nicki R Colledge, Stuart Ralston, Ian Penman 2014. Davidson's Principles and Practice of Medicine, Churchill Livingstone.

Brigitta, Bondy 2002. Pathophysiology of depression and mechanisms of treatment. *Dialogues Clin Neurosci,* 4**,** 7-20.

Burns, A. & Iliffe, S. 2009. Alzheimer's disease. *The BMJ,* 338**,** b158.
Cadwell, Ken 2016. Crosstalk between autophagy and inflammatory signaling pathways: balancing host defence and homeostasis. *Nat Rev Immunol,* 16**,** 661-675.
Cai, Shangli, Huang, Shucai & Hao, Wei 2015. New hypothesis and treatment targets of depression: an integrated view of key findings. *Neurosci. Bull.,* 31**,** 61-74.
Cai, Y. L., Xu, L., Xu, H. W. & Fan, X. T. 2016. SIRT1 and neural cell fate determination. *Mol Neurobiol,* 53**,** 2815-2825.
Cao, Duanfang, Wang, Mingzhu, Qiu, Xiayang, Liu, Dongxiang, Jiang, Hualiang, Yang, Na & Xu, Rui-Ming 2015. Structural basis for allosteric, substrate-dependent stimulation of SIRT1 activity by resveratrol. *Genes Dev,* 29**,** 1316-1325.
Castren, E. & Rantamaki, T. 2010. The role of BDNF and its receptors in depression and antidepressant drug action: Reactivation of developmental plasticity. *Dev Neurobiol,* 70**,** 289-97.
Chang, J. Robert, Ghafouri, Mohammad, Mukerjee, Ruma, Bagashev, Asen, Chabrashvili, Tinatin & Sawaya, Bassel E. 2012. Role of p53 in neurodegenerative diseases. *Neurodegener Dis,* 9**,** 68-80.
Cheepsunthorn, P., Radov, L., Menzies, S., Reid, J. & Connor, J. R. 2001. Characterization of a novel brain-derived microglial cell line isolated from neonatal rat brain. *Glia,* 35**,** 53-62.
Chen, Grace Y. & Nuñez, Gabriel 2010. Sterile inflammation: sensing and reacting to damage. *Nat Rev Immunol,* 10**,** 826-837.
Chen, J., Zhou, Y., Mueller-Steiner, S., Chen, L. F., Kwon, H., Yi, S., Mucke, L. & Gan, L. 2005. SIRT1 protects against microglia-dependent amyloid-beta toxicity through inhibiting NF-kappaB signaling. *J Biol Chem,* 280**,** 40364-74.
Chen, L. F. & Greene, W. C. 2004. Shaping the nuclear action of NF-kappa B. *Nat Rev Mol Cell Biol,* 5**,** 392-401.
Chen, Qi, Luo, Ying, Kuang, Shengnan, Yang, Yang, Tian, Xiaoyan, Ma, Jie, Mai, Shaoshan, Xue, Lai & Yang, Junqing 2017. Cyclooxygenase-2 signalling pathway in the cortex is involved in the pathophysiological mechanisms in the rat model of depression. *Sci Rep,* 7**,** 488.
Chen, X., Wales, P., Quinti, L., Zuo, F., Moniot, S., Herisson, F., Rauf, N. A., Wang, H., Silverman, R. B., Ayata, C., Maxwell, M. M., Steegborn, C., Schwarzschild, M. A., Outeiro, T. F. & Kazantsev, A. G. 2015. The sirtuin-2 inhibitor AK7 is neuroprotective in models of Parkinson's disease but not amyotrophic lateral sclerosis and cerebral ischemia. *PLoS One,* 10**,** e0116919.
Chen, Zhiqing, Zhai, Yi, Zhang, Wei, Teng, Yan & Yao, Ke 2015. Single nucleotide polymorphisms of the sirtuin 1 (SIRT1) gene are associated with age-related macular degeneration in Chinese Han individuals: a case-control pilot study. *Medicine,* 94**,** e2238-e2238.
Cheng, C. K., Luo, J. Y., Lau, C. W., Chen, Z. Y., Tian, X. Y. & Huang, Y. 2019. Pharmacological basis and new insights of resveratrol action in the cardiovascular system. *Br J Pharmacol*.
Chermat, R., Thierry, B., Mico, J. A., Steru, L. & Simon, P. 1986. Adaptation of the tail suspension test to the rat. *J. Pharmacol.,* 17**,** 348-350.
Cheung, Y. T., Lau, W. K., Yu, M. S., Lai, C. S., Yeung, S. C., So, K. F. & Chang, R. C. 2009. Effects of all-trans-retinoic acid on human SH-SY5Y neuroblastoma as in vitro model in neurotoxicity research. *Neurotoxicology,* 30**,** 127-35.
Chopra, V., Quinti, L., Kim, J., Vollor, L., Narayanan, K. L., Edgerly, C., Cipicchio, P. M., Lauver, M. A., Choi, S. H., Silverman, R. B., Ferrante, R. J., Hersch, S. & Kazantsev, A. G. 2012. The sirtuin 2 inhibitor AK-7 is neuroprotective in Huntington's disease mouse models. *Cell Reports,* 2**,** 1492-7.
Clancy, Robert, Varenika, Branko, Huang, Weiqing, Ballou, Les, Attur, Mukundan, Amin, Ashok R. & Abramson, Steven B. 2000. Nitric oxide synthase/COX cross-talk: nitric oxide activates COX-1 but inhibits COX-2-derived prostaglandin production. *J Immunol,* 165**,** 1582-1587.

Constantinescu, R., Constantinescu, A. T., Reichmann, H. & Janetzky, B. 2007. Neuronal differentiation and long-term culture of the human neuroblastoma line SH-SY5Y. *J Neural Transm Suppl***,** 17-28.

Cotter, D., Mackay, D., Landau, S., Kerwin, R. & Everall, I. 2001. Reduced glial cell density and neuronal size in the anterior cingulate cortex in major depressive disorder. *Arch Gen Psychiatry,* 58**,** 545-553.

Crozier, R. A., Bi, C., Han, Y. R. & Plummer, M. R. 2008. BDNF modulation of NMDA receptors is activity dependent. *J Neurophysiol,* 100**,** 3264-74.

Cryan, J. F. 2010. Encyclopedia of behavioral neuroscience.

Cryan, J. F. & Holmes, A. 2005. The ascent of mouse: advances in modelling human depression and anxiety. *Nat Rev Drug Discov,* 4**,** 775-790.

Cui, Qiao, Tashiro, Shin-ichi, Onodera, Satoshi & Ikejima, Takashi 2006. Augmentation of oridonin-induced apoptosis observed with reduced autophagy. *J Pharmcol Sci,* 101**,** 230-239.

Cunha-Santos, J., Duarte-Neves, J., Carmona, V., Guarente, L., Pereira De Almeida, L. & Cavadas, C. 2016. Caloric restriction blocks neuropathology and motor deficits in Machado-Joseph disease mouse models through SIRT1 pathway. *Nat Commun,* 7**,** 11445.

D'agostino, Andrew, English, Clayton D. & Rey, Jose A. 2015. Vortioxetine (brintellix): a new serotonergic antidepressant. *Pharm Ther,* 40**,** 36-40.

Da Rocha, Joana Fernandes, Da Cruz E Silva, Odete A. B. & Vieira, Sandra Isabel 2015. Analysis of the amyloid precursor protein role in neuritogenesis reveals a biphasic SH-SY5Y neuronal cell differentiation model. *J Neurochem,* 134**,** 288-301.

Dallas, S., Block, M. L., Thompson, D. M., Bonini, M. G., Ronaldson, P. T., Bendayan, R. & Miller, D. S. 2013. Microglial activation decreases retention of the protease inhibitor saquinavir: implications for HIV treatment. *J Neuroinflammation,* 10**,** 58.

Daly, Ann K. 2010. Pharmacogenetics and human genetic polymorphisms. *Biochem J,* 429**,** 435-449.

Dantzer, Robert 2004. Cytokine-induced sickness behaviour: a neuroimmune response to activation of innate immunity. *Eur J Pharmacol,* 500**,** 399-411.

Dantzer, Robert, O'connor, Jason C., Freund, Gregory G., Johnson, Rodney W. & Kelley, Keith W. 2008. From inflammation to sickness and depression: when the immune system subjugates the brain. *Nat Rev Neurosci,* 9**,** 46-56.

Davis, Beckley K., Wen, Haitao & Ting, Jenny P. Y. 2011. The inflammasome NLRs in immunity, inflammation, and associated diseases. *Annu Rev Immunol,* 29**,** 707-735.

De Mello, M. F., De Jesus Mari, J., Bacaltchuk, J., Verdeli, H. & Neugebauer, R. 2005. A systematic review of research findings on the efficacy of interpersonal therapy for depressive disorders. *Eur Arch Psychiatry Clin Neurosci,* 255**,** 75-82.

De Oliveira, Rita Machado, Vicente Miranda, Hugo, Francelle, Laetitia, Pinho, Raquel, Szegö, Éva M., Martinho, Renato, Munari, Francesca, Lázaro, Diana F., Moniot, Sébastien, Guerreiro, Patrícia, Fonseca, Luis, Marijanovic, Zrinka, Antas, Pedro, Gerhardt, Ellen, Enguita, Francisco Javier, Fauvet, Bruno, Penque, Deborah, Pais, Teresa Faria, Tong, Qiang, Becker, Stefan, Kügler, Sebastian, Lashuel, Hilal Ahmed, Steegborn, Clemens, Zweckstetter, Markus & Outeiro, Tiago Fleming 2017. The mechanism of sirtuin 2–mediated exacerbation of alpha-synuclein toxicity in models of Parkinson disease. *PLoS Biol,* 15**,** e2000374.

De Vries, Helga E., Blom-Roosemalen, Margret C. M., Oosten, Marijke van, De Boer, Albert G., Van Berkel, Theo J. C., Breimer, Douwe D. & Kuiper, Johan 1996. The influence of cytokines on the integrity of the blood-brain barrier in vitro. *J Neuroimmunol,* 64**,** 37-43.

Deavall, Damian G., Martin, Elizabeth A., Horner, Judith M. & Roberts, Ruth 2012. Drug-induced oxidative stress and toxicity. *J Toxicol,* 2012**,** 645460.

Dedic, Nina, Walser, Sandra & Deussing, Jan 2011. Mouse models of depression. Psychiatric Disorders - Trends and Developments.

Deretic, Vojo, Saitoh, Tatsuya & Akira, Shizuo 2013. Autophagy in infection, inflammation, and immunity. *Nat Rev Immunol,* 13**,** 722-737.

Derubeis, Robert J., Siegle, Greg J. & Hollon, Steven D. 2008. Cognitive therapy vs. medications for depression: Treatment outcomes and neural mechanisms. *Nat Rev Neurosci,* 9**,** 788-796.

Desai, Anu, Kisaalita, William S., Keith, Charles & Wu, Z. Z. 2006. Human neuroblastoma (SH-SY5Y) cell culture and differentiation in 3-D collagen hydrogels for cell-based biosensing. *Biosens Bioelectron,* 21**,** 1483-1492.

Di Fruscia, P., Zacharioudakis, E., Liu, C., Moniot, S., Laohasinnarong, S., Khongkow, M., Harrison, I. F., Koltsida, K., Reynolds, C. R., Schmidtkunz, K., Jung, M., Chapman, K. L., Steegborn, C., Dexter, D. T., Sternberg, M. J., Lam, E. W. & Fuchter, M. J. 2015. The discovery of a highly selective 5,6,7,8-tetrahydrobenzo[4,5]thieno[2,3-d]pyrimidin-4(3H)-one SIRT2 inhibitor that is neuroprotective in an in vitro Parkinson's disease model. *ChemMedChem,* 10**,** 69-82.

Di Maio, L, Squitieri, F, Napolitano, G, Campanella, G, Trofatter, J A & Conneally, P M 1993. Suicide risk in Huntington's disease. *J. Med. Genet.,* 30**,** 293-295.

Di Paolo, Nelson C. & Shayakhmetov, Dmitry M. 2016. Interleukin 1α and the inflammatory process. *Nat Immunol,* 17**,** 906-913.

Diaz-Ruiz, C., Rodriguez-Perez, A. I., Beiroa, D., Rodriguez-Pallares, J. & Labandeira-Garcia, J. L. 2015. Reciprocal regulation between sirtuin-1 and angiotensin-II in the substantia nigra: implications for aging and neurodegeneration. *Oncotarget,* 6**,** 26675-89.

Donmez, G. & Outeiro, T. F. 2013. SIRT1 and SIRT2: emerging targets in neurodegeneration. *EMBO Mol Med,* 5**,** 344-52.

Drago, J., Nurcombe, V. & Bartlett, P. F. 1991. Laminin through its long arm E8 fragment promotes the proliferation and differentiation of murine neuroepithelial cells in vitro. *Exp Cell Res,* 192**,** 256-65.

Du, Yipeng, Hu, Hao, Hua, Chaoju, Du, Kang & Wei, Taotao 2018. Tissue distribution, subcellular localization, and enzymatic activity analysis of human SIRT5 isoforms. *Biochem Biophys Res Commun,* 503**,** 763-769.

Duewell, Peter, Kono, Hajime, Rayner, Katey J., Sirois, Cherilyn M., Vladimer, Gregory, Bauernfeind, Franz G., Abela, George S., Franchi, Luigi, Nuñez, Gabriel, Schnurr, Max, Espevik, Terje, Lien, Egil, Fitzgerald, Katherine A., Rock, Kenneth L., Moore, Kathryn J., Wright, Samuel D., Hornung, Veit & Latz, Eicke 2010. NLRP3 inflammasomes are required for atherogenesis and activated by cholesterol crystals. *Nature,* 464**,** 1357.

Duman, R. S., Malberg, J. & Thome, J. 1999. Neural plasticity to stress and antidepressant treatment. *Biol Psychiatry,* 46**,** 1181-91.

Dwane, Susan, Durack, Edel & Kiely, Patrick A. 2013. Optimising parameters for the differentiation of SH-SY5Y cells to study cell adhesion and cell migration. *BMC Res Notes,* 6**,** 366-366.

Encinas, M., Iglesias, M., Liu, Y., Wang, H., Muhaisen, A., Cena, V., Gallego, C. & Comella, J. X. 2000. Sequential treatment of SH-SY5Y cells with retinoic acid and brain-derived neurotrophic factor gives rise to fully differentiated, neurotrophic factor-dependent, human neuron-like cells. *J Neurochem,* 75**,** 991-1003.

Erburu, M., Munoz-Cobo, I., Diaz-Perdigon, T., Mellini, P., Suzuki, T., Puerta, E. & Tordera, R. M. 2017. SIRT2 inhibition modulate glutamate and serotonin systems in the prefrontal cortex and induces antidepressant-like action. *Neuropharmacology,* 117**,** 195-208.

Erburu, M., Munoz-Cobo, I., Dominguez-Andres, J., Beltran, E., Suzuki, T., Mai, A., Valente, S., Puerta, E. & Tordera, R. M. 2015. Chronic stress and antidepressant induced changes in Hdac5 and Sirt2 affect synaptic plasticity. *Eur Neuropsychopharmacol,* 25**,** 2036-48.

Eyre, H. A., Air, T., Proctor, S., Rositano, S. & Baune, B. T. 2015. A critical review of the efficacy of non-steroidal anti-inflammatory drugs in depression. *Prog Neuropsychopharmacol Biol Psychiatry,* 57**,** 11-6.

Eyre, Harris & Baune, Bernhard T. 2012. Neuroplastic changes in depression: a role for the immune system. *Psychoneuroendocrinology,* 37**,** 1397-1416.

Felger, J. C. & Lotrich, F. E. 2013. Inflammatory cytokines in depression: neurobiological mechanisms and therapeutic implications. *Neuroscience,* 246**,** 199-229.

Feng, X., Liang, N., Zhu, D., Gao, Q., Peng, L., Dong, H., Yue, Q., Liu, H., Bao, L., Zhang, J., Hao, J., Gao, Y., Yu, X. & Sun, J. 2013. Resveratrol inhibits beta-amyloid-induced neuronal apoptosis through regulation of SIRT1-ROCK1 signaling pathway. *PLoS One,* 8**,** e59888.

Ferguson, James M. 2001. SSRI antidepressant medications: adverse effects and tolerability. *Prim Care Companion J Clin Psychiatry,* 3**,** 22-27.

Ferland, C. L., Hawley, W. R., Puckett, R. E., Wineberg, K., Lubin, F. D., Dohanich, G. P. & Schrader, L. A. 2013. Sirtuin activity in dentate gyrus contributes to chronic stress-induced behavior and extracellular signal-regulated protein kinases 1 and 2 cascade changes in the hippocampus. *Biol Psychiatry,* 74**,** 927-35.

Ferland, C. L. & Schrader, L. A. 2011. Regulation of histone acetylation in the hippocampus of chronically stressed rats: a potential role of sirtuins. *Neuroscience,* 174**,** 104-14.

Ferretta, A., Gaballo, A., Tanzarella, P., Piccoli, C., Capitanio, N., Nico, B., Annese, T., Di Paola, M., Dell'aquila, C., De Mari, M., Ferranini, E., Bonifati, V., Pacelli, C. & Cocco, T. 2014. Effect of resveratrol on mitochondrial function: implications in parkin-associated familiar Parkinson's disease. *Biochim Biophys Acta,* 1842**,** 902-15.

Fiebich, Bernd L., Batista, Carla Ribeiro Alvares, Saliba, Soraya Wilke, Yousif, Nizar M. & De Oliveira, Antonio Carlos Pinheiro 2018. Role of Microglia TLRs in Neurodegeneration. *Front Cell Neurosci,* 12.

Fleshner, Monika, Frank, Matthew & Maier, Steven F. 2016. Danger signals and inflammasomes: stress-evoked sterile inflammation in mood disorders. *Neuropsychopharmacology,* 42**,** 36.

Forster, J. I., Köglsberger, S., Trefois, C., Boyd, O., Baumuratov, A. S., Buck, L., Balling, R. & Antony, P. M. A. 2016. Characterization of differentiated SH-SY5Y as neuronal screening model reveals increased oxidative vulnerability. *J Biomol Screen,* 21**,** 496-509.

Frade, J. M., Martinez-Morales, J. R. & Rodriguez-Tebar, A. 1996. Laminin-1 selectively stimulates neuron generation from cultured retinal neuroepithelial cells. *Exp Cell Res,* 222**,** 140-9.

Frank-Cannon, Tamy C., Alto, Laura T., Mcalpine, Fiona E. & Tansey, Malú G. 2009. Does neuroinflammation fan the flame in neurodegenerative diseases? *Mol Neurodegener,* 4**,** 47-47.

Frozza, R. L., Bernardi, A., Hoppe, J. B., Meneghetti, A. B., Battastini, A. M., Pohlmann, A. R., Guterres, S. S. & Salbego, C. 2013. Lipid-core nanocapsules improve the effects of resveratrol against Abeta-induced neuroinflammation. *J Biomed Nanotechnol,* 9**,** 2086-104.

Fu, G., Chen, S., Liang, L., Li, X., Tang, P., Rao, X., Pan, M., Xu, X., Li, Y., Yao, Y., Zhou, Y., Gao, J., Mo, S., Cai, S., Peng, J., Zhang, Z., Clevers, H., Gao, J. & Hua, G. 2021. SIRT1 inhibitors mitigate radiation-induced GI syndrome by enhancing intestinal-stem-cell survival. *Cancer Lett.,* 501**,** 20-30.

Galluzzi, L., Maiuri, M. C., Vitale, I., Zischka, H., Castedo, M., Zitvogel, L. & Kroemer, G. 2007. Cell death modalities: classification and pathophysiological implications. *Cell Death Differ.,* 14**,** 1237-43.

Galluzzi, Lorenzo, Vitale, Ilio, Aaronson, Stuart A., Abrams, John M., Adam, Dieter, Agostinis, Patrizia, Alnemri, Emad S., Altucci, Lucia, Amelio, Ivano, Andrews, David W., Annicchiarico-Petruzzelli, Margherita, Antonov, Alexey V., Arama, Eli, Baehrecke, Eric H., Barlev, Nickolai A., Bazan, Nicolas G., Bernassola, Francesca, Bertrand, Mathieu J. M., Bianchi, Katiuscia, Blagosklonny, Mikhail V., Blomgren, Klas, Borner, Christoph, Boya, Patricia, Brenner, Catherine, Campanella, Michelangelo, Candi, Eleonora, Carmona-Gutierrez, Didac, Cecconi, Francesco, Chan, Francis K. M., Chandel, Navdeep S., Cheng, Emily H., Chipuk, Jerry E., Cidlowski,

John A., Ciechanover, Aaron, Cohen, Gerald M., Conrad, Marcus, Cubillos-Ruiz, Juan R., Czabotar, Peter E., D'angiolella, Vincenzo, Dawson, Ted M., Dawson, Valina L., De Laurenzi, Vincenzo, De Maria, Ruggero, Debatin, Klaus-Michael, Deberardinis, Ralph J., Deshmukh, Mohanish, Di Daniele, Nicola, Di Virgilio, Francesco, Dixit, Vishva M., Dixon, Scott J., Duckett, Colin S., Dynlacht, Brian D., El-Deiry, Wafik S., Elrod, John W., Fimia, Gian Maria, Fulda, Simone, García-Sáez, Ana J., Garg, Abhishek D., Garrido, Carmen, Gavathiotis, Evripidis, Golstein, Pierre, Gottlieb, Eyal, Green, Douglas R., Greene, Lloyd A., Gronemeyer, Hinrich, Gross, Atan, Hajnoczky, Gyorgy, Hardwick, J. Marie, Harris, Isaac S., Hengartner, Michael O., Hetz, Claudio, Ichijo, Hidenori, Jäättelä, Marja, Joseph, Bertrand, Jost, Philipp J., Juin, Philippe P., Kaiser, William J., Karin, Michael, Kaufmann, Thomas, Kepp, Oliver, Kimchi, Adi, Kitsis, Richard N., Klionsky, Daniel J., Knight, Richard A., Kumar, Sharad, Lee, Sam W., Lemasters, John J., Levine, Beth, Linkermann, Andreas, Lipton, Stuart A., Lockshin, Richard A., López-Otín, Carlos, Lowe, Scott W., Luedde, Tom, Lugli, Enrico, Macfarlane, Marion, Madeo, Frank, Malewicz, Michal, Malorni, Walter, Manic, Gwenola, et al. 2018. Molecular mechanisms of cell death: recommendations of the Nomenclature Committee on Cell Death 2018. *Cell Death Differ.*, 25**,** 486-541.

Gan, Li & Mucke, Lennart 2008. Paths of convergence: sirtuins in aging and neurodegeneration. *Neuron,* 58**,** 10-14.

Gao, J., Zhou, R., You, X. T., Luo, F., He, H., Chang, X. Y., Zhu, L. P., Ding, X. S. & Yan, T. H. 2016. Salidroside suppresses inflammation in a D-galactose-induced rat model of Alzheimer's disease via SIRT1/NF-kappa B pathway. *Metab Brain Dis,* 31**,** 771-778.

Garside, R. F., Kay, D. W. K., Wilson, I. C., Deaton, I. D. & Roth, M. 1971. Depressive syndromes and classification of patients. *Psychol Med,* 1**,** 333-338.

Gaynes, Bradley N., Warden, Diane, Trivedi, Madhukar H., Wisniewski, Stephen R., Fava, Maurizio & Rush, A. John 2009. What did STAR*D teach us? results from a large-scale, practical, clinical trial for patients with depression. *Psychiatr Serv,* 60**,** 1439-1445.

Gelder M., Harrison P., Cowen P. 2006. Shorter oxford textbook of psychiatry, Oxford: Oxford University Press.

Gendelman, H. E. 2002. Neural immunity: Friend or foe? *Journal For Neurovirology,* 8**,** 474-9.

Gerhard, Alexander, Pavese, Nicola, Hotton, Gary, Turkheimer, Federico, Es, Meltem, Hammers, Alexander, Eggert, Karla, Oertel, Wolfgang, Banati, Richard B. & Brooks, David J. 2006. In vivo imaging of microglial activation with [11C](R)-PK11195 PET in idiopathic Parkinson's disease. *Neurobiol Dis,* 21**,** 404-412.

Gertz, Melanie, Fischer, Frank, Nguyen, Giang Thi Tuyet, Lakshminarasimhan, Mahadevan, Schutkowski, Mike, Weyand, Michael & Steegborn, Clemens 2013. Ex-527 inhibits sirtuins by exploiting their unique NAD+-dependent deacetylation mechanism. *Proc Natl Acad Sci U S A,* 110**,** E2772-E2781.

Glick, Danielle, Barth, Sandra & Macleod, Kay F. 2010. Autophagy: cellular and molecular mechanisms. *J Pathol,* 221**,** 3-12.

Grabowska, Wioleta, Sikora, Ewa & Bielak-Zmijewska, Anna 2017. Sirtuins, a promising target in slowing down the ageing process. *Biogerontology,* 18**,** 447-476.

Graeber, Manuel B., Li, Wei & Rodriguez, Michael L. 2011. Role of microglia in CNS inflammation. *FEBS Lett,* 585**,** 3798-3805.

Green, K. N., Steffan, J. S., Martinez-Coria, H., Sun, X., Schreiber, S. S., Thompson, L. M. & Laferla, F. M. 2008. Nicotinamide restores cognition in Alzheimer's disease transgenic mice via a mechanism involving sirtuin inhibition and selective reduction of Thr231-phosphotau. *J. Neurosci,* 28**,** 11500-10.

Grozinger, C. M., Chao, E. D., Blackwell, H. E., Moazed, D. & Schreiber, S. L. 2001. Identification of a class of small molecule inhibitors of the sirtuin family of NAD-dependent deacetylases by phenotypic screening. *J Biol Chem,* 276**,** 38837-43.

Guan, Q., Wang, M., Chen, H., Yang, L., Yan, Z. & Wang, X. 2016. Aging-related 1-methyl-4-phenyl-1,2,3,6-tetrahydropyridine-induced neurochemial and behavioral deficits and redox dysfunction: improvement by AK-7. *Exp Gerontol,* 82**,** 19-29.

Guarente, L. 2000. Sir2 links chromatin silencing, metabolism, and aging. *Genes Dev,* 14**,** 1021-6.

Guo, Y. J., Dong, S. Y., Cui, X. X., Feng, Y., Liu, T., Yin, M., Kuo, S. H., Tan, E. K., Zhao, W. J. & Wu, Y. C. 2016. Resveratrol alleviates MPTP-induced motor impairments and pathological changes by autophagic degradation of alpha-synuclein via SIRT1-deacetylated LC3. *Mol Nutr Food Res,* 60**,** 2161-2175.

Han, S., Choi, J. R., Soon Shin, K. & Kang, S. J. 2012. Resveratrol upregulated heat shock proteins and extended the survival of G93A-SOD1 mice. *Brain Res,* 1483**,** 112-7.

Hardingham, G. E., Fukunaga, Y. & Bading, H. 2002. Extrasynaptic NMDARs oppose synaptic NMDARs by triggering CREB shut-off and cell death pathways. *Nat Neurosci,* 5**,** 405-14.

Harry, G. Jean, Christian, Lefebvre d'Hellencourt, A., McPherson Christopher, A., Funk Jason, Mineyoshi, Aoyama & N., Wine Robert 2008. Tumor necrosis factor p55 and p75 receptors are involved in chemical-induced apoptosis of dentate granule neurons. *J Neurochem,* 106**,** 281-298.

Heo, J., Lim, J., Lee, S., Jeong, J., Kang, H., Kim, Y., Kang, J. W., Yu, H. Y., Jeong, E. M., Kim, K., Kucia, M., Waigel, S. J., Zacharias, W., Chen, Y., Kim, I. G., Ratajczak, M. Z. & Shin, D. M. 2017. Sirt1 regulates DNA methylation and differentiation potential of embryonic stem cells by antagonizing Dnmt3I. *Cell Reports,* 18**,** 1930-1945.

Himmerich, Hubertus, Patsalos, Olivia, Lichtblau, Nicole, Ibrahim, Mohammad A. A. & Dalton, Bethan 2019. Cytokine research in depression: principles, challenges, and open questions. *Front. Psychiatry,* 10.

Hirata, T., Otsuka, I., Okazaki, S., Mouri, K., Horai, T., Boku, S., Takahashi, M., Ueno, Y., Sora, I., Shirakawa, O. & Hishimoto, A. 2019. Major depressive disorder-associated SIRT1 locus affects the risk for suicide in women after middle age. *Psychiatry Res.,* 278**,** 141-145.

Honda, T., Segi-Nishida, E., Miyachi, Y. & Narumiya, S. 2006. Prostacyclin-IP signaling and prostaglandin E2-EP2/EP4 signaling both mediate joint inflammation in mouse collagen-induced arthritis. *J Exp Med,* 203**,** 325-35.

Horiuchi, Takahiko, Mitoma, Hiroki, Harashima, Shin-ichi, Tsukamoto, Hiroshi & Shimoda, Terufumi 2010. Transmembrane TNF-alpha: structure, function and interaction with anti-TNF agents. *Rheumatology,* 49**,** 1215-1228.

Horvath, R. J., Nutile-Mcmenemy, N., Alkaitis, M. S. & Deleo, J. A. 2008. Differential migration, LPS-induced cytokine, chemokine, and NO expression in immortalized BV-2 and HAPI cell lines and primary microglial cultures. *J Neurochem,* 107**,** 557-569.

Hou, Xuben, Rooklin, David, Fang, Hao & Zhang, Yingkai 2016. Resveratrol serves as a protein-substrate interaction stabilizer in human SIRT1 activation. *Sci Rep,* 6**,** 38186-38186.

Hou, Y., Dan, X., Babbar, M., Wei, Y., Hasselbalch, S. G., Croteau, D. L. & Bohr, V. A. 2019. Ageing as a risk factor for neurodegenerative disease. *Nat. Reve. Neurol.,* 15**,** 565-581.

Huang, Wen-Juan, Zhang, X. I. A. & Chen, Wei-Wei 2016. Role of oxidative stress in Alzheimer's disease. *Biomed Rep,* 4**,** 519-522.

Huynh, Nhu N. & Mcintyre, Roger S. 2008. What are the implications of the STAR*D trial for primary care? a review and synthesis. *Prim Care Companion J Clin Psychiatry,* 10**,** 91-96.

Hynes, R. O. 2002. Integrins: bidirectional, allosteric signaling machines. *Cell,* 110**,** 673-87.

Innala, Marcus, Riebe, Ilse, Kuzmenko, Volodymyr, Sundberg, Johan, Gatenholm, Paul, Hanse, Eric & Johannesson, Sara 2014. 3D Culturing and differentiation of SH-SY5Y neuroblastoma cells on bacterial nanocellulose scaffolds. *Artif Cells Nanomed Biotechnol,* 42**,** 302-308.

J. Douglas Bremner, Meena Narayan, Eric R. Anderson, Lawrence H. Staib, Helen L. Miller & Dennis S. Charney 2000. Hippocampal volume reduction in major depression. *Am J Psychiatry,* 157**,** 115-118.

Jane S. Paulsen, Carissa Nehl, Karin Ferneyhough Hoth, Jason E. Kanz, Michelle Benjamin, Rachel Conybeare, Bradley Mcdowell & Beth Turner 2005. Depression and stages of Huntington's disease. *J Neuropsychiatry Clin Neurosci,* 17**,** 496-502.

Jaroch, Karol, Jaroch, Alina & Bojko, Barbara 2018. Cell cultures in drug discovery and development: The need of reliable in vitro-in vivo extrapolation for pharmacodynamics and pharmacokinetics assessment. *J. Pharm. Biomed. Anal.,* 147**,** 297-312.

Jellinger, Kurt A. 2010. Basic mechanisms of neurodegeneration: a critical update. *J Cell Mol Med,* 14**,** 457-487.

Jeon, Sang Won & Kim, Yong-Ku 2016. Molecular neurobiology and promising new treatment in depression. *Int J Mol Sci,* 17**,** 381.

Jeong, Jae-Kyo, Moon, Myung-Hee, Lee, You-Jin, Seol, Jae-Won & Park, Sang-Youel 2013. Autophagy induced by the class III histone deacetylase Sirt1 prevents prion peptide neurotoxicity. *Neurobiol Aging,* 34**,** 146-156.

Jesko, H., Wencel, P., Strosznajder, R. P. & Strosznajder, J. B. 2017. Sirtuins and their roles in brain aging and neurodegenerative disorders. *Neurochem Res,* 42**,** 876-890.

Jiang, Kaida, Yu, Xin, Li, Lingjiang & Wang, Gaohua 2010. Psychiatry, Beijing, People's Medical Publishing House.

Jiang, Y., Liu, J., Chen, D., Yan, L. & Zheng, W. 2017. Sirtuin Inhibition: Strategies, Inhibitors, and Therapeutic Potential. *Trends Pharmacol Sci,* 38**,** 459-472.

Kaminska, Bozena, Mota, Mariana & Pizzi, Marina 2016. Signal transduction and epigenetic mechanisms in the control of microglia activation during neuroinflammation. *Biochim Biophs Acta Mol Basis Dis,* 1862**,** 339-351.

Kauppinen, A., Suuronen, T., Ojala, J., Kaarniranta, K. & Salminen, A. 2013. Antagonistic crosstalk between NF-kappaB and SIRT1 in the regulation of inflammation and metabolic disorders. *Cell Signal,* 25**,** 1939-48.

Kawai, T. & Akira, S. 2011. Toll-like receptors and their crosstalk with other innate receptors in infection and immunity. *Immunity,* 34**,** 637-50.

Khairova, Rushaniya A., Machado-Vieira, Rodrigo, Du, Jing & Manji, Husseini K. 2009. A potential role for pro-inflammatory cytokines in regulating synaptic plasticity in major depressive disorder. *Int J Neuropsychopharmacol,* 12**,** 561-578.

Khan, R. S., Fonseca-Kelly, Z., Callinan, C., Zuo, L., Sachdeva, M. M. & Shindler, K. S. 2012. SIRT1 activating compounds reduce oxidative stress and prevent cell death in neuronal cells. *Front Cell Neurosci,* 6**,** 63.

Khemka, Vineet Kumar, Ganguly, Anirban, Bagchi, Debajit, Ghosh, Arindam, Bir, Aritri, Biswas, Atanu, Chattopadhyay, Sita & Chakrabarti, Sasanka 2014. Raised serum proinflammatory cytokines in Alzheimer's disease with depression. *Aging Dis.,* 5**,** 170-176.

Kim, D., Nguyen, M. D., Dobbin, M. M., Fischer, A., Sananbenesi, F., Rodgers, J. T., Delalle, I., Baur, J. A., Sui, G., Armour, S. M., Puigserver, P., Sinclair, D. A. & Tsai, L. H. 2007. SIRT1 deacetylase protects against neurodegeneration in models for Alzheimer's disease and amyotrophic lateral sclerosis. *EMBO J,* 26**,** 3169-79.

Kim, H. D., Hesterman, J., Call, T., Magazu, S., Keeley, E., Armenta, K., Kronman, H., Neve, R. L., Nestler, E. J. & Ferguson, D. 2016. SIRT1 mediates depression-like behaviors in the nucleus accumbens. *J Neurosci,* 36**,** 8441-8452.

Kim, Sangwon F. 2011. The role of nitric oxide in prostaglandin biology; update. *Nitric Oxide,* 25**,** 255-264.

Kishi, T., Yoshimura, R., Kitajima, T., Okochi, T., Okumura, T., Tsunoka, T., Yamanouchi, Y., Kinoshita, Y., Kawashima, K., Fukuo, Y., Naitoh, H., Umene-Nakano, W., Inada, T., Nakamura, J., Ozaki, N. & Iwata, N. 2010. SIRT1 gene is associated with major depressive disorder in the Japanese population. *J Affect Disord,* 126**,** 167-73.

Kiss, Debra L., Windus, Louisa C. E. & Avery, Vicky M. 2013. Chemokine receptor expression on integrin-mediated stellate projections of prostate cancer cells in 3D culture. *Cytokine,* 64**,** 122-130.

Kleman, A. M., Yuan, J. Y., Aja, S., Ronnett, G. V. & Landree, L. E. 2008. Physiological glucose is critical for optimized neuronal viability and AMPK responsiveness in vitro. *J Neurosci Methods,* 167**,** 292-301.

Klionsky, D. J., Abdelmohsen, K., Abe, A., Abedin, M. J., Abeliovich, H., Acevedo Arozena, A., Adachi, H., Adams, C. M., Adams, P. D., Adeli, K., Adhihetty, P. J., Adler, S. G., Agam, G., Agarwal, R., Aghi, M. K., Agnello, M., Agostinis, P., Aguilar, P. V., Aguirre-Ghiso, J., Airoldi, E. M., Ait-Si-Ali, S., Akematsu, T., Akporiaye, E. T., Al-Rubeai, M., Albaiceta, G. M., Albanese, C., Albani, D., Albert, M. L., Aldudo, J., Algul, H., Alirezaei, M., Alloza, I., Almasan, A., Almonte-Beceril, M., Alnemri, E. S., Alonso, C., Altan-Bonnet, N., Altieri, D. C., Alvarez, S., Alvarez-Erviti, L., Alves, S., Amadoro, G., Amano, A., Amantini, C., Ambrosio, S., Amelio, I., Amer, A. O., Amessou, M., Amon, A., An, Z., Anania, F. A., Andersen, S. U., Andley, U. P., Andreadi, C. K., Andrieu-Abadie, N., Anel, A., Ann, D. K., Anoopkumar-Dukie, S., Antonioli, M., Aoki, H., Apostolova, N., Aquila, S., Aquilano, K., Araki, K., Arama, E., Aranda, A., Araya, J., Arcaro, A., Arias, E., Arimoto, H., Ariosa, A. R., Armstrong, J. L., Arnould, T., Arsov, I., Asanuma, K., Askanas, V., Asselin, E., Atarashi, R., Atherton, S. S., Atkin, J. D., Attardi, L. D., Auberger, P., Auburger, G., Aurelian, L., Autelli, R., Avagliano, L., Avantaggiati, M. L., Avrahami, L., Awale, S., Azad, N., Bachetti, T., Backer, J. M., Bae, D. H., Bae, J. S., Bae, O. N., Bae, S. H., Baehrecke, E. H., Baek, S. H., Baghdiguian, S., Bagniewska-Zadworna, A., et al. 2016. Guidelines for the use and interpretation of assays for monitoring autophagy (3rd edition). *Autophagy,* 12**,** 1-222.

Köhler-Forsberg, Ole, Petersen, Liselotte, Ahmed, Kazi Ishtiak, Østergaard, Søren & Gasse, Christiane 2020. Medical diseases prior to first-time depression diagnosis and subsequent risk of admissions for depression: A nationwide study of 117,585 patients. *J Affect Disord*.

Köhler, Ole, Benros, Michael E., Nordentoft, Merete, Farkouh, Michael E., Iyengar, Rupa L., Mors, Ole & Krogh, Jesper 2014. Effect of Anti-inflammatory Treatment on Depression, Depressive Symptoms, and Adverse Effects: A Systematic Review and Meta-analysis of Randomized Clinical Trials. *JAMA Psychiatry,* 71**,** 1381-1391.

Köhler, Ole, Krogh, Jesper, Mors, Ole & Benros, Michael Eriksen 2016. Inflammation in depression and the potential for anti-Inflammatory treatment. *Curr Neuropharmacol,* 14**,** 732-742.

Kono, Hajime & Rock, Kenneth L. 2008. How dying cells alert the immune system to danger. *Nat Rev Immunol,* 8**,** 279-289.

Kostadinov, Ilia, Delev, Delian, Petrova, Atanaska, Stanimirova, Irina, Draganova, Krassimira, Kruzliak, Peter, Kostadinova, Ivanka & Murdjeva, Marianna 2015. Study on anti-inflammatory and immunomodulatory effects of fluoxetine in rat models of inflammation. *Eur J Inflamm,* 13**,** 173-182.

Kovalevich, Jane & Langford, Dianne 2013. Considerations for the use of SH-SY5Y neuroblastoma cells in neurobiology. *Methods Mol Biol,* 1078**,** 9-21.

Krishnadas, R. & Cavanagh, J. 2012. Depression: an inflammatory illness? *J Neurol Neurosurg Psychiatry,* 83**,** 495-502.

Kumar, R., Nigam, L., Singh, A. P., Singh, K., Subbarao, N. & Dey, S. 2017. Design, synthesis of allosteric peptide activator for human SIRT1 and its biological evaluation in cellular model of Alzheimer's disease. *Eur J Med Chem,* 127**,** 909-916.

Kume, Shinji, Uzu, Takashi, Horiike, Kihachiro, Chin-Kanasaki, Masami, Isshiki, Keiji, Araki, Shin-ichi, Sugimoto, Toshiro, Haneda, Masakazu, Kashiwagi, Atsunori & Koya, Daisuke 2010. Calorie restriction enhances cell adaptation to hypoxia through Sirt1-dependent mitochondrial autophagy in mouse aged kidney. *J Clin Invest,* 120**,** 1043-1055.

Landry, J., Sutton, A., Tafrov, S. T., Heller, R. C., Stebbins, J., Pillus, L. & Sternglanz, R. 2000. The silencing protein SIR2 and its homologs are NAD-dependent protein deacetylases. *Proc Natl Acad Sci U S A,* 97**,** 5807-11.

Lavu, S., Boss, O., Elliott, P. J. & Lambert, P. D. 2008. Sirtuins - novel therapeutic targets to treat age-associated diseases. *Nat Rev Drug Discov,* 7**,** 841-853.

Layé, S., Parnet, P., Goujon, E. & Dantzer, R. 1994. Peripheral administration of lipopolysaccharide induces the expression of cytokine transcripts in the brain and pituitary of mice. *Mol Brain Res,* 27**,** 157-62.

Lee, B. H. & Kim, Y. K. 2010. The roles of BDNF in the pathophysiology of major depression and in antidepressant treatment. *Psychiatry Investig,* 7**,** 231-5.

Lee, S H, Soyoola, E, Chanmugam, P, Hart, S, Sun, W, Zhong, H, Liou, S, Simmons, D & Hwang, D 1992. Selective expression of mitogen-inducible cyclooxygenase in macrophages stimulated with lipopolysaccharide. *J Biol Chem,* 267**,** 25934-8.

Lee, Yong Gyu, Reader, Brenda F., Herman, Derrick, Streicher, Adam, Englert, Joshua A., Ziegler, Mathias, Chung, Sangwoon, Karpurapu, Manjula, Park, Gye Young, Christman, John W. & Ballinger, Megan N. 2019. Sirtuin 2 enhances allergic asthmatic inflammation. *JCI Insight,* 4.

Leonard, B. E. 2018. Inflammation and depression: a causal or coincidental link to the pathophysiology? *Acta Neuropsychiatr,* 30**,** 1-16.

Letourneau, P. C., Condic, M. L. & Snow, D. M. 1992. Extracellular matrix and neurite outgrowth. *Curr Opin Genet Dev,* 2**,** 625-34.

Levine, Beth, Mizushima, Noboru & Virgin, Herbert W. 2011. Autophagy in immunity and inflammation. *Nature,* 469**,** 323-335.

Li, L., Sun, Q., Li, Y., Yang, Y., Yang, Y., Chang, T., Man, M. & Zheng, L. 2015. Overexpression of SIRT1 Induced by Resveratrol and Inhibitor of miR-204 Suppresses Activation and Proliferation of Microglia. *J Mol Neurosci,* 56**,** 858-67.

Li, X. M., Zhou, M. T., Wang, X. M., Ji, M. H., Zhou, Z. Q. & Yang, J. J. 2014. Resveratrol pretreatment attenuates the isoflurane-induced cognitive impairment through its anti-inflammation and -apoptosis actions in aged mice. *J Mol Neurosci,* 52**,** 286-93.

Lieb, J., Karmali, R. & Horrobin, D. 1983. Elevated levels of prostaglandin E2 and thromboxane B2 in depression. *Prostaglandins Leukot Med,* 10**,** 361-7.

Liu, Dexiang, Wang, Zhen, Liu, Shangming, Wang, Fuwu, Zhao, Shidou & Hao, Aijun 2011. Anti-inflammatory effects of fluoxetine in lipopolysaccharide(LPS)-stimulated microglial cells. *Neuropharmacology,* 61**,** 592-599.

Liu, L., Zhang, Q., Cai, Y., Sun, D., He, X., Wang, L., Yu, D., Li, X., Xiong, X., Xu, H., Yang, Q. & Fan, X. 2016. Resveratrol counteracts lipopolysaccharide-induced depressive-like behaviors via enhanced hippocampal neurogenesis. *Oncotarget,* 7**,** 56045-56059.

Liu, S. Y., Li, D., Zeng, H. Y., Kan, L. Y., Zou, W., Zhang, P., Gu, H. F. & Tang, X. Q. 2017. Hydrogen sulfide inhibits chronic unpredictable mild stress-induced depressive-like behavior by upregulation of Sirt-1: involvement in suppression of hippocampal endoplasmic reticulum stress. *Int J Neuropsychopharmacol*.

Liu, W., Yan, H., Zhou, D., Cai, X., Zhang, Y., Li, S., Li, H., Li, S., Zhou, D. S., Li, X., Zhang, C., Sun, Y., Dai, J. P., Zhong, J., Yao, Y. G., Luo, X. J., Fang, Y., Zhang, D., Ma, Y., Yue, W., Li, M. & Xiao, X. 2019. The depression GWAS risk allele predicts smaller cerebellar gray matter volume and reduced SIRT1 mRNA expression in Chinese population. *Transl Psychiatry,* 9**,** 333.

Liu, Yiheng, Fu, Yuan, Zhang, Yunxia, Liu, Fangfang, Rose, Gregory M., He, Xiaowen, Yi, Xinan, Ren, Rui, Li, Yiying, Zhang, Yusheng, Wu, Hui, Lv, Chuanzhu & Zhang, Haiying 2020. Butein attenuates the cytotoxic effects of LPS-stimulated microglia on the SH-SY5Y neuronal cell line. *Eur J Pharmacol,* 868**,** 172858.

Lo Iacono, L., Visco-Comandini, F., Valzania, A., Viscomi, M. T., Coviello, M., Giampà, A., Roscini, L., Bisicchia, E., Siracusano, A., Troisi, A., Puglisi-Allegra, S. & Carola, V. 2015. Adversity in childhood and depression: linked through SIRT1. *Transl Psychiatry,* 5**,** e629.

Lobo-Silva, Diogo, Carriche, Guilhermina M., Castro, A. Gil, Roque, Susana & Saraiva, Margarida 2016. Balancing the immune response in the brain: IL-10 and its regulation. *J Neuroinflammation,* 13**,** 297-297.

Long, Katherine R. & Huttner, Wieland B. 2019. How the extracellular matrix shapes neural development. *Open Biol,* 9**,** 180216-180216.

Loonen, Anton J. M. & Ivanova, Svetlana A. 2016. Circuits regulating pleasure and happiness—mechanisms of depression. *Front Hum Neurosci,* 10**,** 571.

Lopez-Castejon, Gloria & Brough, David 2011. Understanding the mechanism of IL-1β secretion. *Cytokine Growth Factor Rev.,* 22**,** 189-195.

Luchtman, Dirk W. & Song, Cai 2010. Why SH-SY5Y cells should be differentiated. *Neurotoxicology,* 31**,** 164-165.

Lukiw, W. J. & Bazan, N. G. 1998. Strong nuclear factor-kappaB-DNA binding parallels cyclooxygenase-2 gene transcription in aging and in sporadic Alzheimer's disease superior temporal lobe neocortex. *J Neurosci Res,* 53**,** 583-92.

Lund, Søren, Christensen, Kenneth Vielsted, Hedtjärn, Maj, Mortensen, Anne Louise, Hagberg, Henrik, Falsig, Jeppe, Hasseldam, Henrik, Schrattenholz, André, Pörzgen, Peter & Leist, Marcel 2006. The dynamics of the LPS triggered inflammatory response of murine microglia under different culture and in vivo conditions. *J Neuroimmunol,* 180**,** 71-87.

Luthi-Carter, R., Taylor, D. M., Pallos, J., Lambert, E., Amore, A., Parker, A., Moffitt, H., Smith, D. L., Runne, H., Gokce, O., Kuhn, A., Xiang, Z., Maxwell, M. M., Reeves, S. A., Bates, G. P., Neri, C., Thompson, L. M., Marsh, J. L. & Kazantsev, A. G. 2010. SIRT2 inhibition achieves neuroprotection by decreasing sterol biosynthesis. *Proc Natl Acad Sci U S A,* 107**,** 7927-32.

Lv, Yanbo, Lin, Shuangyan & Peng, Fang 2017. SIRT1 gene polymorphisms and risk of lung cancer. *Cancer Manag Res,* 9**,** 381-386.

Lyketsos, C. G. & Lee, H. B. 2004. Diagnosis and treatment of depression in Alzheimer's disease. A practical update for the clinician. *Dement. Geriatr. Cogn. Disord.,* 17**,** 55-64.

Lyman, M., Lloyd, D. G., Ji, X. M., Vizcaychipi, M. P. & Ma, D. Q. 2014. Neuroinflammation: The role and consequences. *Neurosci Res,* 79**,** 1-12.

Ma, W., Tavakoli, T., Derby, E., Serebryakova, Y., Rao, M. S. & Mattson, M. P. 2008. Cell-extracellular matrix interactions regulate neural differentiation of human embryonic stem cells. *BMC Dev. Biol.,* 8**,** 90.

Maes, M., Leonard, B. E., Myint, A. M., Kubera, M. & Verkerk, R. 2011. The new '5-HT' hypothesis of depression: Cell-mediated immune activation induces indoleamine 2,3-dioxygenase, which leads to lower plasma tryptophan and an increased synthesis of detrimental tryptophan catabolites (TRYCATs), both of which contribute to the onset of depression. *Prog Neuropsychopharmacol Biol Psychiatry,* 35**,** 702-721.

Mai, A., Massa, S., Lavu, S., Pezzi, R., Simeoni, S., Ragno, R., Mariotti, F. R., Chiani, F., Camilloni, G. & Sinclair, D. A. 2005. Design, synthesis, and biological evaluation of sirtinol analogues as class III histone/protein deacetylase (sirtuin) inhibitors. *J Med Chem,* 48**,** 7789-7795.

Malhi, G. S., Bassett, D., Boyce, P., Bryant, R., Fitzgerald, P. B., Fritz, K., Hopwood, M., Lyndon, B., Mulder, R., Murray, G., Porter, R. & Singh, A. B. 2015. Royal Australian and New Zealand college of psychiatrists clinical practice guidelines for mood disorders. *Aust N Z. J Psychiatry,* 49**,** 1087-206.

Malhi, G. S., Outhred, T., Hamilton, A., Boyce, P. M., Bryant, R., Fitzgerald, P. B., Lyndon, B., Mulder, R., Murray, G., Porter, R. J., Singh, A. B. & Fritz, K. 2018. Royal Australian and New Zealand college of psychiatrists clinical practice guidelines for mood disorders: major depression summary. *Med J Aust,* 208**,** 175-180.

Mancuso, R., Del Valle, J., Modol, L., Martinez, A., Granado-Serrano, A. B., Ramirez-Nunez, O., Pallas, M., Portero-Otin, M., Osta, R. & Navarro, X. 2014. Resveratrol improves motoneuron function and extends survival in SOD1(G93A) ALS mice. *Neurotherapeutics,* 11**,** 419-32.

Markert, C. D., Kim, E., Gifondorwa, D. J., Childers, M. K. & Milligan, C. E. 2010. A single-dose resveratrol treatment in a mouse model of amyotrophic lateral sclerosis. *J Med Food,* 13**,** 1081-5.

Martins, R., Lithgow, G. J. & Link, W. 2016. Long live FOXO: unraveling the role of FOXO proteins in aging and longevity. *Aging cell,* 15**,** 196-207.

Masliah, E., Mallory, M., Alford, M., Deteresa, R., Hansen, L.A., Mckeel, D.W. & Morris, J.C. 2001. Altered expression of synaptic proteins occurs early during progression of Alzheimer's disease. *Neurology,* 56**,** 127-129.

Mathews, D. C., Henter, I. D. & Zarate, C. A. 2012. Targeting the glutamatergic system to treat major depressive disorder: rationale and progress to date. *Drugs,* 72**,** 1313-33.

Maurizio Fava, A. John Rush, Stephen R. Wisniewski, Andrew A. Nierenberg, Jonathan E. Alpert, Patrick J. Mcgrath, Michael E. Thase, Diane Warden, Melanie Biggs, James F. Luther, George Niederehe, Louise Ritz & Madhukar H. Trivedi 2006. A comparison of mirtazapine and nortriptyline following two consecutive failed medication treatments for depressed outpatients: a STAR*D report. *Am J Psychiatry.,* 163**,** 1161-1172.

Mcfarland, A. J., Davey, A. K., Mcdermott, C. M., Grant, G. D., Lewohl, J. & Anoopkumar-Dukie, S. 2018. Differences in statin associated neuroprotection corresponds with either decreased production of IL-1β or TNF-α in an in vitro model of neuroinflammation-induced neurodegeneration. *Toxicol Appl Pharmacol,* 344**,** 56-73.

Mckinney, W. T., Jr. & Bunney, W. E., Jr. 1969. Animal model of depression. I. review of evidence: implications for research. *Arch Gen Psychiatry,* 21**,** 240-8.

Meijering, E., Jacob, M., Sarria, J.-C.F., Steiner, P., Hirling, H. & Unser, M. 2004. Design and validation of a tool for neurite tracing and analysis in fluorescence microscopy images. *Cytometry A,* 58A**,** 167-176.

Melino, G., Thiele, C. J., Knight, R. A. & Piacentini, M. 1997. Retinoids and the control of growth/death decisions in human neuroblastoma cell lines. *J. Neurooncol.,* 31**,** 65-83.

Meyer, Amy, Van Golen, Cynthia M., Kim, Bhumsoo, Van Golen, Kenneth L. & Feldman, Eva L. 2004. Integrin expression regulates neuroblastoma attachment and migration. *Neoplasia (New York, N.Y.),* 6**,** 332-342.

Michan, S. & Sinclair, D. 2007. Sirtuins in mammals: insights into their biological function. *Biochem J,* 404**,** 1-13.

Michishita, Eriko, Park, Jean Y., Burneskis, Jenna M., Barrett, J. Carl & Horikawa, Izumi 2005. Evolutionarily conserved and nonconserved cellular localizations and functions of human SIRT proteins. *Mol Biol Cell,* 16**,** 4623-4635.

Miller, Andrew H. & Raison, Charles L. 2016. The role of inflammation in depression: from evolutionary imperative to modern treatment target. *Nat Rev Immunol,* 16**,** 22-34.

Min, S. W., Cho, S. H., Zhou, Y., Schroeder, S., Haroutunian, V., Seeley, W. W., Huang, E. J., Shen, Y., Masliah, E., Mukherjee, C., Meyers, D., Cole, P. A., Ott, M. & Gan, L. 2010. Acetylation of tau inhibits its degradation and contributes to tauopathy. *Neuron,* 67**,** 953-66.

Min, S. W., Sohn, P. D., Cho, S. H., Swanson, R. A. & Gan, L. 2013. Sirtuins in neurodegenerative diseases: an update on potential mechanisms. *Front Aging Neurosci,* 5**,** 9.

Minghetti, L., Polazzi, E., Nicolini, A., Créminon, C. & Levi, G. 1996. Interferon-gamma and nitric oxide down-regulate lipopolysaccharide-induced prostanoid production in cultured rat microglial cells by inhibiting cyclooxygenase-2 expression. *J Neurochem,* 66**,** 1963-70.

Mishra, Anjuli, Kim, Hee Jung, Shin, Angela H. & Thayer, Stanley A. 2012. Synapse loss induced by interleukin-1β requires pre- and post-synaptic mechanisms. *J. Neuroimmune Pharmacol.,* 7**,** 571-578.

Mizushima, N. 2007. Autophagy: process and function. *Genes Dev,* 21**,** 2861-73.

Moorthi, P., Premkumar, P., Priyanka, R., Jayachandran, K. S. & Anusuyadevi, M. 2015. Pathological changes in hippocampal neuronal circuits underlie age-associated

neurodegeneration and memory loss: positive clue toward SAD. *Neuroscience,* 301**,** 90-105.

Morselli, Eugenia, Mariño, Guillermo, Bennetzen, Martin V., Eisenberg, Tobias, Megalou, Evgenia, Schroeder, Sabrina, Cabrera, Sandra, Bénit, Paule, Rustin, Pierre, Criollo, Alfredo, Kepp, Oliver, Galluzzi, Lorenzo, Shen, Shensi, Malik, Shoaib Ahmad, Maiuri, Maria Chiara, Horio, Yoshiyuki, López-Otín, Carlos, Andersen, Jens S., Tavernarakis, Nektarios, Madeo, Frank & Kroemer, Guido 2011. Spermidine and resveratrol induce autophagy by distinct pathways converging on the acetylproteome. *J Cell Biol,* 192**,** 615-629.

Moussa, C., Hebron, M., Huang, X., Ahn, J., Rissman, R. A., Aisen, P. S. & Turner, R. S. 2017. Resveratrol regulates neuro-inflammation and induces adaptive immunity in Alzheimer's disease. *J Neuroinflammation,* 14.

Mudgal, Jayesh, Basu Mallik, Sanchari, Nampoothiri, Madhavan, Kinra, Manas, Hall, Susan, Grant, Gary D., Anoopkumar-Dukie, Shailendra, Davey, Andrew K., Rao, C. Mallikarjuna & Arora, Devinder 2020. Effect of coffee constituents, caffeine and caffeic acid on anxiety and lipopolysaccharide-induced sickness behavior in mice. *J. Funct. Foods,* 64**,** 103638.

Mudo, G., Makela, J., Di Liberto, V., Tselykh, T. V., Olivieri, M., Piepponen, P., Eriksson, O., Malkia, A., Bonomo, A., Kairisalo, M., Aguirre, J. A., Korhonen, L., Belluardo, N. & Lindholm, D. 2012. Transgenic expression and activation of PGC-1alpha protect dopaminergic neurons in the MPTP mouse model of Parkinson's disease. *Cell Mol Life Sci,* 69**,** 1153-65.

Murray, Christopher J. L., Lopez, Alan D., World Health, Organization, World, Bank & Harvard School of Public, Health 1996. A comprehensive assessment of mortality and disability from diseases, injuries, and risk factors in 1990 and projected to 2020. *In:* MURRAY, C. J. L. & LOPEZ, A. D. (eds.) The global burden of disease. Harvard School of Public Health on behalf of the World Health Organization and the World Bank.

Musiek, Erik S. & Holtzman, David M. 2016. Mechanisms linking circadian clocks, sleep, and neurodegeneration. *Science,* 354**,** 1004-1008.

Na, Cai. , Tim, B Bigdeli. , Warren, Kretzschmar. & Yihan, Li. 2015. Sparse whole-genome sequencing identifies two loci for major depressive disorder. *Nature,* 523**,** 588-591.

Nahas, Z., Marangell, L. B., Husain, M. M., Rush, A. J., Sackeim, H. A., Lisanby, S. H., Martinez, J. M. & George, M. S. 2005. Two-year outcome of vagus nerve stimulation (VNS) for treatment of major depressive episodes. *J Clin Psychiatry,* 66**,** 1097-104.

Narumiya, S. 2009. Prostanoids and inflammation: a new concept arising from receptor knockout mice. *J Mol Med,* 87**,** 1015-22.

Ng, Fanny & Tang, Bor Luen 2013. Sirtuins' modulation of autophagy. *J Cell Physiol,* 228**,** 2262-2270.

Niedzielska, Ewa, Smaga, Irena, Gawlik, Maciej, Moniczewski, Andrzej, Stankowicz, Piotr, Pera, Joanna & Filip, Małgorzata 2016. Oxidative stress in neurodegenerative diseases. *Mol Neurobiol,* 53**,** 4094-4125.

Nimh 2006. National institute of mental health sequenced treatment alternatives to relieve depression (STAR*D) study

Nishida, Yuichiro, Adati, Naoki, Ozawa, Ritsuko, Maeda, Aasami, Sakaki, Yoshiyuki & Takeda, Tadayuki 2008. Identification and classification of genes regulated by phosphatidylinositol 3-kinase- and TRKB-mediated signalling pathways during neuronal differentiation in two subtypes of the human neuroblastoma cell line SH-SY5Y. *BMC Res Notes,* 1**,** 95-95.

Nogueiras, Ruben, Habegger, Kirk M., Chaudhary, Nilika, Finan, Brian, Banks, Alexander S., Dietrich, Marcelo O., Horvath, Tamas L., Sinclair, David A., Pfluger, Paul T. & Tschöp, Matthias H. 2012. Sirtuin 1 and sirtuin 3: physiological modulators of metabolism. *Physiol Rev,* 92**,** 1479-1514.

O'connor, J. C., Lawson, M. A., Andre, C., Moreau, M., Lestage, J., Castanon, N., Kelley, K. W. & Dantzer, R. 2009. Lipopolysaccharide-induced depressive-like behavior is

mediated by indoleamine 2,3-dioxygenase activation in mice. *Mol Psychiatry,* 14**,** 511-22.

Ohishi, Kazuhiro, Ueno, Ryuji, Nishino, Seiji, Sakai, Toshiaki & Hayaishi, Osamu 1988. Increased level of salivary prostaglandins in patients with major depression. *Biol Psychiatry,* 23**,** 326-334.

Orecchia, Angela, Scarponi, Claudia, Di Felice, Francesca, Cesarini, Elisa, Avitabile, Simona, Mai, Antonello, Mauro, Maria Luisa, Sirri, Valentina, Zambruno, Giovanna, Albanesi, Cristina, Camilloni, Giorgio & Failla, Cristina M. 2011. Sirtinol treatment reduces inflammation in human dermal microvascular endothelial cells. *PLoS One,* 6**,** e24307.

Outeiro, T. F., Kontopoulos, E., Altmann, S. M., Kufareva, I., Strathearn, K. E., Amore, A. M., Volk, C. B., Maxwell, M. M., Rochet, J. C., Mclean, P. J., Young, A. B., Abagyan, R., Feany, M. B., Hyman, B. T. & Kazantsev, A. G. 2007. Sirtuin 2 inhibitors rescue alpha-synuclein-mediated toxicity in models of Parkinson's disease. *Science,* 317**,** 516-9.

Ovesna, Z. & Horvathova-Kozics, K. 2005. Structure-activity relationship of trans-resveratrol and its analogues. *Neoplasma,* 52**,** 450-5.

Pais, Teresa Faria, Szegő, Éva M., Marques, Oldriska, Miller-Fleming, Leonor, Antas, Pedro, Guerreiro, Patrícia, De Oliveira, Rita Machado, Kasapoglu, Burcu & Outeiro, Tiago Fleming 2013. The NAD-dependent deacetylase sirtuin 2 is a suppressor of microglial activation and brain inflammation. *EMBO J,* 32**,** 2603-2616.

Pandey, Anand Kumar, Bhattacharya, Pallab, Shukla, Swet Chand, Paul, Sudip & Patnaik, Ranjana 2015. Resveratrol inhibits matrix metalloproteinases to attenuate neuronal damage in cerebral ischemia: a molecular docking study exploring possible neuroprotection. *Neural Regen Res,* 10**,** 568-575.

Paraiso, A. F., Mendes, K. L. & Santos, S. H. 2013. Brain activation of SIRT1: role in neuropathology. *Mol Neurobiol,* 48**,** 681-9.

Patrick J. Mcgrath, Jonathan W. Stewart , Maurizio Fava, Madhukar H. Trivedi, Stephen R. Wisniewski, Andrew A. Nierenberg, Michael E. Thase, Lori Davis, Melanie M. Biggs, Kathy Shores-Wilson, James F. Luther, George Niederehe, Diane Warden & A. John Rush 2006. Tranylcypromine versus venlafaxine plus mirtazapine following three failed antidepressant medication trials for depression: a STAR*D report. *Am J Psychiatry.,* 163**,** 1531-1541.

Paugh, Steven W., Bonten, Erik J., Savic, Daniel, Ramsey, Laura B., Thierfelder, William E., Gurung, Prajwal, Malireddi, R. K. Subbarao, Actis, Marcelo, Mayasundari, Anand, Min, Jaeki, Coss, David R., Laudermilk, Lucas T., Panetta, John C., Mccorkle, J. Robert, Fan, Yiping, Crews, Kristine R., Stocco, Gabriele, Wilkinson, Mark R., Ferreira, Antonio M., Cheng, Cheng, Yang, Wenjian, Karol, Seth E., Fernandez, Christian A., Diouf, Barthelemy, Smith, Colton, Hicks, J. Kevin, Zanut, Alessandra, Giordanengo, Audrey, Crona, Daniel, Bianchi, Joy J., Holmfeldt, Linda, Mullighan, Charles G., Den Boer, Monique L., Pieters, Rob, Jeha, Sima, Dunwell, Thomas L., Latif, Farida, Bhojwani, Deepa, Carroll, William L., Pui, Ching-Hon, Myers, Richard M., Guy, R. Kiplin, Kanneganti, Thirumala-Devi, Relling, Mary V. & Evans, William E. 2015. NALP3 inflammasome up-regulation and CASP1 cleavage of the glucocorticoid receptor causes glucocorticoid resistance in leukemia cells. *Nat Genet,* 47**,** 607-614.

Paulsen, J. S., Ready, R. E., Hamilton, J. M., Mega, M. S. & Cummings, J. L. 2001. Neuropsychiatric aspects of Huntington's disease. *J Neurol Neurosurg Psychiatry,* 71**,** 310-4.

Penn, Elizabeth & Tracy, Derek K. 2012. The drugs don’t work? antidepressants and the current and future pharmacological management of depression. *Ther Adv Psychopharmacol,* 2**,** 179-188.

Pérez-Sánchez, Gilberto, Becerril-Villanueva, Enrique, Arreola, Rodrigo, Martínez-Levy, Gabriela, Hernández-Gutiérrez, María Eugenia, Velasco-Velásquez, Marco A., Alvarez-Herrera, Samantha, Cruz-Fuentes, Carlos, Palacios, Lino, De La Peña, Francisco & Pavón, Lenin 2018. Inflammatory profiles in depressed adolescents treated with fluoxetine: an 8-Week follow-up open study. *Mediators Inflamm.,* 2018**,** 1-12.

Polito, L., Kehoe, P. G., Davin, A., Benussi, L., Ghidoni, R., Binetti, G., Quadri, P., Lucca, U., Tettamanti, M., Clerici, F., Bagnoli, S., Galimberti, D., Nacmias, B., Sorbi, S., Guaita, A., Scarpini, E., Mariani, C., Forloni, G. & Albani, D. 2013. The SIRT2 polymorphism rs10410544 and risk of Alzheimer's disease in two Caucasian case-control cohorts. *Alzheimers Dement,* 9**,** 392-9.

Poljsak, B. & Milisav, I. 2016. NAD plus as the link between oxidative stress, inflammation, caloric restriction, exercise, DNA repair, longevity, and health span. *Rejuv Res,* 19**,** 406-413.

Porcelli, S., Salfi, R., Politis, A., Atti, A. R., Albani, D., Chierchia, A., Polito, L., Zisaki, A., Piperi, C., Liappas, I., Alberti, S., Balestri, M., Marsano, A., Stamouli, E., Mailis, A., Biella, G., Forloni, G., Bernabei, V., Ferrari, B., Lia, L., Papadimitriou, G. N., De Ronchi, D. & Serretti, A. 2013. Association between sirtuin 2 gene rs10410544 polymorphism and depression in Alzheimer's disease in two independent European samples. *J Neural Transm,* 120**,** 1709-15.

Porquet, D., Casadesus, G., Bayod, S., Vicente, A., Canudas, A. M., Vilaplana, J., Pelegri, C., Sanfeliu, C., Camins, A., Pallas, M. & Del Valle, J. 2013. Dietary resveratrol prevents Alzheimer's markers and increases life span in SAMP8. *Age (Dordr),* 35**,** 1851-65.

Prado, R. C. & Barbosa, E. R. 2005. Depression in Parkinson's disease: study of 60 cases. *Arq Neuropsiquiatr,* 63**,** 766-71.

Presgraves, S. P., Ahmed, T., Borwege, S. & Joyce, J. N. 2004. Terminally differentiated SH-SY5Y cells provide a model system for studying neuroprotective effects of dopamine agonists. *Neurotox Res,* 5**,** 579-98.

Qian, Sun, Fan, Jie, Billiar, Timothy R. & Scott, Melanie J. 2017. Inflammasome and autophagy regulation: a two-way street. *Mel Med,* 23**,** 188-195.

Queenslandhealth 2017. The administration of electroconvulsive therapy guideline.

Racagni, G. & Popoli, M. 2008. Cellular and molecular mechanisms in the long-term action of antidepressants. *Dialogues Clin Neurosci,* 10**,** 385-400.

Ramesh, Geeta, Maclean, Andrew G. & Philipp, Mario T. 2013. Cytokines and chemokines at the crossroads of neuroinflammation, neurodegeneration, and neuropathic pain. *Mediators Inflamm.,* 2013**,** 480739.

Reddy, B. R., Maitra, S., Jhelum, P., Kumar, K. P., Bagul, P. K., Kaur, G., Banerjee, S. K., Kumar, A. & Chakravarty, S. 2016. Sirtuin 1 and 7 mediate resveratrol-induced recovery from hyper-anxiety in high-fructose-fed prediabetic rats. *J Biosci,* 41**,** 407-17.

Remus, Jennifer L. & Dantzer, Robert 2016. Inflammation models of depression in rodents: relevance to psychotropic drug discovery. *Int J Neuropsychopharmacol,* 19**,** pyw028.

Ren, N. S. X., Ji, M., Tokar, E. J., Busch, E. L., Xu, X. J., Lewis, D., Li, X. C., Jin, A. W., Zhang, Y. P., Wu, W. K. K., Huang, W. C., Li, L. P., Fargo, D. C., Keku, T. O., Sandler, R. S. & Li, X. L. 2017. Haploinsufficiency of SIRT1 enhances glutamine metabolism and promotes cancer development. *Curr Biol,* 27**,** 483-494.

Rhen, Turk & Cidlowski, John A. 2005. Antiinflammatory action of glucocorticoids — new mechanisms for old drugs. *N Engl J Med,* 353**,** 1711-1723.

Rickards, H. 2006. Depression in neurological disorders: an update. *Curr Opin Psychiatry,* 19**,** 294-8.

Rizk, Sherine M., Shahin, Nancy N. & Shaker, Olfat G. 2016. Association between SIRT1 gene polymorphisms and breast cancer in egyptians. *PLoS One,* 11**,** e0151901.

Rock, Kenneth L., Latz, Eicke, Ontiveros, Fernando & Kono, Hajime 2010. The sterile inflammatory response. *Annu Rev Immunol,* 28**,** 321-342.

Rohwedel, J., Guan, K. & Wobus, A. M. 1999. Induction of cellular differentiation by retinoic acid in vitro. *Cells Tissues Organs,* 165**,** 190-202.

Romeo-Guitart, David, Leiva-Rodríguez, Tatiana, Espinosa-Alcantud, María, Sima, Núria, Vaquero, Alejandro, Domínguez- Martín, Helena, Ruano, Diego & Casas, Caty 2018. SIRT1 activation with neuroheal is neuroprotective but SIRT2 inhibition with AK7 is detrimental for disconnected motoneurons. *Cell Death Dis,* 9**,** 531.

Roos, Elin, Mariosa, Daniela, Ingre, Caroline, Lundholm, Cecilia, Wirdefeldt, Karin, Roos, Per M. & Fang, Fang 2016. Depression in amyotrophic lateral sclerosis. *Neurology,* 86**,** 2271-2277.

Rosenberg, G. A. 2002. Matrix metalloproteinases in neuroinflammation. *Glia,* 39**,** 279-91.

Rosso, Isabelle M., Cintron, Christina M., Steingard, Ronald J., Renshaw, Perry F., Young, Ashley D. & Yurgelun-Todd, Deborah A. 2005. Amygdala and hippocampus volumes in pediatric major depression. *Biol Psychiatry,* 57**,** 21-26.

Rossol, M., Heine, H., Meusch, U., Quandt, D., Klein, C., Sweet, M. J. & Hauschildt, S. 2011. LPS-induced cytokine production in human monocytes and macrophages. *Crit. Rev. Immunol.,* 31**,** 379-446.

Roy, A. & Campbell, M. K. 2013. A unifying framework for depression: bridging the major biological and psychosocial theories through stress. *Clin Invest Med,* 36**,** E170-90.

Rush, A. J., Trivedi, M. H., Wisniewski, S. R., Stewart, J. W., Nierenberg, A. A., Thase, M. E., Ritz, L., Biggs, M. M., Warden, D., Luther, J. F., Shores-Wilson, K., Niederehe, G. & Fava, M. 2006. Bupropion-SR, sertraline, or venlafaxine-XR after failure of SSRIs for depression. *N Engl J Med,* 354**,** 1231-42.

Russo, Matthew & Mcgavern, Dorian B. 2015. Immune surveillance of the CNS following infection and injury. *Trends Immunol,* 36**,** 637-650.

Russo, V. C., Higgins, S., Werther, G. A. & Cameron, F. J. 2012. Effects of fluctuating glucose levels on neuronal cells in vitro. *Neurochem Res,* 37**,** 1768-82.

Sahin, C., Dursun, S., Cetin, M. & Aricioglu, F. 2016. The neuroinflammation perspective of depression: reuniting the outstanding mechanisms of the pathophysiology. *Klinik Psikofarmakol Bulteni,* 26**,** 196-206.

Saitoh, T., Fujita, N., Jang, M. H., Uematsu, S., Yang, B. G., Satoh, T., Omori, H., Noda, T., Yamamoto, N., Komatsu, M., Tanaka, K., Kawai, T., Tsujimura, T., Takeuchi, O., Yoshimori, T. & Akira, S. 2008. Loss of the autophagy protein Atg16L1 enhances endotoxin-induced IL-1beta production. *Nature,* 456**,** 264-8.

Salvemini, D., Misko, T. P., Masferrer, J. L., Seibert, K., Currie, M. G. & Needleman, P. 1993. Nitric oxide activates cyclooxygenase enzymes. *Proc Natl Acad Sci U S A,* 90**,** 7240-4.

Sansone, Randy A. & Sansone, Lori A. 2011. Agomelatine: a novel antidepressant. *Innov Clin Neurosci,* 8**,** 10-14.

Santoni, Giorgio, Cardinali, Claudio, Morelli, Maria Beatrice, Santoni, Matteo, Nabissi, Massimo & Amantini, Consuelo 2015. Danger- and pathogen-associated molecular patterns recognition by pattern-recognition receptors and ion channels of the transient receptor potential family triggers the inflammasome activation in immune cells and sensory neurons. *J Neuroinflammation,* 12**,** 21.

Sanz, J. M. & Di Virgilio, F. 2000. Kinetics and mechanism of ATP-dependent IL-1 beta release from microglial cells. *J Immunol,* 164**,** 4893-8.

Schiepers, Olga J. G., Wichers, Marieke C. & Maes, Michael 2005. Cytokines and major depression. *Prog Neuropsychopharmacol Biol Psychiatry,* 29**,** 201-217.

Schmidt, F. M., Lichtblau, N., Minkwitz, J., Chittka, T., Thormann, J., Kirkby, K. C., Sander, C., Mergl, R., Fasshauer, M., Stumvoll, M., Holdt, L. M., Teupser, D., Hegerl, U. & Himmerich, H. 2014. Cytokine levels in depressed and non-depressed subjects, and masking effects of obesity. *J Psychiatr Res,* 55**,** 29-34.

Schnekenburger, M., Mathieu, V., Lefranc, F., Jang, J. Y., Masi, M., Kijjoa, A., Evidente, A., Kim, H. J., Kiss, R., Dicato, M., Han, B. W. & Diederich, M. 2018. The fungal metabolite eurochevalierine, a sequiterpene alkaloid, displays anti-cancer properties through selective sirtuin 1/2 inhibition. *Molecules,* 23.

Schrag, A., Barone, P., Brown, R. G., Leentjens, A. F., Mcdonald, W. M., Starkstein, S., Weintraub, D., Poewe, W., Rascol, O., Sampaio, C., Stebbins, G. T. & Goetz, C. G. 2007. Depression rating scales in Parkinson's disease: critique and recommendations. *Mov Disord,* 22**,** 1077-92.

Schweichel, J.-U. & Merker, H.-J. 1973. The morphology of various types of cell death in prenatal tissues. *Teratology,* 7**,** 253-266.

Scuderi, C., Stecca, C., Bronzuoli, M. R., Rotili, D., Valente, S., Mai, A. & Steardo, L. 2014. Sirtuin modulators control reactive gliosis in an in vitro model of Alzheimer's disease. *Front Pharmacol,* 5**,** 89.

Shah, S. A., Khan, M., Jo, M. H., Jo, M. G., Amin, F. U. & Kim, M. O. 2017. Melatonin stimulates the SIRT1/Nrf2 signaling pathway counteracting lipopolysaccharide (LPS)-induced oxidative stress to rescue postnatal rat brain. *CNS Neurosci Ther,* 23**,** 33-44.

Shaw, Greg 2013. Polymorphism and single nucleotide polymorphisms (SNPs). *BJU Int,* 112**,** 664-665.

Sheline, Yvette I., Gado, Mokhtar H. & Price, Joseph L. 1998. Amygdala core nuclei volumes are decreased in recurrent major depression. *NeuroReport,* 9**,** 2023-2028.

Shelton, R. C. 2012. Does concomitant use of NSAIDs reduce the effectiveness of antidepressants? *Am J Psychiatry.,* 169**,** 1012-5.

Shi, C. S., Shenderov, K., Huang, N. N., Kabat, J., Abu-Asab, M., Fitzgerald, K. A., Sher, A. & Kehrl, J. H. 2012. Activation of autophagy by inflammatory signals limits IL-1beta production by targeting ubiquitinated inflammasomes for destruction. *Nat Immunol,* 13**,** 255-63.

Shindler, K. S., Ventura, E., Dutt, M., Elliott, P., Fitzgerald, D. C. & Rostami, A. 2010. Oral resveratrol reduces neuronal damage in a model of multiple sclerosis. *J Neuroophthalmol,* 30**,** 328-39.

Shipley, Mackenzie M., Mangold, Colleen A. & Szpara, Moriah L. 2016. Differentiation of the SH-SY5Y human neuroblastoma cell line. *J Vis Exp***,** 53193-53193.

Shoba, Balaji, Lwin, Zin Mar, Ling, Lo Soo, Bay, Boon-Huat, Yip, George W. & Kumar, Srinivasan Dinesh 2009. Function of sirtuins in biological tissues. *Anat Rec,* 292**,** 536-543.

Siegert, R J & Abernethy, D A 2005. Depression in multiple sclerosis: a review. *J Neurol Neurosurg Psychiatry,* 76**,** 469-475.

Silva, D. F., Esteves, A. R., Oliveira, C. R. & Cardoso, S. M. 2016. Mitochondrial metabolism power SIRT2-dependent deficient traffic causing Alzheimer's-Disease related pathology. *Mol Neurobiol,* 54**,** 4021-4040.

Smerker, H. 2014. Weaning and Adaptation of SH-SY5Y Cells to Low Glucose Media for Manganese Exposure Studies. *Proceedings of the National Conference On Undergraduate Research (NCUR) 2014***,** 449-459.

Smith, M. R., Syed, A., Lukacsovich, T., Purcell, J., Barbaro, B. A., Worthge, S. A., Wei, S. R., Pollio, G., Magnoni, L., Scali, C., Massai, L., Franceschini, D., Camarri, M., Gianfriddo, M., Diodato, E., Thomas, R., Gokce, O., Tabrizi, S. J., Caricasole, A., Landwehrmeyer, B., Menalled, L., Murphy, C., Ramboz, S., Luthi-Carter, R., Westerberg, G. & Marsh, J. L. 2014. A potent and selective Sirtuin 1 inhibitor alleviates pathology in multiple animal and cell models of Huntington's disease. *Hum Mol Genet,* 23**,** 2995-3007.

Song, C., Halbreich, U., Han, C., Leonard, B. E. & Luo, H. 2009. Imbalance between pro- and anti-inflammatory cytokines, and between Th1 and Th2 cytokines in depressed patients: the effect of electroacupuncture or fluoxetine treatment. *Pharmacopsychiatry,* 42**,** 182-188.

Song, L., Chen, L., Zhang, X., Li, J. & Le, W. 2014. Resveratrol ameliorates motor neuron degeneration and improves survival in SOD1(G93A) mouse model of amyotrophic lateral sclerosis. *Biomed Res Int,* 2014**,** 483501.

Spires-Jones, T. L., Fox, L. M., Rozkalne, A., Pitstick, R., Carlson, G. A. & Kazantsev, A. G. 2012. Inhibition of sirtuin 2 with sulfobenzoic acid derivative AK1 is non-toxic and potentially neuroprotective in a mouse model of frontotemporal dementia. *Front Pharmacol,* 3**,** 42.

Steckler, T., Holsboer, F. & Reul, J. M. 1999. Glucocorticoids and depression. *Baillieres Best Pract Res Clin Endocrinol Metab,* 13**,** 597-614.

Stein, Dirson J., Vasconcelos, Mailton F., Albrechet-Souza, Lucas, Ceresér, Keila M. M. & De Almeida, Rosa M. M. 2017. Microglial over-activation by social defeat stress contributes to anxiety- and depressive-like behaviors. *Front Behav Neurosci,* 11.

Stein, Liana Roberts & Imai, Shin-ichiro 2012. The dynamic regulation of NAD metabolism in mitochondria. *Trends Endocrinol. Metab.,* 23**,** 420-428.

Steru, L., Chermat, R., Thierry, B., Mico, J. A., Lenegre, A., Steru, M., Simon, P. & Porsolt, R. D. 1987. The automated tail suspension test: a computerized device which differentiates psychotropic drugs. *Prog Neuropsychopharmacol Biol Psychiatry,* 11**,** 659-71.

Stoffels, M., Zaal, R., Kok, N., Van Der Meer, J. W., Dinarello, C. A. & Simon, A. 2015a. ATP-induced IL-1beta specific secretion: true under stringent conditions. *Front Immunol,* 6**,** 54.

Stoffels, Monique, Zaal, Ruben, Kok, Nina, Van Der Meer, Jos W. M., Dinarello, Charles A. & Simon, Anna 2015b. ATP-induced IL-1β specific secretion: true under stringent conditions. *Front Immunol,* 6**,** 54-54.

Stogsdill, Jeff A. & Eroglu, Cagla 2017. The interplay between neurons and glia in synapse development and plasticity. *Curr Opin Neurobiol,* 42**,** 1-8.

Streit, W. J. & Kincaid-Colton, C. A. 1995. The brain's immune system. *Sci Am,* 273**,** 54-5, 58-61.

Sussmuth, S. D., Haider, S., Landwehrmeyer, G. B., Farmer, R., Frost, C., Tripepi, G., Andersen, C. A., Di Bacco, M., Lamanna, C., Diodato, E., Massai, L., Diamanti, D., Mori, E., Magnoni, L., Dreyhaupt, J., Schiefele, K., Craufurd, D., Saft, C., Rudzinska, M., Ryglewicz, D., Orth, M., Brzozy, S., Baran, A., Pollio, G., Andre, R., Tabrizi, S. J., Darpo, B. & Westerberg, G. 2015. An exploratory double-blind, randomized clinical trial with selisistat, a SirT1 inhibitor, in patients with Huntington's disease. *Br J Clin Pharmacol,* 79**,** 465-76.

Sveinbjornsdottir, S. 2016. The clinical symptoms of Parkinson's disease. *J Neurochem,* 139 Suppl 1**,** 318-324.

Sweeney, Gary & Song, Juhyun 2016. The association between PGC-1α and Alzheimer's disease. *Anat Cell Biol,* 49**,** 1-6.

Szepesi, Zsuzsanna, Manouchehrian, Oscar, Bachiller, Sara & Deierborg, Tomas 2018. Bidirectional microglia–neuron communication in health and disease. *Front Cell Neurosci,* 12.

Tandberg, E., Larsen, J. P., Aarsland, D. & Cummings, J. L. 1996. The occurrence of depression in Parkinson's disease: a community-based study. *Arch. Neurol.,* 53**,** 175-9.

Tang, Bor Luen 2017. Sirtuins as modifiers of Parkinson's disease pathology. *J Neurosci Res,* 95**,** 930-942.

Teppola, Heidi, Sarkanen, Jertta-Riina, Jalonen, Tuula O. & Linne, Marja-Leena 2016. Morphological differentiation towards neuronal phenotype of SH-SY5Y neuroblastoma cells by estradiol, retinoic acid and cholesterol. *Neurochem Res,* 41**,** 731-747.

Thase, M. E., Friedman, E. S., Biggs, M. M., Wisniewski, S. R., Trivedi, M. H., Luther, J. F., Fava, M., Nierenberg, A. A., Mcgrath, P. J., Warden, D., Niederehe, G., Hollon, S. D. & Rush, A. J. 2007. Cognitive therapy versus medication in augmentation and switch strategies as second-step treatments: a STAR*D report. *Am J Psychiatry.,* 164**,** 739-52.

Timmerman, Raissa, Burm, Saskia M. & Bajramovic, Jeffrey J. 2018. An overview of in vitro methods to study microglia. *Front Cell Neurosci,* 12**,** 242-242.

Tojima, T. & Ito, E. 2004. Signal transduction cascades underlying de novo protein synthesis required for neuronal morphogenesis in differentiating neurons. *Prog Neurobiol,* 72**,** 183-93.

Trivedi, M. H., Rush, A. J., Wisniewski, S. R., Nierenberg, A. A., Warden, D., Ritz, L., Norquist, G., Howland, R. H., Lebowitz, B., Mcgrath, P. J., Shores-Wilson, K., Biggs, M. M., Balasubramani, G. K., Fava, M. & Team, Star Study 2006a. Evaluation of outcomes with citalopram for depression using measurement-based care in STAR*D: implications for clinical practice. *Am J Psychiatry.,* 163**,** 28-40.

Trivedi, Madhukar H., Fava, Maurizio, Wisniewski, Stephen R., Thase, Michael E., Quitkin, Frederick, Warden, Diane, Ritz, Louise, Nierenberg, Andrew A., Lebowitz, Barry D., Biggs, Melanie M., Luther, James F., Shores-Wilson, Kathy & Rush, A. John 2006b.

Medication augmentation after the failure of SSRIs for depression. *N Engl J Med,* 354**,** 1243-1252.
Uddin, M., Koenen, K. C., Aiello, A. E., Wildman, D. E., De Los Santos, R. & Galea, S. 2011. Epigenetic and inflammatory marker profiles associated with depression in a community-based epidemiologic sample. *Psychol Med,* 41**,** 997-1007.
Valle, C., Salvatori, I., Gerbino, V., Rossi, S., Palamiuc, L., Rene, F. & Carri, M. T. 2014. Tissue-specific deregulation of selected HDACs characterizes ALS progression in mouse models: pharmacological characterization of SIRT1 and SIRT2 pathways. *Cell Death Dis,* 5**,** e1296.
Vallés, Patricia G., Lorenzo, Andrea Gil, Bocanegra, Victoria & Vallés, Roberto 2014. Acute kidney injury: what part do toll-like receptors play? *Int J Nephro Renovasc Dis,* 7**,** 241-251.
Van Dyken, Peter & Lacoste, Baptiste 2018. Impact of metabolic syndrome on neuroinflammation and the blood–brain barrier. *Front Neurosci,* 12.
Vawter, Marquis P., Dillon-Carter, Ora, Tourtellotte, W. W., Carvey, Paul & Freed, William J. 1996. TGFβ1 and TGFβ2 concentrations are elevated in Parkinson's disease in ventricular cerebrospinal fluid. *Exp Neurol,* 142**,** 313-322.
Voican, C. S., Corruble, E., Naveau, S. & Perlemuter, G. 2014. Antidepressant-induced liver injury: a review for clinicians. *Am J Psychiatry.,* 171**,** 404-15.
Von Bernhardi, Rommy, Heredia, Florencia, Salgado, Nicole & Muñoz, Paola 2016. Microglia function in the normal brain. *Adv Exp Med Biol,* 949**,** 67-92.
Wajant, H., Pfizenmaier, K. & Scheurich, P. 2003. Tumor necrosis factor signaling. *Cell Death Differ.,* 10**,** 45-65.
Wang, B., Zhang, Y., Cao, W., Wei, X., Chen, J. & Ying, W. 2016. SIRT2 plays significant roles in lipopolysaccharides-induced neuroinflammation and brain injury in mice. *Neurochem Res,* 41**,** 2490-500.
Wang, J., Zhang, Y., Tang, L., Zhang, N. & Fan, D. 2011. Protective effects of resveratrol through the up-regulation of SIRT1 expression in the mutant hSOD1-G93A-bearing motor neuron-like cell culture model of amyotrophic lateral sclerosis. *Neurosci Lett,* 503**,** 250-5.
Wang, Q., Yan, C., Xin, M. M., Han, L., Zhang, Y. Q. & Sun, M. S. 2017. Sirtuin 1 (Sirt1) overexpression in BaF3 cells contributes to cell proliferation promotion, apoptosis resistance and pro-inflammatory cytokine production. *Med Sci Monitor,* 23**,** 6.
Wang, X., Guan, Q., Wang, M., Yang, L., Bai, J., Yan, Z., Zhang, Y. & Liu, Z. 2015. Aging-related rotenone-induced neurochemical and behavioral deficits: role of SIRT2 and redox imbalance, and neuroprotection by AK-7. *Drug Des Devel Ther,* 9**,** 2553-63.
Wang, X., Wu, H. & Miller, A. H. 2004. Interleukin 1alpha (IL-1alpha) induced activation of p38 mitogen-activated protein kinase inhibits glucocorticoid receptor function. *Mol Psychiatry,* 9**,** 65-75.
Wang, Y. L., Li, S. Y. & Liu, C. F. 2016. Disruption of circadian rhythm function and anti-oxidation via SIRT1-BMAL1 pathway in 6-OHDA induced Parkinson's disease model. *Mov Disord,* 31**,** S41-S41.
Weber, A., Wasiliew, P. & Kracht, M. 2010a. Interleukin-1 (IL-1) pathway. *Sci Signal,* 3**,** 6.
Weber, A., Wasiliew, P. & Kracht, M. 2010b. Interleukin-1beta (IL-1beta) processing pathway. *Sci Signal,* 3**,** cm2.
Wilson, Shruti P. & Cassel, Suzanne L. 2010. Inflammasome mediated autoinflammatory disorders. *Postgrad Med,* 122**,** 125-133.
Wong, Donald, Dorovini-Zis, Katerina & Vincent, Steven R. 2004. Cytokines, nitric oxide, and cGMP modulate the permeability of an in vitro model of the human blood–brain barrier. *Exp Neurol,* 190**,** 446-455.
Xia, Man, Yu, Jin-Tai, Miao, Dan, Lu, Rui-Chun, Zheng, Xue-Ping & Tan, Lan 2014. SIRT2 polymorphism rs10410544 is associated with Alzheimer's disease in a Han Chinese population. *J Neurol Sci,* 336**,** 48-51.
Xiang, Z. & Krainc, D. 2013. Pharmacological upregulation of PGC1alpha in oligodendrocytes: implications for Huntington's Disease. *J Huntingtons Dis,* 2**,** 101-5.

Yaron, Ilana, Shirazi, Idit, Judovich, Rachel, Levartovsky, David, Caspi, Dan & Yaron, Michael 1999. Fluoxetine and amitriptyline inhibit nitric oxide, prostaglandin E2, and hyaluronic acid production in human synovial cells and synovial tissue cultures. *Arthritis Rheum.,* 42**,** 2561-2568.

Ye, J., Liu, Z., Wei, J., Lu, L., Huang, Y., Luo, L. & Xie, H. 2013. Protective effect of SIRT1 on toxicity of microglial-derived factors induced by LPS to PC12 cells via the p53-caspase-3-dependent apoptotic pathway. *Neurosci Lett,* 553**,** 72-7.

Yoshida, R. & Hayaishi, O. 1987. Indoleamine 2,3-dioxygenase. *Methods Enzymol.,* 142**,** 188-95.

Yu, H. & Chen, Z. Y. 2011. The role of BDNF in depression on the basis of its location in the neural circuitry. *Acta Pharmacol Sin,* 32**,** 3-11.

Yuan, Fang, Xu, Zhi-Ming, Lu, Li-Yan, Nie, Hui, Ding, Jun, Ying, Wei-Hai & Tian, Heng-Li 2016a. SIRT2 inhibition exacerbates neuroinflammation and blood-brain barrier disruption in experimental traumatic brain injury by enhancing NF-κB p65 acetylation and activation. *J Neurochem,* 136**,** 581-593.

Yuan, Fang, Xu, Zhi‐Ming, Lu, Li‐Yan, Nie, Hui, Ding, Jun, Ying, Wei‐Hai & Tian, Heng‐Li 2016b. SIRT2 inhibition exacerbates neuroinflammation and blood‐brain barrier disruption in experimental traumatic brain injury by enhancing NF‐κB p65 acetylation and activation. *J Neurochem,* 136**,** 581-593.

Zavvari, Fahime & Nahavandi, Arezo 2020. Fluoxetine increases hippocampal neural survival by improving axonal transport in stress-induced model of depression male rats. *Physiol Behav,* 227**,** 113140.

Zeng, Rong, Chen, Yan, Zhao, Shuai & Cui, Guo-hui 2011. Autophagy counteracts apoptosis in human multiple myeloma cells exposed to oridonin in vitro via regulating intracellular ROS and SIRT1. *Acta Pharmacol Sin,* 33**,** 91.

Zeng, Rong, He, Jing, Peng, Jin, Chen, Yan, Yi, Sha, Zhao, Fei & Cui, Guohui 2012. The time-dependent autophagy protects against apoptosis with possible involvement of Sirt1 protein in multiple myeloma under nutrient depletion. *Ann Hematol,* 91**,** 407-417.

Zhang, Feng, Zhou, Hui, Wilson, Belinda C., Shi, Jing-Shan, Hong, Jau-Shyong & Gao, Hui-Ming 2012. Fluoxetine protects neurons against microglial activation-mediated neurotoxicity. *Parkinsonism Relat Disord,* 18**,** S213-S217.

Zhang, Mingming, Pan, Yida, Dorfman, Robert G., Yin, Yuyao, Zhou, Qian, Huang, Shan, Liu, Jie & Zhao, Shimin 2017. Sirtinol promotes PEPCK1 degradation and inhibits gluconeogenesis by inhibiting deacetylase SIRT2. *Sci Rep,* 7**,** 7-7.

Zhang, Yuqing, Anoopkumar-Dukie, Shailendra, Arora, Devinder & Davey, Andrew K. 2020. Review of the anti-inflammatory effect of SIRT1 and SIRT2 modulators on neurodegenerative diseases. *Eur J Pharmacol,* 867**,** 172847.

Zhao, Chunmei, Deng, Wei & Gage, Fred H. 2008. Mechanisms and functional implications of adult neurogenesis. *Cell,* 132**,** 645-660.

Zheng, Wenwen, Zheng, Xuexing, Liu, Shue, Ouyang, Hongsheng, Levitt, Roy C., Candiotti, Keith A. & Hao, Shuanglin 2012. TNFα and IL-1β are mediated by both TLR4 and Nod1 pathways in the cultured HAPI cells stimulated by LPS. *Biochem Biophys Res Commun,* 420**,** 762-767.

Zou, Wei, Feng, Renjie & Yang, Yuan 2018. Changes in the serum levels of inflammatory cytokines in antidepressant drug-naïve patients with major depression. *PLoS One,* 13**,** e0197267-e0197267.

Zou, X. D., Guo, S. Q., Hu, Z. W. & Li, W. L. 2016. NAMPT protects against 6-hydroxydopamine-induced neurotoxicity in PC12 cells through modulating SIRT1 activity. *Mol Med Rep,* 13**,** 4058-64.